Characterising two genomic islands involved in metabolism in *Neisseria meningitidis*

Adrian Jun Chu

Doctor of Philosophy

University of York

Biology

September 2017

Abstract

Meningococcal meningitis is endemic in sub-Saharan Africa while sporadic outbreaks burden the developed world by preying on the young and immunocompromised. The causal pathogen *Neisseria meningitidis* exclusively colonises the human nasopharynx. With a relatively concise genome, it can invade across multiple bodily compartments, which can be highly debilitating and life-threatening.

Nine genomic "islands" have been identified in *N. meningitidis* and *N. gonorrhoeae*, absent from their commensal cousin *N. lactamica*. Many are predicted to have roles in bacterial transport, metabolism and regulation.

Genomic Island 5 contains three genes and was correctly annotated to encode enzymes involved in the synthesis of the polyamine putrescine, protecting bacteria from oxidative stress. Mutant *N. meningitidis* lacking these genes grew poorly in rich media. The lesion can be restored by putrescine supplementation or gene complementation.

Genomic Island 3 contains two genes poorly annotated to be spermidine-synthesising – a higher polyamine. Mutant *N. meningitidis* lacking these genes, however, grew poorly in chemically-defined media. Shuffling amino acid profiles and culturing with a labelled arginine isotope suggest a role in the acquisition and metabolism of arginine and glutamine, which are key to meningococcal maintenance.

Enhanced systems circumventing host resource-denial, scavenging amino acids and resisting challenges from free radicals are examples of virulence. These islands are believed to support the general fitness of *N. meningitidis* as a highly competitive commensal but paradoxically "accidental" pathogen, where disease is a likely a result of risk-taking lifestyles in response to complex microenvironment changes.

This behaviour is contrasted by *N. gonorrhoeae* which prefers recurrent infection episodes and long-term establishment. The closely-related but phenotypically diverse members of the *Neisseria* genus hence serve as research foci of much interest. In a broader sense, investigating why meningococci conserve such pathogen-specific sequences may help inspire new clinical strategies and provide alternative perspectives towards the biology of similar organisms.

Table of Contents

List of Figures

List of Tables

List of Abbreviations

APS = ammonium persulfate

BBB = blood-brain barrier

BCAA = branched-chain amino acid

BCSFB = blood-cerebrospinal fluid barrier

BLAST = Basic Local Alignment Search Tool

bp = base pair

CBA = Columbia blood Agar

CDC = Centers for Disease Control and Prevention

CDM = chemically-defined medium

cDNA = complementary DNA

cfu = colony forming unit

CNS = central nervous system

CSF = cerebrospinal fluid

DNA = deoxyribonucleic acid

dNTP = deoxyribonucleoside triphosphate

DUS = DNA uptake sequence

ECDC = European Centre for Disease Prevention and Control

EDTA = ethylenediaminetetraacetic acid

Ery^R = erythromycin resistance gene

fHBP = factor H-binding protein

HPLC = high-performance liquid chromatography

Kan^R = kanamycin resistance gene

kbp = kilobase pairs

kDa = kiloDalton

KEGG = Kyoto Encyclopaedia of Genes and Genomes

LB = Lysogeny Broth

LOS = lipo-oligosaccharide

LPS = lipopolysaccharide

Lrp = L-leucine-responsive protein

MALDI = matrix-assisted laser desorption/ionisation

Mbp = Megabase pair

MHB = Müller-Hinton Broth

MS = mass spectrometry

NadA = Neisseria adhesin A

NCBI = National Centre for Biotechnology Information

NO = nitric oxide

OD = optical density

OD_{600} = optical density at wavelength 600 nm

OMV = outer membrane vesicle

Opa = opacity-associated protein

Opc = *Neisseria meningitidis* invasin

PAGE = polyacrylamide gel electrophoresis

PCR = polymerase chain reaction

PorA = Porin A

PorB = Porin B

qPCR = quantitative polymerase chain reaction

RNA = ribonucleic acid

RNase = ribonuclease

RNS = reactive nitrogen species

ROS = reactive oxygen species

rpm = revolutions per minute

SAM = *S*-Adenosyl-L-Methionine

SDS = sodium dodecyl sulphate

SDS-PAGE = sodium dodecyl sulphate-polyacrylamide gel electrophoresis

SOD = superoxide dismutase

$Spec^R$ = spectinomycin resistance gene

spp. = species

STI = sexually-transmitted infection

TBE = Tris-Borate-EDTA buffer

TEMED = tetramethylethylenediamine

TMHMM = transmembrane hidden Markov model (helices prediction programme)

Tris = Tris(hydroxymethyl)aminomethane

TSB = Transformation and Storage Buffer

URT = upper respiratory tract

Acknowledgements

First and foremost, I would like to thank my supervisor Professor James Moir for his insightful guidance and generous support throughout the project.

I would also like to thank my seniors in the Moir Group, Dr. Lindsey Flanagan, Dr. Rachel Yale and Dr. John Thomas, for their invaluable companionship and empathy. Together with all colleagues and fellow students at L1, they were my immediate go-to persons whenever questions arose.

I also thank Professor Maggie Smith and Dr. Jamie Wood for serving as members of my Thesis Advisory Panel. Their thoughtful and critical input helped propel my scientific thinking forward. I wish Professor Smith a happy retirement.

My thanks go to Dr. Tony Larson, Dr. Adam Dowle and Ms Rachel Bates at TF for their technical support in mass spectrometry. I extend my thanks to all at the TF Bioinformatics team as well as the TF Genomics team for their training and counsel.

Thanks also to Dr. Vladimir Pelicic at Imperial College London for providing materials from his *Neisseria* mutant library, which helped accelerate crucial parts of this work.

My heartfelt thanks to all friends and staff I met in York for their encouragement and inspiration.

Last but not least, I thank my family and my girlfriend Tiffany for their love and faith.

Author's Declaration

I declare that this thesis is a presentation of original work and I am the sole author. This work has not previously been presented for an award at this, or any other, University. All sources are acknowledged as References.

Chapter 1 – General Introduction

1.1 Overview of the genus *Neisseria*

Prussian dermato-bacteriologist Albert Neisser first identified *Neisseria gonorrhoeae* as the cause of the sexually-transmitted infection (STI) gonorrhoea in 1879 (Jayakumar and Lipoff, 2017). Named after the Breslau academic, this bacterial genus *Neisseria* belongs to the family Neisseriaceae, under the order Neisseriales and class ß-proteobacteria. Today, the only other species within the genus pathogenic to humans is *Neisseria meningitidis*, which is paradoxically capable of both commensal carriage and life-threatening disease.

With few exceptions, members of the genus are usually 0.6 – 1.9 µm in diameter and normally occur as singlets, in pairs or in tetrads of cocci where adjacent sides appear flattened, while other general features include being haemolytic, oxidase and catalase positive, do not produce exotoxins and are found in mammalian mucosal surfaces (Tønjum, 2015). The sequenced genomes of *N. meningitidis*, *N. gonorrhoeae* and *N. lactamica* strains are very closely related and relatively small in size (around 2.2 Mbp), yet highly diverse as over 10,000 unique sequence types of the three species were deposited at the PubMLST database (Maiden, 2008).

1.1.1 *Neisseria gonorrhoeae*

The diplococcal, non-encapsulated *Neisseria gonorrhoeae* is an obligate human pathogen that causes gonorrhoea, which is characterised by frequent recurrence following treatment (Unemo *et al.*, 2017). Bacterial vaginosis in women is also a predisposition of high risk with strong causal and predictive links to gonorrhoea and other STIs (Wiesenfeld *et al.*, 2003; Gallo *et al.*, 2012). More severe complications include pelvic inflammatory disease, infertility and even ectopic pregnancy, but the disease is further complexed into a major public health concern due to its advanced antibiotic resistance profile (Unemo *et al.*, 2016). Unlike other *Neisseria* species, gonococcal infections are showing increasingly severe cases of antibiotic resistance at alarming rates which are recognised worldwide (Costa-Lourenço *et al.*, 2017). This hallmark trait is facilitated by horizontal gene transfer occurring between other bacterial species and the naturally competent *N. gonorrhoeae* – even from humans (Cehovin and Lewis, 2017; Anderson and Seifert, 2011a; Anderson and Seifert, 2011b). As last resort antibiotics such as extended-spectrum cephalosporins were widely reported to have been compromised, the grave prospect warrants immediate collaborative action by international communities to combat the disease with new drugs and ideally gonococcal vaccines (Wi *et al.*, 2017).

1.1.2 *Neisseria meningitidis*

On the other hand, first identified by Anton Weichselbaum in 1887 from patient cerebrospinal fluid (CSF), *N. meningitidis* is closely related to *N. gonorrhoeae* but without the aforementioned notoriety. While the gonococci infect human genito-urinary tracts resulting in inflammation, pain and discharges, the meningococci infect through the human throat. *N. meningitidis* first colonises the infant nasopharynx along with harmless commensal strains such as *N. lactamica*, and as age increases, meningococcal colonisation becomes increasingly predominant until adolescence (Christensen *et al.*, 2010). Along with *Streptococcus pneumoniae,* Group B *Streptococcus*, *Haemophilus influenzae* and *Listeria monocytogenes*, *N. meningitidis* is one of the major causal pathogens capable of the deadly condition known as bacterial meningitis which has serious clinical consequences (CDC, 2017).

1.1.3 *Neisseria lactamica*

Neisseria lactamica is the most closely-related non-pathogenic species to *N. meningitidis* and is believed to be how infants naturally prime their immunity towards the latter (Gold *et al.*, 1978). In infants, sustained carriage of lactose-fermenting (useful for lactose-rich infant diets) *N. lactamica* – hence the namesake – is accompanied by the presence of anti-meningococcal serum bactericidal antibodies (SBAs) despite relatively low proportions of *N. meningitidis* colonies (Bennett *et al.*, 2005). In adults, this can also be achieved by raising mucosal and systemic humoral immunity against *N. lactamica* where opsonophagocytic antibodies (but not SBAs) cross-react to cover *N. meningitidis* (Evans *et al.*, 2011). This strait had been exploited in the development of some non-universal meningococcal vaccines (Gorringe *et al.*, 2009).

Although they both colonise the nasopharynx, a gradual transition occurs as we progress from childhood to adulthood, during which predominance shifts from the commensal to the pathogen (Bakir *et al.*, 2001). Carriage of *N. lactamica* is usually stable and homogenous in human populations regardless of seasonal variations or the presence of vaccination efforts against its pathogenic cousin (Kristiansen *et al.*, 2012). Although both *N. lactamica* and *N. meningitidis* occupy the same ecological niche and share similar mechanisms in energy acquisition, interactions with host cells differ where the commensal tends to induce expression of pro-inflammatory genes, while the pathogen can down-regulate and evade host defences (Wong *et al.*, 2011). Inoculation with *N. lactamica* was even shown to displace and prevent *N. meningitidis* carriage in young adults through competition (Deasy *et al.*, 2015).

Other non-pathogenic species of *Neisseria* include but are not limited to: *N. sicca, N. mucosa, N. elongata, N. flavescens, N. flava, N. subflava, N perflava, N. cinerea, N. canis, N. weaveri, N. polysaccharea, N. dentiae* etc., which are often found in the human flora as well as other mammalian hosts. Although often underappreciated in comparison to the three human colonisers of outstanding clinical significance (*N. meningitidis*, *N. gonorrhoeae* and *N. lactamica*), this genetically, morphologically and phenotypically diverse genus may have great implications as a model for comparative molecular research (Liu *et al.*, 2015).

1.2 Microbiology of *Neisseria meningitidis*

Neisseria meningitidis is a Gram-negative, fastidious, aerobic bacterium which commonly resides as commensals in the human upper respiratory tract (URT) mucosa, but can also become pathogens. It can grow on a wide range of nutrient-rich media – such as blood agar and Müller-Hinton broth (MHB) used extensively in this study – but requires strict primary carbon sources like pyruvate or glucose. Colonies are round, grey, convex and moist in appearance with clearly-defined edges, growing optimally at around 37°C in the presence of carbon dioxide (Tønjum, 2015). At the heart of the meningococcal central carbon metabolism is the citric acid cycle (Leighton *et al.*, 2001). *N. meningitidis* also possesses high-affinity uptake systems for iron and iron complexes such as lactoferrin, transferrin, haemoglobin, which are both essential to normal metabolism as well as major determinants of pathogenicity (Perkins-Balding *et al.*, 2004). Along with systems that respond to changes in carbon source, metal and oxygen availability, these processes fall under a handful of transcriptional regulators in *N. meningitidis* (Golfieri, 2015). Examples include nitric oxide sensitive repressor (NsrR), fumarate and nitrate reductase regulator protein (FNR), Neisserial adhesin Regulator (NadR) and ferric uptake regulator (Fur) (Grifantini *et al.*, 2004) etc. Regulatory pathways also believed to contribute to pathogenicity include CrgA (Ieva *et al.*, 2005; Deghmane *et al.*, 2000) for attachment and MarR (Nichols *et al.*, 2009) for resistance etc. The Lrp/AsnC family of global regulatory proteins also play a role when *N. meningitidis* grows under nutrient-limiting conditions, an aspect of meningococcal lifestyle explored and discussed in Chapter 5.

N. meningitidis does not possess flagella and hence lacks swimming motility found in other bacteria. In rare cases of invasive pathogenesis, however, *N. meningitidis* may move across the mucosal epithelia and enter the blood stream to cause septicaemia. This “twitching motility” is achieved through the actions of type IV pili, filamentous organelles which allow the bacteria to traverse and adhere to moist surfaces by tethering cells through extension and retraction of thin polymers of pilin (Mattick, 2002). In *N. meningitidis* the

pilins are a source of antigenic variation which contribute to host immune evasion, and characterisation of the meningococcal pili structure demonstrates the organism's heterogeneity and elasticity (Gault *et al.*, 2015; Kolappan *et al.*, 2016).

Another crucial virulence determinant – the endotoxin lipo-oligosaccharide (LOS) – is also a source of antigenic variation in *N. meningitidis*. Unlike the lipopolysaccharides (LPS) of typical enteric Gram-negative bacteria such as *E. coli*, the corresponding meningococcal molecules LOS lack O-antigen repeating units and are localised as small operons in the chromosome, where polymorphisms occur through random rearrangements and contribute to survival in light of selective pressure from host response (Kahler and Stephens, 1998).

As encapsulated bacteria, the 13 meningococcal serogroups – A, B, C, D, H, I, K, L, W-135, X, Y, Z and 29E – were duly classified based on structural variations in capsular polysaccharides (Spinosa *et al.*, 2007). Variations in class II/III (e.g. PorB porin) and class I (e.g. PorA porin) outer membrane proteins determine serotype and serosubtype respectively, while differences in LOS further determines immunotype (Stephens *et al.*, 2007). Together these typical Gram-negative bacteria features contribute towards meningococcal virulence and immunogenicity (Rouphael and Stephens, 2012). Helping *N. meningitidis* adapt and attach to its host are also expression of surface adhesive proteins, mimicry of host antigens as well as high frequency of recombination events, which confers evolutionary advantages through genome plasticity and phenotype diversity (Stephens, 2009). Independent of serogroups, multilocus sequence typing (MLST) has helped identify hypervirulent strains that are highly associated with disease relative to carriage with the use of polymorphisms in 7 "housekeeping" genes (Maiden *et al.*, 1998). This proved to be a vital tool in molecular epidemiology, disease surveillance and prompt investigation of meningococcal outbreaks (Vogel, 2010).

1.3 Carriage, pathogenicity and disease burden of *Neisseria meningitidis*

1.3.1 Aetiology and Epidemiology

About 10% of any non-outbreak population would harbour *N. meningitidis* asymptomatically (Caugant *et al.*, 1994). Disease caused by *N. meningitidis*, on the other hand, primarily affects infants around 1 year of age, adolescents and young adults. Of the 13 *N. meningitidis* serogroups only 6 (A, B, C, W-135, X and Y) are pathogenic in humans, where 5 (A, B, C, W-135 and Y) of them are responsible for most disease outbreaks worldwide. Each of these serogroups distributes differently across the globe (Figure 1.1), where epidemics are usually caused by strains belonging to hypervirulent lineages (Harrison *et al.*, 2009). In Europe, serogroup B strains account for the majority of cases followed by serogroup C (ECDC, 2016). In the US, serogroups B, C and Y are

predominant amid a historic low rate of disease (<1 per 100,000 population) with around 10% case fatality (Cohn *et al.*, 2010). These figures are understandably higher in less-developed endemic regions such as Africa, reaching up to 1000 cases per 100,000 population with an over-representation of serogroup A in terms of prevalence (Gabutti *et al.*, 2015).

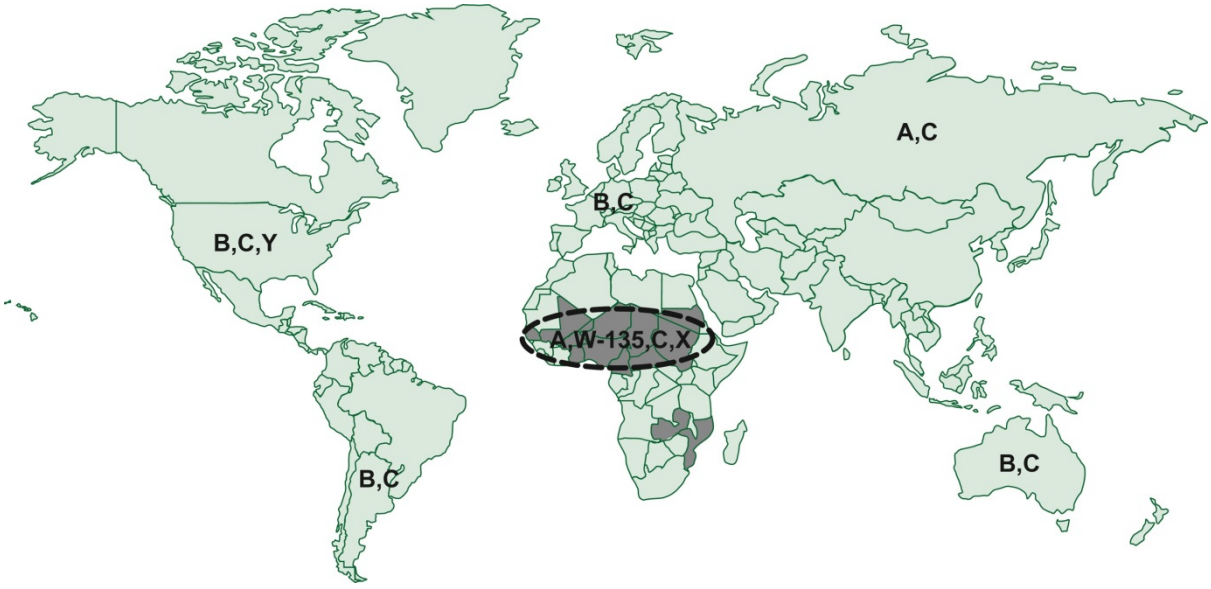

Fig. 1.1 – Worldwide distribution of *N. meningitidis* pathogenic serogroups: A, B, C, X, Y and W-135, with the sub-Saharan "African Meningitis Belt" circled in dashed lines and other endemic regions coloured in grey (from Pelton, 2016).

Circulating strains of *N. meningitidis* can be transiently contracted between humans through aerosolised respiratory droplets or salivary secretions, which results in either 10 – 20% asymptomatic carriage among populations, or invasive disease following an incubation period of 2 – 10 days (WHO, 2015). Apart from residing at or travelling to endemic countries, risk of contact with the bacteria is especially high in enclosed communities such as tertiary educational or military accommodations where adolescents or young adults are in frequent exposure (CDC, 2000). Smoking is also a risk factor as it is believed that damage to the respiratory tract mucosa increases the chances of successful invasion by the meningococci, where there is a positive correlation between disease incidence and smoker prevalence (Norheim *et al.*, 2014). It was also reported that immunocompromised individuals, such as patients with HIV/AIDS, oncological or haematological lesions, those with immature immune systems and those who are on chemotherapy, post-operational or post-transplant prophylaxis, may also be at risk of being infected by *N. meningitidis* (Vogel *et al.*, 2004).

1.3.2 Pathogenesis

Despite the knowledge of a reservoir within the human population, the precise mechanism and stimulus for meningococcal pathogenesis remain unclear. Some suggested that invasive strains are perhaps not a result of within-host evolution where virulence equates bacterial fitness in face of selective pressure, but are simply neutral accumulation of genomic mutations during asymptomatic carriage (Klughammer *et al.*, 2017). More refined upper respiratory tract models for *Neisseria* are required in order to better understand the interactions and dynamics between human hosts and their resident *Nesseria* species (Weyand, 2017). Nonetheless, the multistep invasion process is a demonstration of the remarkable versatility of *N. meningitidis*, where variability in meningococcal capsule expression, in concert with type IV pili-mediated interactions with host cell, are summarily responsible for bacterial survival in at least three diverse bodily compartments (i.e. URT mucosa, blood, CSF) and its ability to breach the barriers in-between (Coureuil *et al.*, 2012). As differences between host compartments amount to distinct ecological niches, a multitude of host-pathogen interactions such as complement-binding via CD46 and CD147, as well as the activation of pro-inflammatory cytokines and chemokines such as tumour necrosis factor α (TNF-α) in the brain, all contribute towards meningococcal survival and translocation (Doran *et al.*, 2016). In particular, the recruitment of factor H (fH), a key regulator of the Alternative Pathway of the complement system, is a hallmark interaction and a major source of host immune evasion in *N. meningitidis* (Schneider *et al.*, 2009). Other factors such as recruitment of negative complement regulators such as complement 4-binding protein (C4BP), the meningococcal polysaccharide capsule and LPS are also necessary to prevent complement-mediated lysis (Schneider *et al.*, 2007). Apart from binding to surface-exposed adhesins (Schubert-Unkmeir, 2017) or eliciting cell signalling to promote internalisation into host cells (Slanina *et al.*, 2014), many genes involved in normal aspects of meningococcal lifestyle (Nassif *et al.*, 1999) are also found to be upregulated for the colonisation of various host sites (Capel *et al.*, 2016).

A major virulence factor, capsule expression influences immunogenicity to the benefit of the meningococci. Clinical strains were found encapsulated while isolates from carriers often lacked capsular antigens, which were believed to confer selective advantages by evading bactericidal phagocytosis or complement-mediated killing (Yazdankhah and Caugant, 2004). The other major virulence factor – type IV pili – enable the normally URT mucosa-bound meningococci to penetrate epithelial cells and enter the bloodstream (See Section 1.2).

1.3.3 Meningococcaemia

Once inside the bloodstream, the pathogen can induce meningococcaemia (meningococcal sepsis) which have severe medical consequences such as acute fever, rashes, disseminated intravascular coagulation (DIC) and eventually death by multiple organ failure as the host complement responses are activated for a systemic inflammation (Takada *et al.*, 2016). Meningococcal septic shock is therefore far more fatal than the exacerbation (meningococcal meningitis) that potentially follows (de Greeff *et al.*, 2008; Brandtzaeg and van Deuren, 2012). Other complications include haemorrhages, tissue necrosis and limb loss, all of which affect recovery (van Deuren *et al.*, 2000). Typical of *Neisseria* spp., however, important components such as porins (PorA and PorB), adhesins, opacity-associated proteins (Opa and Opc), iron metabolism surface proteins, pili (fimbriae) expression and LOS all contribute towards *N. meningitidis* colonisation, nutrient acquisition, establishment in host, evasion of host immune response, cellular invasion and pathogenesis as well as virulence (Coureuil *et al.*, 2012). This paints a complex picture for the meningococci throughout its transition from symbiotic colonisation to parasitic multiplication in the human host.

1.3.4 Meningitis

The blood-brain barrier (BBB) and blood-cerebrospinal fluid barrier (BCSFB) – located at cerebral microvessels and choroid plexus respectively – protect the human central nervous system (CNS) by closely regulating the exchange of solutes and macromolecules by restricting physical permeability of the adherens and tight junctions (Dando *et al.*, 2014). If high level of bacteraemia occurs and is left unchecked, the meningococci can disrupt and cross the BBB within hours of disease onset, triggering a massive inflammatory response towards bacterial proliferation in the CNS (Coureuil *et al.*, 2013). This is achieved by the meningococci type IV pili signalling the recruitment of cortical plaque-forming molecules following initial attachment, which accumulate at cell-cell junctions where microcolonies eventually detach and breach through to the CNS (Miller *et al.*, 2013). As aforementioned, encapsulation enables the meningococci to translocate into CNS by also adhering to the BCSFB-forming human brain microvascular endothelial cells, as well as surviving and replicating in intracellular compartments (Nikulin *et al.*, 2006). The end result is a potentially fatal medical emergency known as meningococcal meningitis, an inflammation of the meninges and CSF-filled subarachnoid space, with clinical manifestations of meningitis ranging from headache, fever and neck stiffness all the way to compromised mental status, impaired consciousness, aphasia, palsies and seizures (van de Beek *et al.*, 2016).

Meningococcal meningitis is a serious condition where fatalities are mostly due to intracranial pressure build-up and herniation, while 8-20% of recovered victims are often scarred with various degrees of highly debilitating audial or neurological sequelae (van Deuren *et al.*, 2000). The morbidity and mortality cause considerable disease burden even in high-income countries, characterised by the financial strain to public health resources associated with follow-up care, outbreak management, lifelong disabilities, the need for rehabilitation as well as societal consequences (Martinón-Torres, 2016).

1.3.5 Treatment and Resistance

Fortunately, prompt treatment by broad-spectrum antibiotics such as ß-lactams is able to drastically reduce mortality in most cases of *N. meningitidis* infection (Dwilow and Fanella, 2015). The challenge lies in the timely identification of any suspected meningococcal infection and applying treatment before waiting for laboratory-confirmed diagnosis, as the disease is fulminant in nature and early clinical presentations were often mistook for their similarities with less severe but more common febrile illnesses (CDC, 2014). Reduced susceptibility to penicillins and third-generation cephalosporins had emerged and was made possible by innate gene exchange mechanisms in the meningococci (Arreaza *et al.*, 2002; Deghmane *et al.*, 2017). Examples are efflux pumps or LOS modification which defend the meningococci against innate killing as well as cationic peptides such as polymixin B (Tzeng *et al.*, 2005; Tzeng and Stephens, 2015). With regards to disease management, resistance is not the major clinical concern as *N. meningitidis* remains susceptible to a wide range of antibiotics (Jorgensen *et al.*, 2005).

1.4 Vaccines for *Neisseria meningitidis*

1.4.1 Vaccines against serogroups A, C, W-135 and Y

As aforementioned, the 6 major disease-causing *N. meningitidis* serogroups (A, B, C, W-135, X and Y) were classified based on their phase and antigenic variations of capsular polysaccharides (Talà *et al.*, 2014). Quadrivalent conjugate polysaccharide vaccines protecting against A, C, Y and W-135 (Menveo® by Novartis; Menomune® and Menactra®, both by Sanofi Pasteur) have long been incorporated as part of routine vaccination programmes in many developed countries (Figure 1.2 (a)). Conjugate vaccines targeting meningococcal serogroup C were also introduced in developed countries which successfully saw decline in incidence through herd immunity effected by reduction in carriage (Figure 1.2 (b)) (Trotter and Maiden, 2009). In addition, MenAfriVac^{TM}, the result of an international charitable effort to deliver affordable vaccines targeting *N. meningitidis* serogroup A to the "African Meningitis Belt" in sub-Saharan Africa, has led to sharp

decreases in incidence, herd immunity as well as eradication of carriage from populations following vaccination (Kristiansen *et al.*, 2013).

Fig. 1.2 (a) – **Meningococcal polysaccharide vaccines**, covering 4 major epidemic serogroups.

Fig. 1.2 (b) – Depending on regional epidemiological patterns and needs, immunisation programmes for children with serogroup C conjugate vaccines may also be found in certain countries Note that Menitorix® is a combined vaccine for *Haemophilus influenzae* type C and *N. meningitidis* serogroup C.

1.4.2 Vaccines against serogroup B: recent advancements and reverse vaccinology

Effective universal vaccines against serogroup B strains, however, had only been approved and licensed for use by regulating authorities in recent years. The peculiar lack of vaccine coverage for serogroup B led it to being responsible for 90% of meningococcal diseases in the UK (Shea, 2013). The major challenge in developing a sufficiently immunogenic vaccine for serogroup B was due to high similarities between its capsular polysaccharides and human sialic acid moieties. The incorporation of polysialic acids in bacterial surface glycans such as the capsule or lipopolysaccharide (LPS, which is LOS in *N. meningitidis*) is a recognised mechanism of host response evasion, but the serogroup B capsule consists of polymers of α(2-8)-linked N-acetylneuraminic acid which share structural identities with human neural cell-adhesion molecule (NCAM) (Hill *et al.*, 2010). Albeit displaying opsonic activity, the result is a reluctance by the host to develop anti-meningococcal SBA in order to prevent autoimmune responses against delicate brain tissue (Christodoulides and Heckels, 2017). This prompted a need for investigating vaccine candidates using sub-capsular antigens and minor proteins which were preferably invariably expressed, accessible, effectively immunogenic and cover all disease-associated strains of meningococci (including hyperinvasive lineages) (Caugant and Maiden, 2009).

The availability of the serogroup B strain MC58 complete genome sequence contributed greatly to this cause by allowing for the comprehensive blind screening of genome-derived surface antigens for potential vaccine candidates (Delany *et al.*, 2013). Termed “reverse vaccinology”, this process was first applied in the development of *N. meningitidis* serogroup B universal vaccines, where the genome was first screened *in silico* for novel

antigens prior to confirming potentially immunogenic candidates with *in vitro* means (Kelly and Rappuoli, 2005; Pizza *et al.*, 2000). In fact, the discovery and subsequent thorough characterisation of factor H-binding protein (fHBP) was a direct beneficiary of this methodology, while also revealing fresh aspects of meningococcal pathogenicity (McNeil *et al.*, 2013). It must be noted that although outer membrane vesicle (OMV)-based vaccines specific against particular epidemic *N. meningitidis* serogroup B strains had been devised during the past decades, the immunogenicity was not broad enough to cover circulating strains where high antigenic variations were often expressed (Acevedo *et al.*, 2014). The lessons learned from OMV vaccine trials and reverse vaccinology resulted in the successful introduction of two serogroup B meningococcal vaccines, rLP2086 (Trumenba® by Pfizer) and 4CMenB (Bexsero® by Novartis but acquired by GSK) within two decades of sequencing the whole genome (Figure 1.2 (c)) (Gandhi *et al.*, 2016; Seib *et al.*, 2015).

Fig. 1.2 (c) – The two commercially-available universal *N. meningitidis* serogroup B vaccines: the fHBP-based Trumenba® marketed by Pfizer and quadrivalent (containing the antigens fHBP, NadA, Neisserial Heparin Binding Antigen plus OMV) Bexsero® developed by Novartis but acquired by GSK.

The first to receive US FDA approval was Trumenba® (Pfizer), a suspension carrying two recombinant lipidated fHBP variants (Brendish and Read, 2015). The second, more expensive one was Bexsero® (originally Novartis, now GSK), a suspension of OMV carrying 4 antigens (Gorringe and Pajón, 2012). The latter had long been approved for use in the EU, Australia and Canada, but only received approval in the UK in late 2013 and in the US in early 2015. In March 2015, the UK commenced its national infant vaccination programme against *N. meningitidis* serogroup B with Bexsero®, which had since "halved" the number of reported cases after the first 10 months (Public Health England, 2016). Following settlement of patent disputes between the two pharmaceutical giants, Trumenba® also received approval for use in the EU in 2017. Aside from infants, both serogroup B vaccines are also recommended by the US FDA for use on adolescents and young adults (high risk populations aged 10 – 25) (Sunasara *et al.*, 2017).

Reverse vaccinology is an invaluable technological advancement and a huge accomplishment for translational research in the combat against vaccine-preventable diseases with such remarkable clinical implications (Rappuoli *et al.*, 2011). With the advent of serogroup B vaccines completing coverage for 5 major pathogenic serogroups,

there is now a rise in previously sporadic cases of invasive meningococcal meningitis caused by serogroup X in endemic African regions where vaccines are needed (Xie *et al.*, 2013). Lessons learned from the development of serogroup B vaccines, however, were revealed to have promising contributions towards the development of potential serogroup X vaccines (Acevedo *et al.*, 2017). Challenges remain to ensure continued success of disease prevention, such as emerging virulent strains not covered by vaccines and the need for multiple doses of delivery (Watson and Turner, 2016; Wang and Pollard, 2017).

1.5 Genomic profile of *Neisseria meningitidis* compared to other bacteria

1.5.1 The value of genomic data

The successful development of serogroup B (*Nm*B) vaccines was largely facilitated by the availability of complete genome of strain MC58 around the start of the millennium (Tettelin *et al.*, 2000). Since then there has been an exponential rise in assembled whole genome sequence data deposited at online databases, which serve as powerful analytic tools for devising improved surveillance, diagnostics and vaccine strategies (Harrison *et al.*, 2017). The protein-coding genomic data allowed for a computational approach which underlies reverse vaccinology in the effort to identify putative vaccine-suitable antigen candidates (Heinson *et al.*, 2015). Regardless of the now-improved coverage of vaccines, the MC58 genome remains an invaluable asset upon which the continuous research effort and further understanding of *N. meningitidis* may be based. As strictly human pathogens both *Neisseria* species pose challenges for the adoption of suitable animal and even primate models (Weyand *et al.*, 2013). Questions as to how the meningococci maintain this unique niche or becomes invasive, for example, as well as foundation work for the understanding of other competing organisms, remain topics of great interest.

1.5.2 Genomic features of *N. meningitidis*

Like *N. gonorrhoeae*, *N. meningitidis* is also naturally competent and, obeying certain constraints, maintains a highly flexible chromosome that is capable of acquiring foreign genetic materials, incorporating such elements into its genome or even conduct intragenic recombination (Schoen *et al.*, 2009). Therefore, the mosaic genomic structure was often speculated to be virulence-associated in its own right, through which pathogenic Neisseriae as well as clinical isolates from other bacteria survive the human immune response (Hughes, 2000). The polygenic nature of meningococcal virulence can be reflected by the multi-faceted recombination strategies that occur in its core genome, where a substantial portion of recombinant genes are often first associated with disease but also turn out to be supportive of bacterial fitness upon closer examination (Joseph *et al.*, 2011).

Small clusters of sequences, believed to evolutionary foreign DNA acquired with integrase and transposase, were first identified exclusively in pathogenic gonococci and meningococci genomes but not in the commensal *N. lactamica* (Perrin *et al.*, 1999). Traits such as G+C content different to the genome and tendencies towards chromosomal integration are all reminiscent of pathogenicity-associated genetic islands first described in *E. coli*, (Hacker *et al.*, 1997). However, those classical islands are often much larger in size (up to 200 kbp) and encode more purposeful, disease-empowering virulence genes such as invasins and toxins (Hacker and Kaper, 2000).

1.5.3 Meningococcal Genomic Islands conserved in pathogenic Neisseriae

A pan-*Neisseria* microarray containing the complete sequences of *N. meningitidis* strains Z2491 (serogroup A), MC58 (serogroup B), FAM18 (serogroup C) and *N. gonorrhoeae* strain FA1090 was constructed and used to analyse both pathogenic and commensal Neisseriae genomes, which revealed genes specific to the disease-causing meningococci and gonococci (Stabler *et al.*, 2005). In an effort to reveal more consistent differences between members of the genus, further sequence analyses eventually led to the identification of 9 small islands in the pathogenic meningococcal genome (Figure 1.3) (Catenazzi, 2013).

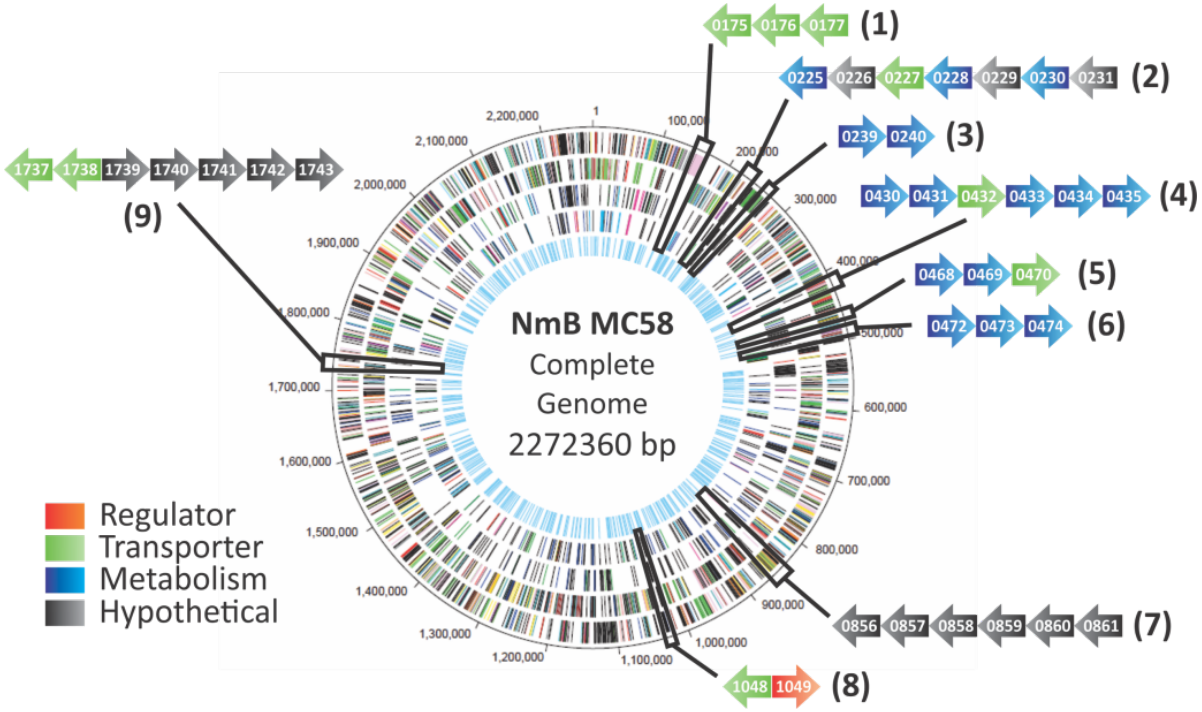

Fig. 1.3 – Complete genome of *N. meningitidis* serogroup B (NmB) strain MC58 and its **9 pathogen-conserved genomic islands**. The designations for coding sequences were adapted from their respective microarray reporter elements, and are to be regarded as gene numberings when referred to henceforth. Brackets denote genomic island numbers. Colours denote the respective annotated functions based on the broad gene ontology of each product. Positions are approximate and not drawn to scale. (Adapted from Catenazzi, 2013)

These clusters of sequences often hold roles in metabolism and transport, but are thought to be disease or pathogenicity-associated as they are found highly conserved in pathogenic *N. meningitidis* strains, mostly conserved in *N. gonorrhoeae,* but absent in commensal *N. lactamica* strains (Perrin *et al.*, 2002). In the 2.27 Mbp circular NmB genome, the largest of these islands is no longer than 10 kbp in size. Several larger regions of genomic sequences with foreign nucleotide signatures – known as "islands of horizontal transfer" (IHT) – were previously identified, but are neither well-conserved amongst pathogenic species nor across the genus and hence should not be confused with those discussed here (Snyder *et al.*, 2005).

Many of these *Neisseria* island genes are still uncharacterised and encode unknown proteins. Preliminary bioinformatics background was obtained using tools such as BLAST and StringDB queries to compare the potential products annotated to be expressed by these *N. meningitidis* sequences (using strain MC58, NCBI GenBank™ accession no.: AE002098.2; genes denoted with prefix "NMB"), their flanking genes (where present) and putative functional homologues in *N. gonorrhoeae* (using strain FA1090, NCBI GenBank™ accession no.: AE004969.1; genes denoted with prefix "NGO") and *N.*

lactamica (using strain 020-06, NCBI GenBank™ accession no.: FN995097.1; genes denoted with prefix "NLA_"). Many homologous flanking genes were often found closely adjacent to each other in commensal Neisseriae (Figures 1.4-1 to -9). Acquisition of these genomic islands was thought to be via horizontal gene transfer, a popular mode of diversification employed among *Neisseria* species (Hotopp *et al.*, 2006).

Genomic Island 1 comprises of three genes and is possibly involved in the oxidation of D-amino acids due to the annotated D-amino acid dehydrogenase (DadA) functionality. It has been shown that the DadA operon, of which a putative subunit is located on Genomic Island 1 in *N. meningitidis* as NMB0176 (Figure 1.4-1), is required in some pathogens such as cystic fibrosis-adapted *Pseudomonas aeruginosa* isolates for the expression of virulence factors (Oliver and Silo-Suh, 2013). Mutants with genetic lesions leading to inability to catabolise D-amino acids show decreased competitiveness in *in vivo* infection models (Boulette *et al.*, 2009). This is believed to confer advantages to bacteria when colonising a wide range of environments, including their respective hosts, by being able to utilise as many forms of nutrient as possible for growth.

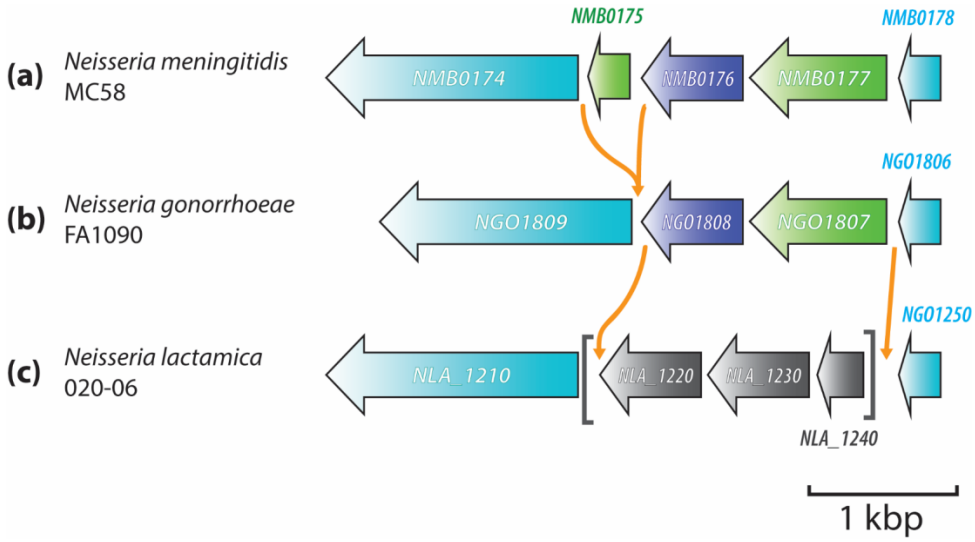

Fig. 1.4-1 – Meningococcal Genomic Island 1. **(a)** Bioinformatics queries annotate: NMB0175 as a zinc transporter (ZupT) homologue; NMB0176 as containing a small D-amino acid dehydrogenase (DadA) subunit, and; NMB0177 as a sodium/alanine symporter homologue, also indicated to be encoded by *NMB0194* and *NMB1647*. **(b)** *N. gonorrhoeae* lacks the NMB0175 homologue but conserves the rest, while **(c)** all three island genes were replaced with three hypothetical proteins in *N. lactamica* not found in the two pathogenic Neisseriae genomes. (Adapted from Catenazzi, 2013)

Genomic Island 2 comprises of 7 genes and, due to the predicted presence of an allophanate hydrolase domain, may possibly be involved in urea and amino acid metabolism. Many bacteria can utilise urea as a nitrogen source. One such mechanism is through the enzyme urea amidolyase (UA), which contains two domains: urea carboxylase (UC) and allophanate hydrolase (AH), of which a putative sub-unit Ahs1 (allophanate hydrolase subunit 1) is located on Genomic Island 2 as NMB0230 (Figure 1.4-2) (Zhao *et al.*, 2018). The domains themselves are enzymatic, and AH works with UC to convert urea into ammonium and carbon dioxide (Fan *et al.*, 2013). The activities of the two are said to be functionally independent, and overall UA contributes to bacterial pathogenicity as it facilitates survival in host immune cells (Lin *et al.*, 2016).

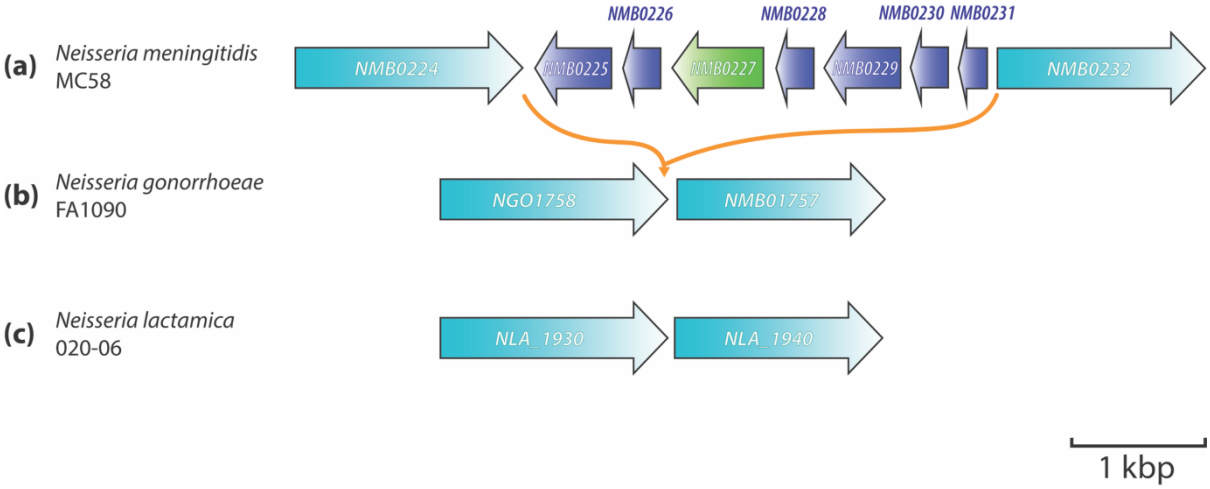

Fig. 1.4-2 – Meningococcal Genomic Island 2. **(a)** Bioinformatics queries annotate: NMB0225 as a member of the IS30 transpose family, also indicated to be encoded by 13 other sequences in NmB; NMB0226 as a hypothetical protein, also indicated to be encoded by *NMB2035*; NMB0227 as a putative transmembrane protein; NMB0228 as a rni3 homologue, a member of the LamB/YcsF family; NMB0229 as a hypothetical protein; NMB0230 as a putative Ahs1 (allophanate hydrolase subunit 1) homologue, and; NMB0231 as a hypothetical protein. This island is completely absent in both **(b)** gonococci and **(c)** *N. lactamica*. (Adapted from Catenazzi, 2013)

Genomic Island 3 comprises of two genes and is possibly involved in the production of the polyamines spermine and spermidine (Figure 1.4-3). This island will be investigated within the thesis and is discussed in detail in Chapter 4.

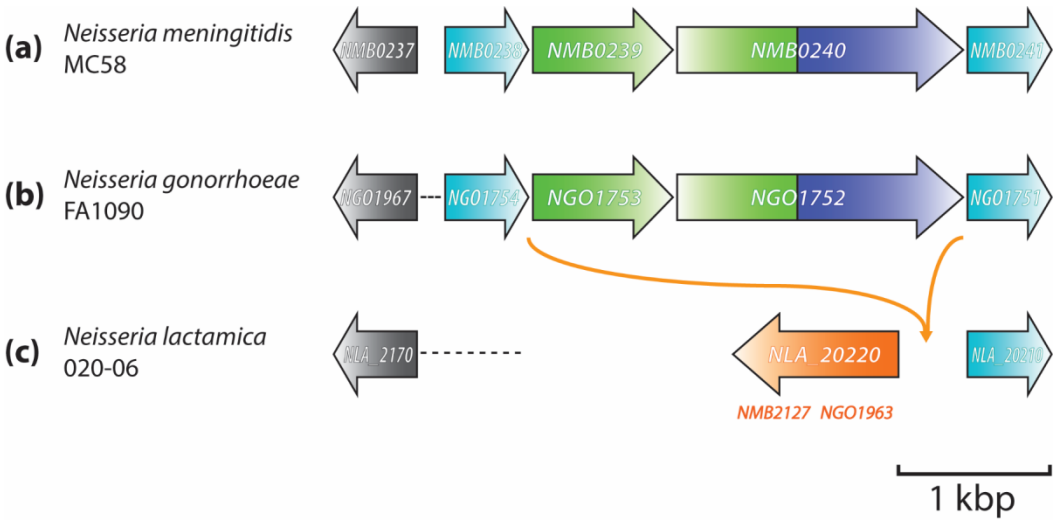

Fig. 1.4-3 – Meningococcal Genomic Island 3. **(a)** Bioinformatics queries annotate: NMB0239 as a putative transmembrane protein with structural motifs reminiscent of major facilitator superfamily 1 (MFS-1), and; NMB0240 as a putative transmembrane protein with a possible spermine/spermidine synthase domain. This island is also **(b)** conserved in gonococci, but **(c)** completely absent in *N. lactamica*. The flanking gene homologous to *NMB0237* was rearranged elsewhere in the gonococcal genome, while the *NMB0238* homologue is not found in *N. lactamica*. (Adapted from Catenazzi, 2013)

Genomic Island 4 comprises of 6 genes and, with a size of 9329 bp, is the largest of the 9 genomic islands (Figure 1.4-4). This island has been has been the subject of study by Catenazzi *et al.* (2014), where characterisation work shows that this *prp* gene cluster enables the meningococci to utilise propionic acid – an end-product of fermentation by neighbouring anaerobes in its niche – as a carbon source, which enhances colonisation capacity but is not central to virulence.

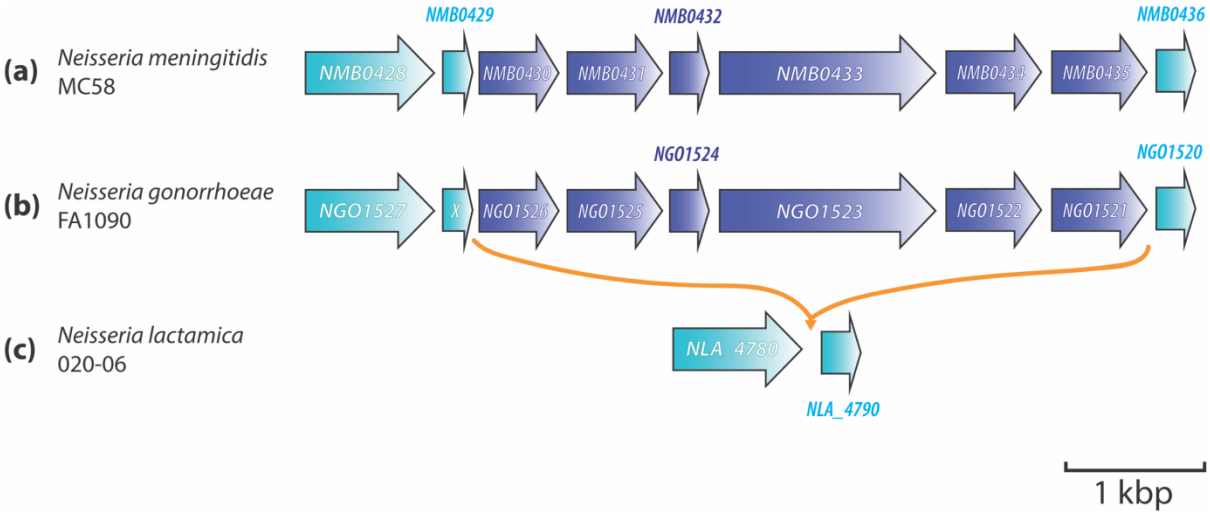

Fig. 1.4-4 – Meningococcal Genomic Island 4. **(a)** Previous work describes or annotates: NMB0430 as a 2-methyl-isocitrate lyase (PrpB) homologue; NMB0431 as a 2-methylcitrate synthase (PrpC) homologue; NMB0432 as a hypothetical transmembrane protein; NMB0433 as a aconitate hydrolase (AcnD) homologue; NMB0434 as a 2-methylcitrate dehydratase (PrpF) homologue, and; NMB0435 as a putative propionate (acetate) kinase (AckA1) homologue. This island is also **(b)** conserved in gonococci but **(c)** completely absent in *N. lactamica*. (Adapted from Catenazzi, 2013)

Genomic Island 5 is possibly involved in the synthesis of the polyamine putrescine due to the predicted presence of a direct pathway comprised of arginine decarboxylase and agmatinase (Figure 1.4-5). This island will be investigated within this thesis and is discussed in detail in Chapter 3.

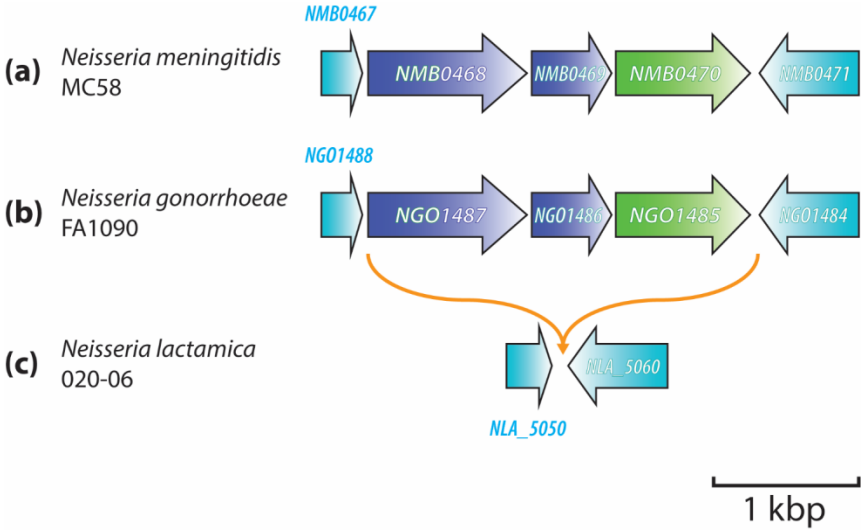

Fig. 1.4-5 – Meningococcal Genomic Island 5. **(a)** Bioinformatics queries annotate: NMB0468 as an arginine decarboxylase (SpeA) homologue; NMB0469 as an agmatinase (SpeB) homologue, and; NMB0470 as a putative transmembrane protein with structural motifs reminiscent of C_4-dicarboxylate transporters. This island is also **(b)** conserved in gonococci but **(c)** completely absent in *N. lactamica*. (Adapted from Catenazzi, 2013)

Genomic Island 6 comprises of three genes and is possibly involved in the production of biotin. Biotin, also known as vitamin H or coenzyme R, is central to the metabolism of many organisms. In bacteria, many species either synthesise biotin *de novo* or encode transporters to acquire them from exogenous sources. In *E. coli* and a number of other bacteria, the bacterial biotin synthesis pathway have been extensively characterised, such as the *bioABCDF* operon (where *bioA* transcribes divergently from the others) and the *bioH* gene (Streit and Entcheva, 2003). Here in *N. meningitidis*, the products of some of these genes, BioF and BioC, are annotated to be located on Genomic Island 6 as NMB0472 and NMB0474 respectively (Figure 1.4-6). In *E. coli* and *S. aureus* the transporter BirA is both responsible for biotin uptake and transcriptional repressor of biotin synthesis genes, where switching between the two roles is thought to be important for bacterial maintenance and virulence (Satiaputra *et al.*, 2016). In the human pathogen *Mycobacterium tuberculosis*, *de novo* biotin synthesis is thought to be vital to both lifestyle and virulence as the pathway is its sole mode of biotin acquisition and close link with the production of key lipid components of the cell membrane (Salaemae *et al.*, 2016).

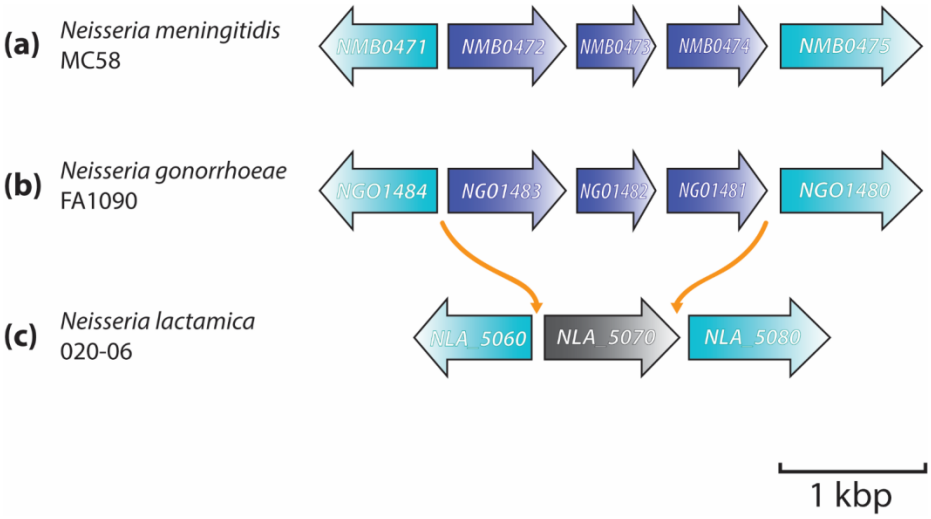

Fig. 1.4-6 – Meningococcal Genomic Island 6. **(a)** Bioinformatics queries annotate: NMB0472 as a 8-amino-7-oxononanoate synthase (BioF); NMB0473 as a hypothetical protein, and; NMB0474 as a putative biotin synthesis protein (BioC) homologue. This island is also **(b)** conserved in gonococci but **(c)** completely absent in *N. lactamica*. In its place is a 1359 bp gene *NLA_5070* which was predicted to encode a tRNA methyltransferase (RlmD), but has no genetic homology to pathogenic Neisseriae apart from a small 95 bp fragment also present in the gap region between *NMB0471* and *NMB0472*. (Adapted from Catenazzi, 2013)

Genomic Island 7 comprises of 6 genes coding for hypothetical proteins, all of which are currently completely uncharacterised and lacking any investigation in literature (Figure 1.4-7).

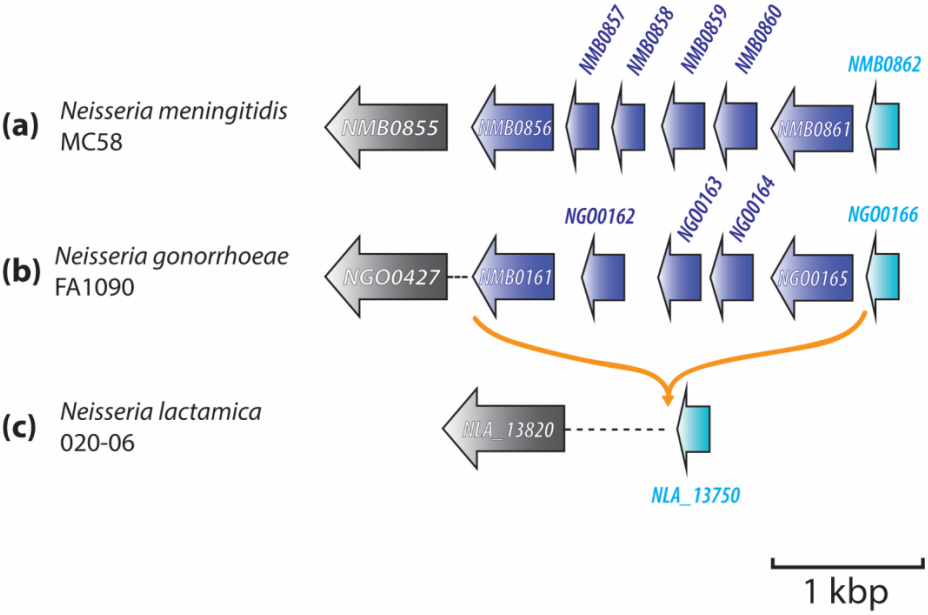

Fig. 1.4-7 – Meningococcal Genomic Island 7. **(a)** Bioinformatics queries return no specific hits for NMB0856 through to NMB0861. The island is also **(b)** conserved in gonococci but **(c)** completely absent in *N. lactamica*. The flanking genes homologous to *NMB0855* were rearranged elsewhere in the gonococcal (*NGO0427*) and commensal (*NLA_13820*) genomes. (Adapted from Catenazzi, 2013)

Genomic Island 8 comprises of two divergently-transcribed uncharacterised genes. Here, the Island gene product NMB1048 is annotated to be involved in sodium pyruvate uptake, under the regulation of an adjacent Island gene product NMB1049, a putative LysR-type regulator (as mentioned in Section 1.2) (Figure 1.4-8). As is the case for many other bacteria, *N. meningitidis* can utilise pyruvate as a carbon source along with glucose under the scrutiny of transcriptional regulators.

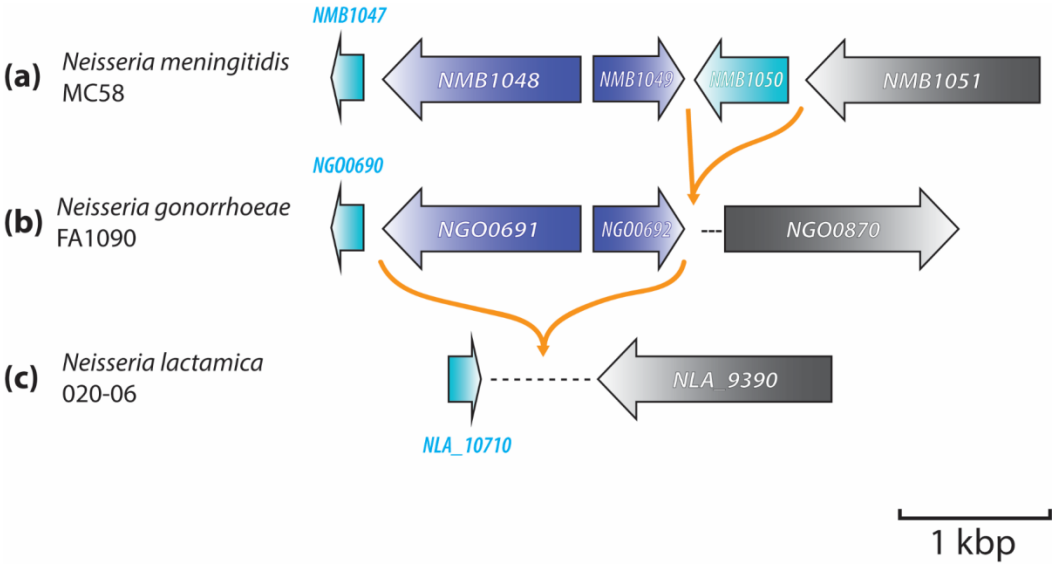

Fig. 1.4-8 – Meningococcal Genomic Island 8. **(a)** Previous work describes and annotates: NMB1048 as a transmembrane protein with unconfirmed involvement in sodium pyruvate transport, and; NMB1049 as containing a domain for LysR-type transcriptional regulator (LTTR) proteins, which regulates expression of *NMB0148*. This island is also **(b)** conserved in gonococci with the exception of the flanking NMB1050 homologue, but **(c)** completely absent in *N. lactamica*. (Adapted from Catenazzi, 2013)

Genomic Island 9 largely comprises of hypothetical and uncharacterised proteins which are incompletely conserved in the pathogenic *N. gonorrhoeae* genome, while both flanks and genes are completely absent from the commensal *N. lactamica*. Some of these genes are loosely annotated to share some motif similarities with the domains of OMP and HlyD secretion proteins, located on Genomic Island 9 as NMB1737 and NMB1738 respectively (Figure 1.4-9). These are common features in Gram negative bacteria and are often linked with drug efflux, hence thought to contribute to virulence through antibiotic resistance.

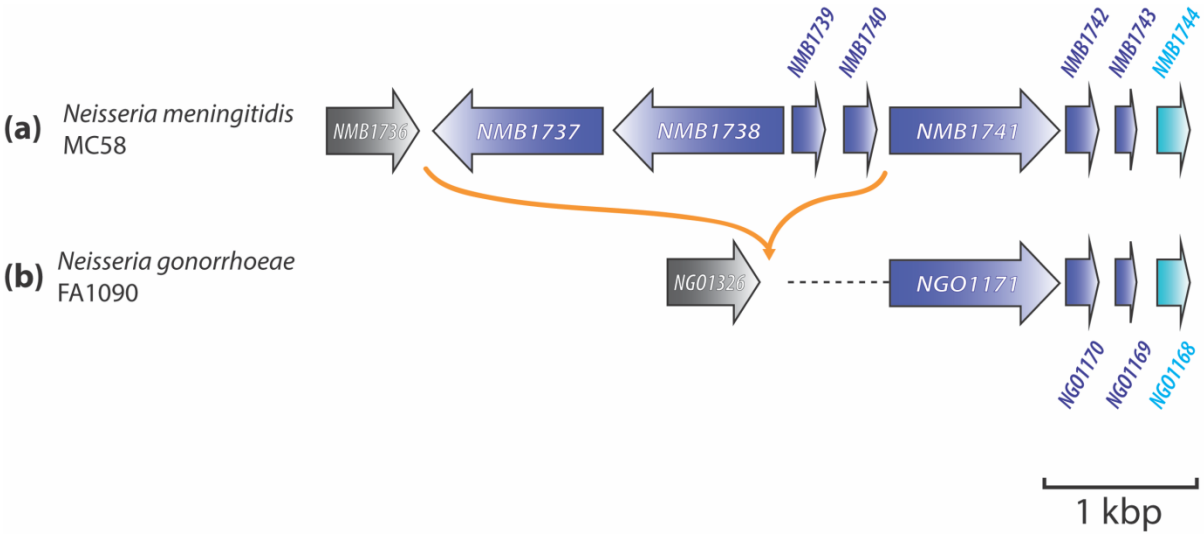

Fig. 1.4-9 – Meningococcal Genomic Island 9. **(a)** Bioinformatics queries annotate: NMB1737 as a putative secretion protein with domain motifs reminiscent of the outer membrane efflux protein (OMP) family; NMB01738 as a putative secretion protein with domain motifs reminiscent of the HlyD family, and; NMB1739 through to NMB1743 as hypothetical proteins. **(b)** Only the last three genes are conserved in gonococci. (Adapted from Catenazzi, 2013)

1.6 Metabolism and stress response in pathogenic *Neisseria*

The overall predicted nature of the above genomic islands re-iterates the importance of metabolism and stress response in able human pathogens such as *N. meningitidis* and its cousin *N. gonorrhoeae.* The fates of metals, carbon sources, stress response regulons and enzymes are often intertwined with one another, contributing to fitness, survival and ultimately enhanced general performance during disease.

1.6.1 Nutrient acquisition

As previously mentioned (Section 1.2), *N. meningitidis* possesses uptake systems for the acquisition of metals such as iron from metalloproteins such as lactoferrin, transferrin and haemoglobin, as well as zinc from calprotectin. Understandably host defences against pathogenic bacteria include restricting them from direct access to metals. This sequestration of nutrients is sometimes referred to as "nutritional immunity", and corresponding bacterial counteraction is therefore vital to survival and pathogenicity (Stork *et al.*, 2013). To this end, both *N. gonorrhoeae* and *N. meningitidis* have devised ingenious mechanisms that hijack bound metal ions from host metalloproteins, thus overcoming host denial of these essential transition metals (McKenna *et al.*, 1988; Neumann *et al.*, 2017). Equally important to bacterial success is the maintenance of equilibrium through metal metabolism, tolerance and even exporters due to the toxic nature of transition metals including manganese (Veyrier *et al.*, 2011; Guilhen *et al.*, 2013).

N. meningitidis is able to utilise glucose, maltose, pyruvate, lactate or certain amino acids as sole carbon sources in growth, which all have varying levels of availability as the bacteria physically traverse from the nasopharynx (e.g. saliva, mucosa and other co-occupying flora), blood to CSF microenvironments (Schoen *et al.*, 2014). Although the meningococci possess pathways necessary for the complete catabolism of glucose and biosynthesis of pyruvate (Baart *et al.*, 2007), preferential acquisition of carbon sources can depend on circumstances such as competition, stress, metabolic or disease progress. For example, lactate can be catabolised at a faster rate than simultaneously available glucose, while its use also contributes to LPS sialylation and hence resistance to complement-mediated killing by host immune responses (Exley *et al.*, 2005a; Smith *et al.*, 2007). Transport of glucose and maltose in *N. meningitidis* are carried out by ion-driven symporters GlcP and MalY (Derkaoui *et al.*, 2016), while transport of lactate is carried out by a lactate permease (LctP) homologue NMB0543 (Exley *et al.*, 2005b). Amino acids such as glutamate can also serve as carbon sources, acquired by two transporter systems in *N. meningitidis*: the ABC-family transporter GltT-GltM and sodium-dependent transporter GltS (Takahashi *et al.*, 2015), but can also utilise its NADP-specific glutamate

dehydrogenase GdhA to synthesise glutamate (Pagliarulo *et al.*, 2004). Interestingly, influx of glutamate via these transporters triggers internalisation of meningococci into host cells which also appears to be a crucial pathogenicity trait when surviving in human blood or CSF (Takahashi *et al.*, 2011). In turn, amino acids and – most importantly – ammonia serve as primary nitrogen sources for *N. meningitidis* (Jyssum, 1959). Other systems implicated in meningococcal nitrogen assimilation include the regulatory protein IIA^{Ntr} (Ren *et al.*, 2005).

Thus, the meningococcal citric acid cycle indeed serves as a highly versatile workhorse which contributes to adaptation towards a plethora of nutrients, fitness and ultimately virulence.

1.6.2 Stress response mechanisms

Both endogenous and exogenous sourced oxidative stress are encountered by *N. meningitidis*, mainly in the form of reactive oxygen species (ROS). Firstly, leakage of electrons from bacterial respiratory chain results in the natural accumulation of peroxides (H_2O_2) and superoxide (O_2^{-}), which can be managed by basal defences. Secondly, the major adversary to meningococcal establishment are patrolling host macrophages capable of generating peroxides as "oxidative bursts" (Duane *et al.*, 1993). This is achieved through the phagosomal NADPH oxidase (NOX) system (DeCoursey and Ligeti, 2005; Panday *et al.*, 2015). The third type consists of competing organisms such as *Streptococcus pneumoniae* which can also generate similar levels of bactericidal peroxides via pyruvate oxidase (SpxB), killing niche co-occupants (i.e. *Haemophilus influenzae*) and contributing to host cytotoxicity (Pericone *et al.*, 2000). Appreciably these challenges are further heightened during pathogenesis, and must therefore be dealt with through dedicated oxidative stress response mechanisms.

N. meningitidis employs a catalase (KatA) expression mechanism tightly regulated by OxyR (Ieva *et al.*, 2008). OxyR also regulates other enzymes such as the two-domain peroxiredoxin-glutaredoxin (Prx) and glutathione oxidoreductase (Gor) which belong to the same operon in *N. gonorrhoeae* (Seib *et al.*, 2007). Other antioxidant enzymes used by *N. meningitidis* include Bcp (of the alkylhydroperoxidase C family AhpC) (Poole, 2005) and GpxA (glutathione peroxidase) (Moore and Sparling, 1995; Moore and Sparling, 1996). Different catalases and peroxidases have varying affinity depending on substrate levels, which arguably confer flexibility enabling *N. meningitidis* to deal with both low and high concentrations of ROS effectively. Another popular method in pathogenic Neisseriae involves metalloenzyme superoxide dismutase (SOD), where *N. gonorrhoeae* sees a

predominantly manganese-cofactered SOD ([Mn]-SOD) system in action while *N. meningitidis* makes use of copper and zinc-cofactored SOD ([Cu,Zn]-SOD) (Dunn *et al.*, 2003; Seib *et al.*, 2004). These periplasmic SODs, together with their cytosolic counterparts, protect bacteria against exogenous and endogenous sources of superoxide damage respectively, which act as major virulence determinants and potentially worthy therapeutic targets (Pratt *et al.*, 2015).

Lastly, the most illustrious case linking metabolism and stress response rests with the partial denitrification pathway in *Neisseria*. In the absence of oxygen, both pathogenic Neisseriae can respire by converting nitrite (NO_2^-) to nitrous oxide (N_2O) via an intermediate nitric oxide (NO). NO is known as a reactive nitrogen species (RNS) and induces nitrosative stress to bacterial cells. Both Neisseriae possesses the copper-containing nitrite reductase (AniA) converting nitrite to NO, while the nitric oxide reductase (NorB) catalyses the detoxification of NO to nitrous oxide (Jen *et al.*, 2015). The anoxic urogenital tract occupied by *N. gonorrhoeae* and the aerobic nasopharynx occupied by *N. meningitidis* may have contributed to differences in regulation and expression of this system (Edwards *et al.*, 2012). In brief, this example describes a scenario where nutrient (metal) acquisition and utilisation, metabolism (respiratory adaptation) and stress response all come together to contribute to the lifestyle of *N. meningitidis*.

1.7 Aims of this work

Prior to invasive disease, exclusive human pathogens such as *N. meningitidis* capable of prolonged periods of asymptomatic carriage first need to demonstrate general fitness in the form of successful colony establishment, where a key combination of host immune evasion, defence against competition and acquisition of nutrients from an ever-changing environment indisputably account for much of that prowess. The 9 genomic islands highly conserved in pathogenic *Neisseria* represent an intriguing aspect of meningococcal research due to their general association with cellular functions that are seldom considered iconic virulence determinants.

The functional characterisation of Genomic Islands 3 and 5 is the focus of this study. The two are of particular interest as bioinformatics suggest a commonality between the two in the form of possible polyamine biosynthesis pathways originating from a mutual amino acid (i.e. arginine) and precursors. Positively-charged polyamines were often associated with protecting bacterial cells against oxidative stress experienced during exponential growth by aiding in the maintenance of normal homeostasis. Although meningococcal pathogenicity is multi-factorial, the fact that genes predicted to encode for such systems are highly conserved in pathogenic strains of *Neisseria* warrants further investigation in an

ongoing effort to determine if they contribute to fitness and to what extent promote disease.

This work aims to characterise the genomic islands by assessing the strength and legitimacy of the preliminary data, confirming their purported functions experimentally and to extrapolate their general significance to the human pathogen with current and potential new findings. It is hoped that new knowledge derived from this work will contribute to combating infectious meningococcal disease, as well as improving understanding of a highly-capable bacteria responsible for only human deaths.

Chapter 2 – Materials and Methods

2.1 Bacterial strains and plasmids used in this work

2.1.1 Bacterial strains used in this work

Strain	Genotype and Description	Source / Reference
Escherichia coli DH5α	For general clong, carrying F$^-$φ80d*lac*ZΔM15 Δ(*lac*ZYA-*arg*F)U169 *rec*A1 *end*A1 *hsd*R17(r_k^-, m_k^+) *pho*A *sup*E44 *thi*-1 *gyr*A96 *rel*A1 λ$^-$	Invitrogen™
N. meningitidis MC58	Wild-type, serogroup B, clonal group ET-5	McGuinness *et al*., 1991
N. meningitidis NMB0240::Spec^R	MC58 with spectinomycin resistance cassette insertion disrupting genomic copy of *NMB0240*	Catenazzi, 2013
N. meningitidis NMB0468::Spec^R	MC58 with spectinomycin resistance cassette insertion disruption genomic copy of *NMB0468*	Catenazzi, 2013
N. meningitidis NMB0468::Spec^R NMB0468$^+$NMB0469$^+$	*NMB0468*$^-$ mutant complemented with intact copies of *NMB0468* and *NMB0469*	This work
N. meningitidis NMB0573::Kan^R	MC58 transformed with disrupted genomic copy of *NMB0573* from *NMV_1850*$^-$ kanamycin resistant mutant serogroup C strain 8013	Dr. V. Pelicic and this work

2.1.2 Plasmids used in this work

Plasmid	Description	Source / Reference
pCR®-Blunt II-TOPO®	For cloning blunt-end PCR product, linearised plasmid cloning vector with kanamycin resistance cassette	Invitrogen™
pKHE2	Vector with erythromycin resistance cassette from pYHS25 plasmid, Opa promoter replaced by pBluescript multiple cloning site	Dr. K. Heurlier

2.2 Culturing bacterial strains

2.2.1 General growth and stocking of *Escherichia coli* DH5α

Once transformed, *E. coli* DH5α works as an intermediate host commonly employed in molecular cloning for the amplification of desired plasmid constructs. The chemical composition of LB media (Table 2.1 (a)) and agar plates (Table 2.1 (b)) are listed accordingly, differing only in the addition of agar powder. Both were mixed and sterilised by autoclaving, but LB agar enters a molten state and should be cooled down to about 40 ˚C in a warm water bath before pouring to Petri dishes 85 mm in diameter (Sterilin®) at 20 ml portions. The appropriate antibiotics can be added to select for mutant strains just before pouring molten agar plates or at the start of freshly inoculated liquid cultures.

To prepare new stocks for storage or obtain fresh culture for experimental work, fresh colonies were spread onto LB agar plates from previous glycerol stocks and incubated at 37 ˚C overnight. For liquid cultures, *E. coli* colonies were then inoculated into 8 ml LB media in 30 ml McCartney bottles and grown overnight under aerobic conditions at 37 ˚C on an Innova® 2000 open air platform shaker (New Brunswick Scientific) at 220 rpm. Glycerol stocks can be created by storing equal volumes of liquid *E. coli* cultured in LB with 50 % (v/v) glycerol/water in appropriately-sized Eppendorf tubes (Sarstedt) at -80 ˚C.

	(a) LB media [g/L]	(b) LB agar plates [g/L]
Tryptone (Melford)	10 g	10 g
Yeast Extract (Formedium™)	5 g	5 g
NaCl (Fisher Chemical)	5 g	5 g
Agar (Formedium™)	N/A	15 g
Deionised H_2O	Topped to a final volume of 1 L	

Table 2.1 – Composition of Lysogeny Broth (LB) (a) media and **(b)** agar plates.

2.2.2 Preparation of chemically-competent *Escherichia coli* DH5α cells

Chemically-competent *E. coli* DH5α cells were used in this work to enable the uptake of pCR®-Blunt II-TOPO® (Invitrogen™) constructs containing desired genetic sequences, which were first amplified by PCR, purified, treated and blunt-end-cloned onto the plasmid according to the manufacturer's instructions. The original non-competent *E. coli* DH5α cells were prepared according to the methodology as described by Hanahan (Hanahan, 1983) before being stored as single-use aliquots at -80 ˚C.

Fresh colonies were spread onto LB agar plates from glycerol stocks and incubated at 37 ˚C overnight. Colonies were picked and inoculated into 50 ml LB media, which were then incubated at 37 ˚C at 200 rpm on an Innova® 2300 open air platform shaker (New Brunswick Scientific) until an OD_{600} (optical density reading at 600 nm) of around 1 (approximately 10^9 cfu/ml) was reached. Cells were harvested by transferring the liquid culture into 50 ml CELLSTAR® Falcon tubes (greiner bio-one) before placing into an Allegra™ X-22R benchtop centrifuge (Beckman Coulter™) to be spun down at 4000 rpm at 4 ˚C for 20 minutes. The supernatant was discarded and the pellet resuspended in 15 ml of ice-cold RF1 Buffer (Table 2.2(a)) before being further centrifuged at 4 ˚C for another 10 minutes. Lastly, the supernatant was again discard and the pellet resuspended in 5 ml of ice-cold RF2 Buffer (Table 2.2(b)) and kept on ice for 15 minutes. At this step, the cells must not be allowed to warm up if they are to remain competent. If the cells were not immediately used for transformation, they may be stored as single-use 400 µl aliquots (100 µl per transformation reaction).

(a) RF1 Buffer	Amount	Final concentration
KCl (Fisher Scientific)	2.4 g	160.94 mM
$MgCl_2$•$6H_2O$ (Fisher Scientific)	2.4 g	59.02 mM
K acetate (Melford)	0.6 g	30.57 mM
$CaCl_2$•$2H_2O$ (Fisher Chemical)	0.3 g	10.20 mM
Glycerol (Sigma-Aldrich®)	30 ml	15 % (w/v)
Deionised H_2O	Topped to a final volume of 200 ml, pH 5.8	
(b) RF2 Buffer	**Amount**	**Final concentration**
0.5 M MOPS, pH 6.8 (Acros Organics)	4 ml	2 % (w/v)
KCl (Fisher Scientific)	0.3 g	20.12 mM
$CaCl_2$•$2H_2O$ (Fisher Chemical)	2.2 g	74.82 mM
Glycerol (Sigma-Aldrich®)	30 ml	15 % (w/v)
Deionised H_2O	Topped to a final volume of 200 ml, pH 5.8	

Table 2.2 – Composition of **(a)** RF1 and **(b)** RF2 Buffers used to chemically render bacterial cells competent and ready for transformation.

2.2.3 General growth, stocking of *Neisseria meningitidis* and bacterial growth curves

The laboratory *Neisseria meningitidis* MC58 used in this work was first donated by Professor Robert Read from the University of Sheffield, and its genome is identical to the completely sequenced serogroup B strain (Tettelin *et al.*, 2000). It was used as a wild-type control in experiments as well as a genomic template for molecular work. To comply with health and safety, all cultures or plates of *N. meningitidis* MC58 wild-type and genetically knocked-out mutant strains were handled inside a Category 2* flow hood to prevent contamination, exposure to air and potential release of meningococcal aerosols.

Fresh colonies of *N. meningitidis* were spread onto horse blood agar (HBA) plates from glycerol stocks and incubated at 37 ˚C in a 5 % CO_2 atmosphere for two overnights. HBA plates were prepared by mixing and autoclaving Columbia Blood Agar (CBA) base (Oxoid), cooling the molten agar to 40 ˚C in a warm water bath, adding defibrinated horse blood (Thermo Scientific) to a final concentration of 5 % (v/v) before pouring to Petri dishes 85 mm in diameter (Sterilin®) at 20 ml portions. The appropriate antibiotics can also be added to select for mutant strains just before pouring molten agar plates or at the start of freshly inoculated liquid cultures.

For liquid cultures, colonies were inoculated into either Müller-Hinton Broth (MHB) (Oxoid) or a minimal, chemically-defined media (CDM) (See Chapter 4 and 5) adapted from the original recipe first described by Catlin (Catlin and Schloer, 1962) (Table 2.3).

CDM	Chemicals used	Stock concentration	Final concentration
Solution 1 (Metals) 40X	$MgCl_2$ (Sigma-Aldrich®)	78 mM	1.95 mM
	$CaCl_2$ (Sigma-Aldrich®)	8.15 mM	0.20 mM
	Ferric citrate (Sigma-Aldrich®)	6.5 mM	0.15 mM
	Dissolved in deionised H_2O, stirred at 50˚C for 3hrs, pH adjusted to 7 and filter sterilised		
Solution 2 (Salts) 20X	NaCl (Fisher Chemical)	2 M	100 mM
	K_2SO_4 (Sigma-Aldrich®)	114.8 mM	5.75 mM
	K_2HPO_4 (Sigma-Aldrich®)	460 mM	23 mM
	NH_4Cl (Fisher Chemical)	360 mM	18 mM
	Dissolved in deionised H_2O, stirred in room temperature for 10 minutes prior to autoclaving		
Solution 3 (Amino Acids) 20X	Glycine (Fisher Chemical)	75.6 mM	3.8 mM
	L-cysteine (Sigma-Aldrich®)	8.3 mM	0.4 mM
	L-arginine (Sigma-Aldrich®)	14 mM	0.7 mM
	L-glutamine (Sigma-Aldrich®)	80 mM	4 mM
	L-serine (Sigma-Aldrich®)	95 mM	4.75 mM
	Dissolved in deionised H2O, stirred at 40˚C for 1h and filter sterilised		
Solution 4 (Carbon Source) 224X	D-glucose (Fisher Chemical)	560 mM	2.5 mM
	Dissolved in deionised H_2O, vortexed until complete dissolution of sodium bicarbonate and filter sterilised		
Solution 5 (CO_2 Source) 100X	$NaHCO_3$ (Fluka)	1 M	10 mM
	Dissolved in deionised H_2O, pH adjusted to 7 and filter sterilised		

Table 2.3 – Chemical composition and preparation method of stock components of the chemically-defined media (CDM) standard to this work. The final CDM solution was prepared prior to liquid culturing by freshly mixing appropriate volumes of Solutions 1, 2, 3, 4 and 5 and topped up with autoclaved deionised H_2O. Final pH should be between 7 to 7.5.

Both media contain a supplement of 10 mM final concentration $NaHCO_3$ (Sigma-Aldrich) which was freshly administered prior to incubation. Inoculated liquid cultures were calibrated to start from an OD_{600} of 0.1 and grown in volumes of 10 ml in 25 ml polypropylene universal tubes (Sarstedt) under aerobic conditions at 37 ˚C in a C25KC incubator shaker (New Brunswick Scientific) at 200 rpm. Glycerol stocks can be created

by storing equal volumes of liquid *N. meningitidis* cultured in MHB with 50 % (v/v) glycerol/MHB in appropriately-sized Eppendorf tubes (Sarstedt) at -80 ˚C.

For growth curve experiments, *N. meningitidis* liquid cultures were grown in biological and technical triplicates over 24-hour periods, collecting data at the first 12 as well as the last hourly time points by measuring OD_{600} using 1.5 ml cuvettes (Kartell Labware) with a Jenway 6300 spectrophotometer (Jenway). Samples were usually diluted at a 1:1 ratio with the appropriate blank (i.e stock MHB or CDM with or without supplemented chemicals) in order to match the optimal sensitivity range of the spectrophotometer while avoiding over-depletion of ongoing culture volumes.

For CDM-based investigations, any chemical component can be introduced on top of existing composition, replace default components or left out from the recipe using the spare water volumes to accommodate for the differences. Individual amino acid stock solutions were prepared by dissolving in deionised H_2O to 100 mM stocks in 50 ml CELLSTAR® Falcon tubes (greiner bio-one) prior to filter-sterilisation with 0.22 μm Millipore filters (Millipore). Alternatively, some amino acids were clustered together into combined stocks (See Chapter 4). Depending on desired final concentrations, amino acids can be freshly mixed into CDM along with other stock components, or spiked with a pipette on a tube-by-tube basis. All amino acid solutions can be unstable and should be kept at 4 ˚C at all times for periods no longer than 1 month, after which fresh new stocks must be prepared in order to prevent abnormal growth. All amino acids apart from L-glycine (Fisher Chemical) were obtained from Sigma-Aldrich.

Results were presented as growth curves (from representative biological replicates), which are joined scatter plots with error bars extrapolated from standard error of the mean (SEM) between technical replicates at each time point. Where necessary, the scales of the y-axes of individual sets of data were adjusted on a case-by-case basis to increase resolution of the figures for better comparison of details, and were therefore not consolidated across the Chapters.

2.2.4 Use of antibiotics

Where applicable, antibiotics were added to directly to liquid media or cooled molten agar if selective plates were desired. The final concentrations of the antibiotics used in *E. coli* and *N. meningitidis* were shown in Table 2.4.

Antibiotic	*E. coli*	*N. meningitidis*
Erythromycin (Ery)	200 μg/ml	5 μg/ml
Kanamycin (Kan)	50 μg/ml	80 μg/ml
Spectinomycin (Spec)	50 μg/ml	50 μg/ml

Table 2.4 – Suitable **final concentrations of antibiotics** in selective media or plates for *E. coli* and *N. meningitidis* respectively.

2.3 Molecular Techniques

2.3.1 Polymerase chain reaction (PCR)

Polymerase chain reactions (PCR) were used to amplify desired genetic fragments for screening or cloning purposes. Primer pairs specific to their complementary templates were first designed, where ideally melting temperatures (T_m) could be synchronised with as little discrepancy as possible. If products were to be digested following amplification, restriction enzyme sites could be created by mismatches towards the 5' end of the primers. Three more bases should extend after the end of the restriction sites. To promote specific binding, G/C clamps should be included towards the 3' end of the primers.

All primers used in this work were custom synthesised as oligonucleotides by Sigma Oligos (Sigma-Aldrich) and listed in their corresponding results chapters (See Tables 3.2, 3.3, 4.2 and 5). Wild-type or mutant *N. meningitidis* MC58 genome served as the central template for obtaining bacterial DNA sequences, while plasmid DNA were used in specific protocols instead. Genomic DNA stock can be extracted from harvested *N. meningitidis* cells using tools such as the Wizard® Genomic DNA Purification Kit (Promega) and stored at -20 ˚C. Template DNA mays also be obtained by picking single colonies with a 10 μl micropipette tip and directly suspending into the PCR reaction mix.

Typical PCR reaction mixes were prepared using GoTaq® G2 DNA Polymerase kit (Promega) and 2.5 mM dNTPs (Lucigen®) (Table 2.5). PCR reactions were run by a programmable Techne TC-3000 PCR Thermo Cycler (Table 2.6). To optimise for specific primers or anticipated PCR product length, annealing temperatures and extension times were adjusted accordingly. If subsequently used for cloning work, the amplified fragments

were purified using the QIAquick PCR Purification Kit (Qiagen) and a Sigma 1-13 microcentrifuge (Sigma) according to the manufacturer's instructions.

Reagent	Final concentration	Amount
100 µM forward primer	2 µM	1 µl
100 µM reverse primer	2 µM	1 µl
5X Green GoTaq® Reaction Buffer	0.5X	10 µl
2.5 mM dNTP Mix	200 µM	4 µl
Sterile deionised H_2O	N/A	33 µl
Template	N/A	0.5 µl or tip-picked colony
GoTaq® G2 DNA Polymerase	5 U/µl	0.5 µl
Final volume	50 µl	

Table 2.5 – Typical 50 µl PCR reaction mixtures for both stock or colony-derived genomic DNA templates, which may be further divided into smaller aliquots. Template concentrations may vary depending on stock concentration or aggregated size of picked colonies.

Programmed step	Stage		Temperature and time
1	Initial denaturation		95 ˚C for 5 mins
2	35 cycles	Denaturation	94 ˚C for 30 sec
		Annealing*	65 ˚C for 30 sec
		Extension**	72 ˚C for 5 mins
3	Final extension		72 ˚C for 8 mins
Hold	Storage		16 ˚C – ∞

Table 2.6 – PCR thermal cycler protocols typically found in this work. PCR reactions were run based on settings input, where annealing (*) and extension (**) times and temperatures could be altered for primer or product length optimisation. During complementation cloning, annealing temperatures varied between 60 – 69 ˚C, while extension times varied between 2 – 10 minutes. 2-step PCR were also attempted using the Q5 High Fidelity DNA Polymerase (New England BioLabs®) i.e. by splitting the 35 cycle counts into 10 and 25 times for different annealing temperature or extension time settings. Individual primer annealing temperatures were projected from the calculated melting temperatures (T_m) of each synthesised oligonucleotide, while extension time was based approximately on an amplification rate of 1 minute per kb of DNA.

2.3.2 Cloning with pCR®-Blunt II-TOPO®

This study made use of Zero Blunt® TOPO® PCR Cloning Kit (Invitrogen™) to clone the complementation genes into the 3.52 kbp pCR®-Blunt II-TOPO® vector containing a kanamycin resistance cassette. Sequencing was done to check the resulting constructs for correctly oriented inserts due to the nature of blunt-end cloning, where there are 50/50 chances of genes ligated in the opposite direction (Figure 2.1).

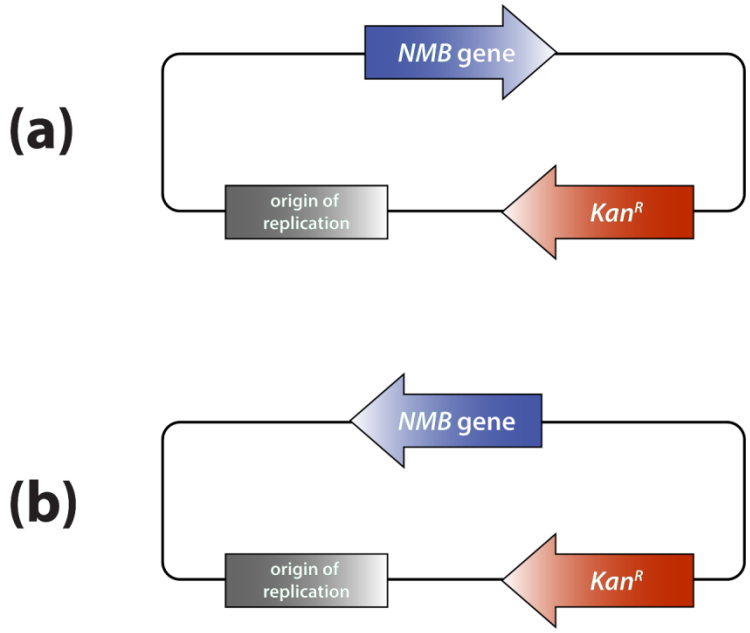

Fig. 2.1 – Map of pCR®-Blunt II-TOPO® plasmid construct ligated with gene of interest in **(a)** normal or **(b)** opposite directions. *Kan*^{R}: kanamycin resistance cassette.

Optimising from the manufacturer's protocol, typical blunt-end cloning reactions were set up in a 1.5 ml Eppendorf tube (Sarstedt), following by mixing 3.5 µl sterile deionised H_2O, 1 µl Salt Solution, 1 µl Control PCR product or purified PCR product and 0.5 µl pCR®-Blunt II-TOPO® vector. The 6 µl mixture was incubated for 5 minutes at room temperature, allowing for the ligation step, after which the reaction was kept on ice.

2.3.3 Restriction digestion of DNA with endonucleases

Restriction digests were performed according to the manufacturer's instructions of each restriction enzyme, which were normally selected for their presence on the genes concerned but not their cloning vectors (i.e. pCR®-Blunt II-TOPO®).

Typical 20 µl DNA digest reactions were conducted in 0.5 ml Eppendorf tubes (Sarstedt) by mixing 12 µl sterile deionised H_2O, 5 µl purified plasmid DNA, 2 µl 10X Restriction Buffer (New England BioLabs®) specific for the enzyme of choice (container caps were colour-coded to match), and 1 µl restriction enzyme (Promega). 0.2 µl 100X BSA (bovine

serum albumin) (New England BioLabs®) may be added optionally to stabilise enzymes in overnight reactions. Reactions were then incubated at 37 ˚C for 1.5 hours, followed by treatment with 0.5 µl calf intestinal alkaline phosphatase (CIP) (New England BioLabs®) for 30 minutes. In the event of sticky-ended products as a result of digestion, 0.5 µl DNA Polymerase I Klenow Fragments (New England BioLabs®) and 0.5 µl 2.5 mM dNTP (Lucigen) may be added 30 minutes before the end of the incubation period. The end products were purified by QIAquick PCR Purification Kit (Qiagen) according to the manufacturer's instructions.

2.3.4 Ligation of DNA fragments

Gene fragments purified from PCR or agarose gels as well as cut plasmids may be ligated together to create intermediate constructs, where sequences of interest may be investigated following transformation or introduced to cells for amplification. Typical ligation reactions consist of 5 µl sterile dH_2O, 3 µl linearised, purified gene of interest, 1 µl 10X T4 DNA Ligase Buffer (Promega) and 1 µl T4 DNA Ligase (Promega), which were mixed and incubated overnight at room temperature. The resulting constructs may be subsequently transformed into competent cells and selected for using the corresponding antibiotics. To check for correctly ligated constructs, transformed plasmids may be restriction digested using the corresponding enzymes as aforementioned (Section 2.3.3), ran on an agarose gel and see if expected DNA fragment sizes were observed before sending purified samples for sequencing for final confirmation.

2.3.5 Agarose gel electrophoresis and DNA gel extraction

Products obtained from PCR (Section 2.3.1) or restriction digests (Section 2.3.3) can be resolved in agarose gel electrophoresis to assess fragment sizes and expression. 1 % agarose gels were typically prepared by fully dissolving 1 g agarose powder (Melford) in 100 ml of 0.5X Tris-Borate-EDTA (TBE) buffer (Table 2.7) under heat in a microwave for about 2-3 minutes. Following cooldown to 40 ˚C by running tap water against the glass container with constant shaking, the molten solution was stained with 10 µl 10,000X SYBR® Safe DNA Gel Stain concentrate (Invitrogen™) for nucleotide visualisation and poured into the desired casting trays with corresponding combs matching required number of lanes.

Reagent	Final concentration	Amount
UltraPure™ Tris (Invitrogen™)	45 mM	54.5 g
Boric acid (Fisher Chemical)	45 mM	27 g
EDTA (Fisher Chemical)	1 mM	3.72 g
Deionised H_2O	Up to 10 L	

Table 2.7 – TBE buffer is a mixture of Tris, boric acid and EDTA in dH_2O, which can be stored at room temperature for several months.

Air bubbles may be prevented by mixing the solution gently or eliminated by dipping an inverted pipette tip on top. The gel was left to set in the tray by cooling down to room temperature for 30 minutes, after which the set-up was placed into an electrophoresis tank and immersed in 0.5X TBE running buffer. Normally, about 8 µl of PCR samples stained with 5X Green GoTaq® Reaction Buffer was directly loaded to each well by careful pipetting, as they already contain blue and yellow loading dyes. Other unstained reaction mixtures such as restriction-digested products or DNA ladders were mixed with 6X Purple Gel Loading Dye (no SDS) (New England BioLabs®) before loading into the wells, e.g. 1 µl of 6X loading dye for 5 µl of sample mixture or ladder. Ideally two flanking lanes of of 7 µl of Low Molecular Weight DNA Ladder (New England BioLabs®), 2-Log DNA Ladder (New England BioLabs®) or 1 kb DNA Ladder (Thermo Scientific) were added as reference according to the expected size ranges of the sample DNA fragments for comparison. Gels were run at 100 V for at least 45 minutes with a PowerPac™ 300 apparatus (Bio-Rad), and may be extended to better resolve bands of similar sizes or to facilitate possible gel excision. DNA was visualised under UV illumination using a GeneGenius BioImaging System apparatus (Syngene) and the GeneSnap software, where digital photos were taken and saved as TIFF files or printed.

DNA fragments of interest may be excised from the gel with a sharp, clean scalpel and placed into 1.5 ml Eppendorf tubes (Sarstedt), which were subsequently purified using the QIAquick Gel Extraction Kit (Qiagen) according to the manufacturer's instructions.

2.3.6 Transformation of chemically-competent *Escherichia coli* DH5α

Plasmid DNA constructs may be introduced into *E. coli* DH5α cells made competent following chemical treatment (Section 2.2.2). 100 µl aliquots of chemically-competent *E. coli* DH5α cells were quickly thawed on ice and mixed with 6 µl blunt-end cloned reaction mixture (Section 2.3.2). The combined mixture was incubated on ice for 30 minutes, heat shocked at 42 ˚C for 90 seconds and finally cooled on ice for a further 2 minutes. As a

recovery stage, the reaction was incubated at 37 ˚C on a SSL1 shaker (Stuart®) at 200 rpm for 1 hour following addition of 800 µl of liquid LB medium. Cells were harvested by centrifugation at 13000 rpm for 60 seconds and the pellet resuspended with 100 µl fresh liquid LB medium, which can then be plated onto corresponding antibiotic LB agar plates i.e. kanamycin in the case of pCR®-Blunt II-TOPO®. Plates were incubated overnight at 37 ˚C for selection and resistant colonies were picked for screening or re-streaked where necessary.

2.3.7 Isolating plasmid DNA

Correct resistant colonies acquired from above (Section 2.3.6) were picked and inoculated into 8 ml of liquid LB medium in 30 ml McCartney bottles. Antibiotics corresponding to the ones used on selective plates were added to the growth medium to maintain selection for cells containing the resistant plasmid constructs. For Minipreps, cells were aerobically cultured on an Innova® 2000 open air platform shaker (New Brunswick Scientific) at 220 rpm at 37 ˚C overnight, and subsequently harvested by spinning at 4500 rpm at 4 ˚C for 10 minutes using a Allegra^{TM} X-22R centrifuge (Beckman Coulter^{TM}). For low yield plasmids such as pKHE2, Midipreps were prepared by growing 50 ml of cells overnight in a sterile 250 ml conical flask on an Innova® 2300 open air platform shaker (New Brunswick Scientific) and harvested using the QIAGEN Plasmid Midi Kit (Qiagen) together with a highspeed Sorval Evolution RC Centrifuge (Sorval). Extraction and purification of plasmidal DNA were carried out with QIAprep Spin Miniprep Kit (Qiagen) with a Sigma 1-13 microcentrifuge (Sigma) according to the manufacturer's instructions. The resulting plasmids were stored at -20 ˚C until further use.

2.3.8 Transformation of *Neisseria meningitidis* strain MC58

Naturally competent *N. meningitidis* cells actively conducts DNA uptake of foreign genetic materials followed by homologous chromosomal recombination. This facilitates transformation of meningococcal strains in molecular biology. Cultures of *N. meningitidis* strain MC58 grown in MHB were prepared as described in Section 2.2.3 until they reach an OD_{600} of approximately 1.0, after which they were placed in 2 ml Eppendorf tubes (Sarstedt) and harvested with a Sigma 1-13 microcentrifuge (Sigma) at 8000 rpm for 5 minutes.

Dr. Melanie Thomson and Dr. Willa Huston devised a protocol for a Transformation and Storage Buffer (TSB), which is a filter-sterilised solution of MHB with 10% PEG 4000, 10 mM $MgCl_2$, 10 mM $MgSO_4$ and 5% DMSO at a final pH of 6.5. 1 ml single-use aliquots were stored at -80 ˚C. Harvested pellets of *N. meningitidis* were resuspended in 200 µl ice-

cold TSB and incubated on ice for 10 minutes. 10 µl of purified plasmid constructs was mixed into the TSB-suspended cells and incubated on ice for a further 50 minutes to allow for transformation. No plasmid was added as a control.

For each transformation reaction, 1.5 ml aliquots of MHB with 10 mM $NaHCO_3$ was pre-warmed to 37 ˚C in 25 ml polypropylene universal tubes (Sarstedt). The reaction mixture was subsequently transferred into the pre-warmed MHB for recovery and cultured aerobically in a C25KC incubator shaker (New Brunswick Scientific) for 1.5 hours at 37 ˚C and 200 rpm. Pellets were harvested by centrifugation at 8000 rpm for 5 minutes and resuspended in 100 µl of fresh MHB prior to plating onto corresponding antibiotic HBA plates. The control was also split and plated on HBA with and without antibiotics to check for spontaneous resistance. Following overnight incubation at 37 ˚C and 5% atmospheric CO_2, antibiotic-resistant mutants were selected and colonies were picked for PCR screening and overnight re-streaking using the same antibiotic plates and conditions. This was to reduce the possibility of seeing wild-type bands from dead wild-type cells in the background during PCR. Multiple colonies were picked again for PCR screening following re-incubation, and glycerol stocks of the colonies yielding the expected DNA fragments were prepared and stored at -80 ˚C.

2.3.9 DNA sequencing

Plasmid DNA was diluted to approximately 100 ng/µl with deionised H_2O and sent for sequencing by the Technology Facility at the University of York using a 16-capillary electrophoresis instrument – ABI 3130*xl* Genetic Analyzer (Applied Biosystems) – and the 3130*xl* Data Collection Software (Applied Biosystems). The data acquired was exported in .ab1 file format which was analysed with the Sequence Scanner Software v2.0 software (Applied Biosystems), or converted to a Word document for analysis with other bioinformatics tools. For constructs derived from the pCR®-Blunt II-TOPO® plasmid, both forward and reverse T7 sequencing primers were used.

2.3.10 Determining DNA or RNA concentrations

Nucleotide concentration and purity were measured and determined using a NanoDrop® ND-1000 Spectrophotometer (Thermo Scientific). Concentration is based on absorbance at wavelength (λ) 260 nm and the respective wavelength-dependent extinction coefficient for DNA ("DNA-50" mode for double-stranded DNA, 50 ng-cm/µl) or RNA ("RNA-40" mode for RNA, 40 ng-cm/µl), on a baseline "zero" absorbance at λ 340 nm.

The ratio 260/280 is commonly used to assess nucleic acid purity in samples and is particularly important in determining DNA contamination in RNA samples. Acceptably pure DNA samples should generally have a ratio value of around 1.8, while for pure RNA samples it should be around 2.0. The ratio 260/230 is commonly used to assess ethanol contamination during respective nucleic acid purification processes, where pure samples should have expected values in the range of 2.0-2.2

Upon each reading, the instrument was blanked with 1.2 µl of Nuclease-Free dH_2O (Ambion®). 1.2 ul of DNA or RNA sample was then pipetted onto the spectrophotometer and the automatic measurements presented in the aforementioned values by the ND-1000 v3.7.1 software.

2.3.11 Extraction of total RNA from *N. meningitidis*

Total RNA from both wild-type and mutant *N. meningitidis* strains were extracted for quantitative PCR (qPCR) experiments. Cells were plated overnight and cultured aerobically in MHB up to a desired OD_{600} as described in previous sections, or up to mid-log phase for about 12 hours. At appropriate time points or the end, 1 ml of each sample was transferred into 1.7 ml RNase-free MaxyClear™ Snaplock microcentrifuge tubes (Axygen®) and harvested with a Sigma 1-13 microcentrifuge (Sigma) at 12000 rpm for 5 minutes. The supernatant was discarded and the pellet quickly stored in -80 ˚C due to instability of bacterial RNA.

A stock solution of Tris-EDTA Buffer 100X (Sigma-Aldrich®) diluted to 1X with Nuclease-Free dH_2O (Ambion®) was prepared and stored indefinitely at room temperature. Nuclease-free Lysozyme Ultrapure (usb®) was dissolved in Nuclease-Free dH_2O (Ambion®) and filter sterilised to give a 10 mg/ml lysozyme solution to be stored at -20 ˚C. 10 µl ß-mercaptoethanol (Sigma-Aldrich®) per 1 ml of Buffer RLT (Qiagen) were mixed to give a Buffer RLT / ß-mercaptoethanol stock solution to be stored at room temperature up to one month. All of the above stock solutions were contained in 1.7 ml RNase-free MaxyClear™ Snaplock microcentrifuge tubes (Axygen®).

Without interruption, all the following steps should be performed in a clean hood or bench sprayed, wiped and dried with ethanol, with minimal clutter and clearly organised work zones to minimise risk of sample contamination. Sterile protective disposable sleeves are also recommended, as well as surgical face masks, hair nets, goggles which are useful if a hood is not available. RNase-free tips (Axygen®), microcentrifuge tubes (Axygen® or Sarstedt) and dedicated pipetting equipment should also be used for RNA work. Adapting from “Protocol 1: Enzymatic Lysis of Bacteria” from RNAprotect® Bacteria Reagent

Handbook version 1/2015 (Qiagen), frozen pellets were resuspended with 1 ml RNAprotect® Bacteria Reagent (Qiagen) and incubated for 10 minutes at room temperature, whilst vortexed for 10 seconds every 2 minutes. Samples were then centrifuged at 13000 rpm for 5 minutes, the supernatant discarded and the pellets resuspended in 180 µl 1X stock Tris-EDTA Buffer. 1 mg/ml lysozyme stock solution was added to each sample and incubated for a further 10 minutes at room temperature, whilst vortexed for 10 seconds every 2 minutes. Afterwards, 700 µl Buffer RLT / ß-mercaptoethanol stock solution was added to each sample and vortexed briefly. If particulates were visible, the samples were centrifuged at 13000 rpm for 2 minutes to retrieve only the supernatant. 500 µl 100% ethanol was mixed into the lysate by gentle pipetting and transferred onto the spin-column provided by the RNeasy® Mini Kit (Qiagen). Following the manufacturer's instructions, "Protocol 7: Purification of Total RNA from Bacterial Lysate Using the RNeasy Mini Kit" version 1/2015 (Qiagen), total RNA was finally extracted. An optional but recommended on-column DNase digestion step can also be carried out according to Appendix B (Qiagen) of the manufacturer's handbook prior to washing and eluting the RNA extract.

Purified RNA samples may be assessed with a NanoDrop spectrophotometer as described in Section 2.3.10 or stored at -80 ˚C until use for the subsequent cDNA synthesis stage.

2.3.12 Synthesis of cDNA

SuperScriptTM II Reverse Transcriptase kit (Invitrogen™) was used to synthesise cDNA copies of total RNA extracts according to the manufacturer's instructions. Typical reverse transcription reactions were set up in 1.7 ml RNase-free MaxyClear™ Snaplock microcentrifuge tubes (Axygen®) by mixing 1 µl 500 µg/ml Random Primers (Promega) and 1 µl 10 mM dNTP Mix PCR Grade (Invitrogen™) to 10 µl purified total RNA. If the stock samples were more concentrated than the recommended range of 1 ng/ml – 5 µg/ml, Nuclease-Free dH_2O (Ambion®) may be used to dilute the total RNA.

The reactions were incubated at 65 ˚C for 5 minutes and quickly cooled on ice for 1 minute before adding 4 µl 5X First-Strand Buffer, 2 µl 0.1 M DTT and 1 µl RNaseOUT™ Recombinant Ribonuclease Inhibitor (40 units/µl) (Invitrogen™). Following an incubation period of 2 minutes at 37 ˚C, 1 µl SuperScript™ II Reverse Transcriptase (200 units) was added to each reaction and incubated for a further 10 minutes at 37 ˚C. The temperature was then increased to 42 ˚C for another 1 hour and 50 minutes, and the reaction finally stopped by inactivating the enzyme at 70 ˚C for 15 minutes.

The final step involves adding 0.5 µl RNase H (5000 units/ml) (New England BioLabs®) to remove remaining RNA complementary to the 20 µl cDNA reaction mixtures, incubating at 37 ˚C for 20 minutes and the enzyme inactivated by heating at 65 ˚C for 20 minutes. The resultant cDNA solution was stored at -80 ˚C until further use.

2.3.13 Quantitative PCR (qPCR) for gene expression analysis

Quantitative PCR (qPCR) was used for the measurement of transcript levels of any target genes of interest. The circumstances for which qPCR was used as well as the qPCR primers designed by the online Primer-BLAST (NCBI) tool in this study were described in Chapter 3 (Section 3.2.1).

Typical qPCR reactions were set-up by mixing 10 µl 2X Fast SYBR® Green Master Mix (Applied Biosystems), 5 µl diluted (at least 20 ng per 20 µl reaction) 0.1X cDNA sample, 1 µl of each forward and reverse primer mixes (at least 200 nM each, working concentration of 10 µM from 100 µM stock), with the difference topped to a final volume of 20 µl using 3 µl Nuclease-Free dH_2O (Ambion®). The reactions were then transferred onto 96-well Optical Reaction Plates (Applied Biosystems) and sealed before inserting into an ABI StepOnePlus™ Real Time PCR System instrument (Applied Biosystems) to be run. No-template control (NTC) wells were also included. Samples were run in triplicates and transcript levels were determined using the threshold cycle (C_T) values (relative expression method) logged by the ABI StepOnePlus™ Software v2.3.

2.4 Analytic chemistry techniques

2.4.1 Nanocontainer-coupled mass spectrometry

This technique was used to measure polyamine levels in culture or solution, where detailed procedures and background knowledge were described in Chapter 3 (Section 3.6).

2.4.2 Labelled isotope MALDI mass spectrometry

This technique was used to detect and assess incorporation of heavier, labelled arginine isotopes in bacterial peptides compared to the naturally occurring form of arginine, where detailed procedures and background knowledge were described in Chapter 4 (Section 4.5).

2.5 Protein techniques

2.5.1 SDS-PAGE

An important step in labelled isotope mass spectrometry (Section 2.4.2, Section 4.5), protein bands from *N. meningitidis* whole cell lysates were visualised, identified and selected by gel staining following resolving with SDS-PAGE. 15% SDS gels were prepared as described in Table 2.8.

Chemical	Resolving gel	Stacking gel
Deionised H_2O	2 ml	700 µl
Resolving gel buffer	1.5 ml	N/A
Stacking gel buffer	N/A	300 µl
10% SDS solution (Melford)	60 µl	12 µl
Ultra Pure ProtoGel® 30% (w/v) acrylamide / 0.8% (w/v) bis-acrylyamide stock solution (37.5:1) (National Diagnostics)	2.4 ml	200 µl
10% (w/v) APS (Sigma-Aldrich®)	50 µl	10 µl
TEMED (Flowgen Bioscience)	10 µl	5 µl

Table 2.8 – Composition of a 15% SDS-PAGE gel, which were typically freshly prepared but can be stored overnight at 4 ˚C once cast. The resolving and stacking layer were added gently to avoid air bubbles during acrylamide polymerisation, both of which required 30 minutes intervals to allow the gel to fully set. Air bubbles on top of the resolving layer can be flattened by gently pipetting a few drops of isopropanol. Once set, the isopropanol can be washed out with deionised H_2O and the last drip dried by inserting a folded strip of filter paper. Air bubbles on top of the stacking layer can be eliminated by overflowing the stacking gel solution and gently inserting the comb.

1X SDS running buffer was prepared by dissolving 25 mM UltraPure™ Tris (Invitrogen™), 125 mM Glycine (Fisher Chemical) and 1.75 mM SDS (Melford). Resolving gel buffer was prepared by dissolving 1.5 M UltraPure™ Tris (Invitrogen™) with 0.4% (w/v) SDS (Melford) calibrated to a final pH of 8.8. Stacking gel buffer was prepared by dissolving 0.5 M UltraPure™ Tris (Invitrogen™) with 0.4% (w/v) SDS (Melford) to a pH of 6.8. 4X Native PAGE Loading Buffer supplemented with 2% SDS (Melford) served as a lysis and dying solution in this work, which is prepared by mixing 0.375 ml 1% Bromophenol Blue dissolved in 100% absolute ethanol (VWR), 6.25 ml 1 M Tris-HCl at pH 6.8 and 8.38 ml deionised H_2O in 100 ml 100% (w/v) glycerol (Sigma-

Aldrich®). 800 µl 4X Native PAGE Loading Buffer were freshly mixed with 200 µl 10% SDS solution (Melford) on the day of SDS-PAGE experiment.

SDS-PAGE gels were cast between glass plates using the Mini-Protean® System (Bio-Rad) to a size of 6 x 8 cm wide and 1 mm thick. Typical 10-well gels can safely hold 15 µl of dyed samples. Protein samples were prepared by mixing harvested pellets from whole cell lysates with 100 µl 2% SDS-supplemented 4X Native PAGE Loading Buffer. Following incubation at room temperature for 1 hour for lysis and 5 minutes of heating at 95 ˚C for protein denaturation, samples were loaded into cast wells, ideally flanked by two lanes of 7 µl PageRuler™ Plus Prestained Protein Ladder (Thermo Scientific). It is recommended that blank wells in between lanes without ladders or samples should be filled with loading-dyed deionised H_2O at volumes equal to that of the samples. This is to prevent lane warping due to unequal pressure caused by large volume differences between lanes. The 15% gel was fastened onto a casket and immersed under 1X SDS running buffer in the aforementioned Bio-Rad gel tank system, and ran with a Power PAC 300 (Bio-Rad) power supply at a constant current of 30 mA for 30 – 60 minutes under room temperature.

2.5.2 Staining of SDS gels

Protein bands SDS gels were stained with either Coomassie Brilliant Blue or Instant*Blue*™ Ultrafast Protein Stain (Expedeon Protein Solutions). Coomassie Brilliant Blue stain was prepared by mixing 20% methanol (Sigma-Aldrich®) and 10% glacial acetic acid (Sigma-Aldrich®) in deionised H_2O, followed by addition of 0.1% (w/v) Coomassie Blue R350. An ethanol or methanol destain solution was also prepared by mixing 10% absolute ethanol (VWR) or 10% methanol (Sigma-Aldrich®) with 10% glacial acetic acid (Sigma-Aldrich®) in deionised H_2O. Both solutions were stored at room temperature indefinitely. Coomassie staining takes about 1 hour while detaining takes at least 1 – 2 hours or overnight until resolved protein bands were clearly visible. The Instant*Blue*™ solution, on the other hand, stains gels in 15 – 30 minutes and destains indefinitely in deionised H_2O, but the solution needs to be kept at 4 ˚C after opening. During both staining and destaining steps, gels retrieved from SDS-PAGE were rinsed with deionised H_2O, kept moist, immersed under the respective solutions and placed on a Gyro-Rocker® STR 9 (BIBBY Stuart) at 20 rpm.

Chapter 3 – Defence against oxidative stress in *Neisseria meningitidis*

3.1 Introduction and Bioinformatics

Oxidative stress management is an important factor in pathogen persistence and virulence. As *Neisseria meningitidis* resides naturally in the human nasopharyngeal region, the mucosal epithelium plays a significant role in maintaining a largely commensal presence for the bacteria. This microenvironment, characteristic of the upper respiratory tract, is rich in nutrients, as well as competing organisms and host immune cells which generate varying levels of oxidative and nitrosative stress upon the meningococci (Eason and Fan, 2014). The highly similar organisms *N. gonorrhoeae* and *N. meningitidis* both possess a complex set of detoxification mechanisms yet with varying priorities, where their overlapping but distinctive roles provide responses to a different profile of endogenous and exogenous stress encountered in the two bacteria's respective ecological niches (Seib *et al.*, 2004).

Reactive oxygen species (ROS) such as hydrogen peroxides (H_2O_2) and superoxide anions (O_2^{-}) are natural products of aerobic respiration where oxygen reacts with leaked electrons to form radicals (Fang, 2011). From the host, activated leukocytes such as polymorphonuclear (PMN) neutrophils or phagocytic monocytes are capable of rapid discharges of ROS known as "oxidative bursts", but are often ineffective against able and well-established human pathogens such as *N. gonorrhoeae* (Seib *et al.*, 2005). Direct detoxification systems such as catalase and superoxide dismutase (SOD) (See Section 1.6.2), together with DNA repair systems, are therefore of great importance in ensuring pathogen survival and in facilitating successful establishment in the host. Alternative mechanisms are also thought to contribute to bacterial defence against oxidative stress, such as the production of polyamines which protect cellular materials through counterion interactions (Tkachenko *et al.*, 2012).

3.1.1 Role of polyamines in bacterial stress response

Polyamines are small, polycationic organic molecules carrying two or more primary amino groups (Figure 3.1-1). Examples are putrescine, spermidine, spermine and cadaverine.

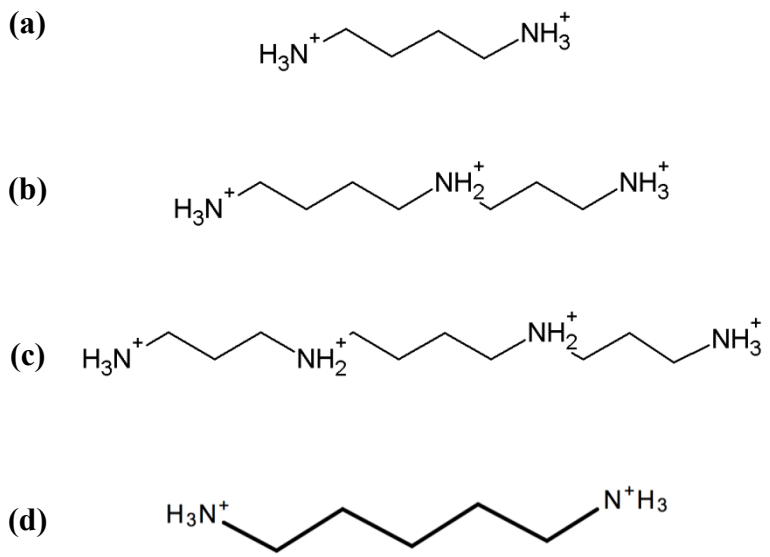

Fig. 3.1-1 – Simplified chemical structures of the primary di-amines **(a)** putrescine (1,4-diaminobutane) and **(d)** cadaverine (1,5-diaminopentane), with the **(b)** tri-amine spermidine and **(c)** tetra-amine spermine. The hallmark regularly-spaced positive charges were shown.

The most important characteristic of polyamines is that their highly positive charges are distributed evenly along the linear, unsaturated hydrocarbon backbone. This enables polyamines to have key roles in metabolism, particularly in rapidly proliferating cells where, for example, polyamines can stabilise the conformation of negatively-charged nucleic acids. Thus they offer protection when challenged by reactive oxygen species (ROS) (Chattopadhyay *et al.*, 2003). As polycations the anti-oxidant properties of polyamines have long been investigated in both mammalian and bacterial cells, but have only received increased recognition in recent years as an important virulence factor. Indeed, in many cases cells deficient in polyamine synthesis often display premature death and impaired invasiveness during pathogenesis (Shah *et al.*, 2011).

In bacteria, polyamines may be synthesised from amino acids such as arginine and glutamate (glutamic acid). Extensive work has been carried out on *E. coli*, the model organism upon which most existing findings on bacterial polyamine metabolism is based (Shah and Swiatlo, 2008). However, analyses with bioinformatics tools show that not all bacteria possess the same enzyme homologues or pathways (Figure 3.1-2).

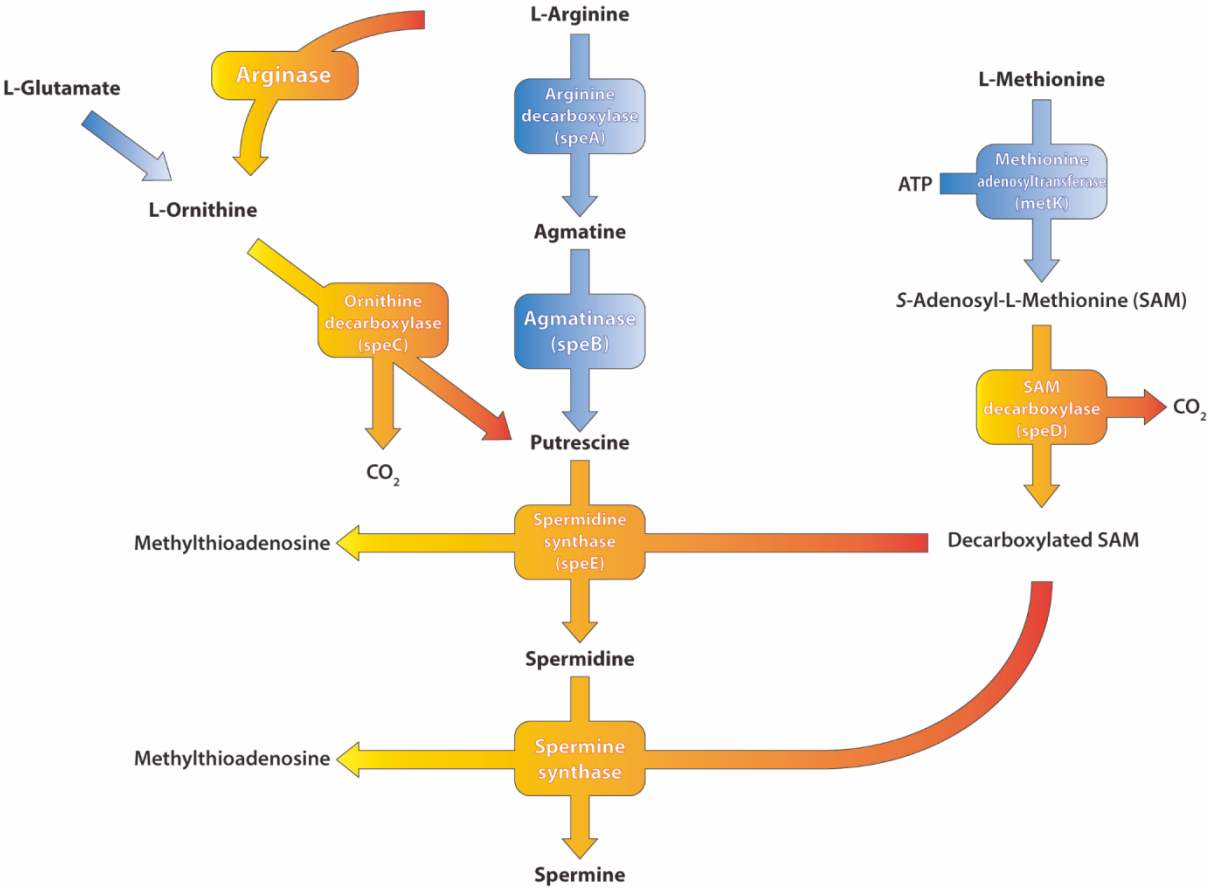

Fig. 3.1-2 – The classical *E. coli* polyamine synthesis pathway, superimposed with that of *N. meningitidis*. All genes, enzymes and pathways shown here are **present in *E. coli***. Colour-coding is used to denote predicted presence (blue) or absence (orange) of functional homologues or simplified pathways in the meningococcal genome. Both spermidine synthase (*E. coli* SpeE homologue; EC 2.5.1.16) and spermine synthase (EC 2.5.1.22) are closely-related aminopropyltransferases that require decarboxylated *S*-Adenosyl-L-Methionine (SAM), but require different substrates resulting in different products.

In *N. meningitidis*, due to the predicted absence of a *S*-Adenosyl-L-Methionine (SAM) decarboxylase (*E. coli* SpeD) homologue, SAM cannot be converted into decarboxylated SAM, which is an essential substrate in the synthesis of the higher polyamines spermidine and spermine from putrescine. Of the two arginine-dependent pathways for putrescine biosynthesis, *N. meningitidis* is not predicted to possess the classic arginase and ornithine decarboxylase (*E. coli* SpeC) homologues more commonly and often simultaneously featured in animals (Morris, 2009). Instead, typical of bacteria and plants, the major route for putrescine production appears to be the one through arginine decarboxylase (*E. coli* SpeA) and agmatinase (*E. coli* SpeB), where arginine is converted to agmatine and finally putrescine and urea (Morris, 2004).

In the *Neisseria meningitidis* genome there are elements that have been annotated for polyamine synthesis (Tettelin *et al.*, 2000). A genomic island conserved among pathogenic *Neisseria* has been predicted to encode a biosynthesis pathway for the di-amine putrescine, indicating a possible role for polyamines in the behaviour of *N. meningitidis* in human colonisation and pathogenicity.

3.1.2 Distribution of Genomic Island 5 in *N. meningitidis*

As previously discussed in Chapter 1, 9 genomic islands were found conserved in all *Neisseria meningitidis* strains, but absent from its closely related commensal cousin *Neisseria lactamica*. One such pathogen-specific island is comprised of three genes of unknown functions, *NMB0468*, *NMB0469* and *NMB0470* in *N. meningitidis* serogroup B strain MC58. The island is present in both pathogenically significant Neisseriae (i.e. *N. meningitidis* and *N. gonorrhoeae*) but is absent from all other *Neisseria* species with complete genomes. It is believed to have been acquired via horizontal gene transfer followed by gene rearrangements (Figure 3.1-3).

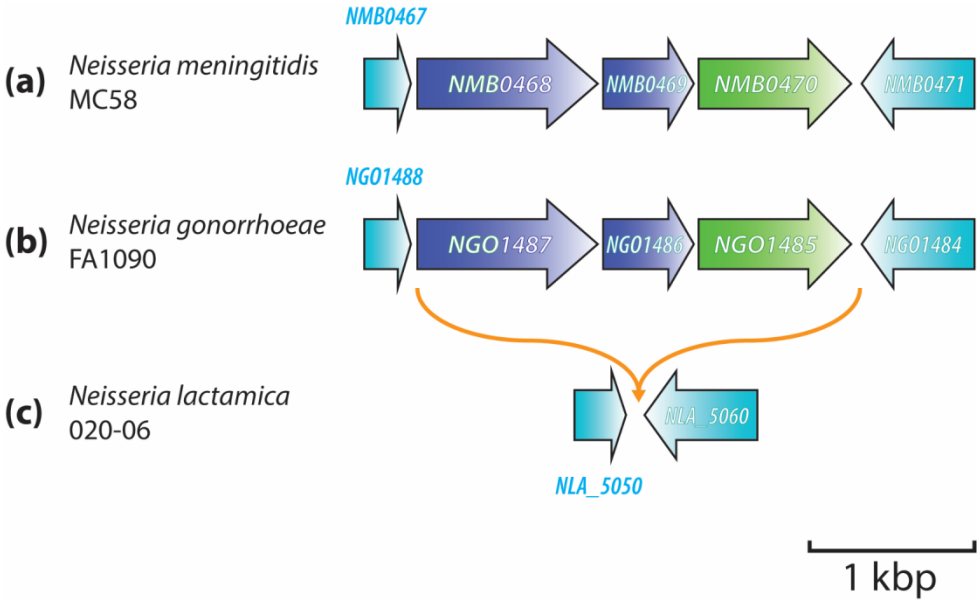

Fig. 3.1-3 – Genomic Island 5 is present in both pathogenic *Neisseria* species but absent in the commensal *N. lactamica*. (a) The meningococcal genes *NMB0468* and *NMB0469* are homologous to **(b)** gonococcal genes *NGO1487* and *NGO1486*. **(c)** The *N. lactamica* gene *NLA5050* corresponds to meningococcal *NMB0467* and gonococcal *NGO1488*, while *NLA5060* corresponds to meningococcal *NMB0471* and gonococcal *NGO1484*. The meningococcal gene *NMB0470* is homologous to gonococcal gene *NGO1485*, and is absent from non-pathogenic *Neisseria* species.

Neisseria meningitidis Genomic Island 5 is a 4579 bp three-gene cluster consisting of the 1893 bp *NMB0468*, 924 bp *NMB0469* and 1467 bp *NMB0470*. The island has a total of 674 bp worth of intergenic regions spanning from just after the end of the flanking gene *NMB0467* to just before the start of the flanking gene *NMB0471*. In comparison there is only an 80 bp distance between the *N. lactamica* flanking homologues *NLA_5050* and *NLA_5060*, which contains the same 12-mer DNA uptake sequence (DUS) 5'-ATGCCGTCTGAA-3' (Duffin and Seifert, 2010) also found in the 166 bp intergenic region between the flanking gene *NMB0467* and island gene *NMB0468.* Protein BLAST analysis revealed specific hits for arginine decarboxylase (*E. coli* SpeA, E.C. 4.1.1.19) active sites, binding sites and catalytic residues in NMB0468 (Table 3.1-1)., while a search with NMB0469 returned specific hits for agmatinase (*E. coli* SpeB, E.C. 3.5.3.11) (Table 3.1-2).

Alignment hit	Query cover	E value	Identity	Accession no.
Arginine decarboxylase (*Kingella kingae*)	100%	0	88%	WP_038316412.1
Arginine decarboxylase (*Alysiella crassa*)	100%	0	84%	WP_034293401.1
Arginine decarboxylase (*Pasteurella multocida*)	99%	0	82%	WP_005757582.1
Arginine decarboxylase (*Pasteurella dagmatis*)	99%	0	82%	WP_032855566.1
Arginine decarboxylase (*Gallibacterium salpingitidis*)	99%	0	80%	WP_066109380.1
Arginine decarboxylase (*Gallibacteria* genomosp. 3)	99%	0	80%	WP_065234030.1
Arginine decarboxylase (*Gallibacterium anatis*)	99%	0	79%	WP_039144822.1
Arginine decarboxylase (*Halfnia alvei*)	98%	0	70%	WP_040046206.1
Arginine decarboxylase (*Yersinia aldovae*)	98%	0	70%	WP_042546832.1
Arginine decarboxylase (*Pectobacterium carotovorum*)	98%	0	70%	WP_039361763.1

Table 3.1-1 – Top 10 hits from protein BLAST results of Genomic Island 5 member *NMB0468* against species outwith *Neisseria*. Redundant hits belonging to the same species are omitted. Accessed 4th May 2017.

Alignment hit	Query cover	E value	Identity	Accession no.
Agmatinase (*Kingella kingae*)	99%	0	92%	WP_032133140.1
Agmatinase (*Alysiella crassa*)	99%	0	77%	WP_034295711.1
Agmatinase (*Pasteurella multocida*)	99%	1e-180	77%	WP_046339245.1
Agmatinase (*Pasteurella dagmatis*)	99%	5e-180	77%	WP_005764265.1
Agmatinase (*Gallibacterium salpingitidis*)	98%	7e-179	78%	WP_066109319.1
Agmatinase (*Gallibacteria* genomosp. 3)	99%	2e-178	77%	WP_065237308.1
Agmatinase (*Gallibacterium anatis*)	99%	3e-178	77%	WP_018347311.1
Agmatinase (*Morganella psychrotolerans*)	99%	3e-173	74%	WP_067360410.1
Agmatinase (*Morganella morganii*)	99%	6e-173	74%	WP_032098326.1
Agmatinase (*Escherichia albertii*)	98%	3e-172	74%	WP_000105568.1

Table 3.1-2 – Top 10 hits from protein BLAST results of Genomic Island 5 member *NMB0469* against species outwith *Neisseria*. Redundant hits belonging to the same species are omitted. Accessed 4th May 2017.

NMB0468 encodes a protein of 630 amino acids (with a predicted molecular mass of 70902), while *NMB0469* encodes a protein of 307 amino acids (with a predicted molecular mass of 33905). Both NMB0468 and NMB0469 are soluble proteins (using online TMHMM software packages by CBS, SOSUI and by SACS). In concordance with initial annotations, multiple alignments and crystal structure comparison revealed that key amino acid residues of NMB0468 are highly conserved and similar to that of the *E. coli* SpeA enzyme arginine decarboxylase (Figure 3.1-4), while NMB0469 is homologous to the *E. coli* SpeB enzyme agmatinase (Ahn *et al.*, 2004; Andréll *et al.*, 2009) (Figure 3.1-5) (see Appendices: Figures A, B).

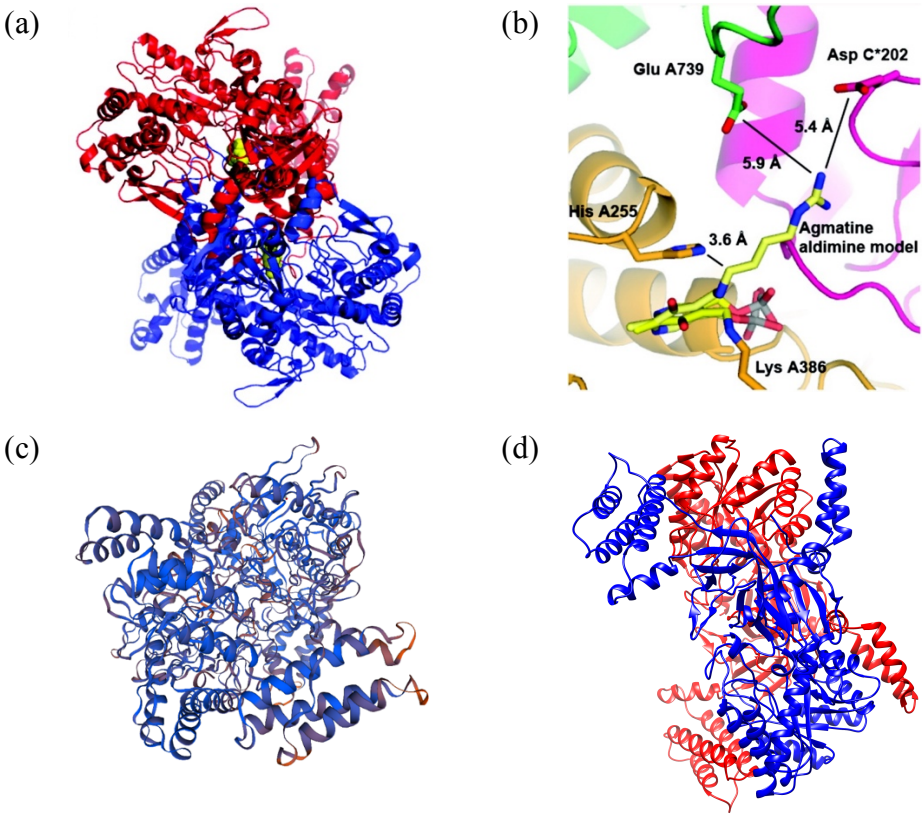

Fig. 3.1-4 – The *E. coli* arginine decarboxylase SpeA: **(a)** crystal structure of the SpeA homodimer from *E. coli* strain BL21 (PDB accession number: 2VYC) and **(b)** key amino acid residues in its active site (from Andréll *et al.*, 2009), compared to **(c)** the predicted structural representation of NMB0468 homodimer generated by the SWISS-MODEL software package (Biasini *et al.*, 2014). SWISS-MODEL used the biosynthetic *E. coli* SpeA homodimer (PDB accession number: 3NZQ) as a template, sharing 68.82% of its sequence identity with NMB0468 and has a decent estimated quality score of 0.83 out of 1. Options for visualising the model online in multicolour, however, is limited, therefore **(d)** when visualised with the offline program UCSF Chimera (Pettersen *et al.*, 2004), the predicted homodimer structure is more visibly comparable to that of the solved SpeA.

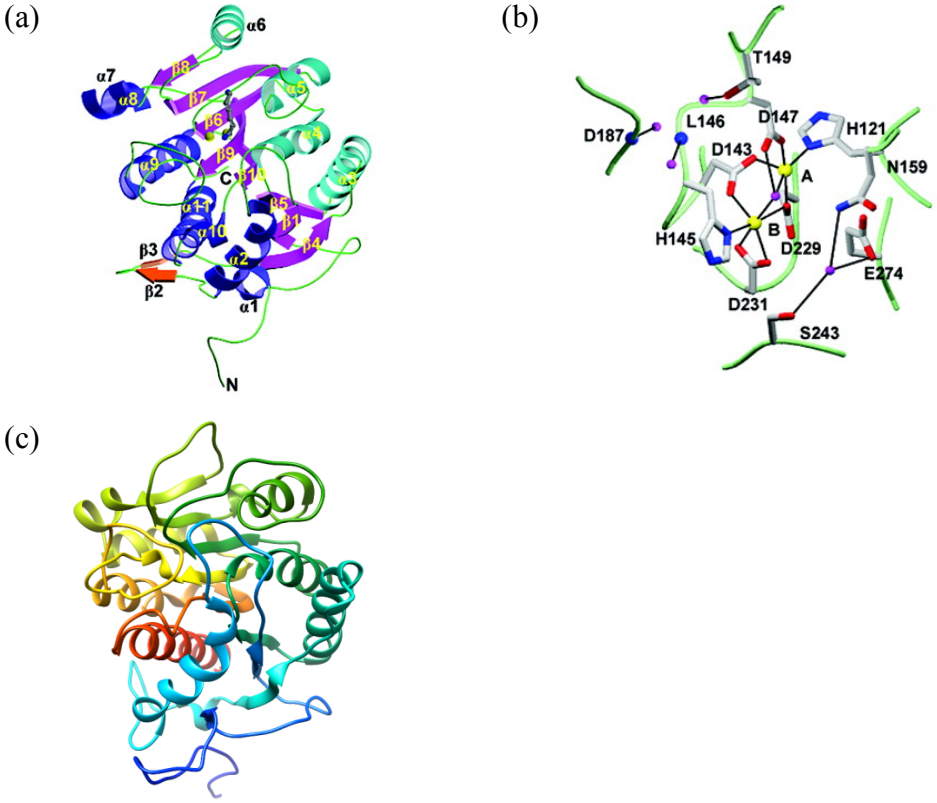

Fig. 3.1-5 – The *E. coli* agmatinase SpeB: (a) crystal structure of manganese-activated (Carvajal *et al.*, 1999) SpeB homologue monomer from *Deinococcus radiodurans* (PDB accession number: 1WOI) (from Ahn *et al.*, 2004) and (b) key amino acid residues in its active site, compared to (c) the predicted structural representation of NMB0469 monomer generated by the RaptorX software package (Källberg *et al.*, 2012) and visualised by UCSF Chimera (Pettersen *et al.*, 2004). RaptorX used the *Burkholderia thailandensis* agmatinase (expressed in *E. coli*) (PDB accession number: 4DZ4) as a template, with 100% of its residues modelled and low estimated modelling error. Options for directing visualising the model online is very limited, hence the file was exported and presented using the offline program UCSF Chimera instead.

NMB0470 encodes a protein of 480 amino acids (with a predicted molecular mass of 51692) which contains around 11 or 12 predicted transmembrane spans (Figure 3.1-6; Figure 3.1-7). Such a structural profile is typical of proteins involved in transport of metabolites (Henderson, 1993). Initial analysis shows it has been annotated as a C_4-dicarboxylate transporter. C_4-dicarboxylates are 4-carbon compounds containing two carboxyl functional groups, such as succinate, fumarate, malate, aspartate, tartate and orotate. However, NMB0470 lacks substantial clusters of charged amino acid residues (Table 3.1-3) typical of known members of the transporter family (Janausch *et al.*, 2002) due to the anionic nature of C_4-dicarboxylates (Kneuper *et al.*, 2005). Moreover, the crystal structures of the known C_4-dicarboxylate transporter family Dcu (DcuA and DcuB) have not yet been resolved for detailed comparison. On the other hand, the crystal structure of a dicarboxylate transporter from the DASS (divalent anion/sodium symporter) family VcINDY (*Vibrio cholerae* I'm not dead yet), a sodium-dependent succinate transporter, had been purified and resolved (Mancusso *et al.*, 2012; Mulligan *et al.*, 2016), but sequence alignments with *NMB0470* do not suggest that they are highly conserved in *N. meningitidis* (see Appendices: Figure C).

(a) (b)

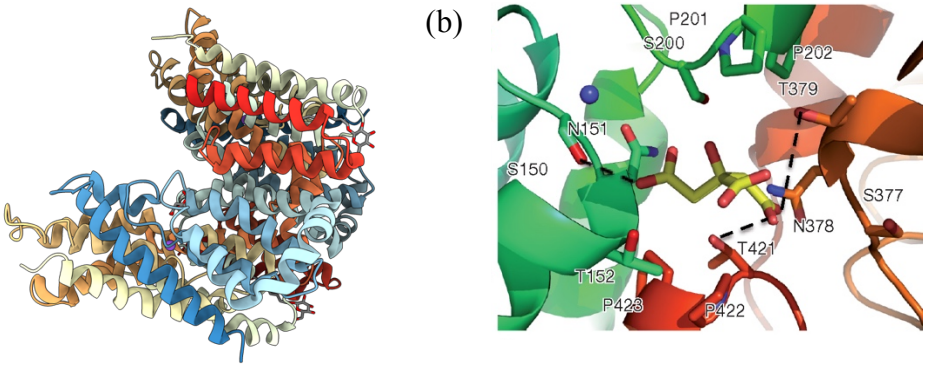

(c)

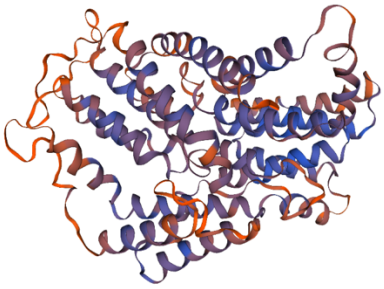

Fig. 3.1-6 – The ***Vibrio cholerae*** **sodium-dependent dicarboxyate transporter VcINDY**: (a) crystal structure of sodium-activated bacterial INDY homologue monomer (PDB accession number: 4F35) (from Mancusso *et al.*, 2012) and (b) key amino acid residues in its active site, compared to (c) the predicted structural representation of NMB0470 monomer generated by the SWISS-MODEL software package (Biasini *et al.*, 2014), which used DASS belonging to the NadC family as templates amid relatively low sequence similarities.

No.	N Terminal	Transmembrane Region	C Terminal	Type	Length
1	58	LYAMM**K**LGF**K**PIPLAIAAVLCAL	80	Primary	23
2	102	VGVIAAIIG**K**AMPLGALSIIAVG	124	Primary	23
3	140	MS**D**ALSAFANPLIWLIAIAVMIS	162	Primary	23
4	250	NPISSAMFITATAPNPLIVNLIA	272	Secondary	23
5	288	WAMAVPGVIAFFVMPLILYFLYP	310	Primary	23
6	335	A**DE**IIMAVIFGILLLLWA**D**VPAL	357	Primary	23
7	368	ATATAFIGLSLLLLSGVLTW**DD**	389	Primary	23
8	399	TIIWFGALIMMAAFLN**K**LGLI**K**W	421	Primary	23
9	429	SVGGLGVSGTAAGVILVLAYMYA	451	Primary	23
10	458	TTA**H**ITAMFGAFFAAAVSLNAPA	480	Secondary	23
11	521	**K**AGFIMSVVNFLIFFVIGSIWW**K**	543	Primary	23

Table 3.1-3 – The **transmembrane domains and charged amino acid residues** (in bold: positives in red; negatives in blue) of NMB0470 from SOSUI. Positives: arginine (R), lysine (K); negatives: glutamate (E), aspartate (D).

(a)

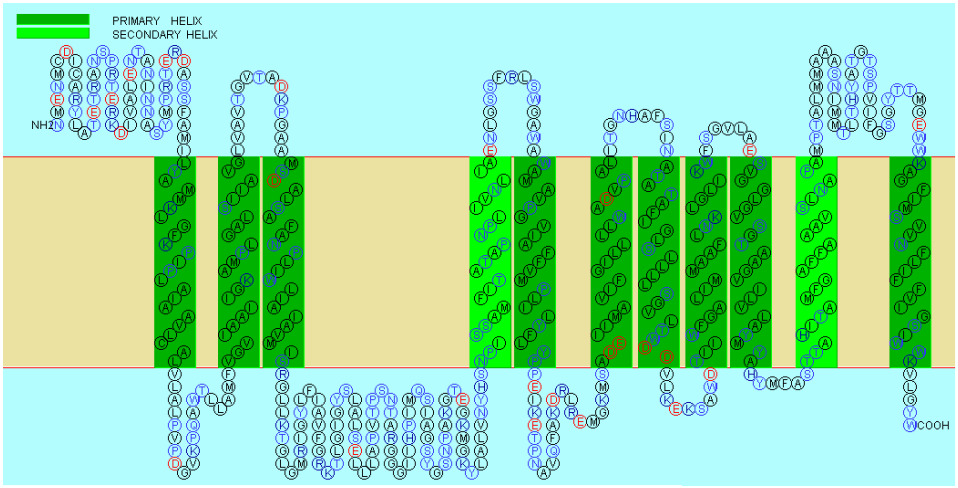

(b)

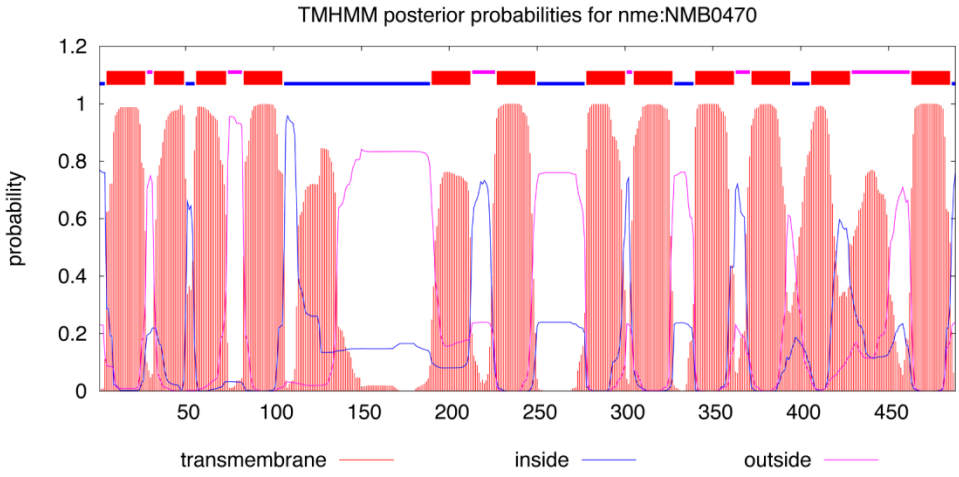

Fig. 3.1-7 – The **11 or 12 predicted transmembrane helices of NMB0470** from **(a)** SOSUI and **(b)** TMHMM by CBS.

Further BLAST searches revealed low sequence identity or coverage for NMB0470 hits outwith the *Neisseria* genus. Non-pathogenic species such as *N. lactamica* returned hits poorly aligned with *NMB0470*. In contrast, the presence of highly-identical, single-copy specific hits for NMB0470 among sequenced *Neisseria meningitidis* and *N. gonorrhoeae* strains suggest strong conservation in the two pathogenic species.

In this chapter, a knockout mutant unable to express intact *NMB0468* was constructed by Catenazzi (2013) for the experimental characterisation of its metabolic properties with an aim of identifying the function(s) of Genomic Island 5.

3.2 Construction of a Genomic Island 5 knockout mutant

A mutant strain of *N. meningitidis* serogroup B strain MC58 unable to synthesise intact copies of the gene *NMB0468* was previously constructed by Catenazzi (2013). All *N. meningitidis* strains used were cultured according to methodologies as previously described (See Chapter 2), while protocols for the molecular work involved are reiterated as follows.

No.	Primer Name	Primer Sequence (5' to 3')	Nucleotide Position
(a)	NMB0468-for	5'-CTTTTCAACACGACAGACGG-3'	488122 – 488141
(b)	NMB0468-rev	5'-GCTTCAGACGGCATATCCGATG-3'	490079 – 490058
(c)	NMB0468bis-for	5'-GTATGGGGCATCAGTCAGGC-3'	489086 – 489105
(d)	NMB0468bis-rev	5'-CGGTAATGGGACAAACAGGG-3'	489602 – 489583

Table 3.2-1 – List of primers used for the construction of a NMB0468-deficient mutant strain of *N. meningitidis* MC58: **(a)** forward and **(b)** reverse cloning primers; **(c)** forward and **(d)** reverse transformation-confirming primers which flank the three *AclI* recognition sites in *NMB0468*. Underlined bases are intended mismatches of the genomic sequence in order to increase frequencies of transformation through the introduction of DNA uptake sequences.

The *NMB0468* gene was amplified from wild-type *N. meningitidis* strain MC58 using the primers shown in Table 3.2-1 (a, b). The resulting 1958-base product was then cloned onto an intermediate vector pCR-Blunt II-TOPO (Invitrogen). The product was digested out with the single-cut restriction enzyme AclI, which has three recognition sites in the *NMB0468* gene (Promega). The sticky ends were rendered blunt by treating with the DNA Polymerase I Klenow Fragment (New England BioLabs®) in the presence of dNTPs. The Ω cassette containing a spectinomycin resistance gene was digested from its 4.3 kbp native vector pHP45Ω (Prentki and Krisch, 1984) with the restriction enzyme SmaI (Promega), which was subsequently ligated with the linearised *NMB0468* clone using T4 DNA ligase (Promega). This yielded a construct containing a cloned copy of *NMB0468* disrupted by

the insertion of a spectinomycin resistance cassette (Figure 3.2-1), which was confirmed by Sanger sequencing.

The above *NMB0468*-knockout construct was then transformed by Catenazzi (2013) into *N. meningitidis* following protocols as previously described by Heurlier *et al.*, (2008), selecting for the mutant strain with 50 µg/ml spectinomycin. The formation of a disrupted *NMB0468* gene through correct chromosomal rearrangement was confirmed by PCR (Figure 3.2-2) using primers (Table 3.2-1(c,d)) that flank the spectinomycin cassette insertion site within *NMB0468* (Figure 3.2-1).

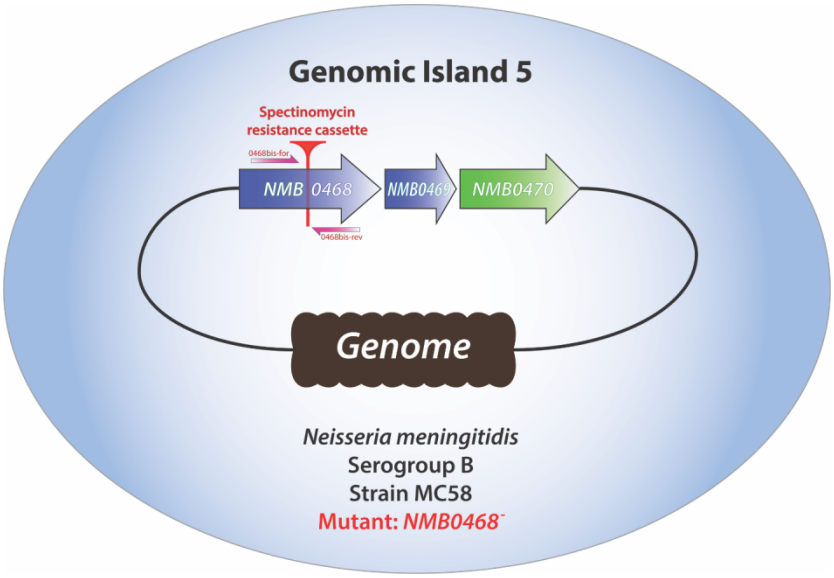

Fig. 3.2-1 – Layout of a *Neisseria meninigitidis* serogroup B strain MC58 Genomic Island 5 mutant. A spectinomycin resistance cassette containing transcription-terminators is inserted into *NMB0468*, resulting in a mutant deficient in intact copies of the gene as well as the rest of the genomic island following chromosomal rearrangement. The primers 0468bis-for and 0468bis-rev confirm the presence of the resistance cassette.

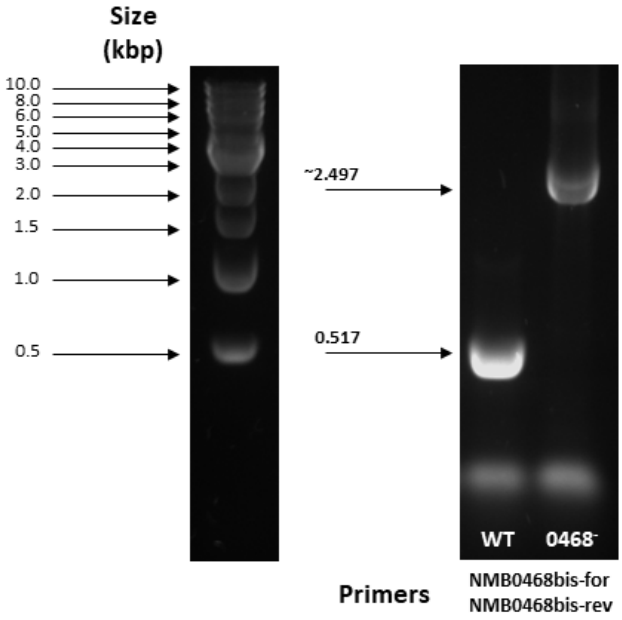

Fig. 3.2-2 – PCR confirmation of spectinomycin resistance cassette insertion by primers NMB0468bis-for and NMB0468bis-rev which flank the site of disruption. The "bis" primers read the wild-type *NMB0468* gene as a 517 bp product and the mutant (0.517 + 1.98 kbp cassette insert) as an approximately 2.497 kbp product. When referring to band weights, 1 kb DNA ladder (New England BioLabs®) was used.

3.2.1 Quantitative PCR confirms the knockout affects expression of *NMB0468* and *NMB0469* but not *NMB0470*

From Section 3.1.2, it was suggested that the third gene in Genomic Island 5 had been inaccurately annotated as a C_4-dicarboxylate transporter, which appears unrelated to the purported functions of the two upstream island members. To assess this implication, quantitative PCR (qPCR) was carried out to compare the expression of *NMB0470* in the *NMB0468*$^-$ knockout mutant, in comparison to *NMB0468* regions both anterior and posterior to the spectinomycin resistance cassette insert as well as *NMB0469*, all normalised against 16S ribosomal RNA (rRNA) and wild-type *N. meningitidis* MC58 expression. The list of primers used are listed in Table 3.2 and were synthesised by Sigma Oligos (Sigma-Aldrich).

No.	Primer Name	Primer Sequence (5' to 3')
(a)	NMB_MC58_16S_A_for	5'-GCCTTCGGGTTGTAAAGGAC-3'
(b)	NMB_MC58_16S_A_rev	5'-GCCGGTGCTTATTCTTCAGG-3'
(c)	NMB0468q_ant_for	5'-TTGATGGGCGAAAAACTGGG-3'
(d)	NMB0468q_ant_rev	5'-TGCCATTTTCCCGAACCTTG-3'
(e)	NMB0468q_post_for	5'-TGTTGTAGGGGAAGACGGAC-3'
(f)	NMB0468q_post_rev	5'-GGCAACGGTGTTTCCTTCAT-3'
(g)	NMB0469q_for	5'-CGTTCCGTACAAATCGGCAT-3'
(h)	NMB0469q_rev	5'-ATTGACTTTAGGGGCGGACA-3'
(i)	NMB0470q_for	5'-CTTCGCCTGTGATTTTCGGT-3'
(j)	NMB0470q_rev	5'-GATAAAACCCGCCTTCCACC-3'

Table 3.2-2 – List of qPCR primers used for determining expression levels of genes *NMB0468*, *NMB0469* and *NMB0470* in both wild-type MC58 and *NMB0468*$^{-}$ mutant strain of *N. meningitidis*, normalised against meningococcal 16S rRNA: **(a)** forward and **(b)** reverse qPCR primers for meningococcal 16S rRNA; **(c)** forward and **(d)** reverse qPCR primers for the region anterior to the spectinomycin resistance cassette insertion site in *NMB0468*; **(e)** forward and **(f)** reverse qPCR primers for the region posterior to the insert in *NMB0468*; **(g)** forward and **(h)** reverse qPCR primers for *NMB0469*, and; **(i)** forward and **(j)** reverse qPCR primers for *NMB0470*.

Liquid cultures of both *N. meningitidis* wild-type and mutant strains were harvested mid-log phase, where their total RNA was extracted, purified and their corresponding cDNA synthesised according to the methodology described in Chapter 2. Upon analysing the qPCR data, it was revealed that the insert had an impact on relative expression level of all probed regions, where the region downstream of the insert in *NMB0468* as well as *NMB0469* were further downregulated by approximately 10-fold (Figure 3.2-2). This was in accordance with the spectinomycin resistance cassette containing strong transcriptional terminators, which indicated at the very least that *NMB0468* and *NMB0469* likely belong to the same operon.

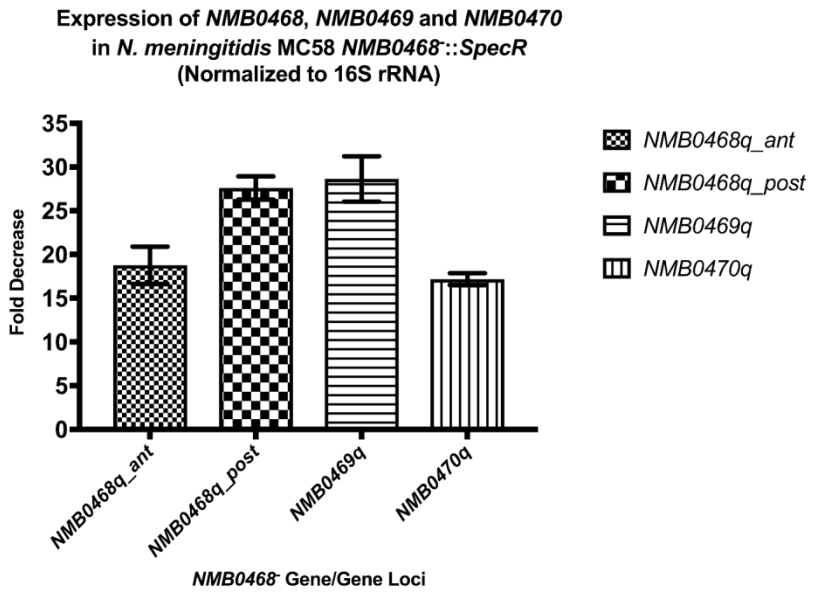

Fig. 3.2-3 – Fold decrease (i.e. **downregulation**) of various regions of Genomic Island 3, normalised against wild-type *N. meningitidis* MC58 and 16S rRNA. The NMB0468q_ant primer pair synthesises the region anterior to the spectinomycin resistance cassette inserted in *NMB0468* in the mutant, while the NMB0468q_post pair reads the posterior region; the NMB0469q and NMB0470q primer pairs monitor expression of *NMB0469* and *NMB0470* respectively. Positive $\Delta\Delta C_T$ values indicate downregulation, and therefore decimals were converted into and expressed as fold change values.

The results did not rule out the possibility of *NMB0470* sharing functional association with *NMB0468* and *NMB0469*, as all Genomic Island 5 genes were collectively downregulated in the mutant strain. The rationale behind the strong incorporation of a putative transporter in pathogenic *Neisseria* genomes and in close proximity to a functionally disparate pathway is unclear, which remains to be explored in the future.

3.3 Complementation of the Genomic Island 5 knockout lesion

To complement the *NMB0468*- knockout mutant in this study, genes from Genomic Island 5 were reintroduced into the cell following protocols as described by Catenazzi (2013). The two adjacent genes *NMB0468* and *NMB0469*, representing the meningococcal putrescine synthesis pathway, were first amplified by polymerase chain reaction (PCR). There was no need to include *NMB0470* in the complementation construct.

No.	Primer Name	Primer Sequence (5' to 3')	Nucleotide Position
(a)	NMB0468c_for	5'-GCTGGATCCTTTGATGGAAAGATGAACC-3'	487982 – 488009
(b)	NMB0469c_rev	5'-CGTGGATCCGATATGCGGCTCCGGGC-3'	491177 – 491152

Table 3.3 – List of primers used for the construction of a plasmid-complemented NMB0468-deficient mutant strain of *N. meningitidis* MC58, in addition to the primers used in Table 3.2-1: **(a)** forward and **(b)** reverse transformation-confirming primers. Underlined bases are intended mismatches of the genomic sequence in order to increase frequencies of transformation through the introduction of DNA uptake sequences.

This combined 2.9 kbp sequence was then cloned onto a pCR®-Blunt II-TOPO® vector (Invitrogen) according to the manufacturer's instructions and transformed into competent *E. coli* DH5α. Colony PCRs were carried out to screen for correct construct, pCR®-Blunt II-TOPO®-*NMB0468-NMB0469,* which was then harvested and purified by QIAprep Spin Miniprep Kit (QIAGEN).

Since the pCR®-Blunt II-TOPO® plasmid cannot be maintained in *N. meningitidis*, the insert was subcloned in *N. meningitidis* via the complementation vector pKHE2 (Heurlier *et al.*, 2009). pKHE2 is an approximately 5 kbp plasmid with an erythromycin resistance cassette derived from pYHS25. To provide some background, pYHS25 itself was in turn a complementation vector containing the tail-to-tail-oriented genes *NMB0102* and *NMB0103* including their intergenic region (Winzer *et al.*, 2002). To construct pKHE2, the multiple cloning site (MCS) and *opa* promoter between two DNA uptake sequences (DUS) were removed from pYHS25 by reverse PCR. In their place, a MCS from the commercially available vector pBlueScript-II KS (Stratagene) was cloned via the (also commercially available) vector pUC6S (Stratagene) and introduced into the BglII restriction site in the aforementioned pYHS25ΔP_{opa}, allowing future cloned inserts to make use of their natural promoters. Promoters from the *opa* multigene family are involved in phase variation of Opa proteins in *Nesseria* spp. and found in their genomes (Belland *et al.*, 1997; Sadarangani *et al.*, 2016). Both pKHE2 and the sequence *NMB0468-0469* were first excised by the single-cut restriction enzyme BamHI, ligated to each other and the resultant construct shown in Figure 3.3-1. This was subsequently transformed into the *N. meningitidis* mutant chromosome as a single-copy insert between chromosomal *NMB0102* and *NMB0103* genes, resulting in a MC58Δ*NMB0468*::*NMB0468-0469*^{ect} (ectopic expression) complemented strain *NMB0468-0469c*.

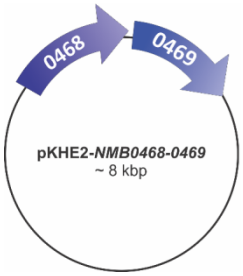

Fig. 3.3-1 – Simplified schematic of the pKHE2 plasmid carrying the genes *NMB0468* and *NMB0469*, resulting in the erythromycin-resistant pKHE-*NMB0468-0469* construct.

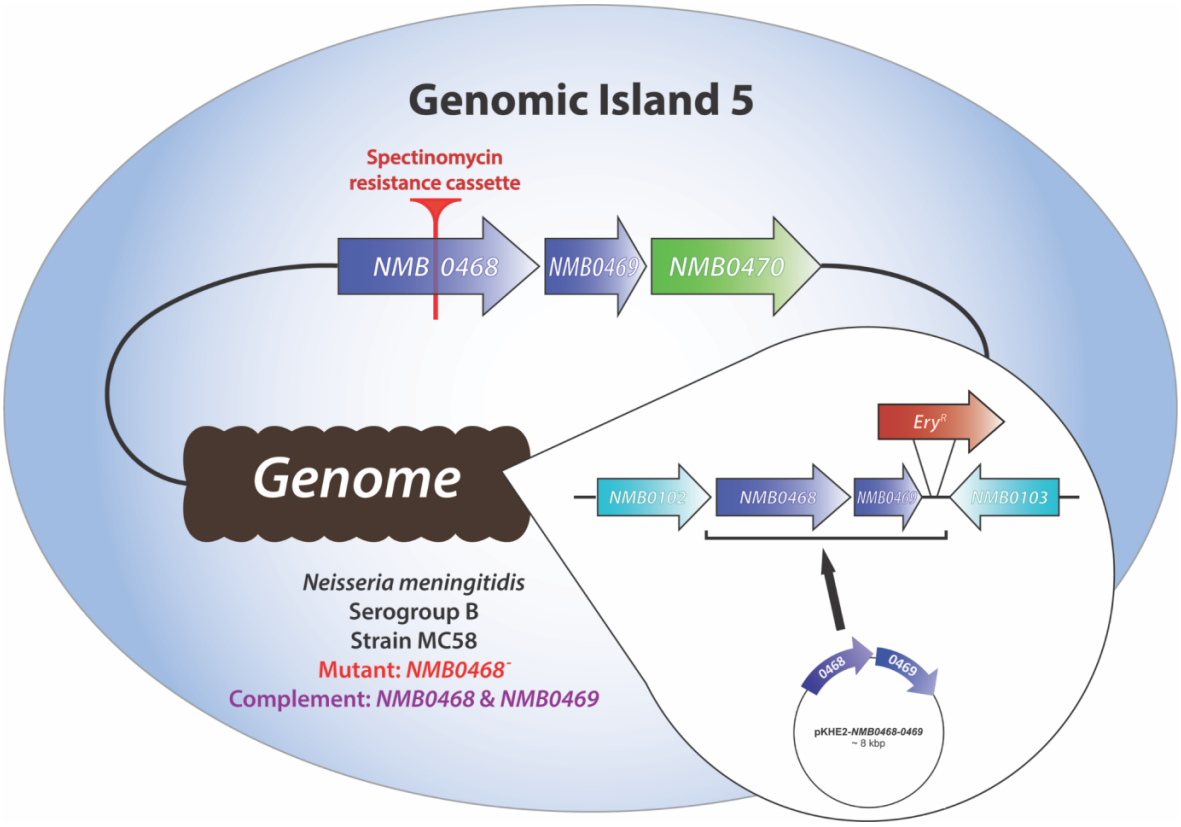

Fig. 3.3-2 (a) – Schematics of the pKHE2-*NMB0468-0469* construct acting as an in-genome insertion under its own promoter within the *NMB0468*$^{-}$ mutant chromosome, as the genes and erythromycin resistance cassette (*Ery*^{R}) crossed over and were incorporated into the intergenic region between *NMB0102* and *NMB0103*.

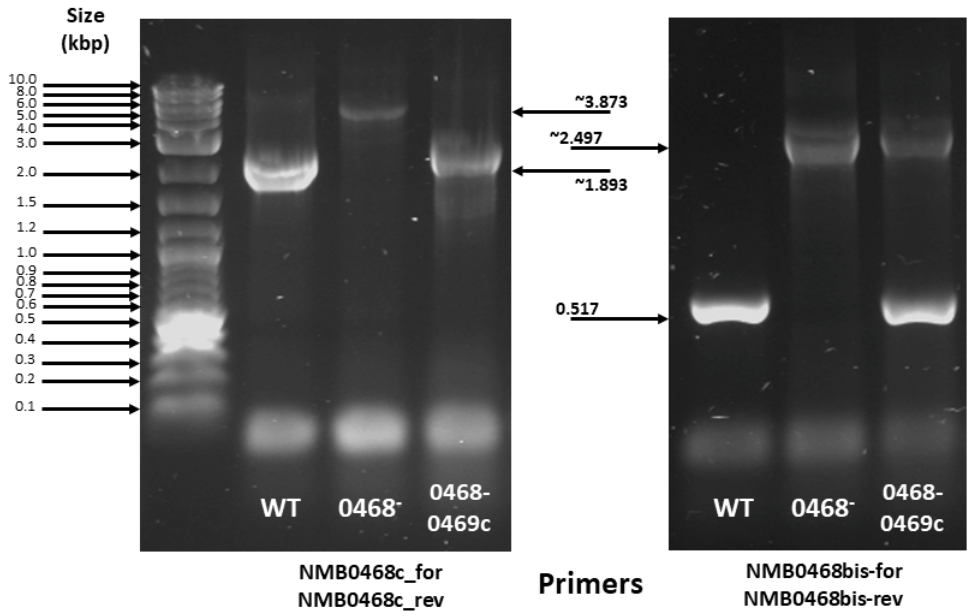

Fig. 3.3-2 (b) – PCR products of the wild type *NMB0468* gene (WT), the disrupted mutant gene (0468$^-$) and the complemented gene (0468-0469c) using (left) the "c" primers that synthesise the entire gene and (right) the "bis" primers that synthesise only the spectinomycin resistance cassette insertion region. When referring to band weights, 2-log DNA ladder (New England BioLabs®) was used.

The *NMB0468-0469*-complemented mutant (*NMB0468-0469c*) was successfully created by reintroducing genes *NMB0468* and *NMB0469* into the *NMB0468*$^-$ mutant chromosome via the erythromycin-resistant vector pKHE2 (Figure 3.3-2 (a)). Sequencing and PCR checks confirm the presence of the pKHE2-*NMB0468-0469* construct (Figure 3.3-2 (b)). The "bis" primers read the short 517 bp region where the 1.98 kbp spectinomycin resistance cassette was inserted, and are able to synthesise both the wild type (or vector-based complement) and the longer, disrupted 2.497 kbp (0.517 + 1.98 kbp) genomic sequences. The "c" primers were used to make the entire sequence inclusive of parts of the intergenic and flanking regions, and preferentially synthesises the shorter, 1.893 kbp wild type (or vector-based complement) product over the longer, approximately 3.893 kbp (1.893 + 1.98 kbp) disrupted genomic *NMB0468* gene. It is therefore possible to recover both intact and disrupted copies of Genomic Island 5 due to the nature of the construct crossing over.

3.4 Effects of putrescine on growth of *N. meningitidis*

3.4.1 Genomic Island 5 mutant grows poorly in MHB compared to wild-type *N. meningitidis*

Müller-Hinton Broth (MHB) (Oxoid) is a rich, undefined liquid media commonly used in microbiology. For more refined analysis of meningococcal growth phenotypes a chemically-defined minimal media (CDM) was used in this study of which the recipe was derived from a modified version of the original Catlin formula (Catlin and Schloer, 1962; Catenazzi, 2013). Details on how to obtain liquid cultures of *N. meningitidis* as well as the complete CDM formula used were described in Chapter 2.

When culturing *N. meningitidis*, aerobic growth of the *NMB0468*$^{-}$ mutant in MHB showed significant impairment in yield and rate compared to the wild-type (Figure 3.4-1 (a)). In light of bioinformatics predictions discussed in Section 3.1, mutant growth was therefore assessed under the more tightly controlled conditions provided by the CDM. While both the wild-type and *NMB0468*$^{-}$ mutant grew noticeably poorer in CDM, significant differences in both yield and rate were observed (Figure 3.4-1 (b)).

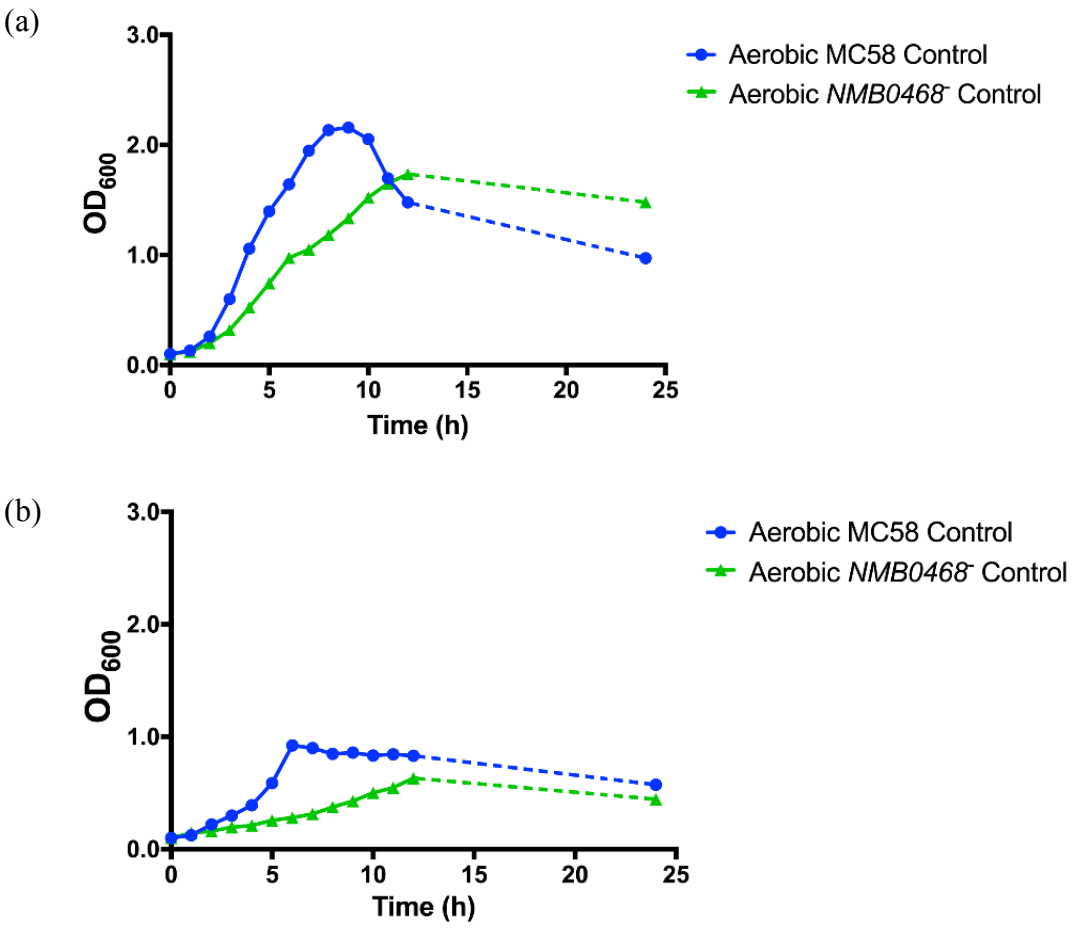

Fig. 3.4-1 – Differences in growth phenotypes of *NMB00468*$^{-}$ mutant compared to wild-type MC58 in **(a)** rich (MHB) and **(b)** minimal media (CDM). The growth curves shown here are representative figures of experiments carried out in technical and biological replicates. The dent in the mutant curve in MHB indicates diauxic growth, where the short lag phase suggests a switch between carbon sources (or other prominent nutrients) during exponential growth (see Section 6.2).

The results were generally in line with the hypothesis that a genetic lesion in the *NMB0468* gene, predicted to be involved in the synthesis of putrescine – which was thought to elicit anti-oxidative effects, was responsible for poorer growth of the meningococci.

3.4.2 Culturing *N. meningitidis* under microaerobic conditions eliminates growth deficit between *NMB0468*$^{-}$ mutant and wild-type

Follow-up to the aforementioned hypothesis (See Section 3.4.1), both the wild-type and *NMB0468*$^{-}$ mutant strains of *N. meningitidis* were cultured in microaerobic conditions. This was achieved by culturing the meningococci in 20 ml of liquid MHB (instead of the usual 10 ml), reducing the volume of air made immediately in contact within the Sterilin® tubes, and reducing the shaker speed to 90 rpm (down from 200 rpm). These settings lowered the oxidative stress incurred upon the bacteria through carefully limiting the rate at which oxygen was made available to proliferating cells.

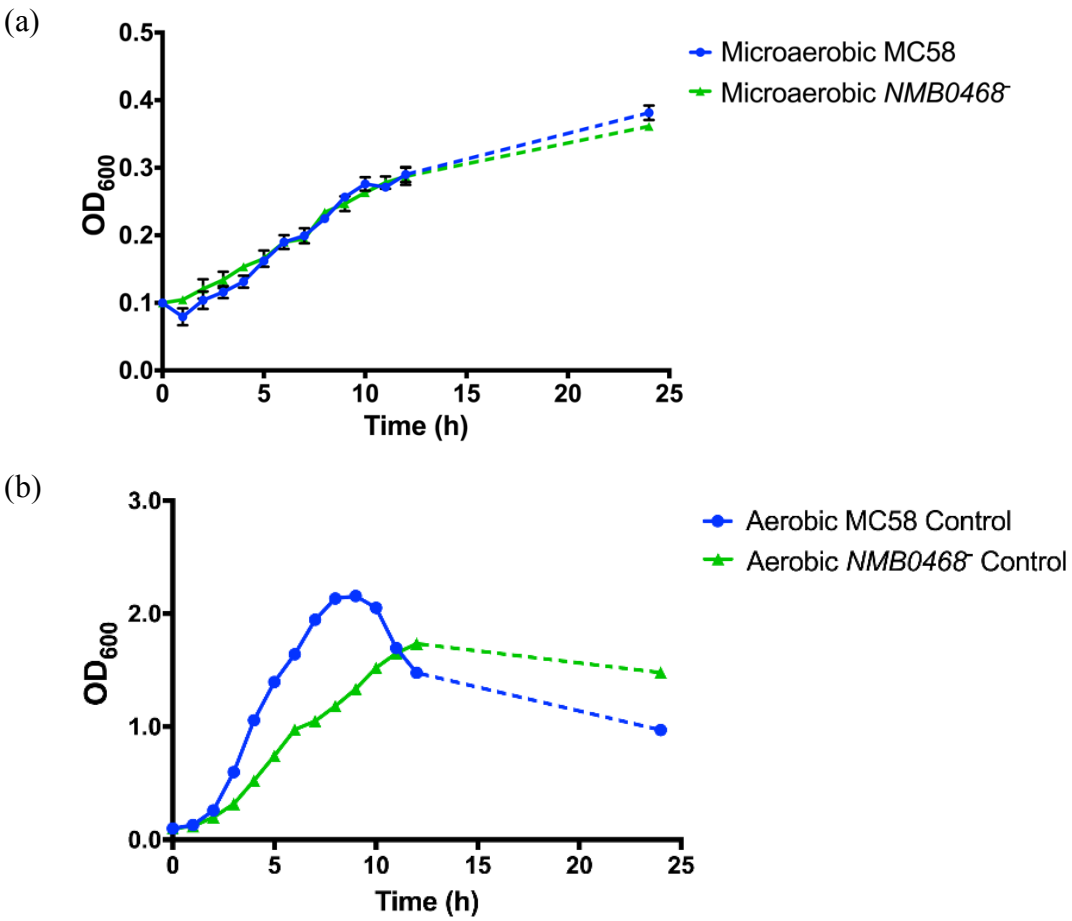

Fig. 3.4-2 – Growth of *N. meningitidis* wild-type MC58 and *NMB0468*$^{-}$ mutant under **(a)** microaerobic and **(b)** aerobic conditions. The growth curves shown here are representative figures of experiments carried out in technical and biological replicates.

The results again provided support for the hypothesis thus far, showing that despite a drastic reduction in both growth rate and yield in both strains (Figure 3.4-2(a)), their growth trends were highly similar to one another when compared to the fully aerobic control (Figure 3.4-2(b)). If Genomic Island 5 was indeed involved in putrescine production, the low oxidative stress present under microaerobic culturing conditions should allow for a growth trend without a marked deficit compared to that of the wild-type through compensating for the inability of the *NMB0468*$^{-}$ mutant to synthesise the polyamine for anti-oxidative purposes. The general slow growth would also be attributable to the limited rate at which oxygen was mixed into the liquid meningococcal culture under microaerobic conditions. This showed that the mutant strain can be similarly sensitive towards such changes when its genetic lesion was accounted for.

3.4.3 Removal of arginine results in poorer *NMB0468*$^{-}$ mutant growth in CDM

To further test for a putrescine biosynthesis pathway in *N. meningitidis*, the starting material L-arginine was removed from the CDM. Both strains were cultured in arginine-

free CDM and the resulting growth trends (Figure 3.4-3(a)) were compared with a control grown in complete CDM (Figure 3.4-3(b)).

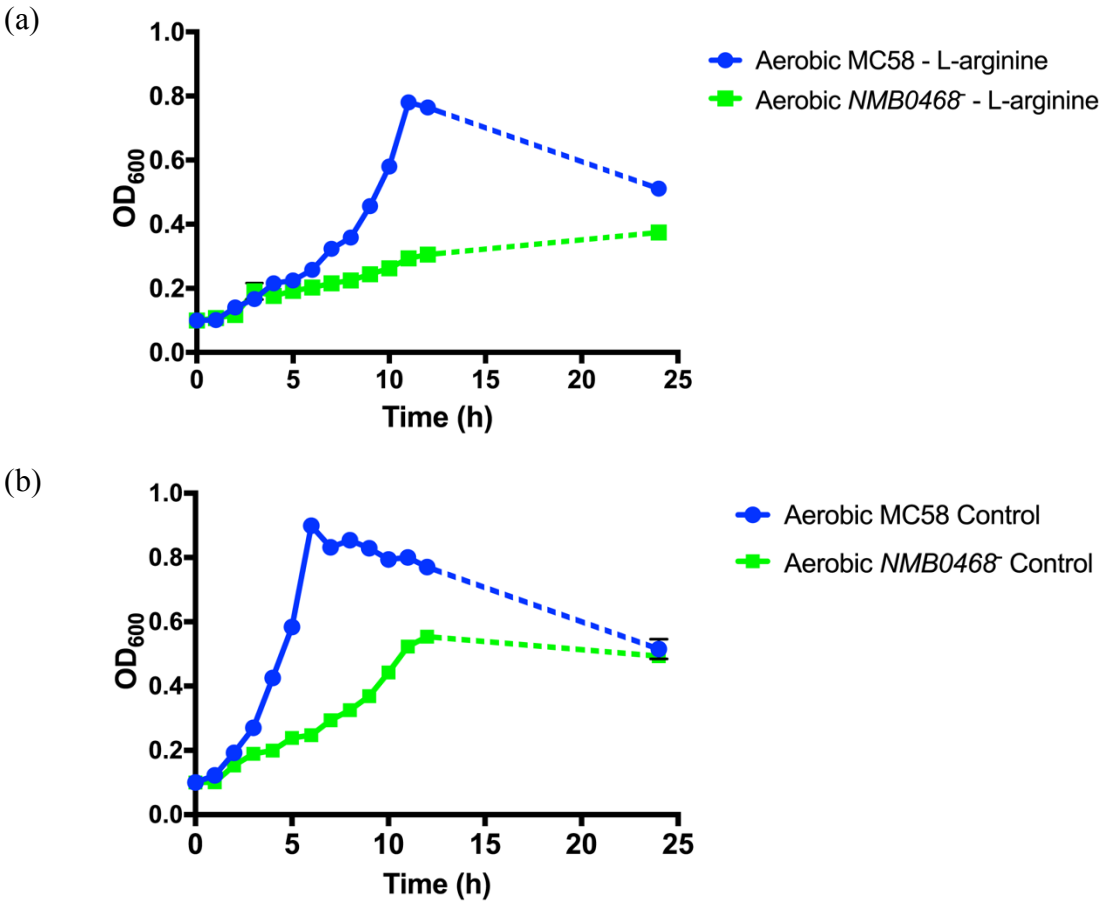

Fig. 3.4-3 – Effects of (a) removal of L-arginine from CDM on *N. meningitidis* wild-type MC58 and *NMB0468*⁻ mutant growth, compared to **(b)** growth of both strains in complete CDM. The growth curves shown here are representative figures of experiments carried out in technical and biological replicates.

The observations fitted with the ongoing hypothesis and bioinformatics predictions (See Chapter 4 for discussion on alternative arginine synthesis pathways). The *NMB0468*⁻ mutant strain appeared to grow significantly poorer in arginine-free CDM than its control in terms of both rate and yield. The wild-type meningococci also displayed a longer lag phase and slower growth rate in arginine-free conditions, suggesting a need to endogenously provide arginine for essential metabolism through alternative means which are energetically less favourable. This was believed to have coupled with the effects of the genetic lesion in the mutant in arginine-free CDM, resulting in both an inability to synthesise putrescine for oxidative protection under aerobic conditions, and a need to utilise other metabolites to synthesise arginine for cellular processes essential to meningococcal maintenance. In summary, arginine removal did not prevent the lesion in the mutant, indicating that the wild-type can still make putrescine (e.g. through

endogenous arginine) in the absence of exogenous arginine albeit experiencing much poorer growth compared to complete CDM.

3.4.4 Exogenous putrescine supplementation restores growth of *NMB0468*⁻ mutant in MHB

Previous findings (See Section 3.4.3) showed that removing L-arginine, the starting material of putrescine biosynthesis pathway, impacted meningococcal growth. To investigate the effects of the end-product, exogenous putrescine was supplemented into MHB at a final concentration of 5 mM (Kurihara *et al.*, 2009) and the growth of both *N. meningitidis* wild-type MC58 and *NMB0468*⁻ mutant were monitored. The results largely conformed to the hypothesis that the mutant was unable to synthesise intact Genomic Island 5, and that adding putrescine appeared to improve both growth rate and yield of the mutant to levels more comparable to that of the wild-type (Figure 3.4-4 (a)) when compared against a putrescine-free plain MHB control (Figure 3.4-4 (b)).

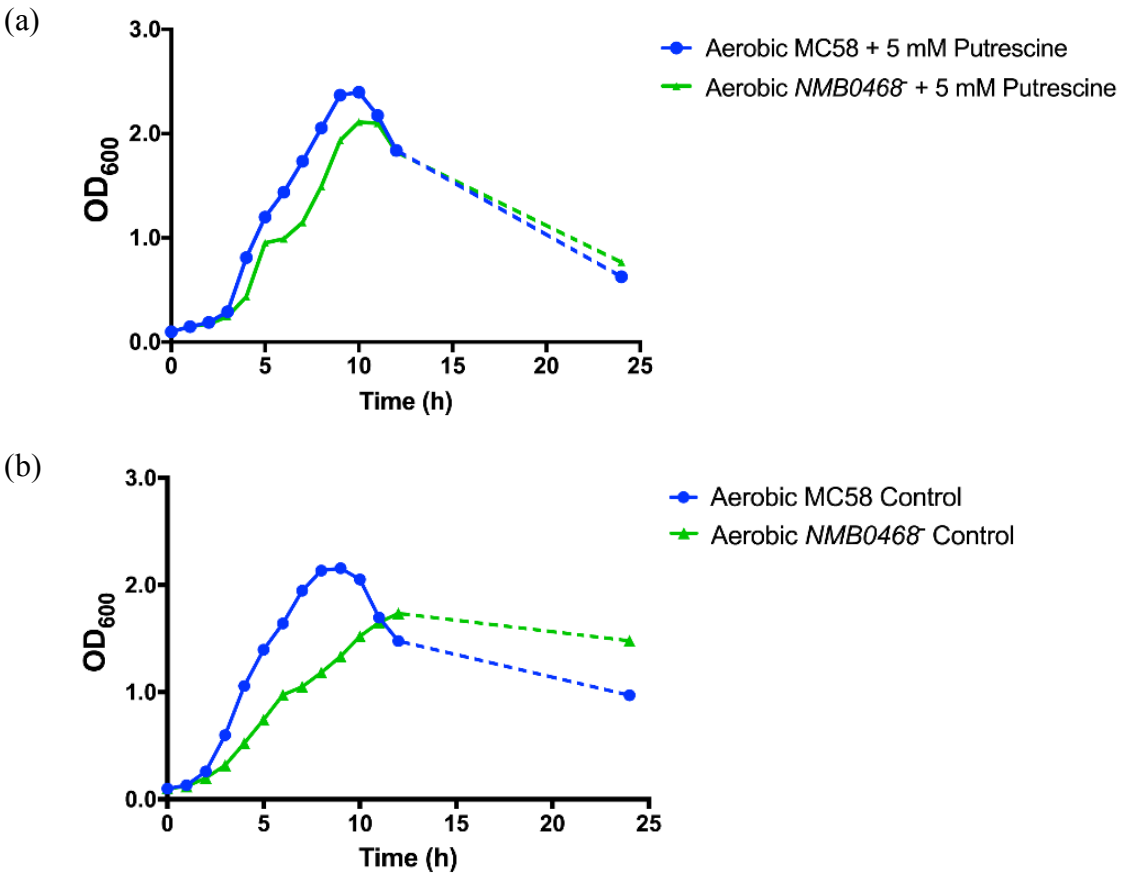

Fig. 3.4-4 – Effects of (a) supplementation by 5 mM putrescine in MHB on *N. meningitidis* wild-type MC58 and *NMB0468*⁻ mutant growth compared to that in **(b)** plain MHB. The growth curves shown here are representative figures of experiments carried out in technical and biological replicates. The lag phase is particularly prominent in the first figure with putrescine (see Section 6.2 for diauxic growth).

For further analysis, these growth conditions were also repeated by supplementing putrescine into CDM. However, the results suggested that it was not possible to rescue growth by adding exogenous putrescine in CDM. Putrescine appeared to incur a certain degree of toxicity towards meningococci at 5 mM, resulting in a prolonged entry into exponential growth phase of the wild-type, as well as lower growth rate and yield of both the wild-type and the mutant strains (Figure 3.4-5(a)).

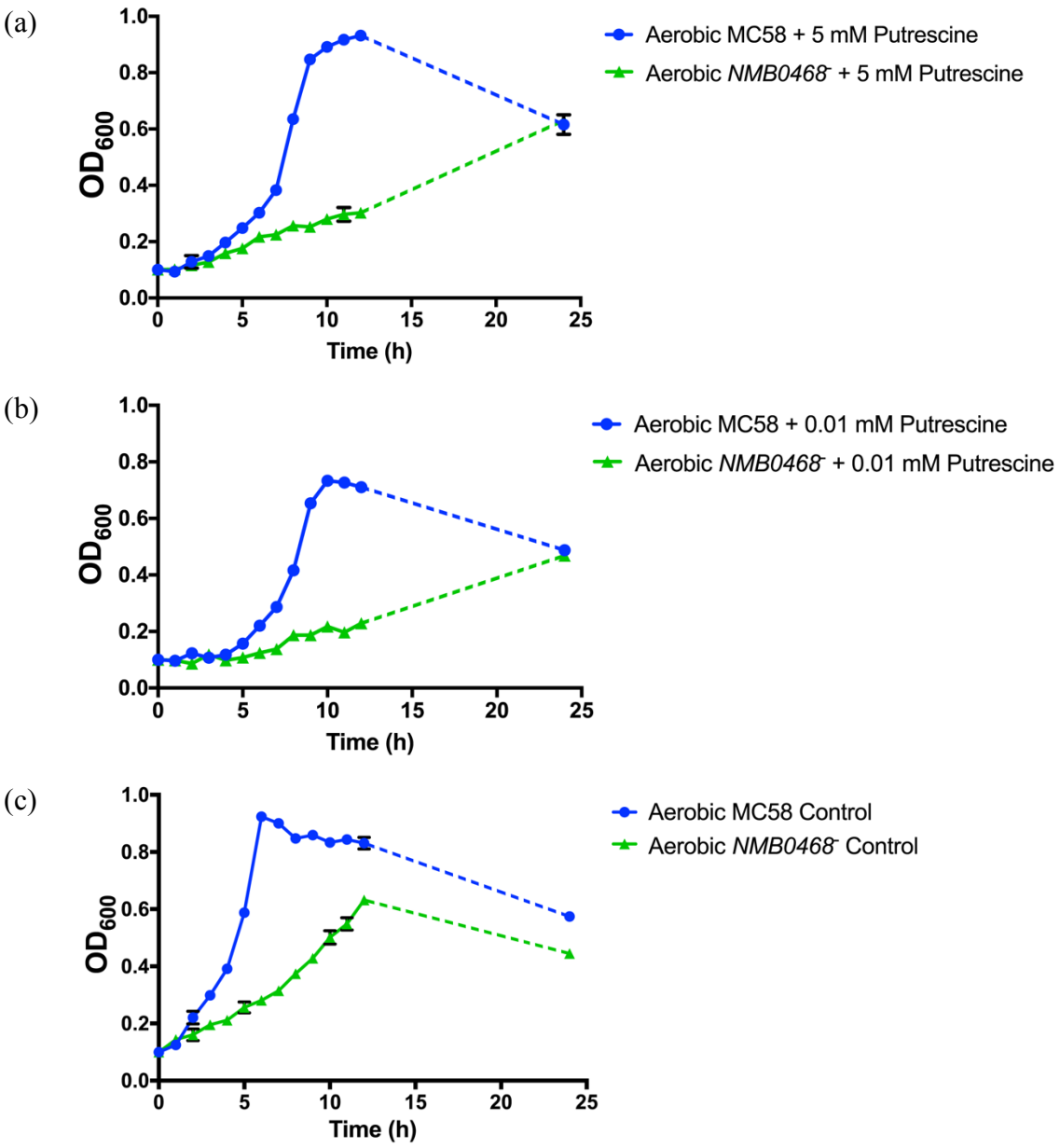

Fig. 3.4-5 – Effects of supplementation by (a) 5 mM and **(b)** 0.01 mM **putrescine** in CDM on *N. meningitidis* wild-type MC58 and *NMB0468*⁻ mutant growth compared to (c) plain CDM. The growth curves shown here are representative figures of experiments carried out in technical and biological replicates.

When compared to putrescine-free CDM-cultured control (Figure 3.4-5 (c)), poorer growth in the form of a longer wild-type lag phase, together with poor growth rate and yield for both strains, were still observed even at low concentrations as 0.01 mM (Figure 3.4-5 (b)). It was possible that competition had arisen between exogenous putrescine and certain CDM-derived metabolites for crucial transporters that resulted in general poor growth, which manifested only in the relatively sensitive nutrient-limited environment of the CDM.

3.4.5 Complementation restores mutant growth to wild-type levels in MHB

Following from Section 3.3, results from culturing the complement construct-transformed MC58Δ*NMB046*::*NMB0468-0469*^{ect} strain showed that exponential growth rate was restored in the *NMB0468*$^{-}$ mutant to wild-type levels (Figure 3.4-6 (a)). The addition of exogenous putrescine also appeared to have no discernible effect on the complemented strain, including the retention of its inability to reach wild-type levels of optimal yield, suggesting possible redundancy of supplementation with construct function and energetic load (Figure 3.4-6 (b)).

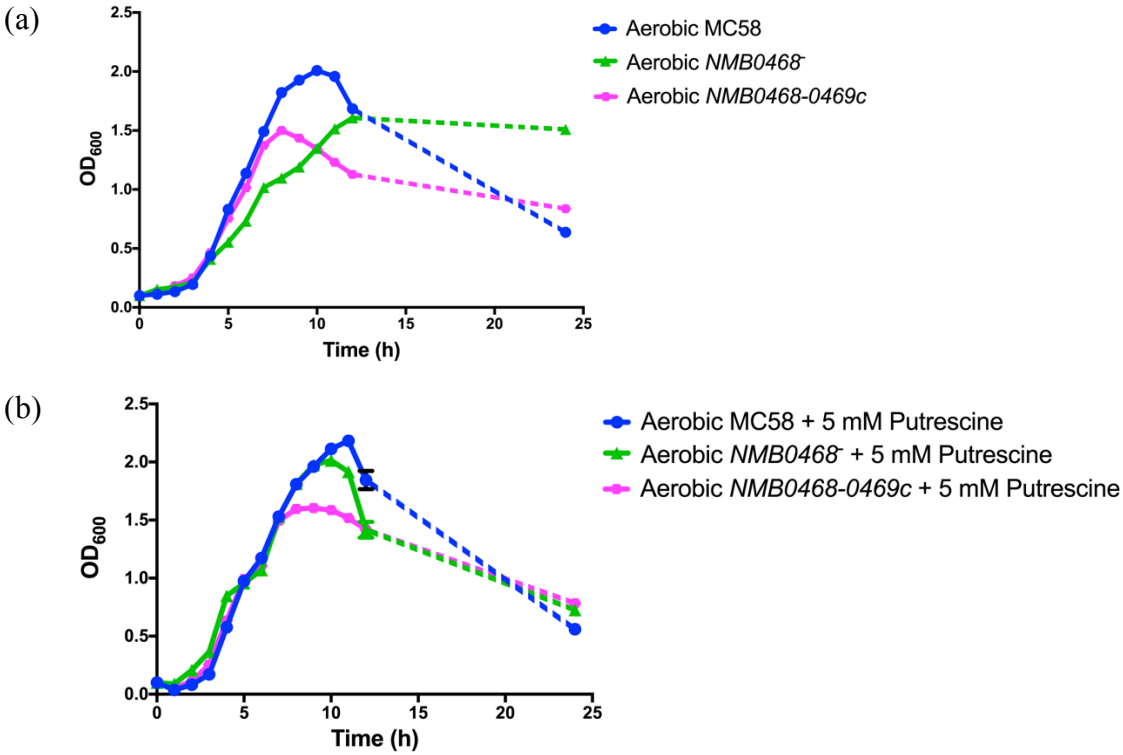

Fig. 3.4-6 – Growth of *N. meningitidis NMB0468*$^{-}$ mutant transformed with erythromycin-resistant pKHE2-*NMB0468-0469* **(a)** construct restores exponential growth of now-complemented mutant to levels comparable to that of wild-type MC58, but **(b)** not yield even in the presence of exogenous putrescine. The growth curves shown here are representative figures of experiments carried out in technical and biological replicates. A noticeable lag phase is present here (see Section 6.2 for diauxic growth).

As part of genetic changes occurring frequently in *N. meningitidis*, the complementation construct crossed over into the intergenic region between *NMB0102* and *NMB0103* on the chromosome. It must therefore be noted that it was possible for intact copies of both wild-type Genomic Island 5 and spectinomycin-disrupted mutant *NMB0468* be recovered.

3.5 Genomic Island 5 is independent of enzymatic defences against oxidative stress

Continuing on the theme of bacterial oxidative stress response mechanisms, catalase and superoxide dismutase (SOD) are enzymes commonly employed by bacteria to deal with reactive oxygen species (ROS). Superoxide dismutase catalyses the breakdown of superoxide radicals into hydrogen peroxide and oxygen, while catalase further breaks down hydrogen peroxide into oxygen and water. In both pathogenic *Neisseria* species, catalase expression is tightly regulated by OxyR (Ieva *et al.*, 2008; Sainsbury *et al.*, 2010; Seib *et al.*, 2006), while both cytosolic and periplasmic metal-cofactored superoxide dismutases protect *N. meningitidis* from host killing (Dunn *et al.*, 2003). Therefore, to explore the possible relationship between Genomic Island 5 and the enzymatic oxidative stress response system, bovine catalase (210U/ml) (from previous work by Fergusson *et al*., unpublished) (Sigma-Aldrich®) and bovine superoxide dismutase (0.01U/ml) (Wilks *et al.*, 1998) (Sigma-Aldrich®) were freshly prepared and supplemented to cultures of *N. meningitidis* wild-type and *NMB0468*$^{-}$ mutant in MHB (Figure 3.5-1).

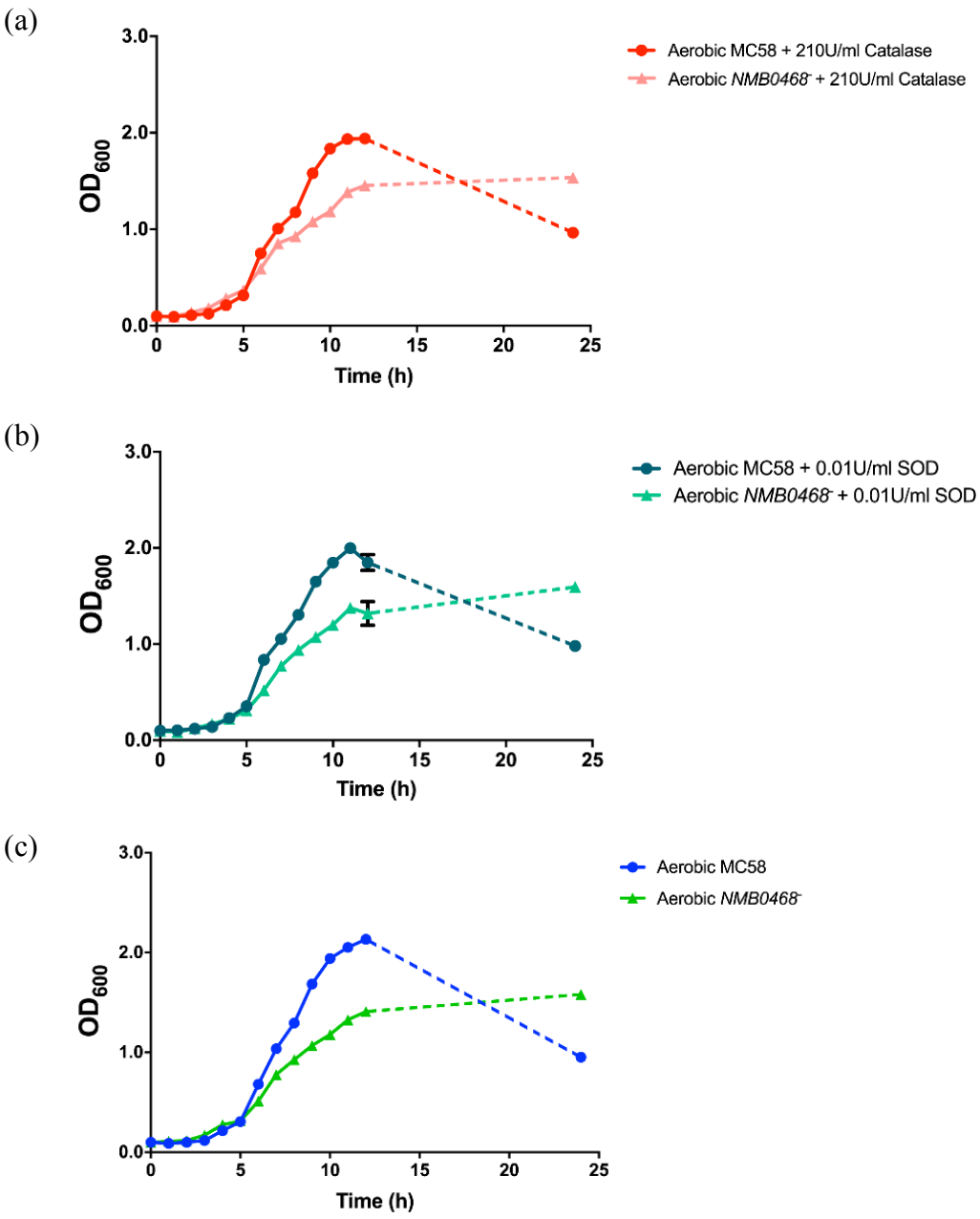

Fig. 3.5-1 – Effects of supplementation of **(a)** catalase and **(b)** superoxide dismutase in MHB on *N. meningitidis* wild-type MC58 and *NMB0468*⁻ mutant growth, compared with growth in **(c)** plain MHB. The growth curves shown here are representative figures of experiments carried out in technical and biological replicates. Some short lag phases can be observed in the figures (see Section 6.2 for diauxic growth).

The results showed that the presence of exogenous catalase and superoxide dismutase had little to no discernible effect on the aerobic growth of both *N. meningitidis* strains in MHB. Both enzymes did not appear to confer any noticeable growth benefits to the mutant, which lacked an intrinsic putrescine synthesis pathway. It is possible that the enzymes acting on oxidative stress response pathways differed from those that normally interact with putrescine, or that putrescine was simply too crucial to omit for *N. meningitidis*. It also remains unclear whether the knockout of the putrescine biosynthesis pathways downregulated the expression of other genes that were vital to meningococcal well-being

which cannot be remedied by catalase and SOD. In summary, the results suggested that enzymatic defences against oxidative stress in *N. meningitidis* was independent of the availability of and ability to synthesise putrescine.

3.6 Measurement of putrescine in *N. meningitidis*

Given its importance as demonstrated by the deficient mutant, it is desirable to be able to quantify or monitor the concentrations of putrescine in culture and within *N. meningitidis* undergoing exponential growth so as to assess how the polyamine may work under physiological conditions. As polyamines do not significantly absorb above 250 nm, it is difficult to achieve direct optical detection using UV. Protocols that involve chemical derivatisation such as benzoylation (i.e. adding benzoyl group to molecule for UV absorbance) prior to analyses by mass spectrometry or HPLC (high-performance liquid chromatography) are commonplace for polyamines but lengthy, while the presence of other molecules impacts assay sensitivity and specificity. Getting separation on typical C18 columns also requires strong ion-pairing reagents which have a tendency of contaminating equipment in the long-term. Advancements in analytical chemistry allow for the use of synthetic, "supramolecular" structures (Anslyn, 2007). By altering the chemical or physical properties of the target molecule, these techniques are believed to be comparatively more selective and robust in its application. Given that polyamines have highly charged yet relatively low molecular weights, detection could be achieved by diluting the samples into an appropriate matrix to obtain a cationic pseudo chromatographic peak through direct infusion into a mass spectrometry system. The polyamine components could subsequently be identified by their *m*/*z* values, as they are intensely protonated at low pHs, by comparing the now-enhanced peaks with that of a suitable internal standard molecule.

Samples were prepared by harvesting fresh cultures of *N. meningitidis* wild-type MC58 and *NMB0468*$^{-}$ mutant strains grown to mid-log phase in MHB. Each 1 ml aliquot was then centrifuged at 12000 rpm, after which the supernatant was carefully separated from the pellet. For safety reasons, both the supernatant and pellet samples were treated with 100 µl 1 M hydrochloric acid (HCl) (Fisher Chemical) for 5 minutes followed by neutralisation with 100 µl 1 M sodium hydroxide (NaOH) (Fisher Chemical) for 5 minutes to allow for thorough killing of the pathogen prior to transport to non-Category 2* laboratory environments. Both the killed pellet and supernatant samples were centrifuged at maximum speed and resuspended in fresh, plain MHB. The samples were then analysed by flow-injection mass spectrometry or frozen until further use.

By coupling free putrescine in solution with a curcubit[7]uril nanocontainer, and using amantadine as an internal standard, the samples were analysed by adapting the protocol described by Galego *et al.*, (2016). As a clean-up step, samples were loaded onto an UltiMate 3000 HPLC system (Thermo Scientific) equipped with a Security Guard™ cartridge C_{18} trap column (2 mm x 4 mm) (Phenomenx) in aqueous 1% (v/v) formic acid. After 2 minutes the eluent was switched to methanol 1% (v/v) formic acid and held for 1.5 minutes. The column was re-equilibrated to aqueous 1% (v/v) formic acid for 0.5 minutes before subsequent injections. A flow rate of 200 µl/min and a column temperature of 40 °C were used throughout.

The HPLC system was interfaced with a maXis HD mass spectrometer (Bruker Daltonics) with an ESI source (Bruker Daltonics). Instrument control, data acquisition and processing were performed using Compass 1.7 software (microTOF control, Hystar and DataAnalysis) (Bruker Daltonics). Positive ESI-MS spectra were acquired using the following instrument settings: ion spray voltage: 4000 V, dry gas: 4 L/min, dry gas temperature 200°C, ion acquisition range: *m/z* 400-1,300, MS spectra rate: 1 Hz, quadrupole low mass: 400 *m/z*, collision RF: 1200 Vpp, transfer time 110.0 µs.

Bruker DataAnalysis 4.4 software was used for peak picking and integration. Extracted ion chromatograms at *m/z* 626.73 and 657.74 were extracted with ± 0.02 *m/z* tolerance. Sum Peak algorithm was used for peak picking with S/N threshold of 1, relative intensity threshold (base peak) 0.1% and absolute threshold 100. Chromatograms were integrated using algorithm version 3.0 MS with sensitivity 99 %, intensity threshold 100 and min peak valley 10%.

To establish a putrescine standard, 1 ml MHB was spiked with putrescine and serially diluted to give final concentrations of 5 mM, 2.5 mM, 1 mM, 0.5 mM, 0.25 mM and 0.05 mM respectively. Analysis of the raw data (Table 3.6-1) showed that putrescine can be confidently identified as low as 0.025 mM (Figure 3.6-1).

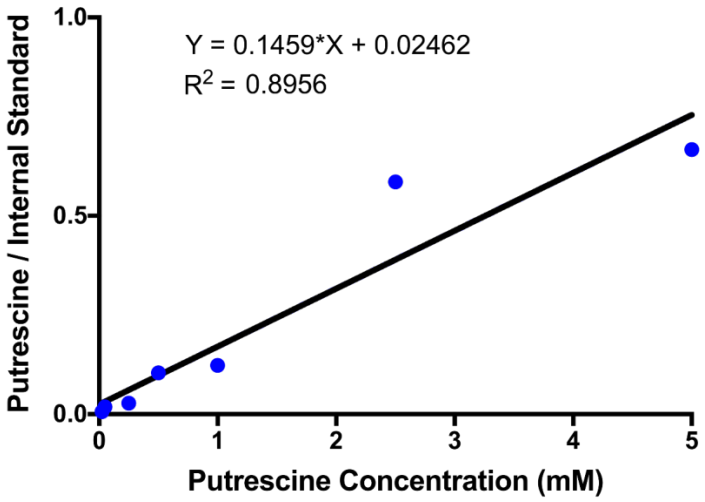

Fig. 3.6-1 – Putrescine standard curve generated through diluting stock **putrescine** solution with MHB in series and the internal standard **amantadine**. The ratio of the area under the peaks of putrescine to that of amantadine is plotted, and a line of best fit extrapolated with the slope equation and R^2 value shown.

Putrescine Concentration (mM)	Putrescine Area	Internal Standard Area	Putrescine / Internal Standard
0.05	10952.9	591081.8	0.0185
0.25	35012.7	1254127.1	0.0279
0.5	85044.1	816295.4	0.1042
1.0	122699.4	994418.0	0.1234
2.5	379616.8	648549.9	0.5853
5.0	779677.4	1168902.6	0.6670

Table 3.6-1 – Raw data used for the generation of the putrescine standard curve from serially-diluted **putrescine** and the internal standard **amantadine** in MHB. The ratio of the area under the peaks of putrescine and amantadine is proportional to their corresponding putrescine concentrations.

However, when analysing the data for the *N. meningitidis* wild-type and *NMB0468*$^-$ mutant supernatant samples, no clearly-defined signal could be observed for putrescine (data not shown). To ensure that putrescine was detectable in the supernatant sample mixtures, they were spiked with a final concentration of 0.05 mM putrescine, from which clear signals could be seen. This implied that the level of putrescine in both supernatant samples, if present, were below the protocol's limit of detection.

The pellet samples of the wild-type and *NMB0468*$^{-}$ mutant strains were analysed similarly but also failed to show detectable signals. Similarly, spiking the pellet mixtures with a final concentration of 5 mM putrescine yielded clear signals for putrescine. This also implied that the level of putrescine in both pellet samples, if present, were below the protocol's limit of detection.

3.7 Discussion

The above findings summarily supported the hypothesis that the two Genomic Island 5 members NMB0468 and NMB0469 form a functional putrescine biosynthesis pathway. This mechanism clearly confered significant advantages to *N. meningitidis* by restoring the exponential phase when aerobically grown in rich media (i.e. MHB), a condition where meningococci were vulnerable to the effects of substantial levels of oxidative stress. Despite inconclusive results, there remained the possibility that differences in putrescine levels existed between wild-type *N. meningitidis* and the *NMB0468*$^{-}$ mutant strains but were below the detection threshold of the instruments employed. It is also possible that biogenic putrescine in culture had been complexed or reacted with other molecules prior to being presented for assay. Intracellular concentration of putrescine is approximately 0.1 – 0.2 mM "in almost all bacteria" (Shah and Swiatlo, 2008). There are exceptions to this generalisation however, as *E. coli* putrescine levels are much higher (around 10 – 30 mM), hence in the case of *N. meningitidis* it is possible for that range to be both considerably higher or lower. Experimentally, *E. coli* had been shown to export up to 50 µM *o*-phthalaldehyde-derivatised putrescine in (per 500 µl, approximately, of) harvested minimal-media-grown culture supernatants (Sugiyama *et al.*, 2016). When taking into consideration of physiological and growth differences between the two bacteria, perhaps the actual intracellular putrescine concentrations in *N. meningitidis* may indeed be much lower as the scale reaches the lower end of the sensitivity of the techniques employed in this study.

An enzyme-coupled assay was previously attempted prior to the use of more sensitive mass spectrometry techniques, known as the spectrophotometric diamine oxidase (DAO) assay (Adapted from Schwelberger, 2012). This relatively simple technique made use of coupling NH_4^+ production in the DAO-catalysed break-down of diamines (such as putrescine) to NH_4^+ consumption in a reaction catalysed by glutamate dehydrogenase (GLDH):

Reaction A: Substrate (diamine) + O_2 + H_3O^+ —**DAO**⟶ Product (aminoaldehyde) + $\mathbf{NH_4^+}$ + H_2O_2

Reaction B: $\mathbf{NH_4^+}$ + α-ketoglutarate + **NADH** —**GLDH**⟶ Glutamate + $\mathbf{NAD^+}$ + H_2O

As one molecule of NADH oxidised by GLDH corresponded to one molecule of substrate converted by DAO, putrescine levels may be quantified in a one-to-one ratio by monitoring the decrease in NADH spectrophotometric absorbance levels through the use of the Beer-Lambert Law $\Delta A = \varepsilon c \ell$ (where ΔA was the change in absorbance; ε was the extinction coefficient; c was the concentration in mM; ℓ was the length of the solution light had to pass through in cm). For the width of a standard 1 ml quartz curvette, ℓ was 1 cm and ε was 6.22 at A_{340} for NADH. Both pellets and supernatants were harvested in a similar manner as in Section 3.6 with the addition of washing with phosphate buffer solution, and the reaction mixture kept in a potassium buffer of pH 7.4. The results (data not shown) failed to distinguish between both *N. meningitidis* wild-type MC58 and *NMB0468*$^-$ knockout mutant, whether the sample was pellet or supernatant. The calculated c values were highly similar, which suggest that the assay was either too non-specific and insensitive for the purpose of putrescine detection in MHB cultures, or that there were other substrates (such as diamines other than putrescine) in play in the meningococcal extracts that complexed the enzyme reactions. It therefore remains a challenge to devise a method to conveniently and economically quantify polyamines in *N. meningitidis* with relative precision.

On the other hand, albeit not having a convincing conclusion to the cause of putrescine toxicity in CDM, one valuable aspect of work carried out in a defined media was that it allowed for the selective inclusion or exclusion of substrates such as L-arginine from the media. This enabled a fine inspection of both ends of cellular pathways in tandem with the construction of mutants with the corresponding lesion, as demonstrated above. Although unable to elicit optimal growth rate and yield for *N. meningitidis*, this is a powerful investigative tool which played a significant role in the characterisation of other meningococcal genomic islands (See Chapter 4) (Catenazzi, 2013).

3.7.1 *NMB0470* is unlikely to be central to Genomic Island 5

The *NMB0468-0469c* complemented mutant was constructed to reinforce the essentiality of the meningococcal arginine decarboxylase and agmatinase homologues in aerobic growth, as well as determining the role of NMB0470. The uncertainty was whether the original *NMB0468*$^-$ knockout mutant is truly unable to express the downstream genes

NMB0469 and *NMB0470*, since it had not been shown whether Genomic Island 5 is an independent operon.

Phenotypes generated from aerobic growth of the *NMB0468-0469c* strain provided no strong implication as to the precise function of the putative transporter NMB0470, as the exclusion of *NMB0470* did not appear to impair the growth of the complemented mutant. In other pathogens such as *Streptococcus pneumoniae*, the genomes contain well-characterised transporters (e.g. *potABCD* family of operons) for polyamines of which deficiency resulted in impaired pneumococcal virulence (Shah *et al.*, 2011). In addition to weak bioinformatics support for its initial annotation as a C_4-dicarboxylate transporter in *N. meningitidis,* there also did not appear to be any similarities between NMB0470 and this ABC (ATP-binding cassette) family of transporters. Although in bacteria such systems may be shared among or dependent on other biogenic molecules (symporters and antiporters) (Driessen *et al.*, 1988), it was entirely possible that NMB0470 was unrelated to exclusive transport or metabolism of polyamines in *N. meningitidis*.

In summary, complementation with *NMB0468* and *NMB0469* restored the growth of a Genomic Island 5 mutant independent of *NMB0470*. Nonetheless, this inconclusive finding of interest warrants future investigation for more thorough characterisation of Genomic Island 5.

3.7.2 Mechanisms for protection against biochemical stress

One of the standing aims of the study was the proposal of a primary mechanism by which putrescine or other polyamines contribute to the protection of *N. meningitidis* against oxidative or nitrosative stress. Literature suggested that it may well be a mix of polyamine-mediated defence mechanisms, interaction with the host microenvironment, as well as transcriptional and translational control of stress response genes.

While there had not been solid evidence, polyamines have been regarded to act as a possible protective charge sink at times due to their highly cationic nature. It was first proposed that the higher polyamines spermidine and spermine prevent DNA conformational changes (Khan *et al.*, 1992). Since then some argued more extensively for polyamines as free radical scavengers aside from DNA association and metal chelation (Ha *et al.*, 1998). Aside from free radical damages, mutant *E. coli* deficient in polyamine biosynthetic pathways were also found to be more susceptible to damage by gastric acid and show impaired host colonisation, and addition of exogenous polyamines restored these traits – essential for food-borne pathogens – by inducing increased expression of acid-resistance genes (Chattopadhyay and Tabor, 2013). Apart from direct biochemical

protection, it is also possible that polyamines play a role in the mediation of transcriptional changes through signalling that confer survival advantages to a pathogen. In drug-resistant *Burkholderia cenocepacia*, exposure to sublethal doses of polymyxin B induced the upregulation of the oxidative stress response regulator *oxyR* and ornithine decarboxylase (i.e. speC in *E. coli* but no predicted meningococcal homologue) (El-Halfawy and Valvano, 2014). It is therefore entirely possible that putrescine may also act in a similar fashion to provide antioxidant coverage to *N. meningitidis*. However, as this study was not able to successfully quantify or monitor putrescine levels during meningococcal growth, it remains an area open to follow-up investigations for exploration.

3.7.3 *N. meningitidis* in face of host immunogenic challenges

Human macrophage represents one of the primary adversaries of *N. meningitidis* in its natural niche, the nasopharyngeal mucosa. Upon induction, activated macrophages are able to mediate the release of reactive oxygen (ROS) and nitrogen species (RNS) to facilitate the killing of pathogens. Mechanisms to resist or evade these antimicrobial radicals are therefore important virulence factors, promoting host colonisation. Constant exposure to nitrosative stress generated by patrolling macrophages as well as its own metabolism has prompted *N. meningitidis* to act as denitrifiers under microaerobic conditions (Anjum *et al.*, 2002). This also contributes towards the ability of *N. meningitidis* in adapting to oxygen-limiting growth conditions in the nasopharynx, as it is able to use nitrite (NO_2^-) as an alternative to oxygen (O_2) (Heurlier *et al.*, 2008).

Apart from RNS, *N. meningitidis* also developed the ability to withstand the onslaught of ROS, such as the aforementioned OxyR-regulated catalase activity and direct dismutation of superoxides. The meningococci had been shown to employ iron-dependent, Fur (ferric uptake regulator)-regulated pathways to defend against oxidative stress generated by peroxides or PMN leukocytes (Grifantini *et al.*, 2004). Fierce competition from other niche occupants like *Streptococcus pneumoniae* and *Haemophilus influenzae* also gave rise to innovative means of sabotage (Shakhnovich *et al.*, 2002), where bacterial oxidative stress can be regarded as weapons against both host and competitor cells (Yesilkaya *et al.*, 2013; Zahlten *et al.*, 2015). These provide solid groundwork and sound reasoning for the ongoing investigation of the extent of the influence of polyamines on the maintenance of the meningococci, where a plausible approach would be the creation of peroxidase/catalase-deficient mutants through the crossing of competent cells. It would be informative if survival assays could be carried out to determine if polyamines elicit protective effects for *N. meningitidis* (mutants) against human macrophages in culture as an assessment of

pathogenicity. Particular care must be paid, however, when selecting the appropriate cell lines in order to uphold relevance of any potential findings to *in vivo* settings.

Chapter 4 – Investigating a pathogen-specific genomic island in *Neisseria meningitidis*

4.1 Introduction and Bioinformatics

A previously discussed in Chapter 1, 9 genomic islands are found highly conserved in *Neisseria meningitidis* strains, but absent from its closely related commensal cousin *Neisseria lactamica*. One such pathogen-specific island is comprised of two genes of unknown function, *NMB0239* and *NMB0240* in *N. meningitidis* serogroup B strain MC58. The island (meningococcal Genomic Island 3) is present in both Neisserial pathogens (i.e. *N. meningitidis* and *N. gonorrhoeae*) but is absent from all other *Neisseria* species with sequenced complete genomes. It is believed to have been acquired via horizontal gene transfer followed by chromosomal rearrangements where flanking genes are of low synteny in *N. lactamica*. As previously shown in Figure 1.4-3, the adjacent divergently transcribed gene in *N. lactamica* could be found elsewhere in the meningococcal and gonococcal genome (i.e. in a circular *N. meningitidis* genome: *NMB2127* is approximately 281 kbp from start of *NMB0240*; in *N. gonorrhoeae*: *NGO1963* is approximately 226 kbp from end of *NGO1752*). Homologues of neighbouring NMB0238 – a hypothetical protein, were predicted to contain similarities to annotated putative IS*1016*-like transposases. In *N. lactamica* the sequence is part of gene *NLA_1870*, which is flanked by repeated DNA uptake sequences (DUS).

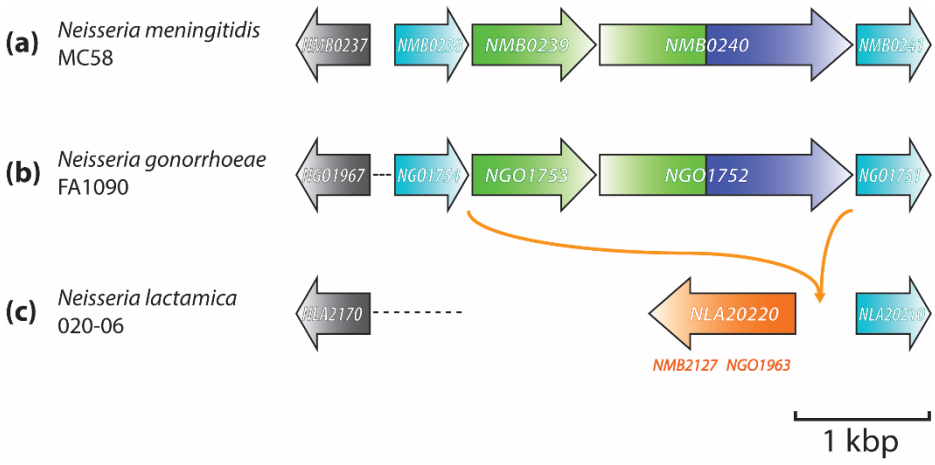

Fig. 4.1-1 – Genomic Island 3 is present in both pathogenic *Neisseria* species but absent in the commensal *N. lactamica*. (a) The meningococcal genes *NMB0239* and *NMB0240* are homologous to **(b)** gonococcal genes *NGO1753* and *NGO1752*. **(c)** the *N. lactamica* gene *NLA20220* corresponds to meningococcal *NMB2127* and gonococcal *NGO1963* located further downstream in their respective genomes. Although *N. lactamica* lacks a homologue of the meningococcal island-flanking gene *NMB0238*, it appears to contain a homologue of the gene further upstream, *NMB0237* (i.e. *NLA2170*). The same also applies to the gonococcal homologue *NGO1967*.

When subject to protein BLAST analysis, the sequence of *NMB0239* returns non-specific hits belonging to a superfamily of proteins with only annotated functions for spermidine synthase (*E. coli* SpeE). When *Neisseria* is excluded, the database only returns hypothetical bacterial proteins with hits of less than 60% sequence identity (Table 4.1). On the other hand, the sequence of *NMB0240* results in specific hits towards the C-terminal (approximately 230 amino acids) for *S*-Adenosyl-L-Methionine (SAM) binding sites typical of spermidine synthases (*E. coli* SpeE) belonging to the SAM-dependent methyltransferase superfamily class I, as well as non-specific hits towards the N-terminal (approximately 170 amino acids) for proteins belonging to the Major Facilitator Superfamily (MFS) of transporters. When *Neisseria* is excluded, the database only returns hits with less than 50% sequence identity, and does not appear to return well-characterised bacterial proteins (Table 4.2).

Alignment hit	Query cover	E value	Identity	Accession number
hypothetical protein F908_00393 (*Acinetobacter* sp. NIPH 284)	99%	2e-69	54%	ENW84791.1
hypothetical protein (*Aggregatibacter aphrophilus*)	100%	4e-66	52%	WP_005702990.1
hypothetical protein (*Acinetobacter* sp. CIP 56.2)	97%	1e-65	54%	WP_004803936.1
hypothetical protein (*Basilea psittacipulmonis*)	97%	2e-65	59%	WP_077315864.1
hypothetical protein (*Aggregatibacter actinomycetemcomitans*)	99%	3e-64	52%	WP_019518403.1
hypothetical protein (*Acinetobacter towneri*)	100%	5e-63	51%	WP_070153804.1
hypothetical protein HMPREF9065_02107 (*Aggregatibacter* sp. oral taxon 458 str. W10330)	98%	4e-62	50%	ERH26145.1
hypothetical protein A2W44_03925 (*Acinetobacter* sp. RIFCSPHIGHO2_12_41_5)	92%	1e-61	56%	OFW94067.1
membrane protein (*Haemophilus ducreyi*)	98%	1e-59	54%	WP_010945191.1
hypothetical protein (*Simonsiella muelleri*)	96%	5e-54	56%	WP_002642737.1

Table 4.1 – Top 10 hits from protein BLAST results of Genomic Island 3 member *NMB0239* against species outwith *Neisseria*. Redundant hits belonging to the same species are omitted. Accessed 4th May 2017.

Alignment hit	Query cover	E value	Identity	Accession number
Hypothetical protein F908_00394 (*Acinetobacter* sp. NIPH 284)	100%	7e-159	45%	ENW84792.1
Hypothetical protein IX83_05845 (*Basilea psittacipulmonis* DSM 24701)	99%	1e-157	47%	AIL32904.1
Hypothetical protein (*Simonsiella muelleri*)	100%	4e-157	49%	WP_002642738.1
Hypothetical protein (*Basilea psittacipulmonis*)	99%	3e-154	47%	WP_077315864.1
Hypothetical protein A2W44_03920 (*Acinetobacter* sp. RIFCSPHIGHO2_12_41_5)	100%	4e-150	45%	OFW94062.1
Hypothetical protein (*Acinetobacter towneri*)	100%	1e-146	44%	WP_070153493.1
Spermidine synthase (*Acinetobacter* sp. CIP 56.2)	100%	2e-142	44%	WP_004803939.1
Spermidine synthase (*Aggregatibacter actinomycetemcomitans*)	99%	3e-139	44%	WP_005568859.1
Spermidine synthase (*Haemophilus ducreyi*)	99%	3e-139	44%	WP_064083169.1
Spermidine synthase (*Aggregatibacter actinomycetemcomitans*)	99%	4e-139	44%	WP_005578206.1

Table 4.2 – Top 10 hits from protein BLAST results of Genomic Island 3 member *NMB0240* against species outwith *Neisseria*. Redundant hits belonging to the same species are omitted. Accessed 4th May 2017.

NMB0239 encodes a protein of 206 amino acids (with a predicted molecular mass of 22298), while *NMB0240* encodes a protein of 483 amino acids (with a predicted molecular mass of 53511). *NMB0239* as well as the 205 N-terminal amino acids of NMB0240 are predominantly hydrophobic, and are predicted to each contain 6 transmembrane helices (using online TMHMM software packages by CBS, SOSUI and by SACS). A soluble periplasmic domain is predicted towards the C-terminal of NMB0240 from amino acids 205-483. Initial analyses have annotated NMB0240 and some of its homologues as spermidine synthase due to the purported presence of SAM-binding domains. However, *N. meningitidis* does not appear to contain functional homologues of the enzyme SAM decarboxylase (*E. coli* SpeD) whose product (decarboxylated SAM) is vital to the function

of spermidine synthases (See Chapter 3). Upon finer inspection, the similarities are low compared to experimentally-validated spermidine synthases (only 21% sequence identity with the *E. coli* SpeE). The domain also lacks 5 key amino acid residues (D88, D158, D161, Y63 and Y226) which are completely conserved and vital for aminopropyltransferase activity, rendering it unfeasible for the encoding of spermidine synthase (Figure 4.1-2).

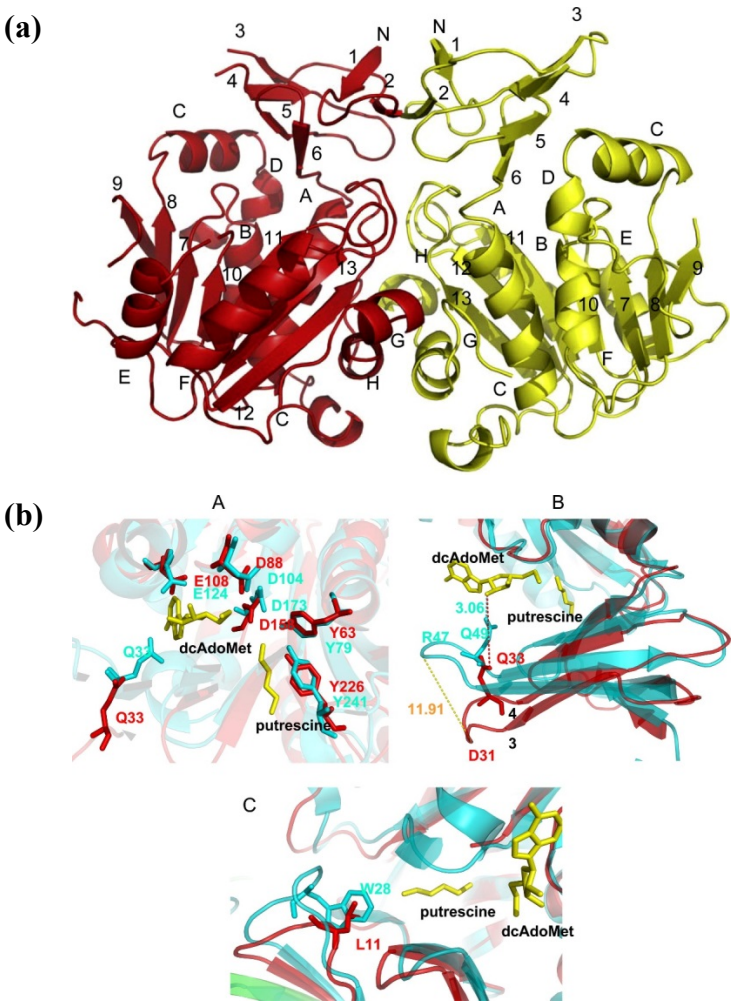

Fig. 4.1-2 – The *E. coli* spermidine synthase SpeE: **(a)** structural representation of SpeE and **(b)** key amino acid residues important for catalysis but not conserved in NMB0240) (from Zhou *et al.*, 2010).

In order to analyse the overall properties of this putative structural element, the sequences of *NMB0239* and the 205 N-terminal amino acids of *NMB0240* were also fused *in silico*. When searched with aforementioned TMHMM software packages, the results yielded a putative protein with similarities to Major Facilitator Superfamily (MFS) transporters consisting of about 12 predicted transmembrane spans and a periplasmic C-terminus (Figure 4.1-3). Such a structural profile is typical of proteins involved in transport of metabolites (Henderson, 1993). Despite not having been previously characterised, the arrangement resembles a transporter consisting of a split membrane-spanning MFS-like

domain fused to a soluble periplasmic domain as a possible expression product, and is suggestive of a transporter for the capture and uptake of small molecule substrates into the meningococcus.

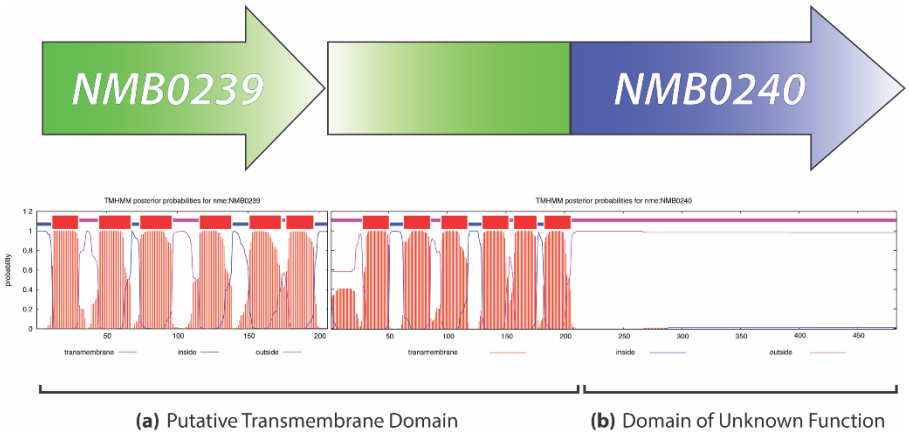

Fig. 4.1-3 – TMHMM predicts the presence of 12 transmembrane spans split across NMB0239 and NMB0240. (a) The 12-helix arrangement is suggestive of (green) transporter functions, while; **(b)** the soluble region is annotated to have a role in (blue) metabolism.

It is therefore hypothesised that Genomic Island 3 encodes for a transport system for the uptake of material(s) crucial to the maintenance and survival of *N. meningitidis* during aerobic growth. The supplementation of such material(s) should elicit a marked response in wild-type growth, which possesses intact copies of the island, while the mutant is not expected to respond to the same change due to the gene lesion.

In this chapter, a knockout mutant unable to express intact *NMB0240* was constructed by Catenazzi (2013) for the experimental characterisation of its metabolic properties with an aim of identifying the function(s) of Genomic Island 3.

4.2 Construction of a Genomic Island 3 knockout mutant via the putative *NMB0240* gene of *N. meningitidis*

A mutant strain of *N. meningitidis* serogroup B strain MC58 unable to synthesise intact copies of the gene *NMB0240* was constructed by Catenazzi (2013). All *N. meningitidis* strains used were cultured according to methodologies as previously described (See Chapter 2), while protocols for the molecular work involved are reiterated as follows.

No.	Primer Name	Primer Sequence (5’ to 3’)	Nucleotide Position
(a)	NMB0240-for	5’-CAGAAAGGATGGATATAGTGAAC-3’	244652 – 244674
(b)	NMB0240-rev	5’-ACCCTTTCAGACGGCTAAATCCC-3’	246167 – 246145
(c)	NMB0240bis-for	5'-CTGTTTGATTTCTGCTG-3'	245187 – 245206
(d)	NMB0240bis-rev	5'-CAGATAGGCACGTTCGATG-3'	245481 – 245463

Table 4.3 – List of primers used for the construction of a NMB0240-deficient mutant strain of *N. meningitidis* MC58: **(a)** forward and **(b)** reverse cloning primers; **(c)** forward and **(d)** reverse transformation-confirming primers. Underlined bases are intended mismatches of the genomic sequence in order to increase frequencies of transformation through the introduction of DNA uptake sequences (Goodman and Scocca, 1988).

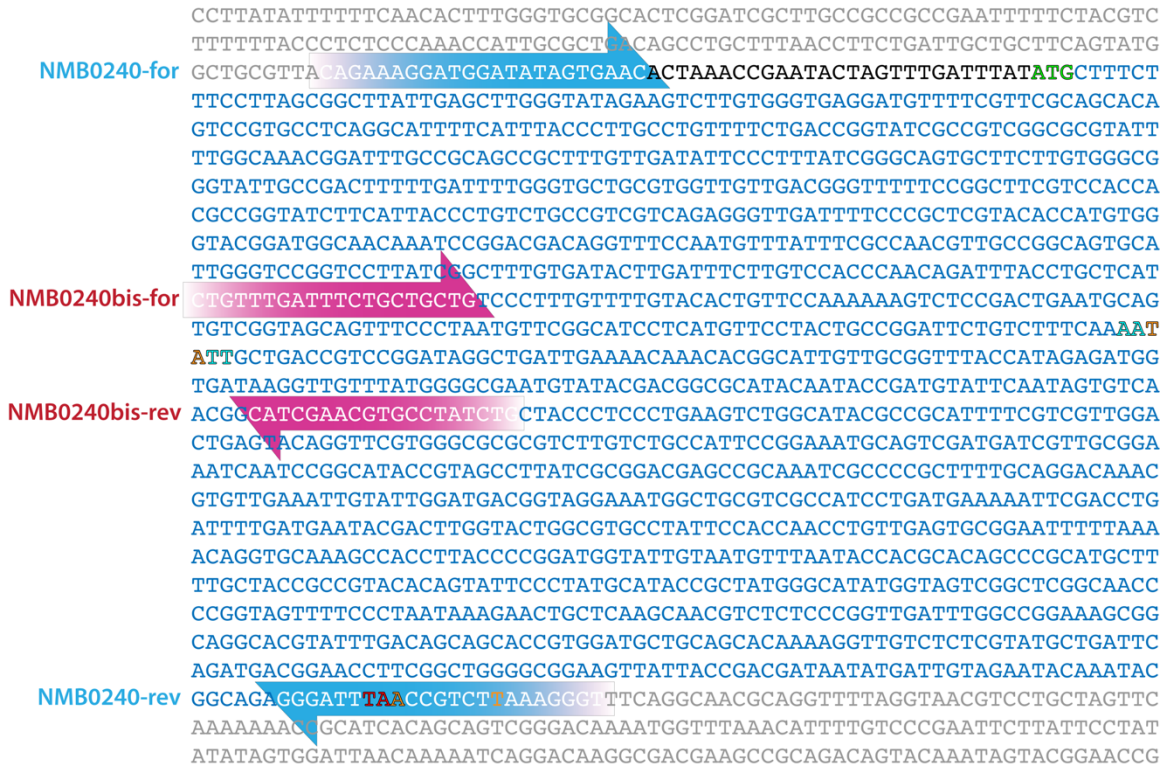

Fig. 4.2-1 – The ***NMB0240*** gene (in blue text) including its flanking regions (in black text), start (green outlined bold text) and stop (red outlined text) codons. Sequences of adjacent genes are denoted in grey text. The SspI restriction site (AATATT: cyan outlined bold text) shows the two bases (orange outlined bold text) where the enzyme cuts. Complementation sites of cloning primers NMB0240-for and NMB0240-rev (white text in blue arrow box) as well as insert-confirming primers NMB0240bis-for and NMB0240bis-rev (white text in pink arrow box) were also shown. Mismatched bases (“A” and “T”: orange text) in the reverse insert-confirming primer NMB0240-rev were considered “G”.

The *NMB0240* gene was amplified from wild-type *N. meningitidis* strain MC58 using the primers shown in Table 4.3 (a, b). Their respective sites of complementation are shown in Figure 4.2-1. The resulting 1516-base product was then cloned into an intermediate vector pCR-BluntII-TOPO (Invitrogen™). The product was digested out with restriction enzyme SspI (only cuts at a single restriction site within the *NMB0240* gene, and not in the rest of the vector) (Promega). The sticky ends were rendered blunt by treating with the DNA polymerase Klenow fragment (New England BioLabs®) in the presence of dNTPs. A spectinomycin resistance gene was digested from its native vector pHP45Ω (Prentki and Krisch, 1984) with the restriction enzyme SmaI (Promega), which was subsequently ligated with the linearised *NMB0240* clone using T4 DNA ligase (Promega). This yields a construct containing a cloned copy of *NMB0240* disrupted by the insertion of a spectinomycin resistance cassette (Figure 4.2-2), which was confirmed by Sanger sequencing.

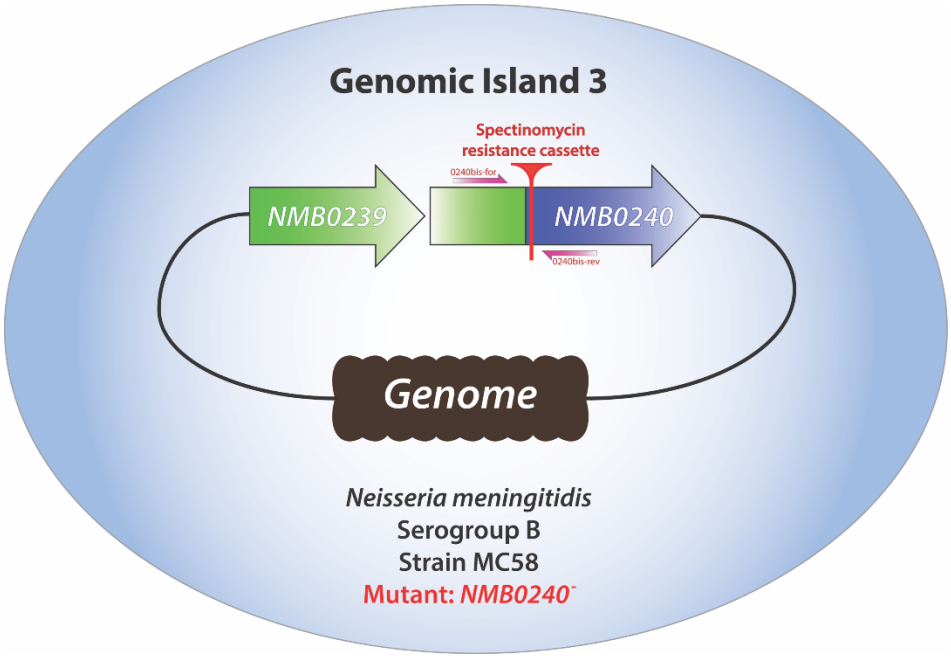

Fig. 4.2-2 – Layout of a *Neisseria meningitidis* serogroup B strain MC58 Genomic Island 3 mutant. A spectinomycin resistance cassette containing transcription-terminators is inserted into *NMB0240*, resulting in a mutant deficient in intact copies of the gene as well as the rest of the genomic island. The cassette is located at the very start of the putative soluble periplasmic domain in *NMB0240* (Prentki and Krisch, 1984).

The above *NMB0240*-knockout construct was then transformed by Catenazzi (2013) into *N. meningitidis* following protocols as previously described by Heurlier *et al.*, 2008, selecting for the mutant strain with 50 µg/ml spectinomycin. The formation of a disrupted *NMB0240* gene was confirmed by PCR (Figure 4.2-3) using primers (Table 4.2 (c,d)) that flank the spectinomycin cassette insertion site within *NMB0240* (Figure 4.2-1).

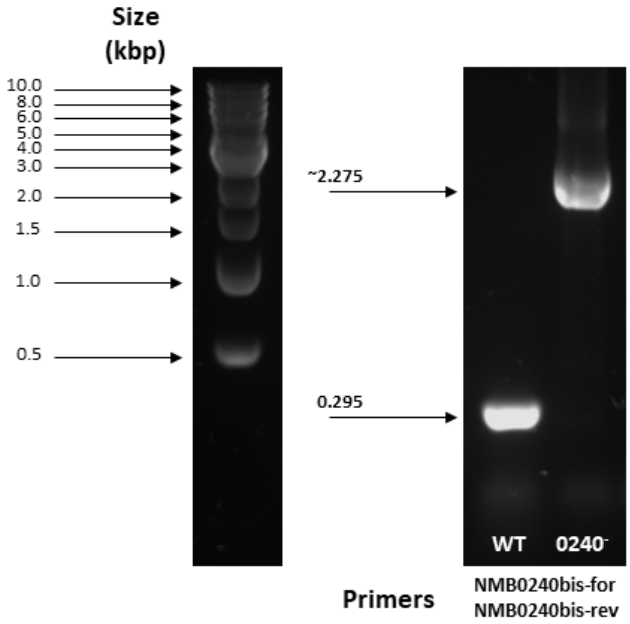

Fig. 4.2-3 – PCR confirmation of spectinomycin resistance cassette insertion by primers NMB0240bis-for and NMB0240bis-rev which flank the site of disruption. The "bis" primers read the wild-type *NMB0240* gene as a 295 bp product and the mutant (0.295 + 1.98 kbp cassette insert) as an approximately 2.275 kbp product. When referring to band weights, 1 kb DNA ladder (New England BioLabs®) was used.

4.3 Effects of rich and minimal media on growth of *N. meningitidis*

Müller-Hinton Broth (MHB) (Oxoid) is a rich, undefined liquid media commonly used in microbiology. It contains dehydrated beef infusion, casein hydrolysates, starch and is maintained at pH 7.3 at room temperature. In contrast, the chemically-defined minimal media (CDM) used in this study was derived from a modified version of the original Catlin formula (Catlin and Schloer, 1962; Catenazzi, 2013) and has a lower total nutrient availability than MHB. Details on how to obtain liquid cultures of *N. meningitidis* as well as the complete CDM formula used are described in Chapter 2 (Table 2.3).

When culturing *N. meningitidis*, aerobic growth of the *NMB0240*$^{-}$ mutant in MHB showed only marginal differences in yield and rate compared to the wild-type despite the presence of the genetic lesion (Figure 4.3-1 (a)). In light of bioinformatics predictions discussed in Section 4.1, mutant growth was therefore assessed under the more tightly controlled conditions provided by the CDM. Although both the wild-type and *NMB0240*$^{-}$ mutant performed noticeably poorer in CDM, significant differences in both yield and rate manifested (Figure 4.3-1 (b)).

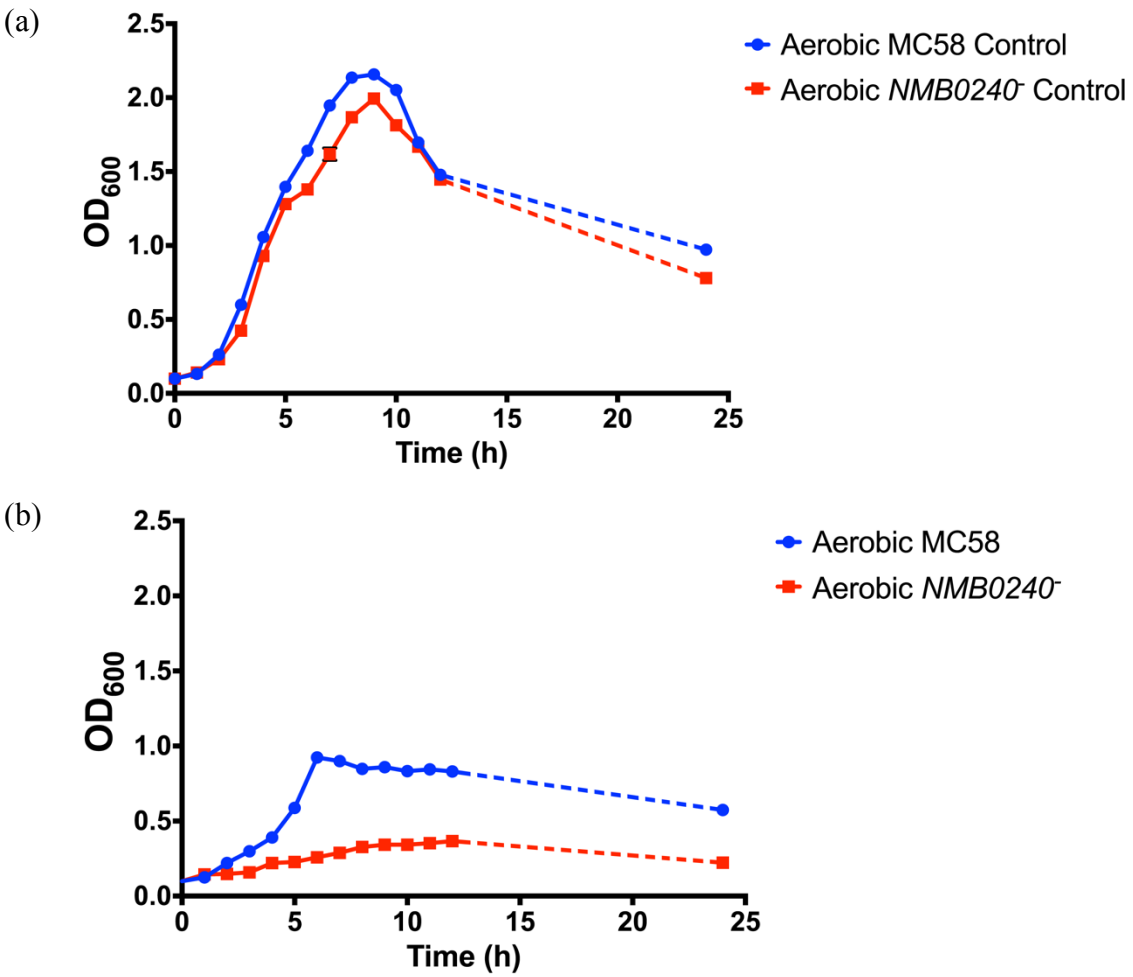

Fig. 4.3-1 – Differences in growth phenotypes of *NMB0240*$^-$ mutant compared to wild-type in **(a)** rich (MHB) and **(b)** minimal media (CDM). The growth curves shown here are representative figures of experiments carried out in technical and biological replicates.

While the relative paucity of nutrients in CDM may be responsible for a general low wild-type growth rate and yield, the *NMB0240*$^-$ knockout mutant took a much steeper downturn in that respect. Owing to the differences in nutritional composition between MHB and CDM, it is believed therein lies possible explanations for the growth differences observed between the two strains and possibly the role played by Genomic Island 3.

Hydrolysed casein is found in MHB, but is also marketed as a separate product sometimes referred to as casamino acids containing all essential amino acids, compared to a default supplementation of only 5 "core" amino acids at known concentrations in CDM. To investigate whether the shortfall in variety and availability of amino acids and peptides would rescue growth of the *NMB0240*$^-$ mutant, 0.1% casamino acids (Fisher Scientific) were supplemented to both strains and their growth was monitored (Figure 4.3-2 (a)). Apart from the 5 "core" amino acids, the other 15 amino acids not present by default in the complete Catlin CDM were also supplemented collectively to both strains for growth monitoring (Figure 4.3-2 (b)). In both cases, the addition of amino acids significantly

reduced the growth impairment of the *NMB0240*⁻ mutant, increasing yields but not rates completely comparable to that of the supplemented wild-type.

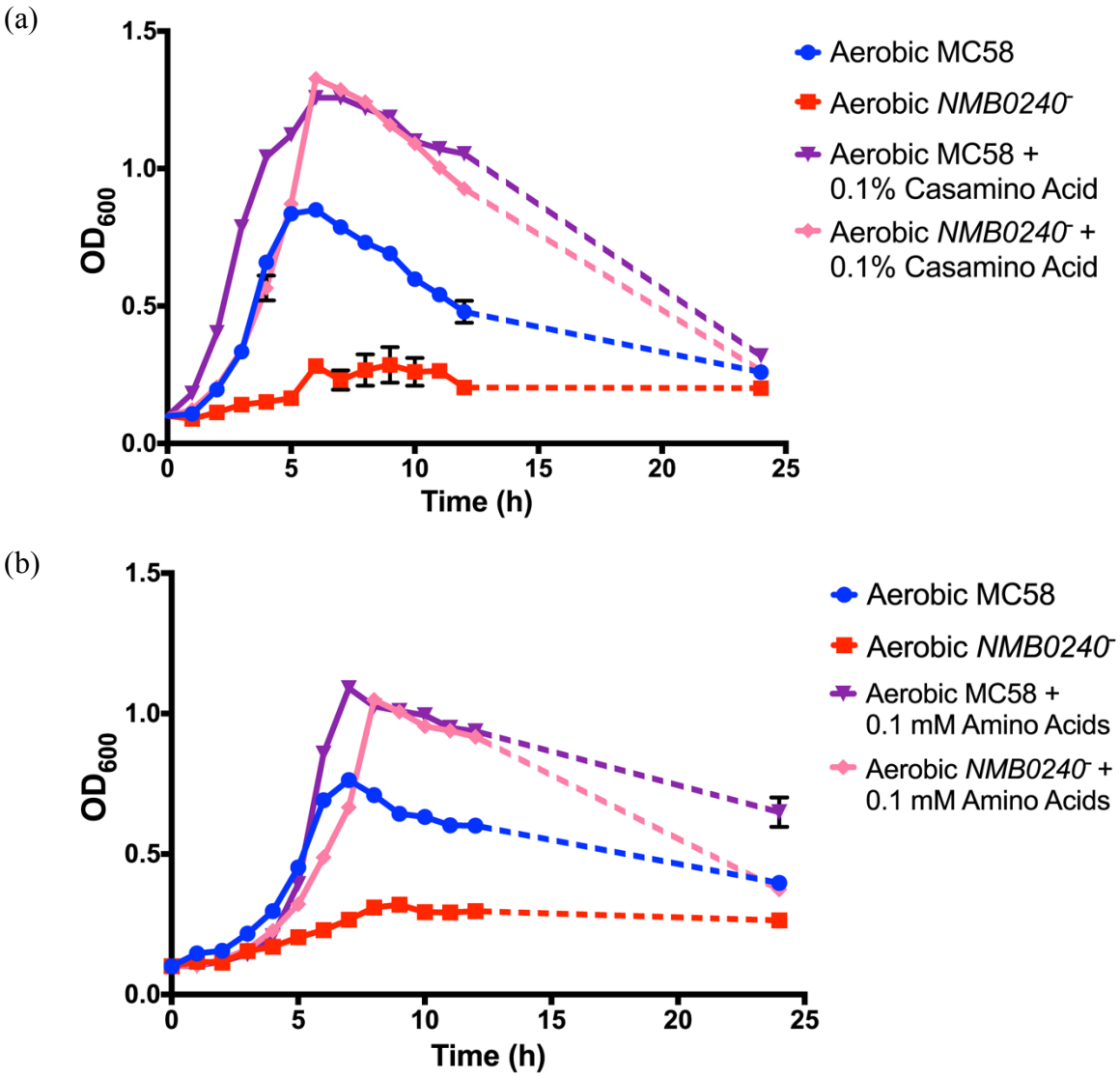

Fig. 4.3-2 – Differences in growth phenotypes of *NMB0240*⁻ mutant compared to wild-type in CDM **(a)** supplemented with 0.1% casamino acids and **(b)** 15 amino acids at 0.1 mM. These amino acids were namely: L-alanine, L-leucine, L-isoleucine, L-valine, L-methionine, L-lysine, L-proline, L-histidine, L-threonine, L-asparagine, L-tyrosine, L-tryptophan, L-phenylalanine, L-aspartate and L-glutamate. Stocks were prepared by dissolving casamino acids or amino acids in water and filter sterilisation, which were then kept at 4 ˚C for up to one month. When supplemented in CDM, volume of sterile dH_2O was adjusted accordingly to make room from the final volume of freshly-mixed CDM stocks. Final pH of CDM should be maintained between 7 and 7.5.

It is therefore proposed that the trends above show that supplementation of amino acids appeared to be able to largely account for the two strains' original differences in growth under plain CDM. Although the initial hypothesis as stated in Section 4.1 no longer appeared relevant to the supplementation approach, as both strains responded with significant growth improvements, this nonetheless prompted further investigation.

4.4 Effects of amino acids on the *NMB0240*$^-$ knockout mutant lesion in *N. meningitidis*

4.4.1 Aliphatic amino acids enable faster growth of both MC58 wild-type and *NMB0240*$^-$ mutant *N. meningitidis*

Based on the observations from above, we set out to determine whether the effects are elicited by a particular set of amino acids. The 15 amino acids that were not originally included in CDM were divided into the following clusters: (a) aliphatic: L-alanine (Sigma-Aldrich®), L-leucine (Sigma-Aldrich®), L-isoleucine (Sigma-Aldrich®), L-valine (Sigma-Aldrich®), L-methionine (Sigma-Aldrich®); (b) hydrophilic: L-lysine (Sigma-Aldrich®), L-proline (Sigma-Aldrich®), L-histidine (Sigma-Aldrich®), L-threonine (Sigma-Aldrich®), L-asparagine (Sigma-Aldrich®); (c) aromatic: L-tyrosine (Sigma-Aldrich®), L-tryptophan (Fisons), L-phenylalanine (Sigma-Aldrich®); (d) acidic: L-aspartate (Sigma-Aldrich®) and L-glutamate (Sigma-Aldrich®). The clusters were then supplemented to complete, plain CDM, where each of the 15 amino acids were at final concentrations of 0.1 mM.

The results show that the aliphatic group of amino acids appears to be able to rescue growth of both wild-type and mutant *N. meningitidis* strains to an extent comparable to that elicited by supplementation of all 15 amino acids or casamino acids (Figure 4.4-1). Differences in growth rates between the two strains are noticeably reduced compared to growth in plain CDM. The yield of the mutant strain also reaches levels increasingly comparable to that of the wild-type. Other clusters of amino acids either resulted in negligible or deleterious effects on meningococcal growth.

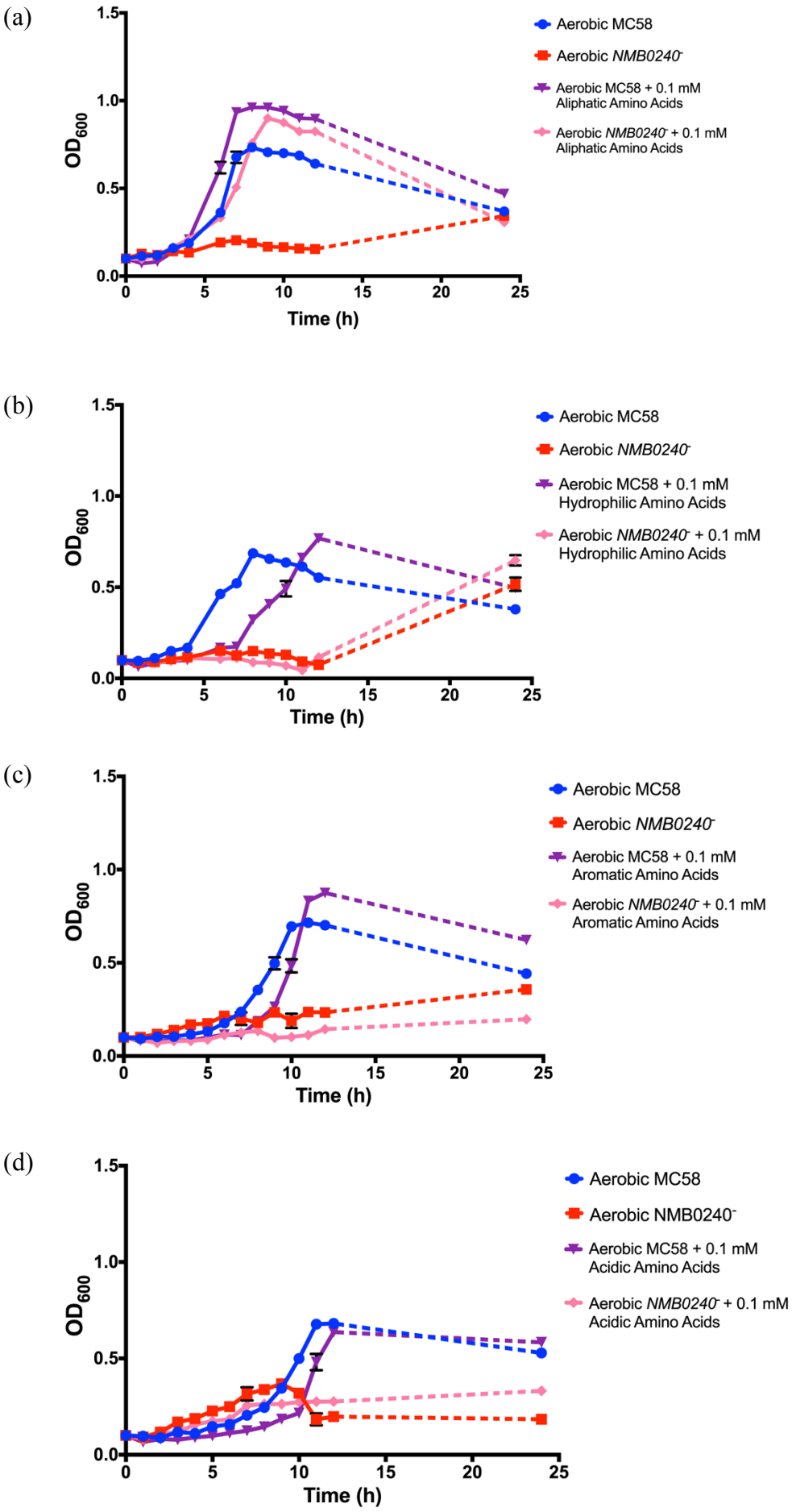

Fig. 4.4-1 – Effects of 15 amino acids supplemented in clusters on *N. meningitidis* growth in CDM, categorised into **(a)** aliphatic; **(b)** hydrophilic; **(c)** aromatic, and; **(d)** acidic.

The results strongly suggest that one or more members of the aliphatic group may be responsible for eliciting the growth trends and effects observed above, prompting specificity questions regarding the amino acids involved. The supplementation of the above materials continued to affect the growth of both strains significantly, which is not in concordance with the initial hypothesis set out in Section 4.1 where solely the wild-type was expected to respond to such changes in CDM composition. The objectives, however, were updated to continue identification as to which specific amino acid(s) could elicit a response in both strains.

4.4.2 Branched-chain amino acids elicit positive effects on growth of *N. meningitidis*

The phenotypes observed above (Section 4.4.1) warranted further investigation into whether the 5 aliphatic amino acids are general or specific in action. To assess their individual effects on meningococcal growth, each aliphatic amino acid – L-alanine, L-leucine, L-isoleucine, L-valine and L-methionine – were supplemented at 0.1 mM to complete, plain CDM for both the wild-type and mutant strains. The results show that mutant growth supplemented by both L-leucine and L-isoleucine, two branched-chain amino acids (BCAAs), significantly mirrored trends found in supplementation by all 5 aliphatic, all 15 amino acids and casamino acids in CDM (Figure 4.4-2a (b)). The remaining BCAA member L-valine, as well as L-methionine, showed negligible effects on meningococcal growth. On the other hand, L-alanine appears to inhibit growth of both strains, of which the delayed entry to log phase could be more easily observed in wild-type MC58 (Figure 4.4-2a (a)).

(a)

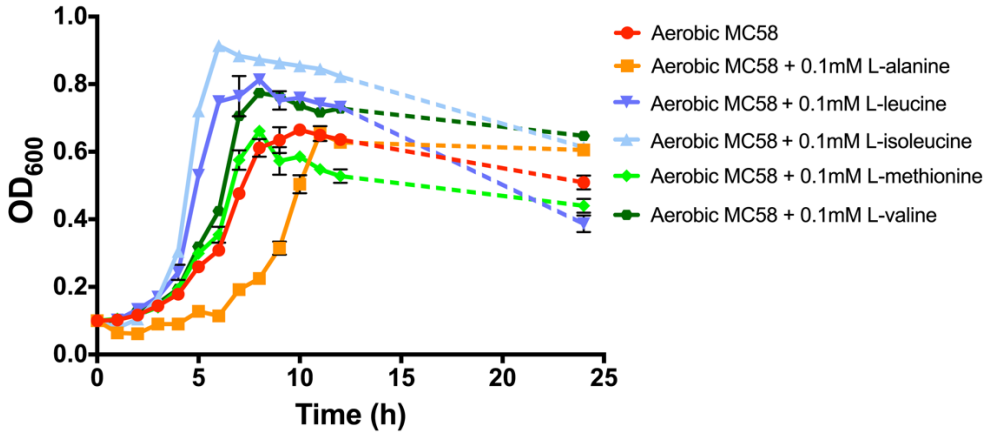

(b)

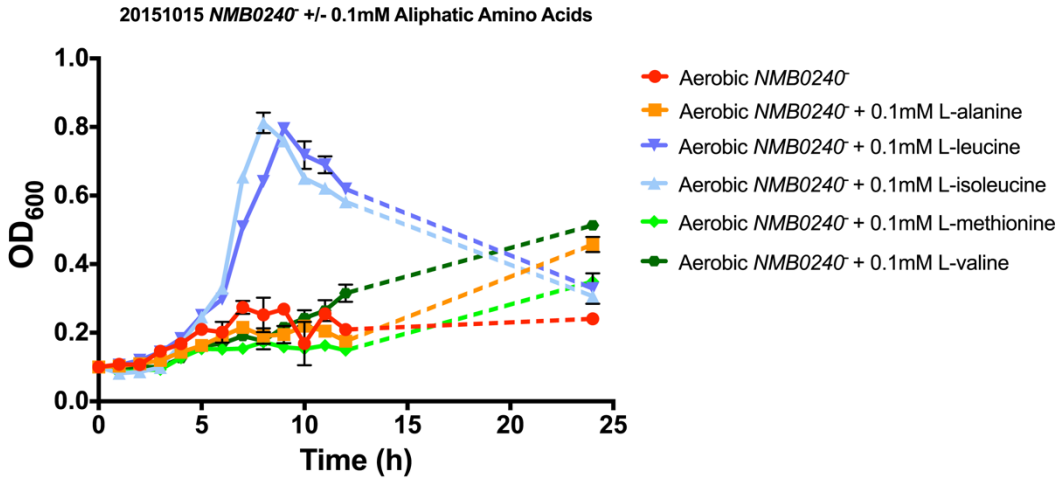

Fig 4.4-2a – Effects of supplementation by 5 aliphatic amino acids in CDM on *N. meningitidis* **(a)** wild-type MC58 and; **(b)** *NMB0240*⁻ mutant growth. The growth curves shown here are representative figures of experiments carried out in technical and biological triplicates.

The supplementation approach in conclusion does not support the initial hypothesis set out in Section 4.1, where the wild-type *N. meningitidis* was expected to respond to supplementation of materials due to its intact putative transporter function predicted for Genomic Island 3 while the knockout mutant was not expected to. In fact, the addition of extra exogenous amino acids in CDM affects both strains, be that positively or negatively. On the other hand, it is worth noting that L-isoleucine supplementation alone appears to distinguish itself as the strongest enhancer of *NMB0240*⁻ mutant growth in CDM thus far. It should however be pointed out that L-isoleucine and L-leucine appear to improve growth of both wild-type and mutant strains. It is also suggested that L-isoleucine supplementation does not account for the *NMB0240*⁻ mutant growth phenotype, as a shortfall in growth rate is still present compared to wild-type growth under the same conditions (Figures 4.4-2b).

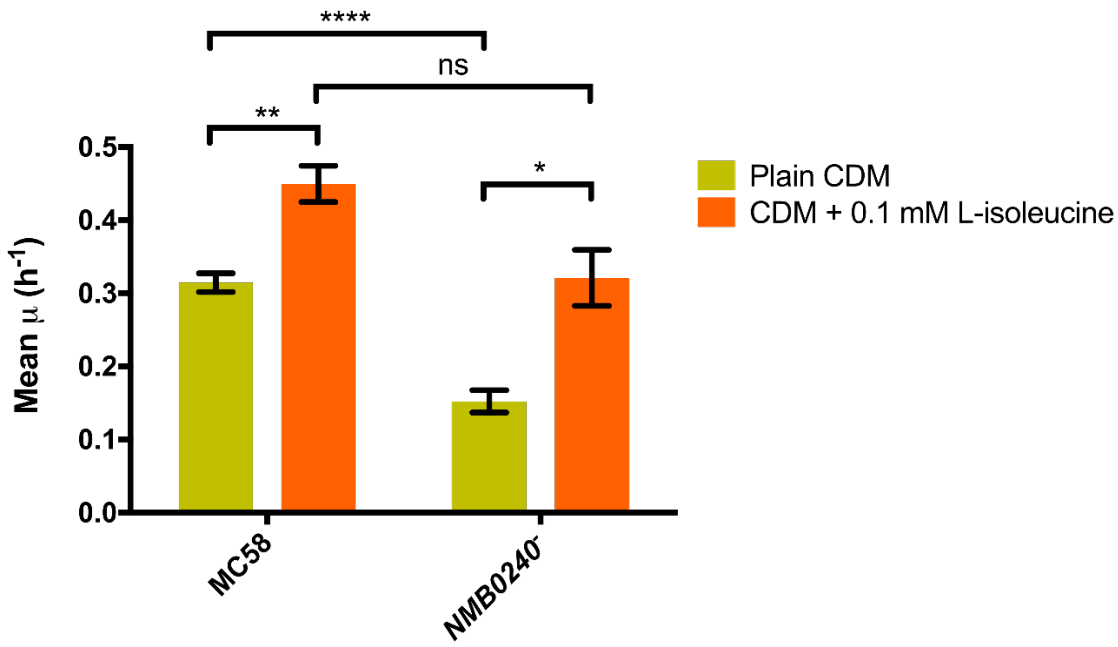

Fig. 4.4-2b – Specific growth rates extrapolated for *N. meningitidis* wild-type MC58 and *NMB0240*⁻ mutant in (gold) plain, complete CDM and (orange) CDM supplemented with minimal isoleucine. For statistical analyses, Student's *t*-tests were carried out to compare growth differences ($P \leq 0.05$). Asterisks are denoted as per formatting of GraphPad PRISM 7, where P-values of: ≥ 0.05 = not significant (ns); 0.01 to 0.05 = significant (*); 0.001 to 0.01 = very significant (**); 0.0001 to 0.001 = extremely significant (***) and; < 0.0001 = extremely significant (****) (GraphPad Software Inc., 2017).

The figure above shows the differences in growth rate of both *N. meningitidis* strains in CDM with and without isoleucine supplementation, where each bar is a relatively objective assessment of growth. These were derived by plotting natural log graphs of each hourly mean OD_{600} reading, from which a slope of best fit (outliers rejected to obtain R^2 values of >0.90, with a minimum of three data points) was extrapolated to obtain the growth rate during exponential phase. The result is known as the specific growth rate (μ) of each growth curve (in h^{-1}). The mean of each experimental condition, grouped by meningococcal strain used and growth media composition, were taken and plotted into bar charts. The analysis method is used extensively and further demonstrated in Section 4.4.4. The implications of the effects of isoleucine on meningococcal growth are discussed further in Chapter 5.

4.4.3 Removal of amino acids from CDM reveals intriguing growth trends from both MC58 wild-type and *NMB0240*$^{-}$ mutant *N. meningitidis*

The above work showed that although the introduction of some exogenous amino acids appears to improve meningococcal growth, a definitive phenotype that may explicitly help identify the function of Genomic Island 3 remains elusive. It was therefore reasoned that the lesion may instead be due to an inability to make use of intrinsic components of the CDM where other nutrients are not present in excess (i.e. MHB). To update the initial hypothesis, the removal – rather than addition – of material(s) from the existing CDM recipe is now expected to affect the growth of the wild-type *N. meningitidis* strain due to its intact copy of Genomic Island 3, being a putative transporter of said material(s), while the mutant would not respond to such changes due to its gene lesion.

As previously mentioned, the standard complete CDM used in our investigations is based on a modified version of the original Catlin recipe, and contains 5 amino acids: L-arginine, L-glycine, L-glutamine, L-serine and L-cysteine. Each of these amino acids were thus removed from CDM individually or in groups, which were then used to culture the two *N. meningitidis* strains. If NMB0239-0240 is a transporter complex for one or more of these amino acids, it may be hypothesised that their respective absence from CDM would result in marked growth deficit for the wild-type MC58 but not the *NMB0240*$^{-}$ knockout mutant.

(a)

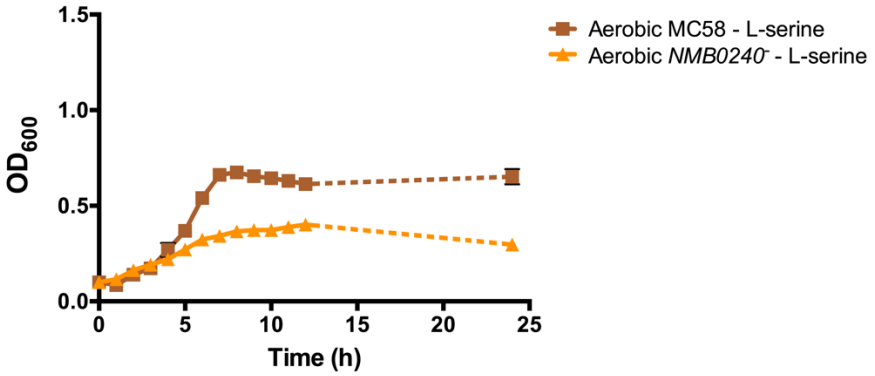

(b)

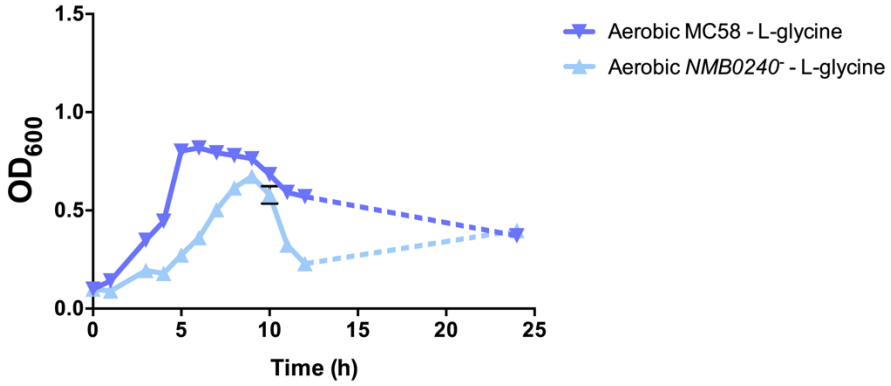

(c)

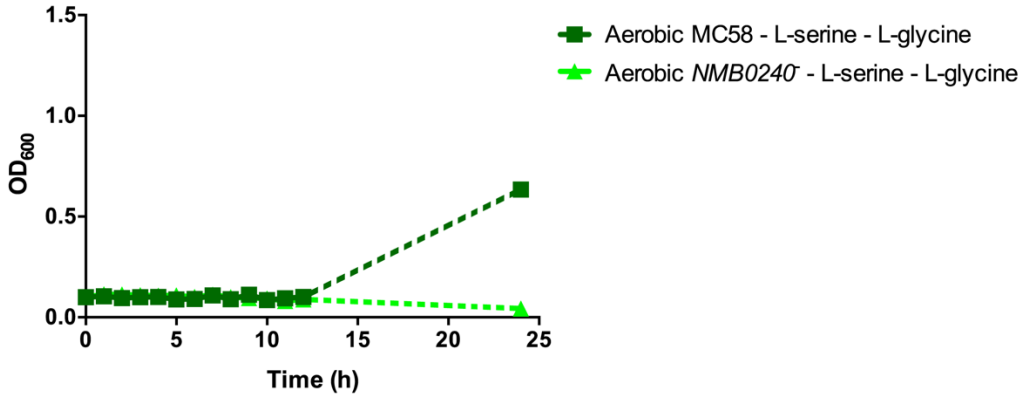

(d)

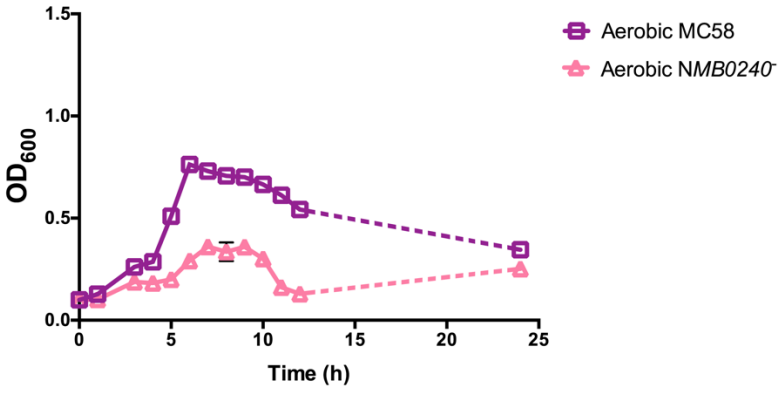

Fig. 4.4-3 (a-d) – Effects of removal of the amino acids L-serine and L-glycine from CDM on *N. meningitidis* wild-type MC58 and *NMB0240*⁻ mutant growth. The presence of a glyA (serine hydroxymethyl transferase) homologue at work serves as a plausible explanation for the trends

observed here where **(a)** only L-serine; **(b)** only L-glycine and; **(c)** both L-serine and L-glycine are withheld from CDM, compared to growth in **(d)** complete CDM. The growth curves shown here are representative figures of experiments carried out in technical and biological replicates.

As shown in Figure 4.4-3 (a), the absence of L-serine alone did not appear to significantly impact either wild-type or mutant meningococcal growth. The absence of L-glycine alone, however, appeared to noticeably improve growth rate and yield of both strains (Figure 4.4-3 (b)) when compared to growth in complete CDM (Figure 4.4-3 (d)). Notably the results showed that *N. meningitidis* growth required at least either L-serine or L-glycine, and cannot grow when both were absent (Figure 4.4-3 (c)). It is believed that this is due to the presence of an annotated meningococcal glyA homologue (serine hydroxymethyl transferase), NMB1055, which catalyses the reversible conversion between L-serine and L-glycine (Blakley, 1960; Schirch *et al.*, 1985). On the other hand, it should be remarked that wild-type *N. meningitidis* did appear to undergo net growth after the first 12 hours of aerobic culturing. It is possible that during that period the meningococci may be attempting to adapt to a nutritional diet different than complete CDM to compensate for the lack of exogenous L-serine and L-glycine.

(e)

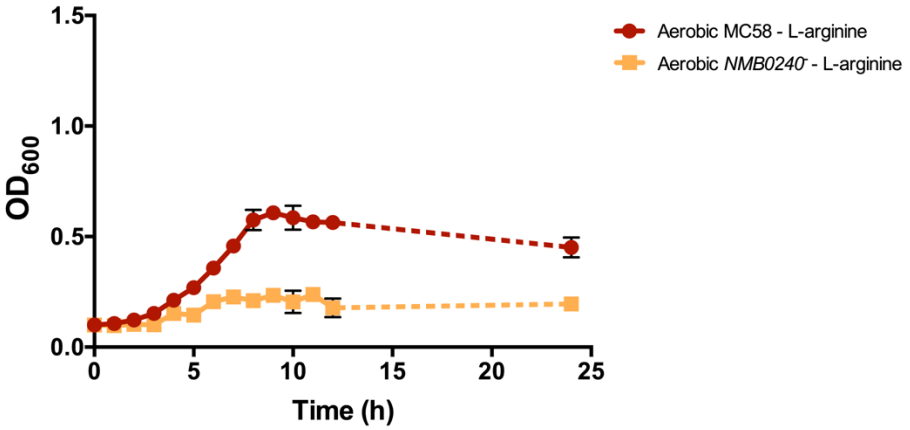

(f)

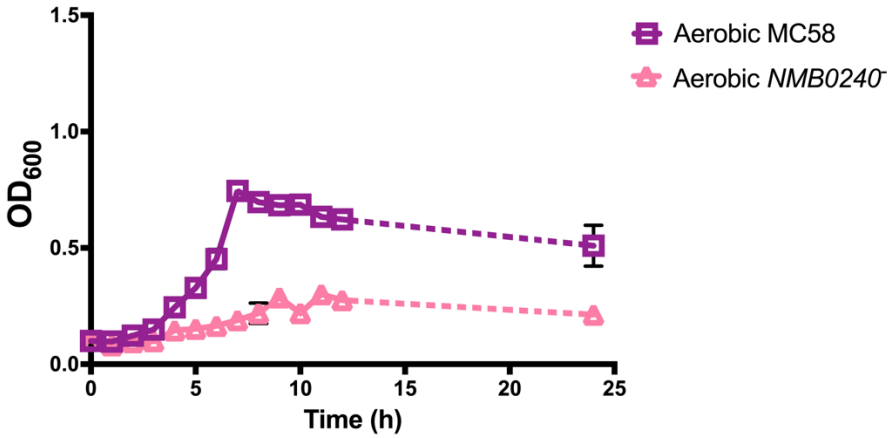

Fig. 4.4-3 (e, f) – Effects of removal of the amino acid L-arginine from CDM on *N. meningitidis* wild-type MC58 and *NMB0240*⁻ mutant growth, shown by the comparison of growth in (e) CDM without L-arginine and; (f) plain, complete CDM as control. The growth curves shown here are representative figures of experiments carried out in technical and biological triplicates.

Compared to growth in complete CDM, the absence of L-arginine has no discernible effect on the growth of the *NMB0240*⁻ mutant, whereas wild-type *N. meningitidis* suffers a decrease in both growth rate and yield (Figure 4.4-3 (e, f)). Although the subsequent compilation of specific growth rates appears to support that there is no statistically significant growth difference between arginine-free wild-type and mutant growth (See Section 4.4.4), cross-comparison with the above growth curves suggests a more complex picture. Since *N. meningitidis* has been annotated to possess alternative pathways for arginine-synthesis (See Section 4.6), it is possible that endogenous arginine may well have accounted for the persistence of the wild-type, which is only experiencing stunted growth.

As this stage, the above results do not fit into the updated hypothesis, as both strains – instead of only the wild-type – responded (whether positively, negatively or neutrally) to the removal of 3 out of the 5 amino acids (individually or in tandem) originally present in the CDM recipe from the media.

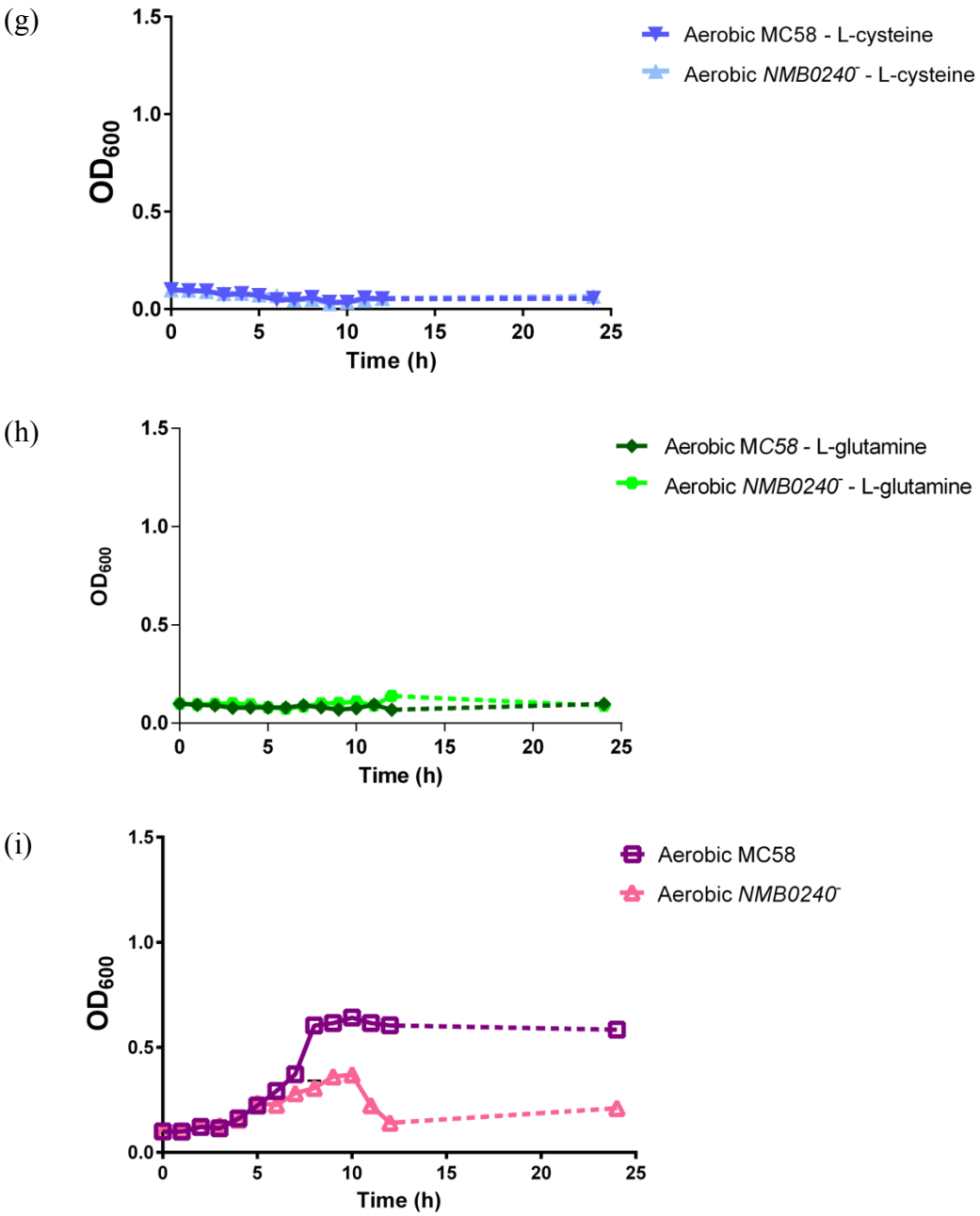

Fig. 4.4-3 (g-i) – Effects of removal of the amino acids L-cysteine and L-glutamine from CDM on *N. meningitidis* wild-type MC58 and *NMB0240*⁻ mutant growth, shown by the comparison of growth in **(g)** CDM without L-cysteine; **(h)** without L-glutamine and; **(i)** plain, complete CDM as control. The growth curves shown here are representative figures of experiments carried out in technical and biological triplicates.

The absence of L-cysteine (Figure 4.4-3 (g)) and L-glutamine (Figure 4.4-3 (h)), on the other hand, appear so debilitating to both strains that there is negligible net growth when compared to the complete CDM control (Figure 4.4 (j)). The relatively poor growth exhibited may be attributable to the fact that glutamine is a crucial substrate in a plethora of biochemical processes. In particular, glutamine serves as a universal nitrogen or amino group donor for biosynthetic processes involving other key amino acids, such as the conversion of pyruvate to serine. Likewise, poor growth tantamount to general cell death

exhibited by both strains in cysteine-free CDM may also be attributable to the fact that cysteine plays a crucial role in the control of oxidative stress due to its ability to undergo redox reactions. Moreover, cells maintain a reduced environment in the cytoplasm by finely balancing the intracellular concentrations of reducing agents such as cysteine (Gaupp *et al.*, 2012).

The above results still do not fit into the updated hypothesis where the wild-type was expected to respond exclusively to the removal of these amino acids. Both strains responded negatively to the removal of the remaining 2 amino acids out of the 5 originally present in media as part of the CDM recipe.

4.4.4 Comparison of specific growth rates of *N. meningitidis* in CDM with various amino acid profiles reveals involvement of Genomic Island 3 in L-arginine and L-glutamine metabolism

Given the limitations in graphical representation, the ability to clearly distinguish differences between the phenotypes of the various experimental conditions involved through direct visual comparison of growth curves decreases over time as data accumulates. It is therefore crucial to adopt a method which allows for the objective assessment of growth trends.

As briefly introduced at the end of Section 4.4.2, natural log graphs of each hourly mean OD_{600} reading were plotted, from which a slope of best fit (outliers rejected to obtain R^2 values of >0.90, with a minimum of three data points) was extrapolated to obtain the growth rate during exponential phase. The result is known as the specific growth rate (μ) of each growth curve (in h^{-1}). The mean of each experimental condition, grouped by *N. meningitidis* strain used and growth media composition, were taken and plotted into bar charts. For statistical analyses, Student's *t*-tests were conducted to compare growth differences ($P \leq 0.05$). With regards to statistical significance, asterisks are denoted as per the plotting software's instructions, where P-values of: ≥ 0.05 = not significant (ns); 0.01 to 0.05 = significant (*); 0.001 to 0.01 = very significant (**); 0.0001 to 0.001 = extremely significant (***) and; < 0.0001 = extremely significant (****) (GraphPad Software Inc., 2017). Error bars are devised from the Standard Error of the Mean (SEM) of each amino acid profile that contains three or more data points. The results are as follows (Figures 4.5-1 & 2):

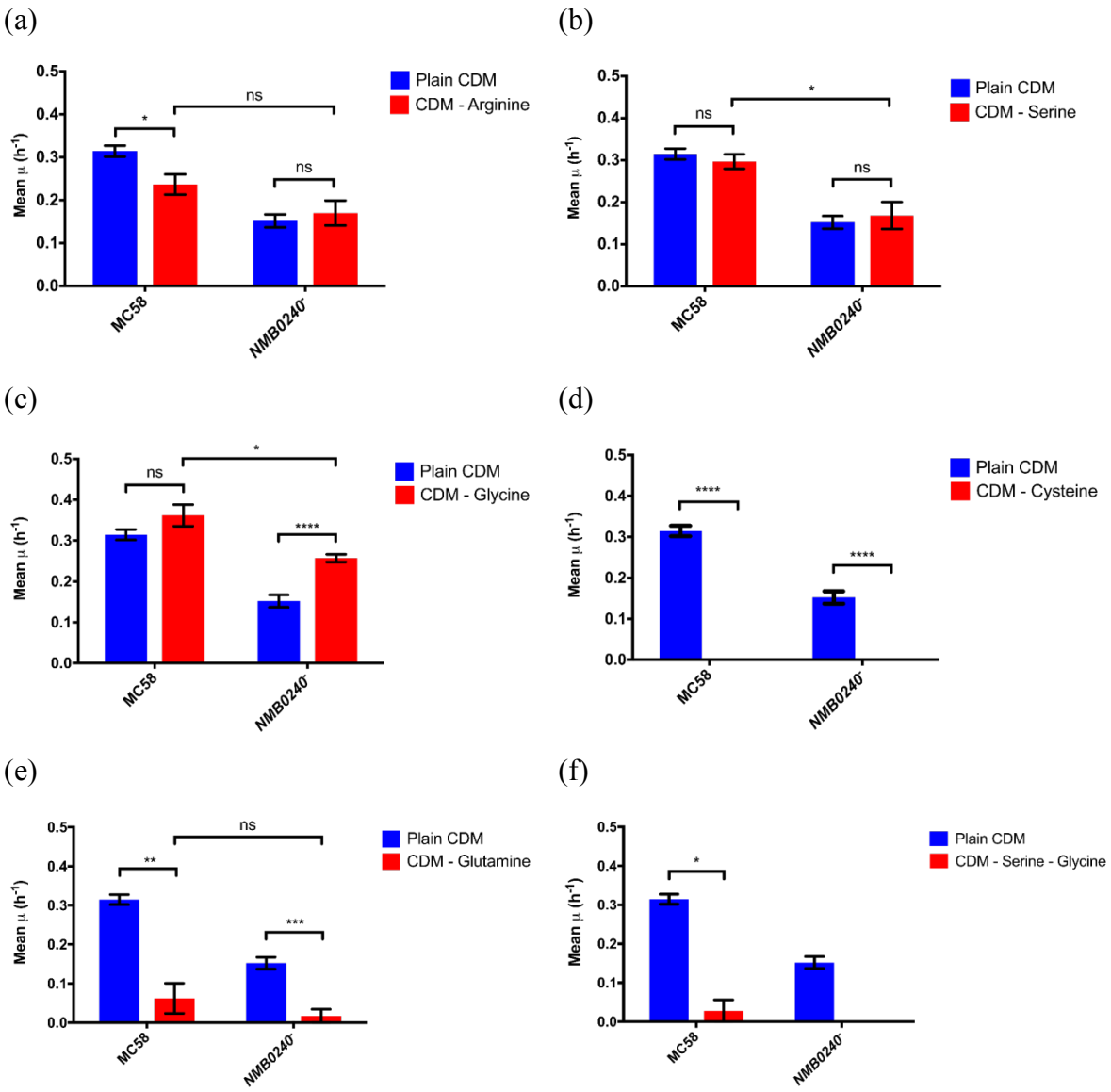

Fig. 4.5-1 – Specific growth rates of *N. meningitidis* wild-type MC58 and *NMB0240*⁻ mutant in (blue) plain, complete CDM and (red) CDM with one or more core amino acids removed: **(a)** arginine; **(b)** serine; **(c)** glycine; **(d)** cysteine; **(e)** glutamine and; **(f)** both serine and glycine. Bars are absent for conditions which did not result in observable net growth and therefore no growth rate extrapolation. For statistical analyses, Student's *t*-tests were carried out to compare growth differences ($P \leq 0.05$). Asterisks are denoted as per formatting of GraphPad PRISM 7, where P-values of: ≥ 0.05 = not significant (ns); 0.01 to 0.05 = significant (*); 0.001 to 0.01 = very significant (**); 0.0001 to 0.001 = extremely significant (***) and; < 0.0001 = extremely significant (****) (GraphPad Software Inc., 2017).

The analysis provides some statistical support for the previously discussed growth curve-based observations. The absence of L-arginine significantly decreases wild-type specific growth rate to an extent where it is no longer statistically different from that of the mutant (Figure. 4.5-1 (a)). The absence of L-serine, cross-compared with results from growth curve experiments, shows small but statistically unapparent loss of growth (Figure 4.5-1(b)). The others reinforce the importance of L-cysteine, L-glutamine and the glyA complex (Figures 4.5-1 (d-f)). The analysis also supports the notion that L-glycine may be preventing *N. meningitidis* from reaching higher levels of growth in CDM (Figure 4.5-1 (c)), of which the implications are discussed in Chapter 5.

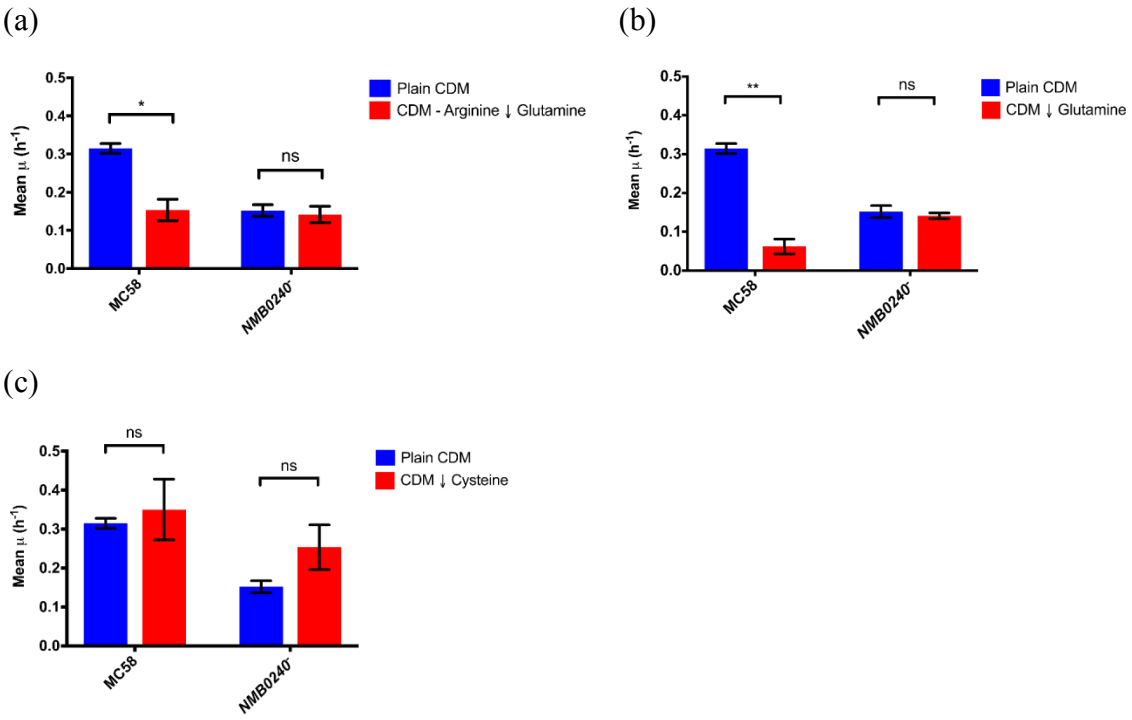

Fig. 4.5-2 – Specific growth rates of *N. meningitidis* wild-type MC58 and *NMB0240*⁻ mutant in (blue) plain, complete CDM and (red) CDM with altered concentrations of core amino acids: **(a)** without arginine and 10-fold lower concentration of glutamine (i.e. from 4 mM to 0.4 mM); **(b)** 10-fold lower concentration of glutamine (i.e from 4 mM to 0.4 mM); **(c)** 10-fold lower concentration of cysteine (i.e. from 0.4 mM to 0.04 mM). **For effects of glutamine-free CDM** on specific growth rate of both strains, refer to Figure 4.5-1 (e) for comparison. For statistical analyses, Student's *t*-tests were carried out to compare growth differences ($P \leq 0.05$). Asterisks are denoted as per formatting of GraphPad PRISM 7, where P-values of: ≥ 0.05 = not significant (ns); 0.01 to 0.05 = significant (*); 0.001 to 0.01 = very significant (**); 0.0001 to 0.001 = extremely significant (***) and; < 0.0001 = extremely significant (****) (GraphPad Software Inc., 2017).

Following up on the results in Figure 4.5-1, L-glutamine and L-cysteine were re-introduced into the CDM at 10-fold lower concentrations compared to complete CDM. Lowering the concentration of L-glutamine in CDM from 4 mM to 0.4 mM results in significantly poorer wild-type growth, while the mutant appears unaffected (Figure 4.5-2 (b), 4.5-3 (b)). Interestingly, lowering the concentration of L-cysteine in CDM from 0.4 mM to 0.04 mM results in a slight increase in both wild-type and mutant growth, albeit not statistically significant (Figure 4.5-2 (c), 4.5-3 (c)). The implications of this is explored in Chapter 5.

From the above, it is also shown that lowered concentrations of L-glutamine, in tandem with the absence of L-arginine, are capable of significantly reducing wild-type *N. meningitidis* growth to mutant levels, whilst having little effect on that of the actual *NMB0240*$^{-}$ mutant strain (Figure 4.5-2 (a)). However, the above analysis has also implied that lowered availability of L-glutamine alone is sufficient to elicit a similar effect on both *N. meningitidis* strains. It is worth noting that the wild-type appears to grow noticeably poorer compared to the mutant in terms of specific growth rate when cultured in lowered concentrations of L-glutamine, albeit the difference is not statistically significant (not shown).

Referring to their respective growth curves (Figure 4.5-3), it can be observed that there appear to be differences in the way that the two amino acid profiles affect the growth of wild-type *N. meningitidis*. In terms of specific growth rates and statistics, however, both the lowered availability of L-glutamine in CDM with and without L-arginine satisfy the criteria for an amino acid profile under which the wild-type grows poorer but the mutant remains unaffected.

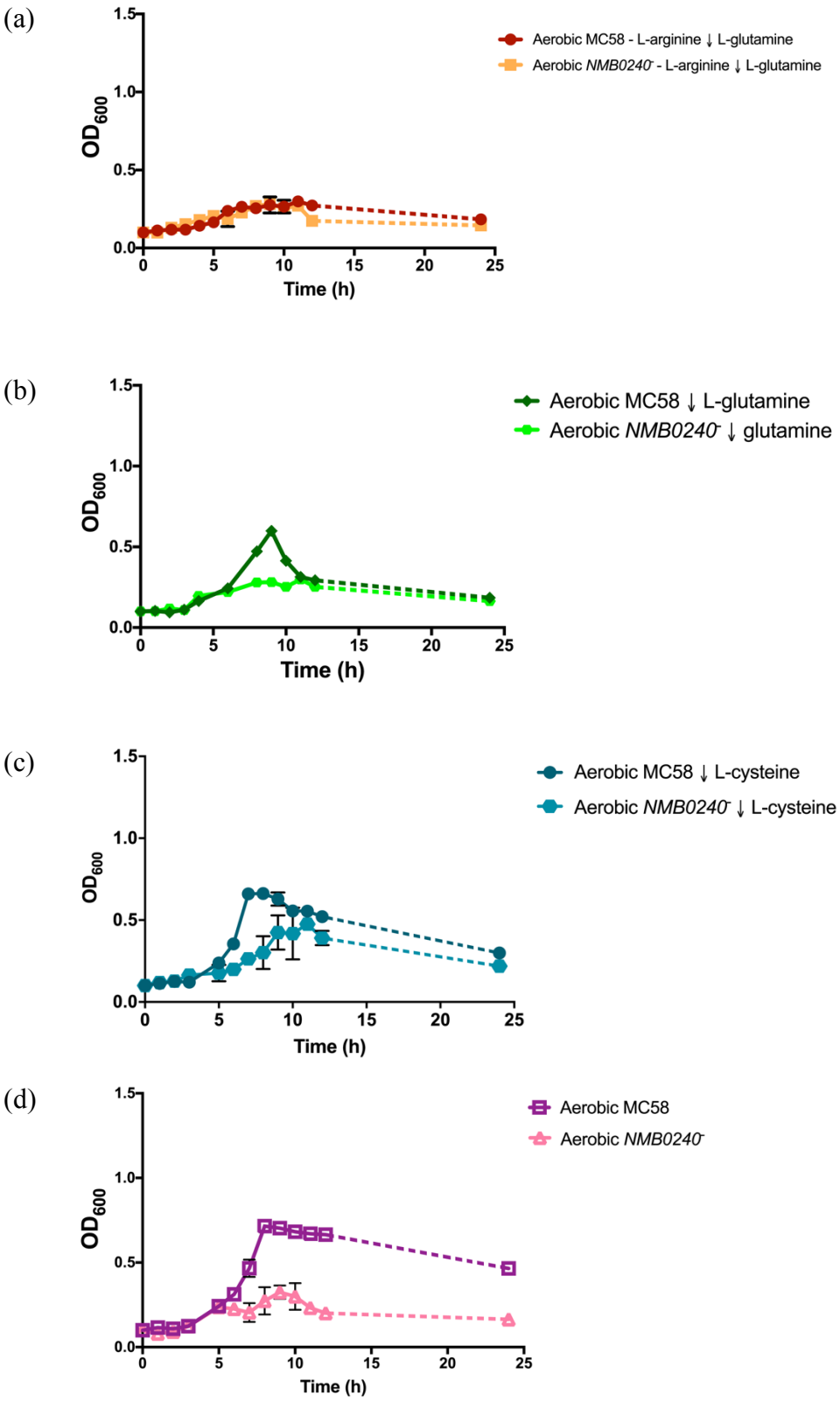

Fig. 4.5-3 – Effects of removal of L-arginine and simultaneously lowered L-glutamine concentrations, **lowered L-glutamine concentrations alone** and **lowered L-cysteine concentrations** from CDM on *N. meningitidis* wild-type MC58 and *NMB0240*⁻ mutant growth, shown by the comparison of growth in **(a)** CDM without arginine and 10-fold lowered availability of glutamine (i.e. from 4 mM to 0.4 mM); **(b)** CDM with 10-fold lowered availability of glutamine alone (i.e. from 4 mM to 0.4 mM); **(c)** CDM with 10-fold lowered availability of cysteine (i.e. from 0.4 mM to 0.04 mM), and; **(d)** plain, complete CDM as control. The growth curves shown here are representative figures of experiments carried out in technical and biological triplicates.

It is possible that wild-type *N. meningitidis* attempts unsuccessfully to adapt its nutritional requirements around the low availability of L-glutamine, displaying a brief exponential growth before falling victim to the exhaustion of an amino acid whose biochemical importance to bacterial cell metabolism has previously been stressed. When coupled with the loss of L-arginine, it is also possible that a metabolic demand has arisen in the meningococci to utilise the limited L-glutamine in an attempt to compensate cellular processes that depend on the availability of L-arginine through its biosynthesis from L-glutamine (See Section 4.6). Consequently, for the wild-type, the results are early depletion of free L-glutamine in solution and growth that is not energetically sustained in a favourable manner – not unlike that experienced by the *NMB0240*$^{-}$ knockout mutant.

In summary, the effects of removing L-arginine from CDM and lowering L-glutamine concentrations in CDM in tandem do appear to support the updated hypothesis of Genomic Island 3 as a putative transporter of amino acid(s) (i.e. L-arginine), as only the wild-type was impacted by the change while the mutant was largely unaffected.

4.5 Genomic Island 3 can transport arginine

To confirm whether Genomic Island 3 is involved in the transport of exogenous L-arginine, potential movement of the amino acid across either side of the bacterial membrane was monitored, and the results compared between wild-type and *NMB0240*$^{-}$ knockout mutant *N. meningitidis* strains. The null hypothesis is that Genomic Island 3 does not play any role in the meningococcal intake of L-arginine; if true, a mutant deficient in the expression of the intact Island products would not see any reduction in L-arginine incorporation in peptides.

To test this, *N. meningitidis* was cultured in complete CDM with either the naturally-occurring L-arginine isotope, or replaced with a labelled isotope containing two ^{15}N atoms in the guanidineimino side chain (Sigma-Aldrich®) at equal concentrations. Cell pellets were harvested from each strain respectively at mid-log phase by centrifuging 1 ml aliquots of liquid culture in 1.5 ml Eppendorf tubes at 12000 rpm for 5 minutes. The supernatant was discarded and the pellets were resuspended in 200 µl sample buffer with loading dye and 10% SDS, after which the lysis reaction was allowed to take place for one hour. SDS-PAGE of the samples were performed as described in Chapter 2, after which the gel was stained for 30 minutes with InstantBlue™ (Expedeon) and destained overnight with dH_2O. Definitive bands across the samples with the same molecular mass were excised and trypsin-digested. The resulting trypsin-derived peptides were analysed by MALDI-MS/MS using a Bruker ultraflex III MALDI TOF/TOF instrument (Bruker) according to the manufacturer's protocol.

The tandem mass spectra obtained were searched against the unrestricted UniProt database for matches with known *N. meningitidis* proteins. The next step was to use the search result to locate arginine-containing peptides within the samples, which is facilitated by the fact that trypsin cleaves peptides exclusively C-terminal to arginine or lysine (Olsen *et al.*, 2004).

(a)

MT						
Peptide Identified	Peptide Expect Score	Intensity L	Intensity H	Ratio (H/L)	Log2(Ratio H/L)	Percent H MT
VSVGYDFGGWR	5.9 x 10-6	20011	55498	2.77	1.47	73.50
IAADYASYR	4.40E-03	2429	8387	3.45	1.79	77.54
ISTVSDYFR	5.4 x 10-5	2532	8833	3.49	1.80	77.72
SPYYVQADLAYAAER	2.9 x 10-9	29995	82187	2.74	1.45	73.26
				Mean	1.63	75.51
			Geometric Ratio Mean	3.09		

WT						
Peptide Identified	Peptide Expect Score	Intensity L	Intensity H	Ratio (H/L)	Log2(Ratio H/L)	Percent H WT
VSVGYDFGGWR	5.9 x 10-6	11202	62650	5.59	2.48	84.83
IAADYASYR	4.40E-03	1575	12084	7.67	2.94	88.47
ISTVSDYFR	5.4 x 10-5	1964	13587	6.92	2.79	87.37
SPYYVQADLAYAAER	2.9 x 10-9	20680	116232	5.62	2.49	84.90
				Mean	2.68	86.39
			Geometric Mean	6.39		

(b)

MT						
Peptide Identified	Peptide Expect Score	Intensity L	Intensity H	Ratio (H/L)	Log2(Ratio H/L)	Percent H MT
DVQFGNEVR	0.023	70	235	3.36	1.75	77.05
YVTAGMNPTDLKR	0.059	12	55	4.58	2.20	82.09
AAVEEGVVAGGGVALLR	1.8 x 10-6	389	1346	3.46	1.79	77.58
SLENELDVVEGMQFDR	2.7 x 10-1	90	527	5.86	2.55	85.41
ENTTIIDGFGDAAQIEAR	7.3 x 10-11	234	1068	4.56	2.19	82.03
				Mean	2.09	80.83
			Geometric Ratio Mean	4.27		

WT						
Peptide Identified	Peptide Expect Score	Intensity L	Intensity H	Ratio (H/L)	Log2(Ratio H/L)	Percent H WT
DVQFGNEVR	3.3 x 10-4	84	1038	12.36	3.63	92.51
YVTAGMNPTDLKR	0.032	30	290	9.67	3.27	90.63
AAVEEGVVAGGGVALLR	1.8 x 10-10	579	4722	8.16	3.03	89.08
SLENELDVVEGMQFDR	1.3 x 10-11	246	2950	11.99	3.58	92.30
ENTTIIDGFGDAAQIEAR	1.4 x 10-14	362	3823	10.56	3.40	91.35
				Mean	3.38	91.17
			Geometric Mean	10.40		

(c)

MT						
Peptide Identified	Peptide Expect Score	Intensity L	Intensity H	Ratio (H/L)	Log2(Ratio H/L)	Percent H MT
APVALVNEEAAR	0.62	29	203	7.00	2.81	87.50
SVTVETLENLER	6.6 x 10-3	12	91	7.58	2.92	88.35
VTASVGDAEVDQTVEILR	3.6 x 10-6	13	213	16.38	4.03	94.25
				Mean	3.25	90.03
			Geometric Ratio Mean	9.55		

WT						
Peptide Identified	Peptide Expect Score	Intensity L	Intensity H	Ratio (H/L)	Log2(Ratio H/L)	Percent H WT
APVALVNEEAAR	0.14	15	206	13.73	3.78	93.21
SVTVETLENLER	1.1 x 10-3	8	105	13.13	3.71	92.92
VTASVGDAEVDQTVEILR	9.3 x 10-8	5	318	63.60	5.99	98.45
				Mean	4.49	94.86
			Geometric Mean	22.55		

Table. 4.4 (a-c) – Results of **MALDI-MS/MS** analyses of trypsin-derived peptides from three sets of protein bands excised at three different molecular mass respectively, showing incorporation of heavy (H) $^{15}N_2$-labelled L-arginine isotope compared with light (L) natural L-arginine in percentages and as ratios of their signal intensities (from respective relative peak areas) in both wild-type (WT) and *NMB0240*$^-$ knockout mutant (MT) *N. meningitidis* strains. All trypsin-derived peptides shown are cleaved C-terminal to arginine (R). The above data are biological triplicates.

The results show that approximately 90% of incorporated L-arginine belongs to the heavy labelled isotope in wild-type *N. meningitidis*, while the *NMB0240*$^{-}$ knockout mutant sees approximately 81% heavy L-arginine incorporation (Table 4.4). This is equivalent to a two-fold increase in incorporation of light labelled L-arginine isotope in the mutant compared to the wild-type. Note that the difference between the two meningococci strains in Table 4.4 (c) is statistically significant when analysed as pairs. Differences in mean incorporation of heavy isotope between wild-type and mutant strains may vary from run to run, which may be attributable to more complex MS spectra resulting in more confounding signals. In addition, the supplied labelled isotope is 98% in purity. Together with activity from possible arginine biosynthesis pathways via other present CDM components and residual incorporation from rich agar incubation, this can result in samples grown with heavy L-arginine not being completely free from the lighter naturally-occurring L-arginine isotope. It must be noted that, however, a relatively minor reduction in percentage incorporation of imported L-arginine in bacterial peptides observed does not necessarily reflect the extent of which meningococcal biomass yield and growth rate are reduced. It is possible that pathways that attempt to compensate for the need for arginine incorporation in protein synthesis are more energetically demanding in the *NMB0240*$^{-}$ mutant, leading to stress, which in turn may lead to halved specific growth rate and yield compared to that of the wild-type meningococci.

4.6 Discussion

Neisseria meningitidis and *N. gonorrhoeae* strains possess 9 highly conserved genomic islands not found in their commensal relative *N. lactamica*. Characterisation of their functions may provide new insights into their biology through distinguishing pathogenic from non-pathogenic *Neisseria* species. *N. meningitidis* serogroup B strain MC58 Genomic Island 3 consists of the genes *NMB0239*/*0240* which are absent from all other members of the order Neisseriales apart from disease-causing meningococci and gonococci. Through the use of a chemically-defined media (CDM), the effects of various growth media constituents on the phenotype of a knockout mutant deficient in NMB0240 were investigated in a bid to uncover the functions of this putative island. This powerful tool enabled the identification of the role of Genomic Island 3 in the uptake of arginine. This is not an exclusive way of transport for these amino acids, however, as the *NMB0240*$^{-}$ knockout mutant appears to still be able to acquire them from exogenous sources. Nonetheless, the gene lesion does appear to have a significant impact on meningococcal growth, especially under nutrient-limiting conditions. Given the growth of the MC58 wild-type (but not the *NMB0240*$^{-}$ knockout mutant) benefits from the presence of arginine, the

results from growth experiments at first suggested the possibility of Genomic Island 3 being the sole route of arginine uptake. Subsequent work involving the use of isotope-labelled arginine, however, indicated that that the mutant is still capable of taking up externally-supplemented arginine at reduced efficiency compared to that of the wild-type. Although complemented by existing endogenous pathways for arginine biosynthesis, it appears that meningococci deficient in Genomic Island 3 would come to rely on that more heavily, resulting in a lower general growth rate. In summary, the results suggest that Genomic Island 3 can transport L-arginine, but can be complemented by the availability of L-glutamine at defined concentrations through mechanisms beyond the scope of this investigation.

Overall, experimental results from the inclusion and exclusion of amino acid supplements in growth media reveals a rather complex metabolic requirement in *N. meningitidis*. Under conditions described in previous sections, glutamine and cysteine are crucial to the survival of *N. meningitidis*. With the predicted presence of a glyA (serine hydroxymethyltransferase) homologue, at least one of serine or glycine is also required. Arginine confers advantages to growth, and at least one arginine biosynthesis pathway – from glutamate – has been predicted in *N. meningitidis* (KEGG; www.kegg.jp). Despite the absence of a dedicated glutamate synthase homologue, ammonium normally present in CDM can serve as a nitrogen source for the NADP-specific glutamate dehydrogenase GdhA, providing a likely and alternative pathway for the biosynthesis of glutamate (Schoen *et al.*, 2014). The presence of an annotated meningococcal glutamine synthetase homologue NMB0359 (*E. coli* GlnA), although normally responsible for catalysing the biosynthesis of L-glutamine from L-glutamate using ammonium, implies that synthesis of L-glutamate is also a likely product as hydrolysis of L-glutamine can occur (Eisenberg *et al.*, 2000). It appears, however, that although endogenous supply of arginine supports meningococcal survival, it was not sufficient for sustaining growth at optimal levels demonstrated only in the presence of exogenous arginine. Last but not least, arginine is also a starting material for meningococcal polyamine biosynthesis, of which putrescine can be synthesised from arginine via agmatine in the presence of the relevant enzyme homologues as described in Chapter 3.

Glutamine transport in another meningitis-causing pathogen Group B streptococci is carried out by GlnQ with great implications in virulence (Tamura *et al.*, 2002). The meningococcal homologue NMB0787 and gonococcal homologue NGO0372 are involved in glutamine uptake in pathogenic Neisseriae, where exogenous glutamine as a substrate can induce upregulation of the *N. gonorrhoeae* clusters of ABC transporter genes and

mediate expression of other virulence-associated genes (Friedrich *et al.*, 2007). In that work L-glutamine was added at 2 mM to a glutamine-free culture 3 hours into gonococcal growth to elicit positive transcriptional changes, which was similar to the original glutamine concentration of 4 mM in CDM in this study. By lowering glutamine levels to 0.4 mM, it is not inconceivable for it to have a profound effect on wild-type growth. The *NMB0240*$^{-}$ mutant, however, appeared unaffected by this change. The highly comparable phenotypes between the two strains therefore make the case for Genomic Island 3 in also having a (non-exclusive) role in glutamine uptake.

Supplementation with some amino acids appears to prevent *N. meningitidis* from achieving higher yields during exponential growth, such as alanine and glycine. A possible theory would be that exogenous alanine and glycine, the two smallest amino acids, compete for the use of transporters shared by other key meningococcal nutrients, and hence the absence of alanine and removal of glycine from CDM may have facilitated the effective utilisation of compounds that were previously difficult to access. Cysteine, which forms a core part of the original chemically-defined media recipe, appears to be more advantageous to meningococcal growth rate (but deleterious to yield) at lower concentrations. Cysteine toxicity can impair bacterial growth particularly in minimal media, and multiple mechanisms that tightly regulate its effects have been reported in various Enterobacteriaceae (Kari *et al.*, 1971; Ohtsu *et al.*, 2010; Oguri *et al.*, 2012; Takumi and Nonaka, 2016). In *N. meningitidis* cysteine has been demonstrated as a growth-limiting media component, where depletion can lead to lowered tolerance to oxidative stress (van de Waterbeemd *et al.*, 2013). The exact mechanisms in play here, however, is unclear.

The above findings appear to have painted an interesting picture with regards to the highly specific nature of CDM. The fact that the *N. meningitidis* wild-type strain used here (serogroup B MC58) is highly sensitive to alterations in amino acid composition demonstrates the versatility of the CDM used. Although very well designed, there appears to be some redundancy among the CDM components. In fact, it is not uncommon that minimal media often require more bespoke, strain-specific adjustments in order to achieve optimal growth which facilitates the conduction of experiments. Together with the generally growth-promoting effects of isoleucine which is relatable to global transcriptional upregulation, the implications of these are explored in Chapter 5.

In conclusion, it is fundamental for pathogens to access host nutrient in order to survive and successfully establish themselves in their respective niches prior to pathogenesis. Many pathogenic bacteria have evolved ways to scavenge nutrients such as amino acids from the microenvironment, whilst evading the mechanisms employed by the host

response to starve them through limiting their availability (Zhang and Rubin, 2013). Some have even coined the term “nutritional virulence” (Abu Kwaik and Bumann, 2013). *N. meningitidis*, compounded by its relatively small genome size of ~2.3 Mbp, does not appear to possess a typical repertoire of virulence genes, and yet has become increasingly evident that metabolic adaption is the key determinant of the meningococcal capability to invade (Schoen *et al.*, 2014). It therefore remains important that the characterisation of genes possibly involved in the mundane transport of metabolic products and cellular building blocks conserved only in pathogenic strains be given the same degree of attention as those which codes for direct means of cellular invasion.

Chapter 5 – Role of isoleucine in *N. meningitidis* regulation and chemically-defined minimal media

5.1 Introduction

In Section 4.4.2, the exogenous supplementation of L-isoleucine to liquid cultures of *Neisseria meningitidis* in chemically-defined media (CDM) was shown to universally enhance growth of both wild-type strain MC58 as well as that of the *NMB0240*$^{-}$ (Genomic Island 3) knockout mutant. Similarly, the removal or lowering the concentrations of certain amino acids also resulted in marked growth improvements. Here the implications of the aforementioned trends are explored in order to optimise the CDM for growth of *N. meningitidis*. The genetic basis for the impact of isoleucine on *N. meningitidis* growth was also examined.

5.2 Isoleucine and the meningococcal *lrp* regulon

As mentioned in Chapter 1, *N. meningitidis* consists of a handful of transcriptional regulator systems which monitor the uptake of essential nutrients, metabolism and respond to changes in their availability, one of which is Lrp. Lrp (L-leucine-responsive protein) is a small (~15 kDa) transcriptional regulator with homologues widely distributed as multimers in bacteria as well as archaea (Brinkman *et al.*, 2003; Unoarumhi *et al.*, 2016; Peeters and Charlier, 2010). Many operons important for bacterial maintenance and survival are controlled by this member of the Lrp/AsnC family, and thus Lrp is known as a global regulator. It is so named because the presence or absence of L-leucine mediates the activation or inhibition of pathways and cellular processes that are regulated by Lrp. *E. coli* as a model organism was used extensively to characterise Lrp, where lesions in the gene result in both positive and negative effects on the expression of many proteins arguably involved in adaptation to major environmental changes (Ernsting *et al.*, 1992). Lrp had been shown to significantly affect transcription of about 10% of all *E. coli* genes, indicating a large regulatory network involving more than 400 genes (Tani *et al.*, 2002). Despite its namesake, intracellular leucine levels or presence do not always have an effect on potentiating or antagonising Lrp-mediated genes (Calvo and Matthews, 1994). Nonetheless it was broadly suggested that leucine abundance together with that of Lrp are responsible for oversight in bacterial transition between “feast and famine” (Landgraf *et al.*, 1996).

Lrp orthologs from many genera collectively respond to wide range of amino acids aside from leucine (Hart and Blumenthal, 2011). The set of genes controlled by the Lrp regulon had been analysed *in silico* in *E. coli* using leucine as the signalling molecule (Cho *et al.*,

2008). Additionally, it was also shown in *Corynebacterium glutamicum* that all branched chain amino acids (BCAAs) – L-leucine, L-isoleucine, L-valine, as well as the closely-related (nominally aliphatic) L-methionine – were able to stimulate significant global expression changes induced by direct Lrp binding when supplemented in minimal media (Lange *et al.*, 2012). This showed that for Lrp to function leucine is not always the exclusive effector amino acid, and that this depends on the species containing the Lrp homologue.

Neisseria meningitidis encodes NMB0573 and NMB1650, which are two paralogous gene products that were annotated as members of the Lrp/AsnC family of regulators. In some instances, *NMB1650* was regarded as the *lrp* gene (Hey *et al.*, 2013). Solving the crystal structure of the NMB0573 octamer, however, provided a stronger case for *NMB0573*, where the protein was duly characterised as the meningococcal Lrp homologue (gene incorrectly annotated as *asnC*) responding to both leucine and methionine as ligands (Ren *et al.*, 2007). Microarray analyses from the same work also showed that *NMB0240* (part of Genomic Island 3) was upregulated in a *NMB0573*$^{-}$ knockout model, which provided a putative link between possible Lrp activity and the phenotypes induced by isoleucine supplementation in CDM.

5.3 Effects of isoleucine on growth of *N. meningitidis* under various amino acid profiles of CDM

In Section 4.4.2, among the branched chain amino acids (BCAAs) the inclusion of isoleucine in CDM was shown to be sufficient to bring about statistically significant enhanced growth rate and yield to both wild-type and *NMB0240*$^{-}$ mutant strains of *N. meningitidis* (shown below again as Figure 5.1).

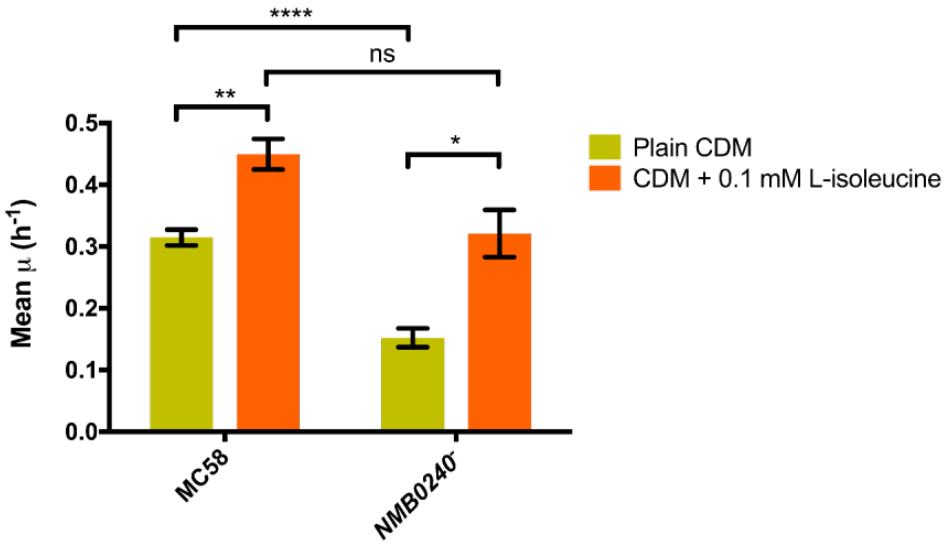

Fig. 5.1 – Specific growth rates extrapolated for *N. meningitidis* wild-type MC58 and *NMB0240*⁻ mutant in (green ochre) plain, complete CDM and (orange) CDM supplemented with minimal isoleucine. For statistical analyses, Student's *t*-tests were carried out to compare growth differences ($P \leq 0.05$). Asterisks are denoted as per formatting of GraphPad PRISM 7, where P-values of: ≥ 0.05 = not significant (ns); 0.01 to 0.05 = significant (*); 0.001 to 0.01 = very significant (**); 0.0001 to 0.001 = extremely significant (***) and; < 0.0001 = extremely significant (****) (GraphPad Software Inc., 2017).

As pointed out, this improved growth did not account for *NMB0240*⁻ mutant growth phenotype, since a difference in growth remained between that and the wild-type (See Chapter 4). Moreover, when isoleucine was supplemented to CDM under varying amino acid profiles, in most cases both wild-type (Figure 5.2) and the *NMB0240*⁻ mutant (Figure 5.3) meningococci similarly experienced substantial improvements in terms of specific growth rate. Although it did not address the specific hypotheses discussed in Chapter 4, it was subsequently speculated that enhancement of growth by isoleucine might be a consequence of transcriptional changes mediated by the global regulator Lrp through a response to the presence of exogenous BCAAs.

To test this hypothesis, a knockout mutant unable to express intact meningococcal Lrp homologue was constructed in this study.

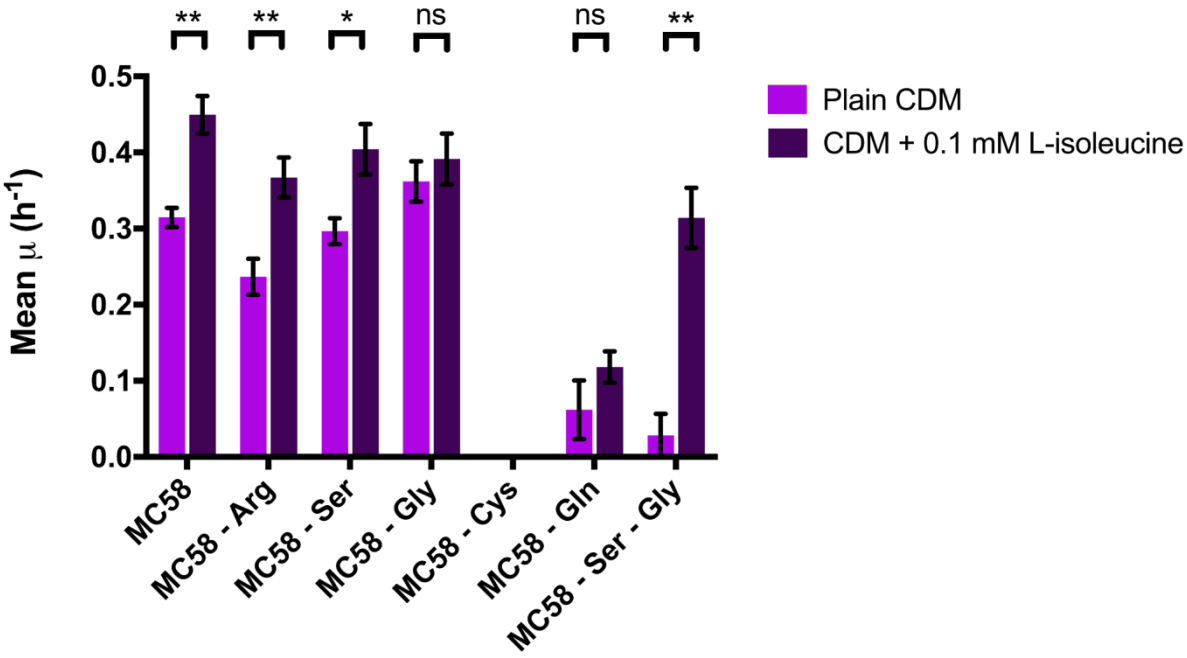

Fig. 5.2 – Specific growth rates of *N. meningitidis* wild-type MC58 in (light purple) plain, complete CDM and (dark purple) CDM with altered concentrations of core amino acids: **(from left to right)** control; without arginine; without serine; without glycine; without cysteine; without glutamine, and; without both serine and glycine. Bars are absent for conditions which did not result in observable net growth and therefore no growth rate extrapolation. For statistical analyses, Student's *t*-tests were carried out to compare growth differences ($P \leq 0.05$). Asterisks are denoted as per formatting of GraphPad PRISM 7, where P-values of: ≥ 0.05 = not significant (ns); 0.01 to 0.05 = significant (*); 0.001 to 0.01 = very significant (**); 0.0001 to 0.001 = extremely significant (***) and; < 0.0001 = extremely significant (****) (GraphPad Software Inc., 2017).

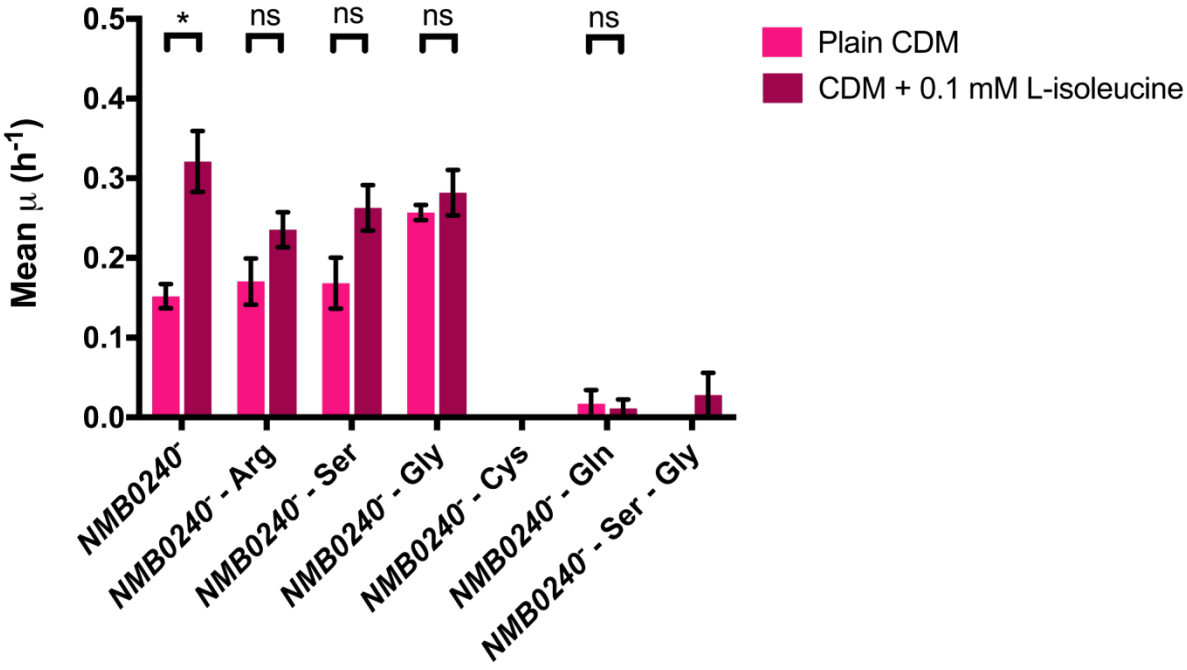

Fig. 5.3 – Specific growth rates of *N. meningitidis NMB0240*⁻ mutant strain in (pink) plain, complete CDM and (rose) CDM with altered concentrations of core amino acids: **(from left to right)** control; without arginine; without serine; without glycine; without cysteine; without glutamine, and; without both serine and glycine. Bars are absent for conditions which did not result in observable net growth and therefore no growth rate extrapolation. For statistical analyses, Student's *t*-tests were carried out to compare growth differences ($P \leq 0.05$). Asterisks are denoted as per formatting of GraphPad PRISM 7, where P-values of: ≥ 0.05 = not significant (ns); 0.01 to 0.05 = significant (*); 0.001 to 0.01 = very significant (**); 0.0001 to 0.001 = extremely significant (***) and; < 0.0001 = extremely significant (****) (GraphPad Software Inc., 2017).

5.4 Construction of a knockout mutant for the *NMB0573* gene of *N. meningitidis*

Dr. Vlaimir Pelicic from Imperial College kindly provided a total genomic DNA (gDNA) extraction of a NMV_1850-deficient (i.e. homologous to NMB0573-deficient) mutant from a library of kanamycin-resistant *N. meningitidis* serogroup C strain 8013 (Rusniok *et al.*, 2009). This was based on the *Himar1 mariner*-based transposon-mediated high-throughput *in vitro* mutagenesis of and subsequent chromosomal transposition into naturally competent *N. meningitidis* (Pelicic *et al.*, 2000), resulting in thousands of randomly-generated mutants (Geoffroy *et al.*, 2003).

In this study, the gDNA (Figure 5.4-2) was transformed into *N. meningitidis* serogroup B strain MC58 wild-type according to the TSB protocol as described in Chapter 2 and selected for using 80 µg/ml kanamycin, and subsequently confirmed with colony PCR (primers shown in Table 5; sites of complementation shown in Figure 5.4-1; bands shown in Figure 5.4-3).

No.	Primer Name	Primer Sequence (5' to 3')	Nucleotide Position
(a)	NMB0573_for	5'-CCGAAAACAAAATTTGTCCCGG-3'	601049 – 601070
(b)	NMB0573_rev	5'-TTTGCAGATTGCACGTGCGGG-3'	601671 – 601691

Table 5 – List of primers used for the PCR confirmation of the NMB0573-deficient mutant strain of *N. meningitidis* MC58: **(a)** forward and **(b)** reverse screening primers.

Fig. 5.4-1 – The ***NMB0573*** gene (in blue text) including its flanking regions (in black text), start (green outlined bold text) and stop (red outlined text) codons. Sequences of adjacent genes are denoted in grey text. Complementation sites of cloning/confirmation primers NMB0573_for and NMB0573_rev (white text in blue arrow box) were also shown, binding to intergenic sequences and ensuring inclusion of all *NMB0573* coding sequences.

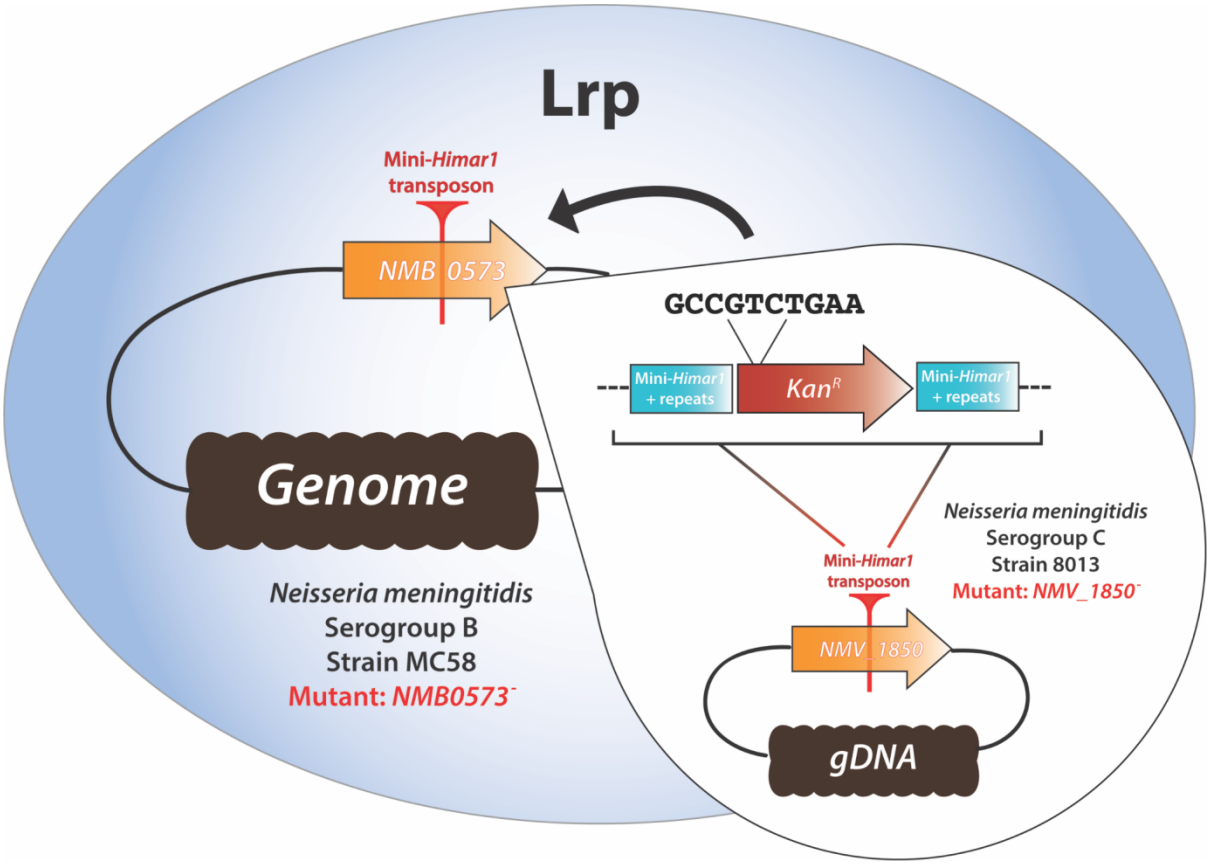

Fig. 5.4-2 – Schematics of *NMB0573*$^{-}$ (*lrp*) mutagenesis by *Himar1* transposon, based on a protocol first described by Akerley *et al.* (1998). The first and last 100 bp from the *Himar1 mariner* transposon (Lampe *et al.*, 1996) were cloned ("Mini-*Himar1*"). Summarily, the 1.6 kbp "minitransposon" constructed by Pelicic *et al.* (2000) consisted of a 1.5 kbp *Neisseria* kanamycin resistance cassette (*Kan*^{R}) with a neisserial uptake sequence (GCCGTCTGAA) flanked by the Mini-*Himar1* and inverted repeats. The insert remains stable at site after transposition into meningococcal chromosome and random mutagenesis. A *NMV_1850*$^{-}$ mutant 8013 strain was generated from this, and the purified genomic DNA extract was used to create a *NMB0573*$^{-}$ mutant MC58 strain for this study following transformation and chromosomal rearrangement.

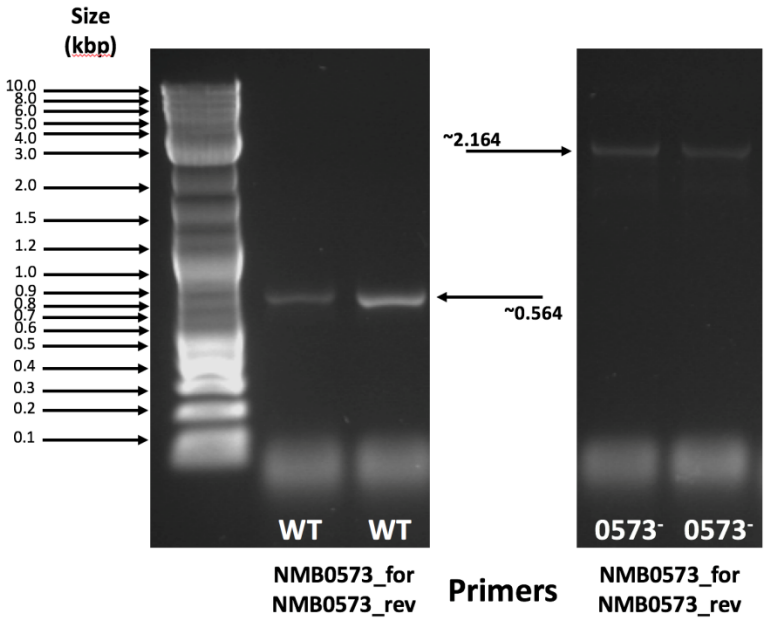

Fig. 5.4-3 – PCR products of the wild type *NMB0573* gene (WT) and the disrupted mutant gene (0573^{-}) using the NMB0573 screening primers in Table 5. Although *NMB_1850* is 483 bp long, *NMB0573* is slightly longer at 564 bp while perfectly aligned with *NMV_1850* (See Appendices: Figure D). Therefore, the size of MC58 homologue *NMB0573* (564 bp) plus the 1.6 kbp minitransposon described above (Pelicic *et al.*, 2000) resulted in a 2.164 kbp product. This heavier product is present in *N. meningitidis* serogroup B strain MC58 successfully transformed with serogroup C strain 8013 mutant gDNA which is deficient in NMV_1850, which is now deficient in NMB0573.

The resulting *NMB0573*$^{-}$ mutant strain (transformed MC58) displayed faster growth than the wild-type MC58 in CDM, while there were no observable differences between the two when cultured in MHB (Figure 5.4-4). This suggested that Lrp normally represses aerobic meningococcal growth under conditions present in nutrient-poor environments but not in the nutrient-rich MHB.

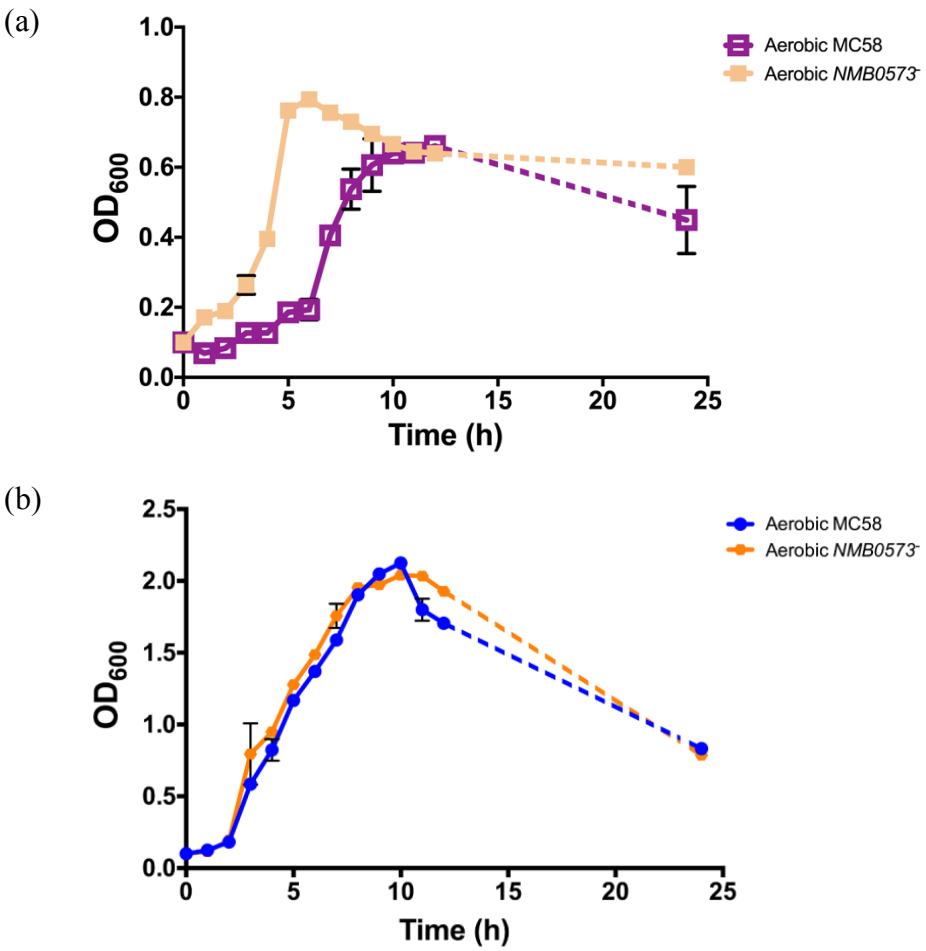

Fig. 5.4-4 – Differences in growth phenotypes of *NMB0573*$^{-}$ mutant compared to wild-type, showing **(a)** a significantly higher growth rate compared to that of wild-type MC58 when cultured in **CDM**, and; **(b)** highly comparable levels of exponential growth when cultured in **MHB**. The growth curves shown here are representative figures of experiments carried out in technical and biological triplicates.

It can be argued that Lrp may have been preventing rapid depletion of nutrients when exposed to nutrient-limited environments by providing close regulation for balanced meningococcal proliferation (i.e. "feast and famine"). This can be supported by the fact that despite a faster growth rate during log phase, the *NMB0573*$^{-}$ mutant reached a similar maximum yield as the wild-type MC58 when cultured in CDM before levelling off.

Likewise, as the role played by Lrp on *N. meningitidis* is global in effect, so are the respective changes exhibited when it is knocked out. A plethora of meningococcal genes were either upregulated or downregulated by the *lrp* lesion (Ren *et al.*, 2007), and it would require additional efforts to ascertain which global changes in particular led to such growth phenotypes. A possible explanation for the almost identical growth phenotypes in MHB is that the rich media likely contains an excess of isoleucine. Overall the trends suggest that Lrp is not essential for *N. meningitidis* growth in a nutrient-rich environment.

5.5 *Lrp* knockout ablates effect of isoleucine on *N. meningitidis* growth

To test the effects of exogenous isoleucine supplementation on meningococcal growth in CDM, wild-type MC58 and *NMB0573*$^{-}$ knockout mutant strains were cultured accordingly and cross-compared (Figure 5.5-1).

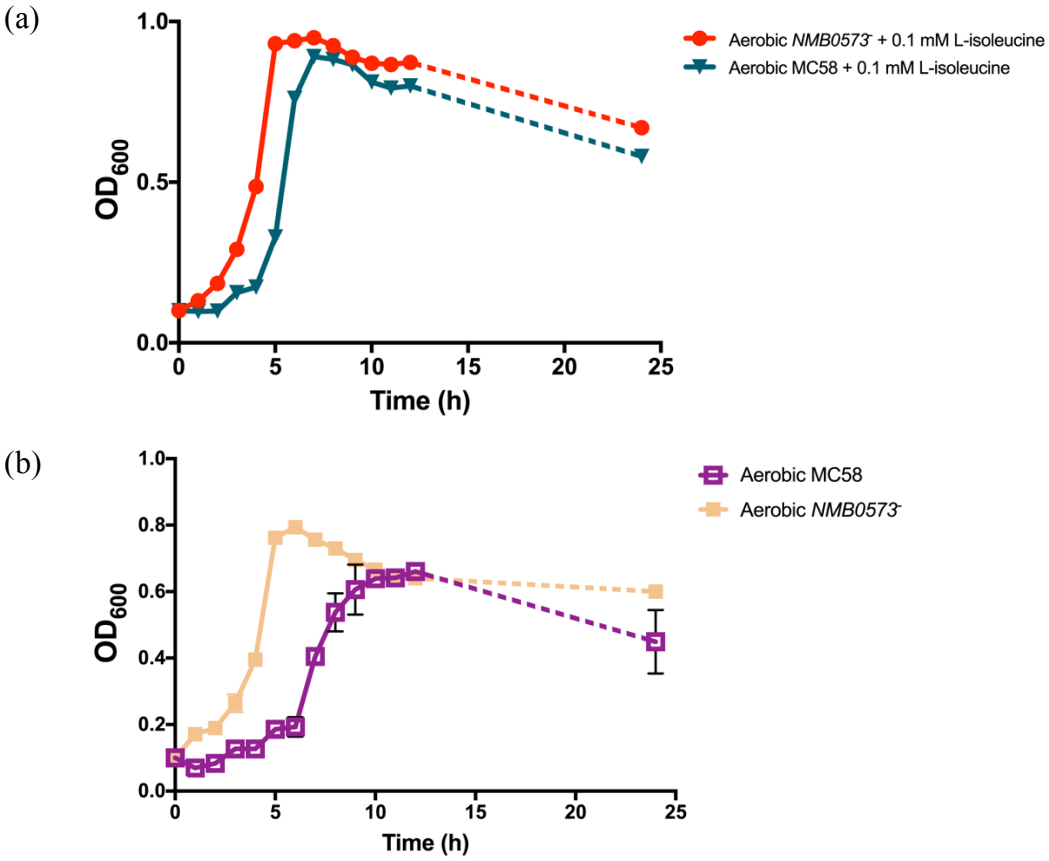

Fig. 5.5-1 – Effects of L-isoleucine supplementation in CDM on *N. meningitidis*: **(a)** wild-type MC58 and *NMB0573*$^{-}$ knockout mutant growth in CDM with isoleucine, compared to; **(b)** wild-type MC58 and *NMB0573*$^{-}$ knockout mutant growth in plain, complete CDM as control. The growth curves shown here are representative figures of experiments carried out in technical and biological replicates.

If isoleucine indeed plays the role of an effector in meningococcal global regulation (See Section 5.3), at first glance it was questionable as to why the Lrp mutant strain would seemingly respond to the presence of isoleucine in CDM (Figure 5.5-1 (a)). Despite appearances, however, the addition of isoleucine did not confer statistically significant growth benefits to the *NMB0573*$^{-}$ mutant in CDM (Figure 5.5-2). The specific growth rates of the *NMB0573*$^{-}$ mutant were also highly similar to those of isoleucine-supplemented wild-type (i.e. all between 0.4 to 0.5 h^{-1}). Taking into account of the predicted upregulation of *NMB0240* expression (intact here) that accompanies an Lrp mutation, this did not appear to result in growth changes that may distinguish the *NMB0573*$^{-}$ mutant phenotype from that of the isoleucine-supplemented wild-type.

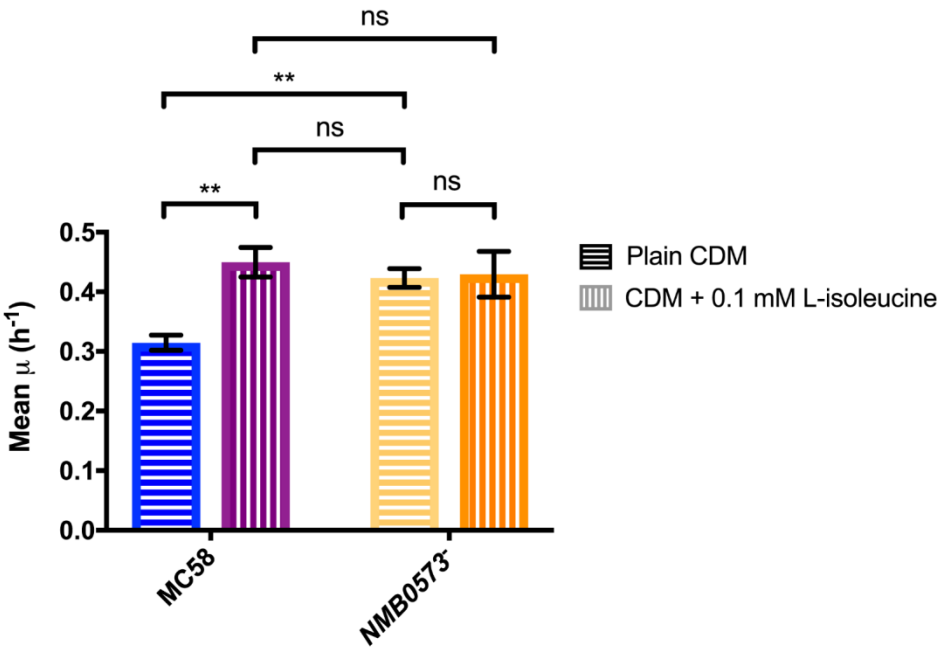

Fig. 5.5-2 – Specific growth rates of *N. meningitidis* (blue and purple) wild-type MC58 and (sand and orange) *NMB0573*$^{-}$ mutant in (horizontal stripes) plain, complete CDM and (vertical stripes) CDM supplemented with exogenous L-isoleucine. For statistical analyses, Student's *t*-tests were carried to compare growth differences ($P \leq 0.05$). Asterisks are denoted as per formatting of GraphPad PRISM 7, where P-values of: ≥ 0.05 = not significant (ns); 0.01 to 0.05 = significant (*); 0.001 to 0.01 = very significant (**); 0.0001 to 0.001 = extremely significant (***) and; < 0.0001 = extremely significant (****) (GraphPad Software Inc., 2017).

The results suggested that regulation by Lrp can explain the effects of isoleucine on *N. meningitidis* in CDM. A wide range of pathways were both up-regulated and down-regulated following knock out of NMB0573, resulting in significantly improved meningococcal growth. Supplementing CDM with exogenous isoleucine similarly resulted in marked growth improvements. Although not all changes in the meningococcal *lrp*$^{-}$ mutant can be unitarily replicable in the wild-type by isoleucine, this parallelism summarily implied that the effects of isoleucine on growth in CDM were ablated when the *NMB0573* was knocked out.

5.6 An improved CDM optimised for *N. meningitidis* MC58

From the above, it was found that the effects of isoleucine on *N. meningitidis* growth can be explained as being due to its interaction with the global regulator Lrp. In practical terms, however, L-isoleucine would serve to greatly improve the potency of the CDM by making it easier to observe growth trends in future investigations into *N. meningitidis* response to nutritional changes.

From Figure 4.5-2 (d), 4.5-3 (c), it was observed that lowering the concentration of L-cysteine in CDM elicited a slight but statistically insignificant increase in growth on both *N. meningitidis* wild-type MC58 and *NMB0240*⁻ mutant. Taking into account the ameliorative effects shown by the removal of L-glycine from CDM and the fact that L-isoleucine appeared to act as a general growth factor in culture, it was hypothesised that the combination of all three conditions may be able to generate the highest-performing meningococcal growth seen in CDM. The result, however, suggested otherwise (Figure 5.6-1).

(a)

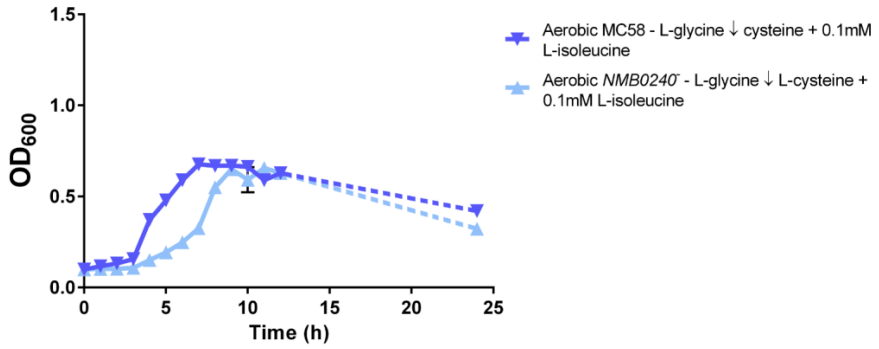

(b)

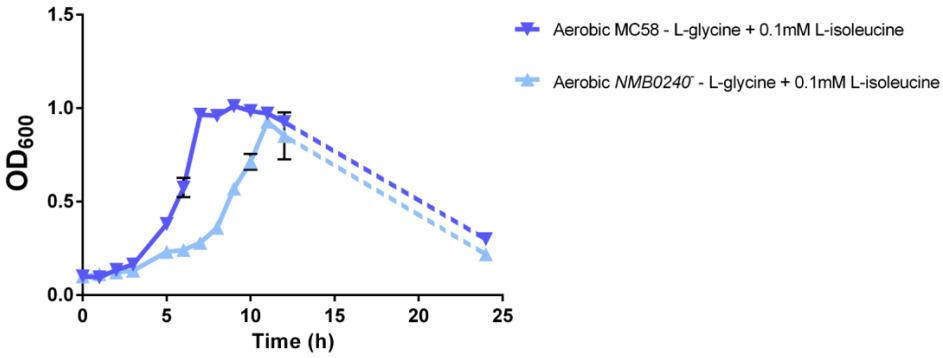

(c)

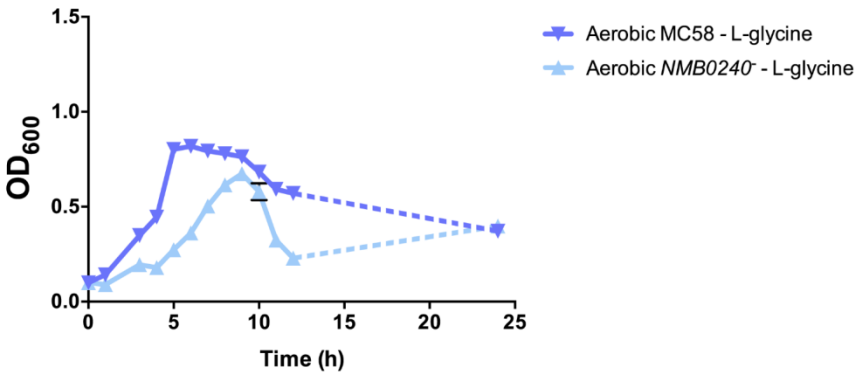

(d)

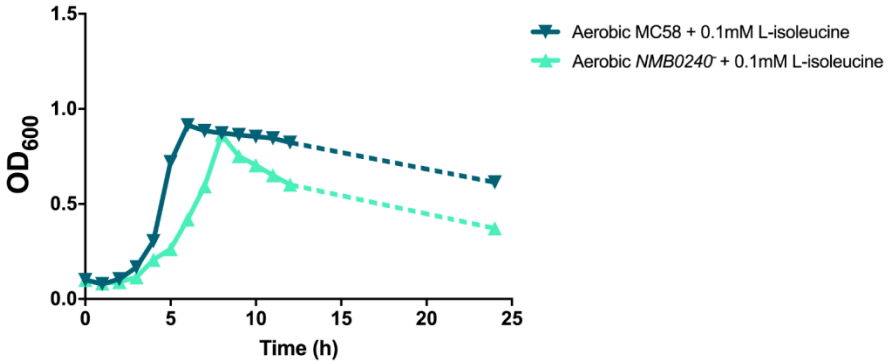

(e)

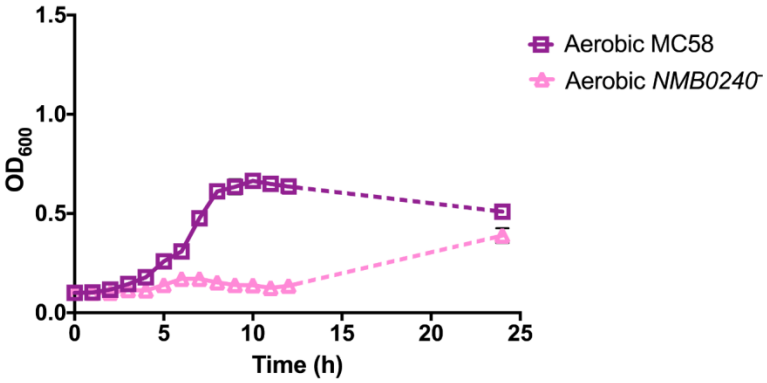

Fig. 5.6-1 – Effects of removal of L-glycine, lowered L-cysteine concentrations and L-isoleucine supplementation in CDM on *N. meningitidis* wild-type MC58 and *NMB0240*⁻ mutant growth, shown by comparison of growth in **(a)** CDM without L-glycine, 10-fold lowered availability of L-cysteine (i.e. from 0.4 mM to 0.04 mM) and addition of L-isoleucine; **(b)** CDM without L-glycine and addition of L-isoleucine; **(c)** CDM without L-glycine; **(d)** CDM with L-isoleucine, and; **(e)** plain, complete CDM. The growth curves shown here are representative figures of experiments carried out in technical and biological triplicates.

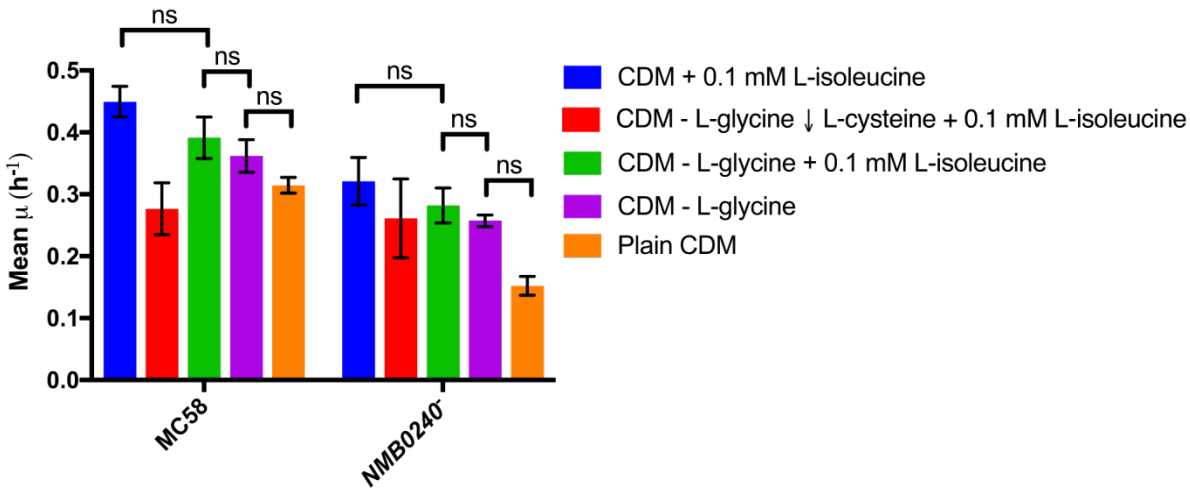

Fig. 5.6-2 – Specific growth rates of *N. meningitidis* wild-type MC58 and *NMB0240*⁻ mutant in (blue) CDM with isoleucine; (red) CDM without glycine, 10-fold lower concentrations of cysteine (i.e. from 0.4 mM to 0.04 mM) and addition of isoleucine; (green) CDM without glycine and addition of isoleucine; (purple) CDM without glycine, and; (orange) plain, complete CDM. For statistical analyses, Student's *t*-tests were carried out where there are comparisons of growth differences ($P \leq 0.05$). Asterisks are denoted as per formatting of GraphPad PRISM 7, where P-values of: ≥ 0.05 = not significant (ns); 0.01 to 0.05 = significant (*); 0.001 to 0.01 = very significant (**); 0.0001 to 0.001 = extremely significant (***) and; < 0.0001 = extremely significant (****) (GraphPad Software Inc., 2017).

The specific growth rates (Figure 5.6-2) reinforced the message conveyed by the growth curves above. Lowering the availability of cysteine resulted in poorer growth than the replacement of glycine with isoleucine alone, while excluding glycine from isoleucine-supplemented CDM resulted in slightly poorer growth compared to isoleucine supplementation alone. The importance of cysteine and glycine had been discussed in Chapter 4. Overall apart from that between complete CDM without or without isoleucine, the above variations in CDM compositions amounted to no statistically significant differences with each other.

5.7 Conclusions

Chemically-defined medium for nutritional investigations of *N. meningitidis* was first proposed more than three-quarters of a century ago (Frantz, 1942). It had subsequently seen numerous modifications. The original formulae upon which this study adapted its CDM from had been devised more than half a century ago in both agar and fluid forms for "quantitative genetic studies", where the authors explicitly admitted that L-glycine was not essential and was only included because it had a slight stimulatory effect on colony counts of *N. meningitidis* strain 15 (Catlin and Schloer, 1962). In fact, chemically-defined media were often altered slightly in their composition for different strains or study aims. For example, some investigators would use L-cystine instead of L-cysteine (Catenazzi, 2013). In addition, a "maximal" media was also reported where L-isoleucine can be present in meningococcal or gonococcal cultures at a final concentration of 0.23 mM (Catlin, 1973).

Together with the experimental results above, there is a case for an improved CDM tailored specifically for *N. meningitidis* serogroup B strain MC58 by introducing L-isoleucine. In scenarios where the presence of L-isoleucine is not desirable, the exclusion of L-glycine from CDM would also be beneficial to meningococcal growth. As faster growth rates and higher yields often facilitate observation of growth phenotypes, this would be especially useful for mutant strains with growth-impairing lesions.

Chapter 6 – General Discussion and Future Directions

6.1 General Discussion

Determinants of virulence and pathogenicity are often intertwined with that of bacterial metabolism and fitness whilst residing in a host (Snyder and Saunders, 2006). To establish a steady presence in humans, bacteria need to evade host immune responses by showing variability or mimicry. The driving forces embodied by the various environmental challenges are met with a genomic readiness to embrace changes. Naturally competent bacteria can achieve this through their capacity to accommodate foreign genetic materials both inter- and intra-species of origin. Systems such as the Lrp/AsnC family or small regulatory RNAs also allow for switching between "feast or famine" metabolic phenotypes (Yokoyama *et al.*, 2006; Pannekoek *et al.*, 2017).

Carriage of obligate commensals such as *Neisseria meningitidis* can normally be rendered harmless, as long as competition from other niche occupants keeps them at bay while immunosurveillance keeps them in check. When risk factors compromise such defences, this arguably provides a window for any capable bacteria to seize the opportunity and pursue more myopic but high-return lifestyles. Nonetheless, it can be suggested that the proportionally small sizes of the pathogen-specific genomic islands reflect a preference for more conservative, localised genomic changes while fundamentally preserving speciation. The purported functions involved range from various amino acids, biotin to the more recently characterised propionic acid metabolism – arguably traits which one might not instinctively associate with pathogenicity.

This trend was reflected by the findings of this work. In general, the pathways investigated oversaw the transport, utilisation and biosynthesis of amino acids and their derivatives. The three-gene Genomic Island 5 synthesises the polyamine putrescine by expressing arginine decarboxylase (NMB0468) and agmatinase (NMB0469), as well as containing a putative transporter (NMB0470) of unknown function. Although the most straightforward finding of this work was confirming the function of NMB0468 and NMB0469, it was not possible to quantify the amount of putrescine present in culture. Considering the bacteria was very sensitive towards even minimal amounts of putrescine in terms of toxicity, perhaps the physiological levels of putrescine required to complement *N. meningitidis* was either very low, or that they fulfil their role in meningococci lifestyle and disease through less traditional, unclear means. The role of the transmembrane protein NMB0470 also remains open for future investigations, as its initial predicted function had no strong homology to

known C_4-dicarboxylate transporters, and showed neither essentiality nor immediate connection to putrescine biosynthesis.

Genomic Island 3 contains two genes (*NMB0239* and *NMB0240*) which have a role in meningococcal arginine and possibly glutamine metabolism under nutrient-limiting conditions. Misleading initial predictions suggested its involvement in synthesising spermine or spermidine due to query hits with low homology, which was contradicted with the absence of crucial precursor substrates and upstream pathways. With that route rejected, we endeavoured to the best of our efforts to identify nutritional conditions which may explain growth trends displayed by the mutant strain. When arginine and (to a large extent) glutamine were withheld from the defined media, wild-type growth was impaired to levels highly-comparable to the mutant strain deficient in these genes. Subsequent labelled-isotope assays reinforced the notion that Genomic Island 3 is required for optimal uptake and utilisation of arginine and glutamine in *N. meningitidis*.

A common theme was the role and fate of arginine in meningococcal maintenance. Preferably acquired from exogenous sources, intrinsic synthesis of arginine appeared to invoke substantial energetic stress as the meningococci attempt to compensate using alternative materials and mechanisms. Arginine is a key component in many metabolic processes and also the starting material for the meningococcal putrescine synthesis pathway. The clinical importance of such a system had also been previously explored in pathogenic *N. gonorrhoeae* (Gong *et al.*, 2016). However, it is uncertain whether the mechanisms encoded by both Genomic Islands 3 and 5 are critical for virulence. Aside from further characterisation work, *ex vivo* techniques using suitable models may also help address their real-world relevance and determine whether mutant behaviours can be aptly reflected *in vivo*.

Interestingly, the absence of Genomic Island 3 was not entirely detrimental to meningococcal replication under nutrient-rich media, while the same could be said for both islands when cultured under microaerobic conditions. We propose that the essentiality and activity of these genomic islands are environment-dependent. Overall this work continues to broadly reflect a highly elastic genetic structure which empowers *N. meningitidis* to adapt to different environmental conditions likely to be encountered *in vivo*, whether it is the nasopharyngeal mucosa, the bloodstream or the CSF. It should be noted that, whilst tempting to attribute so, “nutritional virulence” describes specialised means through which pathogens scavenge nutrients or compromise host denial mechanisms in order to enrich their own supply (Abu Kwaik and Bumann, 2013). Although this aspect is increasingly

relevant in meningococcal research (Schoen *et al.*, 2014), such paradigm has not yet been observed amongst the genomic islands in question.

A widely accepted notion is that virulent *N. meningitidis* strains are "accidental" pathogens, given that host death terminates further bacterial propagation through the more harmonious state of commensal co-existence (Moxon and Jansen, 2005). On the other hand, *N. gonorrhoeae* is capable of recurrent infections which establishes a comparatively more long-term presence within its host. The high degree of genetic similarities between all strains of the genus *Neisseria* was contrasted by their diverse phenotypes, especially among the very definitive pathogenic species (Maiden, 2008). Extensive polymorphisms such as phase and antigenic variations were often displayed by pathogenic Neisseriae and allowed for very different behaviours and specialisations (Marri *et al.*, 2010). Many of these genes are key to both meningococcal pathogenicity and commensalism, such as capsular antigens, outer membrane proteins and adhesins (Caugant, 2008). Evolutionary gain or loss of function in genes of individual *Neisseria* strains is also possible as the bacteria adapts accordingly to its typical microenvironment (Moir, 2011). Summarily, the core to both meningococcal success in outgrowth and downfall by host fatality lies in its enhanced flexibility in face of change (Schoen *et al.*, 2007).

6.2 Future Directions

In general, follow-up work should involve further exploration of the relationship between polyamines and the expression of oxidative stress response genes in *N. meningitidis*, as this project contains preliminary data that may serve as a foundation. This would complement the current knowledge on Genomic Island 5, where ideally the function of the third gene product NMB0470 may also be ascertained. Putting *Neisseria* research into clinical context, future prospects must include the alleviation of the antibiotic crisis with effective universal vaccines (Lipsitch and Siber, 2016). This is of utmost relevance to the genus given the notoriety of *N. gonorrhoeae* (Baarda *et al.*, 2017).

Specifically, future works may include the creation of a NMB0470-deficient mutant strain to ascertain the precise effects of the knocking out of this gene on meningococcal growth. The creation of a *NMB0240*$^{-}$ and *NMB0573*$^{-}$ double mutant strain can also be used to verify the predicted relationship between Lrp and Genomic Island 3, for example by comparing growth with the single mutant strains. Despite its crystal structure has not yet been solved, investigating the nature of the alternative Lrp/AsnC regulator NMB1650 is also encouraged, as its characterisation may serve as important groundwork for studies on meningococcal regulation. The apparent diauxic growth displayed in many putrescine-

related growth curves in Chapter 3 is also worthy of closer investigation, as it would be useful to understand what changes were taking place and what triggered these phenomena.

Taking a broader perspective, the comparison of results form a similar analysis in alternate *Neisseria* spp. such as *N. lactamica* would reveal the importance of the possession of these genomic islands and how commensal species cope with their absence. The relevance of the findings in this study to host-pathogen interactions is of particular interest. It would be of great significance if an infection model could be devised to investigate the role played by the genomic islands in pathogenesis, possibly by co-culturing human cell lines (e.g. macrophages) with mutant strains and comparing observations to that cultured with wild-type *N. meningitidis*. General ecological and evolutionary questions associated with *N. meningitidis* that arose from these results may also be explored in future works. A closing remark would be the re-emphasis of the usefulness of a dedicated plate reader/incubator for growth curve-based experiments with pathogenic *Neisseria*, as this could greatly alleviate logistical constraints and free-up invaluable resources for other investigations.

6.3 Final Conclusion

In conclusion, *N. meningitidis* is a small, versatile bacterium with a relatively humble arms profile, but is willing to adapt, and, using limited resources, punches above its weight. Aside from clinical implications, this brings food for thought regarding the relationship between mankind and its microbiota.

Appendix A – Sequence alignment: *speA* and *NMB0468*

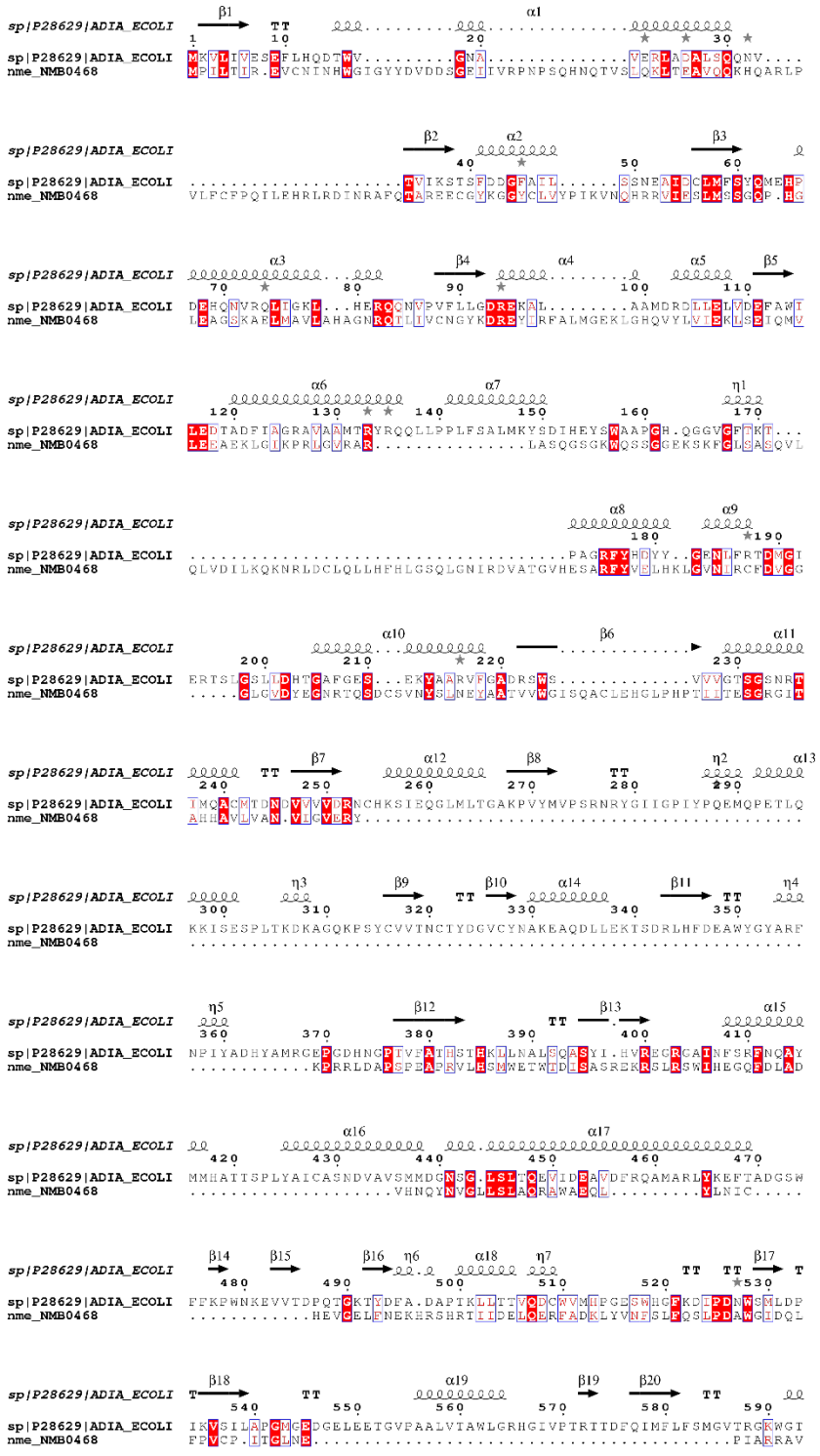

(Figure continued in next page)

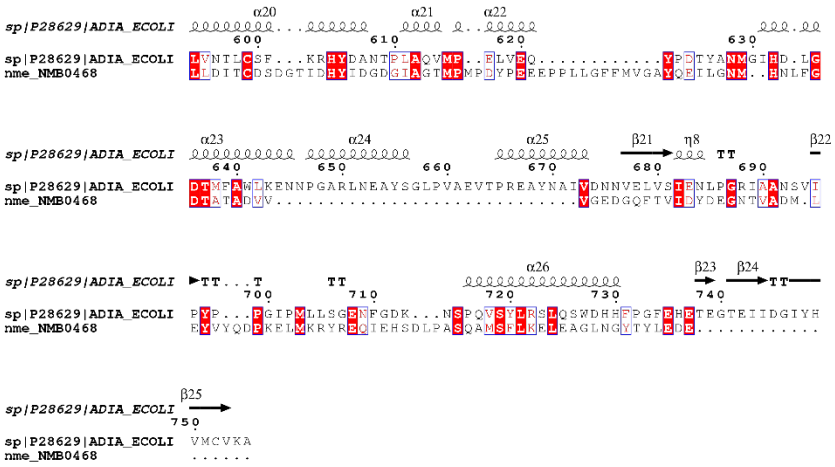

Fig. A – Structure-based alignment of (top to bottom) *E. coli* strain BL21 *speA* (NCBI GenBank™ accession no.: NP418541) (from Andréll *et al.*, 2009) and *N. meningitidis NMB0468* (NCBI GenBank™ accession no.: NP273515). Conserved key amino acid residues: D202; Not conserved: H255, K386, E739. Sequences were aligned using T-Coffee (http://tcoffee.vital-it.ch; Di Tommaso *et al.*, 2011) and displayed with secondary structures using ESPript 3 (http://espript.ibcp.fr; Robert and Gouet, 2014).

Appendix B – Sequence alignment: *speB* and *NMB0469*

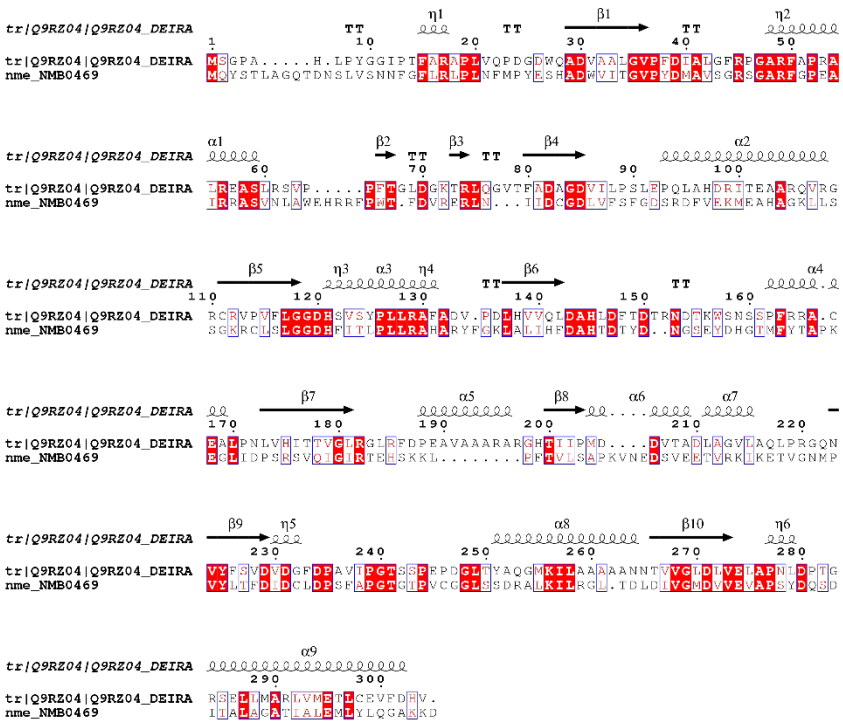

Fig. B – Structure-based alignment of (top to bottom) *Deinococcus radiodurans* manganese-activated *speB* (NCBI GenBank™ accession no.: NP285473) (from Ahn *et al.*, 2004) and *N. meningitidis NMB0469* (NCBI GenBank™ accession no.: NP273516). Conserved key amino acid residues: H121, D143, H145, D147, D229, D231, E274; Not conserved: L146, T149, N159, D187, S243. Sequences were aligned using T-Coffee (http://tcoffee.vital-it.ch; Di Tommaso *et al.*, 2011) and displayed with secondary structures using ESPript 3 (http://espript.ibcp.fr; Robert and Gouet, 2014).

Appendix C – Sequence alignment: *VcINDY* and *NMB0470*

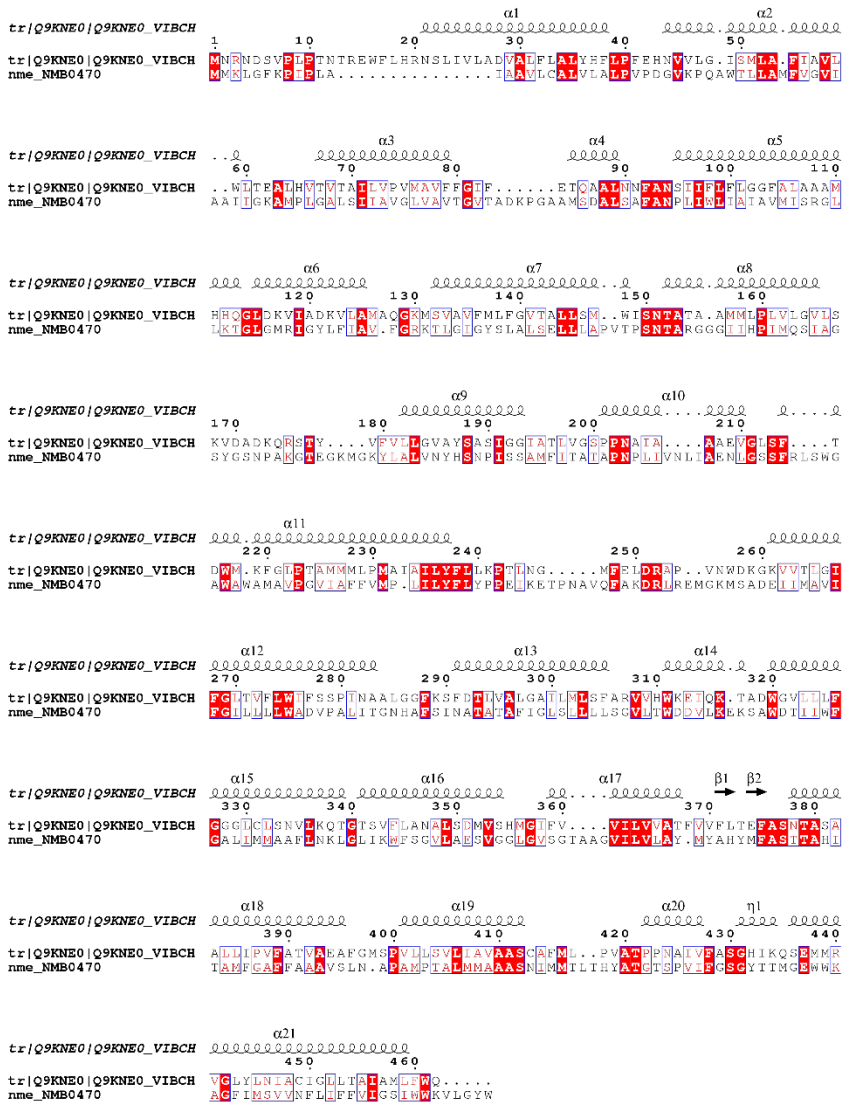

Fig. C – Structure-based alignment of (top to bottom) *Vibrio cholerae* sodium-dependent dicarboxylate transporter *INDY* (*VcINDY*) (NCBI GenBank™ accession no.: NP232426) (from Mancusso *et al.*, 2012) and *N. meningitidis NMB0470* (NCBI GenBank™ accession no.: NP273517). Conserved key amino acid residues: S150, N151, T152, P202, S377, T379, T421; Not conserved: S200, P201, N378, P422, P423. Sequences were aligned using T-Coffee (http://tcoffee.vital-it.ch; Di Tommaso *et al.*, 2011) and displayed with secondary structures using ESPript 3 (http://espript.ibcp.fr; Robert and Gouet, 2014).

Appendix D – Sequence alignment: *lrp, NMB0573* and *NMV_1850*

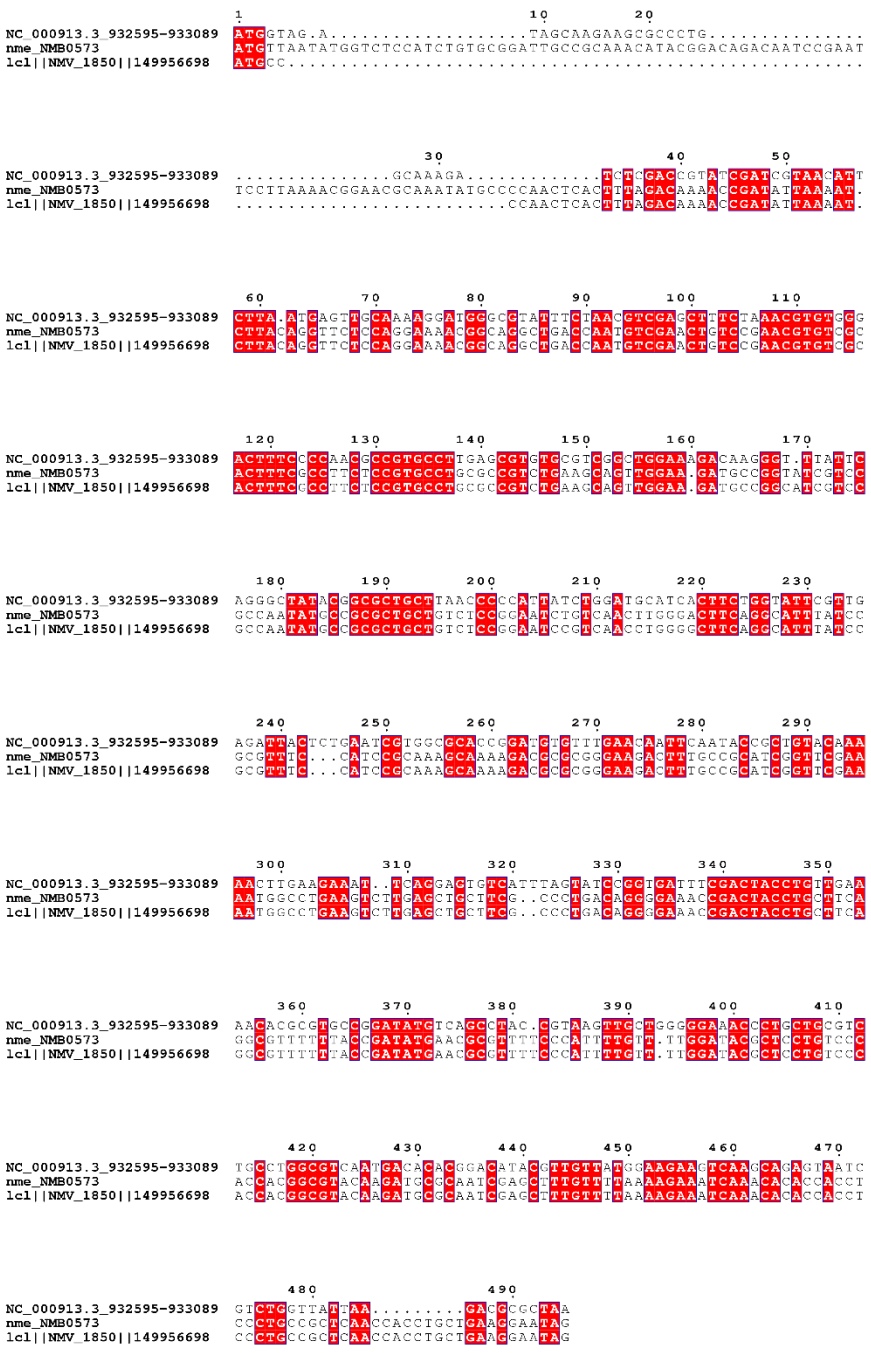

Fig. D – Alignment of (top to bottom) *E. coli* strain K12 *lrp* (NCBI GenBank™ accession number NP415409)*, N. meningitidis* serogroup B strain MC58 *NMB0573* (NCBI GenBank™ accession number NP273617) and serogroup C strain 8013 *NMV_1850* (NCBI GenBank™ accession number CAX50652). Sequences were aligned using T-Coffee (http://tcoffee.vital-it.ch; Di Tommaso *et al.*, 2011) and displayed with secondary structures using ESPript 3 (http://espript.ibcp.fr; Robert and Gouet, 2014).

References

Abu Kwaik, Y., Bumann, D. (2013) Microbial quest for food in vivo: 'nutritional virulence' as an emerging paradigm. *Cellular Microbiology*. **15**(6), 882–890.

Acevedo, R., Fernández, S., Zayas, C., Acosta, A., Sarmiento, M.E., Ferro, V.A., Rosenqvist, E., Campa, C., Cardoso, D., Garcia, L., Perez, J.L. (2014) Bacterial Outer Membrane Vesicles and Vaccine Applications. *Frontiers in Immunology*. **5**.

Acevedo, R., Zayas, C., Norheim, G., Fernández, S., Cedré, B., Aranguren, Y., Cuello, M., Rodriguez, Y., González, H., Mandiarote, A., Pérez, M., Hernández, M., Hernández-Cedeño, M., González, D., Brorson, S.-H., Rosenqvist, E., Naess, L., Tunheim, G., Cardoso, D., García, L. (2017) Outer membrane vesicles extracted from Neisseria meningitidis serogroup X for prevention of meningococcal disease in Africa. *Pharmacological Research*. **121**, 194–201.

Ahn, H.J., Kim, K.H., Lee, J., Ha, J.-Y., Lee, H.H., Kim, D., Yoon, H.-J., Kwon, A.-R., Suh, S.W. (2004) Crystal Structure of Agmatinase Reveals Structural Conservation and Inhibition Mechanism of the Ureohydrolase Superfamily. *Journal of Biological Chemistry*. **279**(48), 50505–50513.

Akerley, B.J., Rubin, E.J., Camilli, A., Lampe, D.J., Robertson, H.M., Mekalanos, J.J. (1998) Systematic identification of essential genes by in vitro mariner mutagenesis. *Proceedings of the National Academy of Sciences of the United States of America*. **95**(15), 8927–8932.

Anderson, M.T., Seifert, H.S. (2011a) Neisseria gonorrhoeae and humans perform an evolutionary LINE dance. *Mobile Genetic Elements*. **1**(1), 85–87.

Anderson, M.T., Seifert, H.S. (2011b) Opportunity and Means: Horizontal Gene Transfer from the Human Host to a Bacterial Pathogen. *mBio*. **2**(1).

Andréll, J., Hicks, M.G., Palmer, T., Carpenter, E.P., Iwata, S., Maher, M.J. (2009) Crystal Structure of the Acid-Induced Arginine Decarboxylase from Escherichia coli: Reversible Decamer Assembly Controls Enzyme Activity. *Biochemistry*. **48**(18), 3915–3927.

Anjum, M.F., Stevanin, T.M., Read, R.C., Moir, J.W.B. (2002) Nitric Oxide Metabolism in Neisseria meningitidis. *Journal of Bacteriology*. **184**(11), 2987–2993.

Anslyn, E.V. (2007) Supramolecular Analytical Chemistry. *The Journal of Organic Chemistry*. **72**(3), 687–699.

Arreaza, L., Salcedo, C., Alcalá, B., Vázquez, J.A. (2002) What about antibiotic resistance in Neisseria lactamica? *Journal of Antimicrobial Chemotherapy*. **49**(3), 545–547.

Baarda, B.I., Emerson, S., Proteau, P.J., Sikora, A.E. (2017) Deciphering the Function of New Gonococcal Vaccine Antigens Using Phenotypic Microarrays. *Journal of Bacteriology*. **199**(17), e00037-17.

Baart, G.J., Zomer, B., de Haan, A., van der Pol, L.A., Beuvery, E.C., Tramper, J., Martens, D.E. (2007) Modeling Neisseria meningitidis metabolism: from genome to metabolic fluxes. *Genome Biology*. **8**(7), R136.

Bakir, M., Yagci, A., Ulger, N., Akbenlioglu, C., Ilki, A., Soyletir, G. (2001) Asymtomatic carriage of Neisseria meningitidis and Neisseria lactamica in relation to Streptococcus pneumoniae and Haemophilus influenzae colonization in healthy children: apropos of 1400 children sampled. *European Journal of Epidemiology*. **17**(11), 1015–1018.

van de Beek, D., Brouwer, M., Hasbun, R., Koedel, U., Whitney, C.G., Wijdicks, E. (2016) Community-acquired bacterial meningitis. *Nature Reviews Disease Primers*. **2**, nrdp201674.

Belland, R.J., Morrison, S.G., Carlson, J.H., Hogan, D.M. (1997) Promoter strength influences phase variation of neisserial opa genes. *Molecular Microbiology*. **23**(1), 123–135.

Bennett, J.S., Griffiths, D.T., McCarthy, N.D., Sleeman, K.L., Jolley, K.A., Crook, D.W., Maiden, M.C.J. (2005) Genetic Diversity and Carriage Dynamics of Neisseria lactamica in Infants. *Infection and Immunity*. **73**(4), 2424–2432.

Biasini, M., Bienert, S., Waterhouse, A., Arnold, K., Studer, G., Schmidt, T., Kiefer, F., Cassarino, T.G., Bertoni, M., Bordoli, L., Schwede, T. (2014) SWISS-MODEL: modelling protein tertiary and quaternary structure using evolutionary information. *Nucleic Acids Research*. **42**(Web Server issue), W252–W258.

Blakley, R.L. (1960) A spectrophotometric study of the reaction catalysed by serine transhydroxymethylase. *Biochemical Journal*. **77**(3), 459–465.

Boulette, M.L., Baynham, P.J., Jorth, P.A., Kukavica-Ibrulj, I., Longoria, A., Barrera, K., Levesque, R.C., Whiteley, M. (2009) Characterization of Alanine Catabolism in Pseudomonas aeruginosa and Its Importance for Proliferation In Vivo. *Journal of Bacteriology*. **191**(20), 6329–6334.

Brandtzaeg, P., van Deuren, M. (2012) Classification and Pathogenesis of Meningococcal Infections. In *Neisseria meningitidis*. Methods in Molecular Biology. Humana Press, pp. 21–35.

Brendish, N.J., Read, R.C. (2015) Neisseria meningitidis serogroup B bivalent factor H binding protein vaccine. *Expert Review of Vaccines*. **14**(4), 493–503.

Brinkman, A.B., Ettema, T.J.G., De Vos, W.M., Van Der Oost, J. (2003) The Lrp family of transcriptional regulators. *Molecular Microbiology*. **48**(2), 287–294.

Calvo, J.M., Matthews, R.G. (1994) The leucine-responsive regulatory protein, a global regulator of metabolism in Escherichia coli. *Microbiological Reviews*. **58**(3), 466–490.

Capel, E., Zomer, A.L., Nussbaumer, T., Bole, C., Izac, B., Frapy, E., Meyer, J., Bouzinba-Ségard, H., Bille, E., Jamet, A., Cavau, A., Letourneur, F., Bourdoulous, S., Rattei, T., Nassif, X., Coureuil, M. (2016) Comprehensive Identification of Meningococcal Genes and Small Noncoding RNAs Required for Host Cell Colonization. *mBio*. **7**(4).

Carvajal, N., López, V., Salas, M., Uribe, E., Herrera, P., Cerpa, J. (1999) Manganese Is Essential for Catalytic Activity ofEscherichia coliAgmatinase. *Biochemical and Biophysical Research Communications*. **258**(3), 808–811.

Catenazzi, M.C.E. (2013) *Characterisation of genomic islands in Neisseria meningitidis*. Thesis. University of York.

Catenazzi, M.C.E., Jones, H., Wallace, I., Clifton, J., Chong, J.P.J., Jackson, M.A., Macdonald, S., Edwards, J., Moir, J.W.B. (2014) A large genomic island allows Neisseria meningitidis to utilize propionic acid, with implications for colonization of the human nasopharynx. *Molecular Microbiology*. **93**(2), 346–355.

Catlin, B.W. (1973) Nutritional Profiles of Neisseria gonorrhoeae, Neisseria meningitidis, and Neisseria lactamica in Chemically Defined Media and the Use of Growth Requirements for Gonococcal Typing. *The Journal of Infectious Diseases*. **128**(2), 178–194.

Catlin, B.W., Schloer, G.M. (1962) A defined agar medium for genetic transformation of Neisseria meningitidis. *Journal of Bacteriology*. **83**, 470–474.

Caugant, D.A. (2008) Genetics and evolution of Neisseria meningitidis: Importance for the epidemiology of meningococcal disease. *Infection, Genetics and Evolution*. **8**(5), 558–565.

Caugant, D.A., Høiby, E.A., Magnus, P., Scheel, O., Hoel, T., Bjune, G., Wedege, E., Eng, J., Frøholm, L.O. (1994) Asymptomatic carriage of Neisseria meningitidis in a randomly sampled population. *Journal of Clinical Microbiology*. **32**(2), 323–330.

Caugant, D.A., Maiden, M.C.J. (2009) Meningococcal carriage and disease—Population biology and evolution. *Vaccine*. **27**(4), B64–B70.

CDC (2017) Meningitis | About Bacterial Meningitis Infection | CDC. [online]. Available from: https://www.cdc.gov/meningitis/bacterial.html [Accessed August 11, 2017].

CDC (2000) Meningococcal Disease and College Students. [online]. Available from: https://www.cdc.gov/mmwr/preview/mmwrhtml/rr4907a2.htm [Accessed August 11, 2017].

CDC (2014) Surveillance Manual | Meningococcal | Vaccine Preventable Diseases | CDC. [online]. Available from: https://www.cdc.gov/vaccines/pubs/surv-manual/chpt08-mening.html#f7 [Accessed August 20, 2017].

Cehovin, A., Lewis, S.B. (2017) Mobile genetic elements in Neisseria gonorrhoeae: movement for change. *Pathogens and Disease*. **75**(6).

Chattopadhyay, M.K., Tabor, C.W., Tabor, H. (2003) Polyamines protect Escherichia coli cells from the toxic effect of oxygen. *Proceedings of the National Academy of Sciences*. **100**(5), 2261–2265.

Chattopadhyay, M.K., Tabor, H. (2013) Polyamines Are Critical for the Induction of the Glutamate Decarboxylase-dependent Acid Resistance System in Escherichia coli. *Journal of Biological Chemistry*. **288**(47), 33559–33570.

Cho, B.-K., Barrett, C.L., Knight, E.M., Park, Y.S., Palsson, B.Ø. (2008) Genome-scale reconstruction of the Lrp regulatory network in Escherichia coli. *Proceedings of the National Academy of Sciences*. **105**(49), 19462–19467.

Christensen, H., May, M., Bowen, L., Hickman, M., Trotter, C.L. (2010) Meningococcal carriage by age: a systematic review and meta-analysis. *The Lancet Infectious Diseases*. **10**(12), 853–861.

Christodoulides, M., Heckels, J. (2017) Novel approaches to Neisseria meningitidis vaccine design. *Pathogens and Disease*. **75**(3).

Cohn, A.C., MacNeil, J.R., Harrison, L.H., Hatcher, C., Theodore, J., Schmidt, M., Pondo, T., Arnold, K.E., Baumbach, J., Bennett, N., Craig, A.S., Farley, M., Gershman, K., Petit, S., Lynfield, R., Reingold, A., Schaffner, W., Shutt, K.A., Zell, E.R., Mayer, L.W., Clark, T., Stephens, D., Messonnier, N.E. (2010) Changes in Neisseria meningitidis Disease Epidemiology in the United States, 1998–2007: Implications for Prevention of Meningococcal Disease. *Clinical Infectious Diseases*. **50**(2), 184–191.

Costa-Lourenço, A.P.R. da, Barros dos Santos, K.T., Moreira, B.M., Fracalanzza, S.E.L., Bonelli, R.R. (2017) Antimicrobial resistance in Neisseria gonorrhoeae: history, molecular mechanisms and epidemiological aspects of an emerging global threat. *Brazilian Journal of Microbiology*.

Coureuil, M., Join-Lambert, O., Lécuyer, H., Bourdoulous, S., Marullo, S., Nassif, X. (2012) Mechanism of meningeal invasion by Neisseria meningitidis. *Virulence*. **3**(2), 164–172.

Coureuil, M., Join-Lambert, O., Lécuyer, H., Bourdoulous, S., Marullo, S., Nassif, X. (2013) Pathogenesis of Meningococcemia. *Cold Spring Harbor Perspectives in Medicine*. **3**(6), a012393.

Dando, S.J., Mackay-Sim, A., Norton, R., Currie, B.J., John, J.A.S., Ekberg, J.A.K., Batzloff, M., Ulett, G.C., Beacham, I.R. (2014) Pathogens Penetrating the Central Nervous System: Infection Pathways

and the Cellular and Molecular Mechanisms of Invasion. *Clinical Microbiology Reviews.* **27**(4), 691–726.

Deasy, A.M., Guccione, E., Dale, A.P., Andrews, N., Evans, C.M., Bennett, J.S., Bratcher, H.B., Maiden, M.C.J., Gorringe, A.R., Read, R.C. (2015) Nasal Inoculation of the Commensal Neisseria lactamica Inhibits Carriage of Neisseria meningitidis by Young Adults: A Controlled Human Infection Study. *Clinical Infectious Diseases*. **60**(10), 1512–1520.

DeCoursey, T.E., Ligeti, E. (2005) Regulation and termination of NADPH oxidase activity. *Cellular and Molecular Life Sciences CMLS*. **62**(19–20), 2173–2193.

Deghmane, A.-E., Hong, E., Taha, M.-K. (2017) Emergence of meningococci with reduced susceptibility to third-generation cephalosporins. *Journal of Antimicrobial Chemotherapy*. **72**(1), 95–98.

Deghmane, A.-E., Petit, S., Topilko, A., Pereira, Y., Giorgini, D., Larribe, M., Taha, M.-K. (2000) Intimate adhesion of Neisseria meningitidis to human epithelial cells is under the control of the crgA gene, a novel LysR-type transcriptional regulator. *The EMBO Journal*. **19**(5), 1068–1078.

Delany, I., Rappuoli, R., Seib, K.L. (2013) Vaccines, Reverse Vaccinology, and Bacterial Pathogenesis. *Cold Spring Harbor Perspectives in Medicine*. **3**(5).

Derkaoui, M., Antunes, A., Abdallah, J.N., Poncet, S., Mazé, A., Pham, Q.M.M., Mokhtari, A., Deghmane, A.-E., Joyet, P., Taha, M.-K., Deutscher, J. (2016) Transport and Catabolism of Carbohydrates by Neisseria meningitidis. *Journal of Molecular Microbiology and Biotechnology*. **26**(5), 320–332.

van Deuren, M., Brandtzaeg, P., van der Meer, J.W.M. (2000) Update on Meningococcal Disease with Emphasis on Pathogenesis and Clinical Management. *Clinical Microbiology Reviews*. **13**(1), 144–166.

Di Tommaso, P., Moretti, S., Xenarios, I., Orobitg, M., Montanyola, A., Chang, J.-M., Taly, J.-F., Notredame, C. (2011) T-Coffee: a web server for the multiple sequence alignment of protein and RNA sequences using structural information and homology extension. *Nucleic Acids Research*. **39**(Web Server issue), W13–W17.

Doran, K.S., Fulde, M., Gratz, N., Kim, B.J., Nau, R., Prasadarao, N., Schubert-Unkmeir, A., Tuomanen, E.I., Valentin-Weigand, P. (2016) Host–pathogen interactions in bacterial meningitis. *Acta Neuropathologica*. **131**, 185–209.

Driessen, A.J., Smid, E.J., Konings, W.N. (1988) Transport of diamines by Enterococcus faecalis is mediated by an agmatine-putrescine antiporter. *Journal of Bacteriology*. **170**(10), 4522–4527.

Duane, P.G., Rubins, J.B., Weisel, H.R., Janoff, E.N. (1993) Identification of hydrogen peroxide as a Streptococcus pneumoniae toxin for rat alveolar epithelial cells. *Infection and Immunity*. **61**(10), 4392–4397.

Duffin, P.M., Seifert, H.S. (2010) DNA Uptake Sequence-Mediated Enhancement of Transformation in Neisseria gonorrhoeae Is Strain Dependent. *Journal of Bacteriology*. **192**(17), 4436–4444.

Dunn, K.L.R., Farrant, J.L., Langford, P.R., Kroll, J.S. (2003) Bacterial [Cu,Zn]-Cofactored Superoxide Dismutase Protects Opsonized, Encapsulated Neisseria meningitidis from Phagocytosis by Human Monocytes/Macrophages. *Infection and Immunity*. **71**(3), 1604–1607.

Dwilow, R., Fanella, S. (2015) Invasive Meningococcal Disease in the 21st Century—An Update for the Clinician. *Current Neurology and Neuroscience Reports*. **15**(3), 2.

Eason, M.M., Fan, X. (2014) The role and regulation of catalase in respiratory tract opportunistic bacterial pathogens. *Microbial Pathogenesis*. **74**, 50–58.

ECDC (2016) Invasive meningococcal disease - Annual Epidemiological Report 2016 [2014 data]. *European Centre for Disease Prevention and Control*. [online]. Available from: http://ecdc.europa.eu/en/publications-data/invasive-meningococcal-disease-annual-epidemiological-report-2016-2014-data [Accessed August 17, 2017].

Edwards, J., Quinn, D., Rowbottom, K.-A., Whittingham, J.L., Thomson, M.J., Moir, J.W.B. (2012) Neisseria meningitidis and Neisseria gonorrhoeae are differently adapted in the regulation of denitrification: single nucleotide polymorphisms that enable species-specific tuning of the aerobic–anaerobic switch. *Biochemical Journal*. **445**(1), 69–79.

Eisenberg, D., Gill, H.S., Pfluegl, G.M.U., Rotstein, S.H. (2000) Structure–function relationships of glutamine synthetases1. *Biochimica et Biophysica Acta (BBA) - Protein Structure and Molecular Enzymology*. **1477**(1–2), 122–145.

El-Halfawy, O.M., Valvano, M.A. (2014) Putrescine Reduces Antibiotic-Induced Oxidative Stress as a Mechanism of Modulation of Antibiotic Resistance in Burkholderia cenocepacia. *Antimicrobial Agents and Chemotherapy*. **58**(7), 4162–4171.

Ernsting, B.R., Atkinson, M.R., Ninfa, A.J., Matthews, R.G. (1992) Characterization of the regulon controlled by the leucine-responsive regulatory protein in Escherichia coli. *Journal of Bacteriology*. **174**(4), 1109–1118.

Evans, C.M., Pratt, C.B., Matheson, M., Vaughan, T.E., Findlow, J., Borrow, R., Gorringe, A.R., Read, R.C. (2011) Nasopharyngeal Colonization by Neisseria lactamica and Induction of Protective Immunity against Neisseria meningitidis. *Clinical Infectious Diseases*. **52**(1), 70–77.

Exley, R.M., Goodwin, L., Mowe, E., Shaw, J., Smith, H., Read, R.C., Tang, C.M. (2005) Neisseria meningitidis Lactate Permease Is Required for Nasopharyngeal Colonization. *Infection and Immunity*. **73**(9), 5762–5766.

Exley, R.M., Shaw, J., Mowe, E., Sun, Y., West, N.P., Williamson, M., Botto, M., Smith, H., Tang, C.M. (2005) Available carbon source influences the resistance of Neisseria meningitidis against complement. *The Journal of Experimental Medicine*. **201**(10), 1637–1645.

Fan, C., Li, Z., Yin, H., Xiang, S. (2013) Structure and Function of Allophanate Hydrolase. *The Journal of Biological Chemistry*. **288**(29), 21422–21432.

Fang, F.C. (2011) Antimicrobial Actions of Reactive Oxygen Species. *mBio*. **2**(5), e00141-11.

Frantz, I.D. (1942) Growth Requirements of the Meningococcus. *Journal of Bacteriology*. **43**(6), 757–761.

Friedrich, A., Arvidson, C.G., Shafer, W.M., Lee, E.-H., So, M. (2007) Two ABC Transporter Operons and the Antimicrobial Resistance Gene mtrF Are pilT Responsive in Neisseria gonorrhoeae. *Journal of Bacteriology*. **189**(14), 5399–5402.

Gabutti, G., Stefanati, A., Kuhdari, P. (2015) Epidemiology of Neisseria meningitidis infections: case distribution by age and relevance of carriage. *Journal of Preventive Medicine and Hygiene*. **56**(3), E116–E120.

Galego, L.R., Rodrigues, M.A.A., Mendes, D.C., Jockusch, S., Da Silva, J.P. (2016) Quantitative analysis of biogenic polyamines in distilled drinks by direct electrospray ionization tandem mass spectrometry using a nanocontainer. *Rapid Communications in Mass Spectrometry*. **30**(17), 1963–1968.

Gallo, M.F., Macaluso, M., Warner, L., Fleenor, M.E., Hook, E.W., Brill, I., Weaver, M.A. (2012) Bacterial Vaginosis, Gonorrhea, and Chlamydial Infection Among Women Attending a Sexually Transmitted Disease Clinic: A Longitudinal Analysis of Possible Causal Links. *Annals of Epidemiology*. **22**(3), 213–220.

Gandhi, A., Balmer, P., York, L.J. (2016) Characteristics of a new meningococcal serogroup B vaccine, bivalent rLP2086 (MenB-FHbp; Trumenba®). *Postgraduate Medicine*. **128**(6), 548–556.

Gault, J., Ferber, M., Machata, S., Imhaus, A.-F., Malosse, C., Charles-Orszag, A., Millien, C., Bouvier, G., Bardiaux, B., Péhau-Arnaudet, G., Klinge, K., Podglajen, I., Ploy, M.C., Seifert, H.S., Nilges, M., Chamot-Rooke, J., Duménil, G. (2015) Neisseria meningitidis Type IV Pili Composed of Sequence Invariable Pilins Are Masked by Multisite Glycosylation. *PLOS Pathogens*. **11**(9), e1005162.

Gaupp, R., Ledala, N., Somerville, G.A. (2012) Staphylococcal response to oxidative stress. *Frontiers in Cellular and Infection Microbiology*. **2**.

Geoffroy, M.-C., Floquet, S., Métais, A., Nassif, X., Pelicic, V. (2003) Large-Scale Analysis of the Meningococcus Genome by Gene Disruption: Resistance to Complement-Mediated Lysis. *Genome Research*. **13**(3), 391–398.

Gold, R., Goldschneider, I., Lepow, M.L., Draper, T.F., Randolph, M. (1978) Carriage of Neisseria meningitidis and Neisseria lactamica in infants and children. *The Journal of Infectious Diseases*. **137**(2), 112–121.

Golfieri, G. (2015) *Regulatory networks of Neisseria meningitidis and their implications for pathogenesis*. Tesi di dottorato. alma.

Gong, Z., Tang, M.M., Wu, X., Phillips, N., Galkowski, D., Jarvis, G.A., Fan, H. (2016) Arginine- and Polyamine-Induced Lactic Acid Resistance in Neisseria gonorrhoeae. *PLOS ONE*. **11**(1), e0147637.

Goodman, S.D., Scocca, J.J. (1988) Identification and arrangement of the DNA sequence recognized in specific transformation of Neisseria gonorrhoeae. *Proceedings of the National Academy of Sciences of the United States of America*. **85**(18), 6982–6986.

Gorringe, A.R., Pajón, R. (2012) Bexsero: A multicomponent vaccine for prevention of meningococcal disease. *Human Vaccines & Immunotherapeutics*. **8**(2), 174–183.

Gorringe, A.R., Taylor, S., Brookes, C., Matheson, M., Finney, M., Kerr, M., Hudson, M., Findlow, J., Borrow, R., Andrews, N., Kafatos, G., Evans, C.M., Read, R.C. (2009) Phase I Safety and Immunogenicity Study of a Candidate Meningococcal Disease Vaccine Based on Neisseria lactamica Outer Membrane Vesicles. *Clinical and Vaccine Immunology*. **16**(8), 1113–1120.

de Greeff, S.C., de Melker, H.E., Schouls, L.M., Spanjaard, L., van Deuren, M. (2008) Pre-admission clinical course of meningococcal disease and opportunities for the earlier start of appropriate intervention: a prospective epidemiological study on 752 patients in the Netherlands, 2003–2005. *European Journal of Clinical Microbiology & Infectious Diseases*. **27**(10), 985.

Grifantini, R., Frigimelica, E., Delany, I., Bartolini, E., Giovinazzi, S., Balloni, S., Agarwal, S., Galli, G., Genco, C., Grandi, G. (2004) Characterization of a novel Neisseria meningitidis Fur and iron-regulated operon required for protection from oxidative stress: utility of DNA microarray in the assignment of the biological role of hypothetical genes. *Molecular Microbiology*. **54**(4), 962–979.

Guilhen, C., Taha, M.-K., Veyrier, F.J. (2013) Role of transition metal exporters in virulence: the example of Neisseria meningitidis. *Frontiers in Cellular and Infection Microbiology*. **3**.

Ha, H.C., Sirisoma, N.S., Kuppusamy, P., Zweier, J.L., Woster, P.M., Casero, R.A. (1998) The natural polyamine spermine functions directly as a free radical scavenger. *Proceedings of the National Academy of Sciences*. **95**(19), 11140–11145.

Hacker, J., Blum-Oehler, G., Mühldorfer, I., Tschäpe, H. (1997) Pathogenicity islands of virulent bacteria: structure, function and impact on microbial evolution. *Molecular Microbiology*. **23**(6), 1089–1097.

Hacker, J., Kaper, J.B. (2000) Pathogenicity Islands and the Evolution of Microbes. *Annual Review of Microbiology*. **54**(1), 641–679.

Hanahan, D. (1983) Studies on transformation of Escherichia coli with plasmids. *Journal of Molecular Biology*. **166**(4), 557–580.

Harrison, L.H., Trotter, C.L., Ramsay, M.E. (2009) Global epidemiology of meningococcal disease. *Vaccine*. **27**, B51–B63.

Harrison, O.B., Schoen, C., Retchless, A.C., Wang, X., Jolley, K.A., Bray, J.E., Maiden, M.C.J. (2017) Neisseria genomics: current status and future perspectives. *Pathogens and Disease*. **75**(6).

Hart, B.R., Blumenthal, R.M. (2011) Unexpected Coregulator Range for the Global Regulator Lrp of Escherichia coli and Proteus mirabilis. *Journal of Bacteriology*. **193**(5), 1054–1064.

Heinson, A.I., Woelk, C.H., Newell, M.-L. (2015) The promise of reverse vaccinology. *International Health*. **7**(2), 85–89.

Henderson, P.J. (1993) The 12-transmembrane helix transporters. *Current Opinion in Cell Biology*. **5**(4), 708–721.

Heurlier, K., Thomson, M.J., Aziz, N., Moir, J.W.B. (2008) The Nitric Oxide (NO)-Sensing Repressor NsrR of Neisseria meningitidis Has a Compact Regulon of Genes Involved in NO Synthesis and Detoxification. *Journal of Bacteriology*. **190**(7), 2488–2495.

Heurlier, K., Vendeville, A., Halliday, N., Green, A., Winzer, K., Tang, C.M., Hardie, K.R. (2009) Growth Deficiencies of Neisseria meningitidis pfs and luxS Mutants Are Not Due to Inactivation of Quorum Sensing. *Journal of Bacteriology*. **191**(4), 1293–1302.

Hey, A., Li, M.-S., Hudson, M.J., Langford, P.R., Kroll, J.S. (2013) Transcriptional Profiling of Neisseria meningitidis Interacting with Human Epithelial Cells in a Long-Term In Vitro Colonization Model. *Infection and Immunity*. **81**(11), 4149.

Hill, D.J., Griffiths, N.J., Borodina, E., Virji, M. (2010) Cellular and molecular biology of Neisseria meningitidis colonization and invasive disease. *Clinical Science (London, England : 1979)*. **118**(Pt 9), 547–564.

Hotopp, J.C.D., Grifantini, R., Kumar, N., Tzeng, Y.L., Fouts, D., Frigimelica, E., Draghi, M., Giuliani, M.M., Rappuoli, R., Stephens, D.S., Grandi, G., Tettelin, H. (2006) Comparative genomics of Neisseria meningitidis: core genome, islands of horizontal transfer and pathogen-specific genes. *Microbiology*. **152**(12), 3733–3749.

Hughes, D. (2000) Evaluating genome dynamics: the constraints on rearrangements within bacterial genomes. *Genome Biology*. **1**, reviews0006.

Ieva, R., Alaimo, C., Delany, I., Spohn, G., Rappuoli, R., Scarlato, V. (2005) CrgA Is an Inducible LysR-Type Regulator of Neisseria meningitidis, Acting both as a Repressor and as an Activator of Gene Transcription. *Journal of Bacteriology*. **187**(10), 3421–3430.

Ieva, R., Roncarati, D., Metruccio, M.M.E., Seib, K.L., Scarlato, V., Delany, I. (2008) OxyR tightly regulates catalase expression in Neisseria meningitidis through both repression and activation mechanisms. *Molecular Microbiology*. **70**(5), 1152–1165.

Janausch, I.G., Zientz, E., Tran, Q.H., Kröger, A., Unden, G. (2002) C4-dicarboxylate carriers and sensors in bacteria. *Biochimica et Biophysica Acta (BBA) - Bioenergetics*. **1553**(1), 39–56.

Jayakumar, K.L., Lipoff, J.B. (2017) Albert Ludwig Sigesmund Neisser, MD—A Life of Discovery and Controversy in Dermatology. *JAMA Dermatology*. **153**(6), 574–574.

Jen, F.E.-C., Djoko, K.Y., Bent, S.J., Day, C.J., McEwan, A.G., Jennings, M.P. (2015) A genetic screen reveals a periplasmic copper chaperone required for nitrite reductase activity in pathogenic Neisseria. *The FASEB Journal*. **29**(9), 3828–3838.

Jorgensen, J.H., Crawford, S.A., Fiebelkorn, K.R. (2005) Susceptibility of Neisseria meningitidis to 16 Antimicrobial Agents and Characterization of Resistance Mechanisms Affecting Some Agents. *Journal of Clinical Microbiology*. **43**(7), 3162–3171.

Joseph, B., Schwarz, R.F., Linke, B., Blom, J., Becker, A., Claus, H., Goesmann, A., Frosch, M., Müller, T., Vogel, U., Schoen, C. (2011) Virulence Evolution of the Human Pathogen Neisseria meningitidis by Recombination in the Core and Accessory Genome. *PLoS ONE*. **6**(4), e18441.

Jyssum, K. (1959) Assimilation of nitrogen in meningococci grown with the ammonium ion as sole nitrogen source. *Acta Pathologica Et Microbiologica Scandinavica*. **46**, 320–332.

Kahler, C.M., Stephens, D.S. (1998) Genetic basis for biosynthesis, structure, and function of meningococcal lipooligosaccharide (endotoxin). *Critical Reviews in Microbiology*. **24**(4), 281–334.

Källberg, M., Wang, H., Wang, S., Peng, J., Wang, Z., Lu, H., Xu, J. (2012) Template-based protein structure modeling using the RaptorX web server. *Nature Protocols*. **7**(8), 1511–1522.

Kari, C., Nagy, Z., Kovács, P., Hernádi, F. (1971) Mechanism of the growth inhibitory effect of cysteine on Escherichia coli. *Journal of General Microbiology*. **68**(3), 349–356.

Kelly, D.F., Rappuoli, R. (2005) Reverse Vaccinology and Vaccines for Serogroup B Neisseria meningitidis. In *Hot Topics in Infection and Immunity in Children II*. Advances in Experimental Medicine and Biology. Springer, Boston, MA, pp. 217–223.

Khan, A.U., Mascio, P.D., Medeiros, M.H., Wilson, T. (1992) Spermine and spermidine protection of plasmid DNA against single-strand breaks induced by singlet oxygen. *Proceedings of the National Academy of Sciences*. **89**(23), 11428–11430.

Klughammer, J., Dittrich, M., Blom, J., Mitesser, V., Vogel, U., Frosch, M., Goesmann, A., Müller, T., Schoen, C. (2017) Comparative Genome Sequencing Reveals Within-Host Genetic Changes in Neisseria meningitidis during Invasive Disease. *PLOS ONE*. **12**(1), e0169892.

Kneuper, H., Janausch, I.G., Vijayan, V., Zweckstetter, M., Bock, V., Griesinger, C., Unden, G. (2005) The Nature of the Stimulus and of the Fumarate Binding Site of the Fumarate Sensor DcuS of Escherichia coli. *Journal of Biological Chemistry*. **280**(21), 20596–20603.

Kolappan, S., Coureuil, M., Yu, X., Nassif, X., Egelman, E.H., Craig, L. (2016) Structure of the *Neisseria meningitidis* Type IV pilus. *Nature Communications*. **7**, ncomms13015.

Kristiansen, P.A., Diomandé, F., Ba, A.K., Sanou, I., Ouédraogo, A.-S., Ouédraogo, R., Sangaré, L., Kandolo, D., Aké, F., Saga, I.M., Clark, T.A., Misegades, L., Martin, S.W., Thomas, J.D., Tiendrebeogo, S.R., Hassan-King, M., Djingarey, M.H., Messonnier, N.E., Préziosi, M.-P., LaForce,

F.M., Caugant, D.A. (2013) Impact of the Serogroup A Meningococcal Conjugate Vaccine, MenAfriVac, on Carriage and Herd Immunity. *Clinical Infectious Diseases*. **56**(3), 354–363.

Kristiansen, P.A., Diomandé, F., Ouédraogo, R., Sanou, I., Sangaré, L., Ouédraogo, A.-S., Ba, A.K., Kandolo, D., Thomas, J.D., Clark, T.A., Préziosi, M.-P., LaForce, F.M., Caugant, D.A. (2012) Carriage of Neisseria lactamica in 1- to 29-Year-Old People in Burkina Faso: Epidemiology and Molecular Characterization. *Journal of Clinical Microbiology*. **50**(12), 4020–4027.

Kurihara, S., Tsuboi, Y., Oda, S., Kim, H.G., Kumagai, H., Suzuki, H. (2009) The Putrescine Importer PuuP of Escherichia coli K-12. *Journal of Bacteriology*. **191**(8), 2776–2782.

Lampe, D.J., Churchill, M.E., Robertson, H.M. (1996) A purified mariner transposase is sufficient to mediate transposition in vitro. *The EMBO Journal*. **15**(19), 5470–5479.

Landgraf, J.R., Wu, J., Calvo, J.M. (1996) Effects of nutrition and growth rate on Lrp levels in Escherichia coli. *Journal of Bacteriology*. **178**(23), 6930–6936.

Lange, C., Mustafi, N., Frunzke, J., Kennerknecht, N., Wessel, M., Bott, M., Wendisch, V.F. (2012) Lrp of Corynebacterium glutamicum controls expression of the brnFE operon encoding the export system for l-methionine and branched-chain amino acids. *Journal of Biotechnology*. **158**(4), 231–241.

Leighton, M.P., Kelly, D.J., Williamson, M.P., Shaw, J.G. (2001) An NMR and enzyme study of the carbon metabolism of Neisseria meningitidis. *Microbiology*. **147**(6), 1473–1482.

Lin, Y., Boese, C.J., St Maurice, M. (2016) The urea carboxylase and allophanate hydrolase activities of urea amidolyase are functionally independent. *Protein Science: A Publication of the Protein Society*. **25**(10), 1812–1824.

Lipsitch, M., Siber, G.R. (2016) How Can Vaccines Contribute to Solving the Antimicrobial Resistance Problem? *mBio*. **7**(3), e00428-16.

Liu, G., Tang, C.M., Exley, R.M. (2015) Non-pathogenic Neisseria: members of an abundant, multi-habitat, diverse genus. *Microbiology*. **161**(7), 1297–1312.

Maiden, M.C. (2008) Population genomics: diversity and virulence in the Neisseria. *Current Opinion in Microbiology*. **11**(5), 467–471.

Maiden, M.C.J., Bygraves, J.A., Feil, E., Morelli, G., Russell, J.E., Urwin, R., Zhang, Q., Zhou, J., Zurth, K., Caugant, D.A., Feavers, I.M., Achtman, M., Spratt, B.G. (1998) Multilocus sequence typing: A portable approach to the identification of clones within populations of pathogenic microorganisms. *Proceedings of the National Academy of Sciences of the United States of America*. **95**(6), 3140–3145.

Mancusso, R., Gregorio, G.G., Liu, Q., Wang, D.-N. (2012) Structure and mechanism of a bacterial sodium-dependent dicarboxylate transporter. *Nature*. **491**(7425), 622–626.

Marri, P.R., Paniscus, M., Weyand, N.J., Rendón, M.A., Calton, C.M., Hernández, D.R., Higashi, D.L., Sodergren, E., Weinstock, G.M., Rounsley, S.D., So, M. (2010) Genome Sequencing Reveals Widespread Virulence Gene Exchange among Human Neisseria Species. *PLOS ONE*. **5**(7), e11835.

Martinón-Torres, F. (2016) Deciphering the Burden of Meningococcal Disease: Conventional and Under-recognized Elements. *The Journal of Adolescent Health: Official Publication of the Society for Adolescent Medicine*. **59**(2 Suppl), S12-20.

Mattick, J.S. (2002) Type IV Pili and Twitching Motility. *Annual Review of Microbiology*. **56**(1), 289–314.

McKenna, W.R., Mickelsen, P.A., Sparling, P.F., Dyer, D.W. (1988) Iron uptake from lactoferrin and transferrin by Neisseria gonorrhoeae. *Infection and Immunity*. **56**(4), 785–791.

McNeil, L.K., Zagursky, R.J., Lin, S.L., Murphy, E., Zlotnick, G.W., Hoiseth, S.K., Jansen, K.U., Anderson, A.S. (2013) Role of Factor H Binding Protein in Neisseria meningitidis Virulence and Its Potential as a Vaccine Candidate To Broadly Protect against Meningococcal Disease. *Microbiology and Molecular Biology Reviews : MMBR*. **77**(2), 234–252.

Miller, F., Lécuyer, H., Join-Lambert, O., Bourdoulous, S., Marullo, S., Nassif, X., Coureuil, M. (2013) Neisseria meningitidis colonization of the brain endothelium and cerebrospinal fluid invasion. *Cellular Microbiology*. **15**(4), 512–519.

Moir, J.W. (2011) A snapshot of a pathogenic bacterium mid-evolution: Neisseria meningitidis is becoming a nitric oxide-tolerant aerobe. *Biochemical Society Transactions*. **39**(6), 1890–1894.

Moore, T.D., Sparling, P.F. (1996) Interruption of the gpxA gene increases the sensitivity of Neisseria meningitidis to paraquat. *Journal of Bacteriology*. **178**(14), 4301–4305.

Moore, T.D., Sparling, P.F. (1995) Isolation and identification of a glutathione peroxidase homolog gene, gpxA, present in Neisseria meningitidis but absent in Neisseria gonorrhoeae. *Infection and Immunity*. **63**(4), 1603–1607.

Morris, S.M. (2004) Recent advances in arginine metabolism. *Current Opinion in Clinical Nutrition and Metabolic Care*. **7**(1), 45–51.

Morris, S.M. (2009) Recent advances in arginine metabolism: roles and regulation of the arginases. *British Journal of Pharmacology*. **157**(6), 922–930.

Moxon, E.R., Jansen, V.A.A. (2005) Phage variation: understanding the behaviour of an accidental pathogen. *Trends in Microbiology*. **13**(12), 563–565.

Mulligan, C., Fenollar-Ferrer, C., Fitzgerald, G.A., Vergara-Jaque, A., Kaufmann, D., Li, Y., Forrest, L.R., Mindell, J.A. (2016) The bacterial dicarboxylate transporter VcINDY uses a two-domain elevator-type mechanism. *Nature Structural & Molecular Biology*. **23**(3), 256–263.

Nassif, X., Pujol, C., Morand, P., Eugène, E. (1999) Interactions of pathogenic Neisseria with host cells. Is it possible to assemble the puzzle? *Molecular Microbiology*. **32**(6), 1124–1132.

Neumann, W., Hadley, R.C., Nolan, E.M. (2017) Transition metals at the host–pathogen interface: How Neisseria exploit human metalloproteins for acquiring iron and zinc. *Essays in biochemistry*. **61**(2), 211–223.

Nichols, C.E., Sainsbury, S., Ren, J., Walter, T.S., Verma, A., Stammers, D.K., Saunders, N.J., Owens, R.J. (2009) The structure of NMB1585, a MarR-family regulator from Neisseria meningitidis. *Acta Crystallographica Section F: Structural Biology and Crystallization Communications*. **65**(3), 204–209.

Nikulin, J., Panzner, U., Frosch, M., Schubert-Unkmeir, A. (2006) Intracellular survival and replication of Neisseria meningitidis in human brain microvascular endothelial cells. *International journal of medical microbiology: IJMM*. **296**(8), 553–558.

Norheim, G., Sadarangani, M., Omar, O., Yu, L.-M., Mølbak, K., Howitz, M., Olcén, P., Haglund, M., Ende, A. van der, Pollard, A.J. (2014) Association between population prevalence of smoking and incidence of meningococcal disease in Norway, Sweden, Denmark and the Netherlands between 1975 and 2009: a population-based time series analysis. *BMJ Open*. **4**(2), e003312.

Oguri, T., Schneider, B., Reitzer, L. (2012) Cysteine Catabolism and Cysteine Desulfhydrase (CdsH/STM0458) in Salmonella enterica Serovar Typhimurium. *Journal of Bacteriology*. **194**(16), 4366–4376.

Ohtsu, I., Wiriyathanawudhiwong, N., Morigasaki, S., Nakatani, T., Kadokura, H., Takagi, H. (2010) The l-Cysteine/l-Cystine Shuttle System Provides Reducing Equivalents to the Periplasm in Escherichia coli. *Journal of Biological Chemistry*. **285**(23), 17479–17487.

Oliver, K.E., Silo-Suh, L. (2013) Impact of d-amino acid dehydrogenase on virulence factor production by a Pseudomonas aeruginosa. *Canadian Journal of Microbiology*. **59**(9), 598–603.

Olsen, J.V., Ong, S.-E., Mann, M. (2004) Trypsin Cleaves Exclusively C-terminal to Arginine and Lysine Residues. *Molecular & Cellular Proteomics*. **3**(6), 608–614.

Pagliarulo, C., Salvatore, P., De Vitis, L.R., Colicchio, R., Monaco, C., Tredici, M., Talà, A., Bardaro, M., Lavitola, A., Bruni, C.B., Alifano, P. (2004) Regulation and differential expression of gdhA encoding NADP-specific glutamate dehydrogenase in Neisseria meningitidis clinical isolates. *Molecular Microbiology*. **51**(6), 1757–1772.

Panday, A., Sahoo, M.K., Osorio, D., Batra, S. (2015) NADPH oxidases: an overview from structure to innate immunity-associated pathologies. *Cellular & Molecular Immunology*. **12**(1), 5–23.

Pannekoek, Y., Huis in 't Veld, R.A.G., Schipper, K., Bovenkerk, S., Kramer, G., Brouwer, M.C., van de Beek, D., Speijer, D., van der Ende, A. (2017) Neisseria meningitidis Uses Sibling Small Regulatory RNAs To Switch from Cataplerotic to Anaplerotic Metabolism. *mBio*. **8**(2).

Peeters, E., Charlier, D. (2010) The Lrp Family of Transcription Regulators in Archaea. *Archaea*. **2010**.

Pelicic, V., Morelle, S., Lampe, D., Nassif, X. (2000) Mutagenesis of Neisseria meningitidis by In Vitro Transposition of Himar1 mariner. *Journal of Bacteriology*. **182**(19), 5391–5398.

Pelton, S.I. (2016) The Global Evolution of Meningococcal Epidemiology Following the Introduction of Meningococcal Vaccines. *Journal of Adolescent Health*. **59**(2), S3–S11.

Pericone, C.D., Overweg, K., Hermans, P.W.M., Weiser, J.N. (2000) Inhibitory and Bactericidal Effects of Hydrogen Peroxide Production by Streptococcus pneumoniae on Other Inhabitants of the Upper Respiratory Tract. *Infection and Immunity*. **68**(7), 3990–3997.

Perkins-Balding, D., Ratliff-Griffin, M., Stojiljkovic, I. (2004) Iron Transport Systems in Neisseria meningitidis. *Microbiology and Molecular Biology Reviews*. **68**(1), 154–171.

Perrin, A., Bonacorsi, S., Carbonnelle, E., Talibi, D., Dessen, P., Nassif, X., Tinsley, C. (2002) Comparative Genomics Identifies the Genetic Islands That Distinguish Neisseria meningitidis, the Agent of Cerebrospinal Meningitis, from Other Neisseria Species. *Infection and Immunity*. **70**(12), 7063–7072.

Perrin, A., Nassif, X., Tinsley, C. (1999) Identification of Regions of the Chromosome of Neisseria meningitidis and Neisseria gonorrhoeae Which Are Specific to the Pathogenic Neisseria Species. *Infection and Immunity*. **67**(11), 6119–6129.

Pettersen, E.F., Goddard, T.D., Huang, C.C., Couch, G.S., Greenblatt, D.M., Meng, E.C., Ferrin, T.E. (2004) UCSF Chimera—A visualization system for exploratory research and analysis. *Journal of Computational Chemistry*. **25**(13), 1605–1612.

Pizza, M., Scarlato, V., Masignani, V., Giuliani, M.M., Aricò, B., Comanducci, M., Jennings, G.T., Baldi, L., Bartolini, E., Capecchi, B., Galeotti, C.L., Luzzi, E., Manetti, R., Marchetti, E., Mora, M.,

Nuti, S., Ratti, G., Santini, L., Savino, S., Scarselli, M., Storni, E., Zuo, P., Broeker, M., Hundt, E., Knapp, B., Blair, E., Mason, T., Tettelin, H., Hood, D.W., Jeffries, A.C., Saunders, N.J., Granoff, D.M., Venter, J.C., Moxon, E.R., Grandi, G., Rappuoli, R. (2000) Identification of Vaccine Candidates Against Serogroup B Meningococcus by Whole-Genome Sequencing. *Science*. **287**(5459), 1816–1820.

Poole, L.B. (2005) Bacterial defenses against oxidants: mechanistic features of cysteine-based peroxidases and their flavoprotein reductases. *Archives of Biochemistry and Biophysics*. **433**(1), 240–254.

Pratt, A.J., DiDonato, M., Shin, D.S., Cabelli, D.E., Bruns, C.K., Belzer, C.A., Gorringe, A.R., Langford, P.R., Tabatabai, L.B., Kroll, J.S., Tainer, J.A., Getzoff, E.D. (2015) Structural, Functional, and Immunogenic Insights on Cu,Zn Superoxide Dismutase Pathogenic Virulence Factors from Neisseria meningitidis and Brucella abortus. *Journal of Bacteriology*. **197**(24), 3834–3847.

Prentki, P., Krisch, H.M. (1984) In vitro insertional mutagenesis with a selectable DNA fragment. *Gene*. **29**(3), 303–313.

Public Health England Vaccine cuts cases of meningitis and septicaemia in UK infants - GOV.UK. [online]. Available from: https://www.gov.uk/government/news/vaccine-cuts-cases-of-meningitis-and-septicaemia-in-uk-infants [Accessed August 17, 2017].

Rappuoli, R., Black, S., Lambert, P.H. (2011) Vaccine discovery and translation of new vaccine technology. *The Lancet*. **378**(9788), 360–368.

Ren, J., Sainsbury, S., Berrow, N.S., Alderton, D., Nettleship, J.E., Stammers, D.K., Saunders, N.J., Owens, R.J. (2005) Crystal structure of nitrogen regulatory protein IIANtr from Neisseria meningitidis. *BMC Structural Biology*. **5**, 13.

Ren, J., Sainsbury, S., Combs, S.E., Capper, R.G., Jordan, P.W., Berrow, N.S., Stammers, D.K., Saunders, N.J., Owens, R.J. (2007) The Structure and Transcriptional Analysis of a Global Regulator from Neisseria meningitidis. *Journal of Biological Chemistry*. **282**(19), 14655–14664.

Robert, X., Gouet, P. (2014) Deciphering key features in protein structures with the new ENDscript server. *Nucleic Acids Research*. **42**(W1), W320–W324.

Rouphael, N.G., Stephens, D.S. (2012) Neisseria meningitidis: Biology, Microbiology, and Epidemiology. In M. Christodoulides, ed. *Neisseria meningitidis*. Methods in Molecular Biology. Humana Press, pp. 1–20.

Rusniok, C., Vallenet, D., Floquet, S., Ewles, H., Mouzé-Soulama, C., Brown, D., Lajus, A., Buchrieser, C., Médigue, C., Glaser, P., Pelicic, V. (2009) NeMeSys: a biological resource for narrowing the gap between sequence and function in the human pathogen Neisseria meningitidis. *Genome Biology*. **10**, R110.

Sadarangani, M., Hoe, J.C., Makepeace, K., Ley, P. van der, Pollard, A.J. (2016) Phase variation of Opa proteins of Neisseria meningitidis and the effects of bacterial transformation. *Journal of Biosciences*. **41**(1), 13–19.

Sainsbury, S., Ren, J., Nettleship, J.E., Saunders, N.J., Stuart, D.I., Owens, R.J. (2010) The structure of a reduced form of OxyR from Neisseria meningitidis. *BMC Structural Biology*. **10**, 10.

Salaemae, W., Booker, G.W., Polyak, S.W. (2016) The Role of Biotin in Bacterial Physiology and Virulence: a Novel Antibiotic Target for Mycobacterium tuberculosis. *Microbiology Spectrum*. **4**(2).

Satiaputra, J., Shearwin, K.E., Booker, G.W., Polyak, S.W. (2016) Mechanisms of biotin-regulated gene expression in microbes. *Synthetic and Systems Biotechnology*. **1**(1), 17–24.

Schirch, V., Hopkins, S., Villar, E., Angelaccio, S. (1985) Serine hydroxymethyltransferase from Escherichia coli: purification and properties. *Journal of Bacteriology*. **163**(1), 1–7.

Schneider, M.C., Exley, R.M., Ram, S., Sim, R.B., Tang, C.M. (2007) Interactions between Neisseria meningitidis and the complement system. *Trends in Microbiology*. **15**(5), 233–240.

Schneider, M.C., Prosser, B.E., Caesar, J.J.E., Kugelberg, E., Li, S., Zhang, Q., Quoraishi, S., Lovett, J.E., Deane, J.E., Sim, R.B., Roversi, P., Johnson, S., Tang, C.M., Lea, S.M. (2009) Neisseria meningitidis recruits factor H using protein mimicry of host carbohydrates. *Nature*. **458**(7240), 890–893.

Schoen, C., Joseph, B., Claus, H., Vogel, U., Frosch, M. (2007) Living in a changing environment: Insights into host adaptation in Neisseria meningitidis from comparative genomics. *International Journal of Medical Microbiology*. **297**(7), 601–613.

Schoen, C., Kischkies, L., Elias, J., Ampattu, B.J. (2014) Metabolism and virulence in Neisseria meningitidis. *Frontiers in Cellular and Infection Microbiology*. **4**.

Schoen, C., Tettelin, H., Parkhill, J., Frosch, M. (2009) Genome flexibility in Neisseria meningitidis. *Vaccine*. **27**, B103–B111.

Schubert-Unkmeir, A. (2017) Molecular mechanisms involved in the interaction of Neisseria meningitidis with cells of the human blood–cerebrospinal fluid barrier. *Pathogens and Disease*. **75**(2).

Seib, K.L., Scarselli, M., Comanducci, M., Toneatto, D., Masignani, V. (2015) Neisseria meningitidis factor H-binding protein fHbp: a key virulence factor and vaccine antigen. *Expert Review of Vaccines*. **14**(6), 841–859.

Seib, K.L., Simons, M.P., Wu, H.-J., McEwan, A.G., Nauseef, W.M., Apicella, M.A., Jennings, M.P. (2005) Investigation of Oxidative Stress Defenses of Neisseria gonorrhoeae by Using a Human Polymorphonuclear Leukocyte Survival Assay. *Infection and Immunity*. **73**(8), 5269–5272.

Seib, K.L., Tseng, H.-J., McEwan, A.G., Apicella, M.A., Jennings, M.P. (2004) Defenses against Oxidative Stress in Neisseria gonorrhoeae and Neisseria meningitidis: Distinctive Systems for Different Lifestyles. *The Journal of Infectious Diseases*. **190**(1), 136–147.

Seib, K.L., Wu, H.-J., Kidd, S.P., Apicella, M.A., Jennings, M.P., McEwan, A.G. (2006) Defenses against Oxidative Stress in Neisseria gonorrhoeae: a System Tailored for a Challenging Environment. *Microbiology and Molecular Biology Reviews*. **70**(2), 344–361.

Seib, K.L., Wu, H.-J., Srikhanta, Y.N., Edwards, J.L., Falsetta, M.L., Hamilton, A.J., Maguire, T.L., Grimmond, S.M., Apicella, M.A., McEwan, A.G., Jennings, M.P. (2007) Characterization of the OxyR regulon of Neisseria gonorrhoeae. *Molecular Microbiology*. **63**(1), 54–68.

Shah, P., Nanduri, B., Swiatlo, E., Ma, Y., Pendarvis, K. (2011) Polyamine biosynthesis and transport mechanisms are crucial for fitness and pathogenesis of Streptococcus pneumoniae. *Microbiology*. **157**(2), 504–515.

Shah, P., Swiatlo, E. (2008) A multifaceted role for polyamines in bacterial pathogens. *Molecular Microbiology*. **68**(1), 4–16.

Shakhnovich, E.A., King, S.J., Weiser, J.N. (2002) Neuraminidase Expressed by Streptococcus pneumoniae Desialylates the Lipopolysaccharide of Neisseria meningitidis and Haemophilus influenzae: a Paradigm for Interbacterial Competition among Pathogens of the Human Respiratory Tract. *Infection and Immunity*. **70**(12), 7161–7164.

Shea, M.W. (2013) The Long Road to an Effective Vaccine for Meningococcus Group B (MenB). *Annals of Medicine and Surgery*. **2**(2), 53–56.

Slanina, H., Mündlein, S., Hebling, S., Schubert-Unkmeir, A. (2014) Role of Epidermal Growth Factor Receptor Signaling in the Interaction of Neisseria meningitidis with Endothelial Cells. *Infection and Immunity*. **82**(3), 1243–1255.

Smith, H., Tang, C.M., Exley, R.M. (2007) Effect of Host Lactate on Gonococci and Meningococci: New Concepts on the Role of Metabolites in Pathogenicity. *Infection and Immunity*. **75**(9), 4190–4198.

Snyder, L.A., Saunders, N.J. (2006) The majority of genes in the pathogenic Neisseria species are present in non-pathogenic Neisseria lactamica, including those designated as 'virulence genes'. *BMC Genomics*. **7**(1), 128.

Snyder, L.A.S., Davies, J.K., Ryan, C.S., Saunders, N.J. (2005) Comparative overview of the genomic and genetic differences between the pathogenic Neisseria strains and species. *Plasmid*. **54**(3), 191–218.

Spinosa, M.R., Progida, C., Talà, A., Cogli, L., Alifano, P., Bucci, C. (2007) The Neisseria meningitidis Capsule Is Important for Intracellular Survival in Human Cells. *Infection and Immunity*. **75**(7), 3594–3603.

Stabler, R.A., Marsden, G.L., Witney, A.A., Li, Y., Bentley, S.D., Tang, C.M., Hinds, J. (2005) Identification of pathogen-specific genes through microarray analysis of pathogenic and commensal Neisseria species. *Microbiology*. **151**(9), 2907–2922.

Stephens, D.S. (2009) Biology and pathogenesis of the evolutionarily successful, obligate human bacterium Neisseria meningitidis. *Vaccine*. **27**(Suppl 2), B71–B77.

Stephens, D.S., Greenwood, B., Brandtzaeg, P. (2007) Epidemic meningitis, meningococcaemia, and Neisseria meningitidis. *The Lancet*. **369**(9580), 2196–2210.

Stork, M., Grijpstra, J., Bos, M.P., Mañas Torres, C., Devos, N., Poolman, J.T., Chazin, W.J., Tommassen, J. (2013) Zinc Piracy as a Mechanism of Neisseria meningitidis for Evasion of Nutritional Immunity. *PLoS Pathogens*. **9**(10).

Streit, W.R., Entcheva, P. (2003) Biotin in microbes, the genes involved in its biosynthesis, its biochemical role and perspectives for biotechnological production. *Applied Microbiology and Biotechnology*. **61**(1), 21–31.

Sugiyama, Y., Nakamura, A., Matsumoto, M., Kanbe, A., Sakanaka, M., Higashi, K., Igarashi, K., Katayama, T., Suzuki, H., Kurihara, S. (2016) A Novel Putrescine Exporter SapBCDF of Escherichia coli. *Journal of Biological Chemistry*. **291**(51), 26343–26351.

Sunasara, K., Cundy, J., Srinivasan, S., Evans, B., Sun, W., Cook, S., Bortell, E., Farley, J., Griffin, D., Bailey Piatchek, M., Arch-Douglas, K. (2017) Bivalent rLP2086 (Trumenba®): Development of a well-characterized vaccine through commercialization. *Vaccine*.

Takada, S., Fujiwara, S., Inoue, T., Kataoka, Y., Hadano, Y., Matsumoto, K., Morino, K., Shimizu, T. (2016) Meningococcemia in Adults: A Review of the Literature. *Internal Medicine*. **55**(6), 567–572.

Takahashi, H., Kim, K.S., Watanabe, H. (2011) Meningococcal internalization into human endothelial and epithelial cells is triggered by the influx of extracellular L-glutamate via GltT L-glutamate ABC transporter in Neisseria meningitidis. *Infection and Immunity*. **79**(1), 380–392.

Takahashi, H., Yanagisawa, T., Kim, K.S., Yokoyama, S., Ohnishi, M. (2015) Multiple Functions of Glutamate Uptake via Meningococcal GltT-GltM l-Glutamate ABC Transporter in Neisseria meningitidis Internalization into Human Brain Microvascular Endothelial Cells. *Infection and Immunity*. **83**(9), 3555–3567.

Takumi, K., Nonaka, G. (2016) Bacterial Cysteine-Inducible Cysteine Resistance Systems. *Journal of Bacteriology*. **198**(9), 1384–1392.

Talà, A., Cogli, L., De Stefano, M., Cammarota, M., Spinosa, M.R., Bucci, C., Alifano, P. (2014) Serogroup-Specific Interaction of Neisseria meningitidis Capsular Polysaccharide with Host Cell Microtubules and Effects on Tubulin Polymerization. *Infection and Immunity*. **82**(1), 265–274.

Tamura, G.S., Nittayajarn, A., Schoentag, D.L. (2002) A Glutamine Transport Gene, glnQ, Is Required for Fibronectin Adherence and Virulence of Group B Streptococci. *Infection and Immunity*. **70**(6), 2877–2885.

Tani, T.H., Khodursky, A., Blumenthal, R.M., Brown, P.O., Matthews, R.G. (2002) Adaptation to famine: A family of stationary-phase genes revealed by microarray analysis. *Proceedings of the National Academy of Sciences of the United States of America*. **99**(21), 13471–13476.

Tettelin, H., Saunders, N.J., Heidelberg, J., Jeffries, A.C., Nelson, K.E., Eisen, J.A., Ketchum, K.A., Hood, D.W., Peden, J.F., Dodson, R.J., Nelson, W.C., Gwinn, M.L., DeBoy, R., Peterson, J.D., Hickey, E.K., Haft, D.H., Salzberg, S.L., White, O., Fleischmann, R.D., Dougherty, B.A., Mason, T., Ciecko, A., Parksey, D.S., Blair, E., Cittone, H., Clark, E.B., Cotton, M.D., Utterback, T.R., Khouri, H., Qin, H., Vamathevan, J., Gill, J., Scarlato, V., Masignani, V., Pizza, M., Grandi, G., Sun, L., Smith, H.O., Fraser, C.M., Moxon, E.R., Rappuoli, R., Venter, J.C. (2000) Complete Genome Sequence of Neisseria meningitidis Serogroup B Strain MC58. *Science*. **287**(5459), 1809–1815.

Tkachenko, A.G., Akhova, A.V., Shumkov, M.S., Nesterova, L.Y. (2012) Polyamines reduce oxidative stress in Escherichia coli cells exposed to bactericidal antibiotics. *Research in Microbiology*. **163**(2), 83–91.

Tønjum, T. (2015) Neisseria. In *Bergey's Manual of Systematics of Archaea and Bacteria*. John Wiley & Sons, Ltd.

Trotter, C.L., Maiden, M.C. (2009) Meningococcal vaccines and herd immunity: lessons learned from serogroup C conjugate vaccination programs. *Expert Review of Vaccines*. **8**(7), 851–861.

Tzeng, Y.-L., Ambrose, K.D., Zughaier, S., Zhou, X., Miller, Y.K., Shafer, W.M., Stephens, D.S. (2005) Cationic Antimicrobial Peptide Resistance in Neisseria meningitidis. *Journal of Bacteriology*. **187**(15), 5387–5396.

Tzeng, Y.-L., Stephens, D.S. (2015) Antimicrobial peptide resistance in Neisseria meningitidis. *Biochimica et Biophysica Acta (BBA) - Biomembranes*. **1848**(11, Part B), 3026–3031.

Unemo, M., Bradshaw, C.S., Hocking, J.S., de Vries, H.J.C., Francis, S.C., Mabey, D., Marrazzo, J.M., Sonder, G.J.B., Schwebke, J.R., Hoornenborg, E., Peeling, R.W., Philip, S.S., Low, N., Fairley, C.K. (2017) Sexually transmitted infections: challenges ahead. *The Lancet Infectious Diseases*. **17**(8), e235–e279.

Unemo, M., del Rio, C., Shafer, W.M. (2016) Antimicrobial resistance expressed by Neisseria gonorrhoeae: a major global public health problem in the 21st century. *Microbiology spectrum*. **4**(3).

Unoarumhi, Y., Blumenthal, R.M., Matson, J.S. (2016) Evolution of a global regulator: Lrp in four orders of γ-Proteobacteria. *BMC Evolutionary Biology*. **16**.

Veyrier, F.J., Boneca, I.G., Cellier, M.F., Taha, M.-K. (2011) A Novel Metal Transporter Mediating Manganese Export (MntX) Regulates the Mn to Fe Intracellular Ratio and Neisseria meningitidis Virulence. *PLoS Pathogens*. **7**(9).

Vogel, U. (2010) Molecular epidemiology of meningococci: Application of DNA sequence typing. *International Journal of Medical Microbiology*. **300**(7), 415–420.

Vogel, U., Claus, H., Müller, L. von, Bunjes, D., Elias, J., Frosch, M. (2004) Bacteremia in an Immunocompromised Patient Caused by a Commensal Neisseria meningitidis Strain Harboring the Capsule Null Locus (cnl). *Journal of Clinical Microbiology*. **42**(7), 2898–2901.

Wang, N.Y., Pollard, A.J. (2017) The next chapter for group B meningococcal vaccines. *Critical Reviews in Microbiology*, 1–17.

van de Waterbeemd, B., Zomer, G., van den IJssel, J., van Keulen, L., Eppink, M.H., van der Ley, P., van der Pol, L.A. (2013) Cysteine Depletion Causes Oxidative Stress and Triggers Outer Membrane Vesicle Release by Neisseria meningitidis; Implications for Vaccine Development. *PLoS ONE*. **8**(1).

Watson, P.S., Turner, D.P.J. (2016) Clinical experience with the meningococcal B vaccine, Bexsero®: Prospects for reducing the burden of meningococcal serogroup B disease. *Vaccine*. **34**(7), 875–880.

Weyand, N.J. (2017) Neisseria models of infection and persistence in the upper respiratory tract. *Pathogens and Disease*. **75**(3).

Weyand, N.J., Wertheimer, A.M., Hobbs, T.R., Sisko, J.L., Taku, N.A., Gregston, L.D., Clary, S., Higashi, D.L., Biais, N., Brown, L.M., Planer, S.L., Legasse, A.W., Axthelm, M.K., Wong, S.W., So, M. (2013) Neisseria infection of rhesus macaques as a model to study colonization, transmission, persistence, and horizontal gene transfer. *Proceedings of the National Academy of Sciences*. **110**(8), 3059–3064.

WHO (2015) WHO | Meningococcal meningitis. *Meningococcal meningitis*. [online]. Available from: http://www.who.int/mediacentre/factsheets/fs141/en/ [Accessed August 11, 2017].

Wi, T., Lahra, M.M., Ndowa, F., Bala, M., Dillon, J.-A.R., Ramon-Pardo, P., Eremin, S.R., Bolan, G., Unemo, M. (2017) Antimicrobial resistance in Neisseria gonorrhoeae: Global surveillance and a call for international collaborative action. *PLOS Medicine*. **14**(7), e1002344.

Wiesenfeld, H.C., Hillier, S.L., Krohn, M.A., Landers, D.V., Sweet, R.L. (2003) Bacterial Vaginosis Is a Strong Predictor of Neisseria gonorrhoeae and Chlamydia trachomatis Infection. *Clinical Infectious Diseases*. **36**(5), 663–668.

Wilks, K.E., Dunn, K.L.R., Farrant, J.L., Reddin, K.M., Gorringe, A.R., Langford, P.R., Kroll, J.S. (1998) Periplasmic Superoxide Dismutase in Meningococcal Pathogenicity. *Infection and Immunity*. **66**(1), 213–217.

Winzer, K., Sun, Y., Green, A., Delory, M., Blackley, D., Hardie, K.R., Baldwin, T.J., Tang, C.M. (2002) Role of Neisseria meningitidis luxS in Cell-to-Cell Signaling and Bacteremic Infection. *Infection and Immunity*. **70**(4), 2245–2248.

Wong, H.E.E., Li, M.-S., Kroll, J.S., Hibberd, M.L., Langford, P.R. (2011) Genome Wide Expression Profiling Reveals Suppression of Host Defence Responses during Colonisation by Neisseria meningitides but not N. lactamica. *PLOS ONE*. **6**(10), e26130.

Xie, O., Pollard, A.J., Mueller, J.E., Norheim, G. (2013) Emergence of serogroup X meningococcal disease in Africa: Need for a vaccine. *Vaccine*. **31**(27), 2852–2861.

Yazdankhah, S.P., Caugant, D.A. (2004) Neisseria meningitidis: an overview of the carriage state. *Journal of Medical Microbiology*. **53**(9), 821–832.

Yesilkaya, H., Andisi, V.F., Andrew, P.W., Bijlsma, J.J.E. (2013) Streptococcus pneumoniae and reactive oxygen species: an unusual approach to living with radicals. *Trends in Microbiology*. **21**(4), 187–195.

Yokoyama, K., Ishijima, S.A., Clowney, L., Koike, H., Aramaki, H., Tanaka, C., Makino, K., Suzuki, M. (2006) Feast/famine regulatory proteins (FFRPs): Escherichia coli Lrp, AsnC and related archaeal transcription factors. *FEMS Microbiology Reviews*. **30**(1), 89–108.

Zahlten, J., Kim, Y.-J., Doehn, J.-M., Pribyl, T., Hocke, A.C., García, P., Hammerschmidt, S., Suttorp, N., Hippenstiel, S., Hübner, R.-H. (2015) Streptococcus pneumoniae–Induced Oxidative Stress in Lung Epithelial Cells Depends on Pneumococcal Autolysis and Is Reversible by Resveratrol. *The Journal of Infectious Diseases*. **211**(11), 1822–1830.

Zhang, Y.J., Rubin, E.J. (2013) Feast or famine: the host-pathogen battle over amino acids. *Cellular Microbiology*. **15**(7), 1079–1087.

Zhao, J., Zhu, L., Fan, C., Wu, Y., Xiang, S. (2018) Structure and function of urea amidolyase. *Bioscience Reports*. **38**(1).

Zhou, X., Chua, T.K., Tkaczuk, K.L., Bujnicki, J.M., Sivaraman, J. (2010) The crystal structure of Escherichia coli spermidine synthase SpeE reveals a unique substrate-binding pocket. *Journal of Structural Biology*. **169**(3), 277–285.